



Université catholique de Louvain

Faculté d'ingénierie biologique, agronomique et environnementale

Unravelling genetic components of apple russeting

Sylvain Legay

Doctoral thesis in

Agronomical sciences and biological engineering

Committee:

Prof. Francois Chaumont, UCL (president)
Prof. Marc Boutry, UCL (supervisor)
Dr. Jean-François Hausman, LIST (supervisor)
Dr. Christelle André, LIST
Prof. Xavier Draye, UCL
Prof. Charles Hachez, UCL
Prof. Frédéric Domergue, CNRS

Abstract

Russeting, a major concern for the apple production sector, is due to the accumulation of suberin in the inner part of the cell wall of the epidermal cell layer. Since the 60s, many studies have been performed to better understand the tight relationship occurring between the cuticle development and the suberization process. However, the genetic factors which drive the russeting process, as well as the metabolic genes which are involved in the suberization process, remain unclear.

The first aim of this thesis was to identify the different genetic actors of the russeting process. For this, a transcriptomic approach comparing waxy and russeted tissues was used to investigate the different pathways which are involved in this particular trait. Among the identified genes, a large number involved in the cuticle biosynthesis had their expression repressed in the russeted skin. Conversely, genes likely involved in the suberization process were identified and displayed an enhanced expression in these tissues. A lipid surface analysis of the russeted and waxy apple skins in a semi-russeted apple confirmed these results. Interestingly, cell wall modification genes seemed to be also involved in this russeting program.

In a second step, candidate transcription factor genes, which might be involved in the regulation of russeting, were investigated. Among these, MdMYB93, which is able to trigger the expression of a large part of the genes identified in our transcriptomic studies, is now considered as a master regulator of suberin biosynthesis in apple.

Altogether the present thesis provides answers which help to better understand the mechanisms leading to russeting. It also opens new insights for further work

aiming at unravelling the remaining unexplored processes involved in apple russeting and, more generally, in the plant suberization process.

Acknowledgements

For more than fifteen years, I have been working with passion in plant biology research. I joined the CRP-Gabriel Lippmann in 2007, which became later the Luxembourg Institute of Science and Technology (LIST). During these years, I learnt how to perform the different tasks that are a researcher's daily responsibility. In 2013, the LIST supported my professional development giving me the opportunity to carry out a PhD. I enthusiastically accepted as I considered this proposal as a challenging professional validation of the work that I have been producing these last years, as well as an ideal framework for my future personal and professional development. However, I would have never succeeded in this task without the support of colleagues, relatives and friends.

I would like first to thank **Dr. Danièle Evers**, who initiated this new challenge. She was my scientific mentor and for 8 years, I have really appreciated her professionalism and humanity. I am thankful to **Dr. Jean-François Hausman**, who accepted to be my local supervisor, thesis promoter and group leader. For 10 years, he has taught me a lot about the work of a scientist and our exchanges were extremely prolific for my professional development. I also thank **Prof. Marc Boutry**, who accepted to be my thesis promoter at the UCL. I met a highly professional and passionate scientist, who was always available when I needed support.

I will never thank enough **Dr. Gea Guerriero**, who supported me, helped me in the lab, criticized my work and proposed me solutions. I was often impressed by her knowledgeable advice in the field of molecular biology and plant cell wall. I realize that I have met a precious colleague, with whom I can share my crazy ideas or found solutions to the different pitfalls we can meet at work.

I am also grateful to **Dr. Christelle André**, who is my referent colleague when I needed to discuss about apples. She was involved a lot in the present work. I was always excited to share with her my latest updates in our common field of experiment. Our discussions were always fruitful and I really appreciated her sharp comments on my work. I also thank her to accept to be part of my thesis committee with **Prof. Xavier Draye**, who helped me with the administrative procedures, which I partially forgot during these long years out of university.
I would like to thank **Prof. François Chaumont**, who accepted to be the foreman of the jury. I also thank **Dr. Frédéric Domergue** and **Prof. Charles Hachez** to be part of this jury.

Of course, I thank a lot all the people who were involved in this project. I extend my sincere thanks to **Dr. Marc Lateur**, who provided us the apple cultivars and shared a lot of data as well as his knowledge on the apple germplasm. I also thank **Prof. Owen Rowland**, who accepted to join our work and shared his strong expertise in plant surface lipids.

I also want to express my gratitude to **Dr. Cédric Guignard** and **Emmanuelle Cocco**, who taught me, supported me and participated in the development and the analysis of the apple lipid surface components. I thank **Dr Jenny Renaut**, **Céline Leclerq** and **Sébastien Planchon**, who spent a lot of time in the analysis of the proteome of the apple skin. Finally, I thank **Sophie Charton**, who performed and analyzed the data obtained from the UPLC-tripleTOF.

I especially thank our two technicians, **Aude Corvisy** and **Laurent Solinhac**, who helped me a lot in my other projects. This allowed me to spend more time for this work, which was highly valuable in this short timeframe.

I thank all the students I supervised, **Mélanie Roland**, **Ben Jacob**, **Sagynbek Aaliev**, **Farhod Bobokalonov** and **Nurullo Muhsimov**, who participated in the activities of my thesis and research work. I am convinced that they will have a great professional development in the future.

I am thankful to the colleagues that supported me in my decision to carry out a PhD thesis, notably **Matias**, **Thommaso**, **Daniel**, **Sébastien, Kjell**, **Christos**, **Phillipe**. I also thank my PhD fellows, **Marc**, **Sébastien, Kahina, Blandine** and **Annelie**. I am sure they will succeed in their PhD.

I am highly indebted to my **family** and especially to my **parents**, who were always behind me. I thank my **grandmother**, who always asked 'is the work OK?', and I think a lot to my **grandfather**... Despite the fact that I have not seen some of them for a long time, I would like to thank my close friends, who gave me a bit of 'fresh air' along these last years. I thank particularly **Etienne**, **Xavier**, **David**, **Anton**, **Steve**, **Pierre**, **Jo**, **Mathilde**, **Ludovic** and **Caroline**.

These last years were quite eventful with good and bad moments. Because of this, I would like to say that I am so proud to have **Aurélie** in my life. She has always been supporting me with intelligence and kindness, keeping me in the right behavior to achieve my objectives. This is invaluable… I will keep forever in mind this period of our life and measure each day the chance I have to be with her. Thank you so much!!!

Thesis achievements

Published in the thesis frame

Legay S, Guerriero G, Deleruelle A, Lateur M, Evers D, André CM, Hausman, J-F. 2015. Apple russeting as seen through the RNA-seq lens: strong alterations in the exocarp cell wall. *Plant Molecular Biology* **88**: 21-40.

Legay S, Guerriero G, André CM, Guignard C, Cocco E, Charton S, Boutry M, Rowland O, Hausman JF. 2016. MdMyb93 is a regulator of suberin deposition in russeted apple fruit skins. *New phytologist* Epub head of print.

Published in the apple russeting topic

Andre CM, Legay S, Deleruelle A, Nieuwenhuizen N, Punter M, Brendolise C, Cooney JM, Lateur M, Hausman JF, Larondelle Y, Laing WA. 2016. Multifunctional oxidosqualene cyclases and cytochrome P450 involved in the biosynthesis of apple fruit triterpenic acids. *New Phytologist* **211**: 1279-1294.

Published out of the topic

Andre CM, Legay S, Iammarino C, Ziebel J, Guignard C, Larondelle Y, Hausman JF, Evers D, Miranda Miranda L. 2014. The Potato in the Human Diet: a Complex Matrix with Potential Health Benefits. *Potato Research* **57**: 201-214.

Guerriero G, Legay S, Hausman JF. 2014. Alfalfa Cellulose synthase gene expression under abiotic stress: a Hitchhiker's guide to RT-qPCR normalization. *PLoS One* **9**: e103808.

Behr M, Legay S, Hausman JF, Guerriero G. 2015. Analysis of cell wall-related genes in organs of *Medicago sativa* L. under different abiotic stresses. *International Journal of Molecular Sciences* **16**: 16104-16124.

Georgantzopoulou A, Skoczyńska E, Van den Berg JH, Brand W, Legay S, Klein SG, Rietjens IM, Murk AJ. 2014. P-gp efflux pump inhibition potential of common environmental contaminants determined in vitro. *Environmental Toxicolology and Chemistry* **33**: 804-813.

Elnar AA, Desor F, Legay S, Nemos C, Yen FT, Oster T, Bohn T, Soulimani R. 2015. No evidence for oxidative stress in the cerebellar tissues or cells of juvenile male mice exposed via lactation to the 6 non-dioxin-like PCBs at levels below the regulatory safe limits for humans. *Toxicology Letters* **245**: 7-14.

Guerriero G, Hausman JF, Legay S. 2016. Silicon and the Plant Extracellular Matrix. *Frontiers in Plant Science* **7**: 463.

Kaulmann A, Legay S, Schneider YJ, Hoffmann L, Bohn T. 2016. Inflammation related responses of intestinal cells to plum and cabbage digesta with differential carotenoid and polyphenol profiles following simulated gastrointestinal digestion. *Molecular Nutrition & Food Research* **60**: 992-1005.

Article in preparation

Legay S, Cocco E, Guerriero G, André CM, Guignard C, Hausman JF. Differential accumulation of cutin, suberin and their associated waxes in the semi-russeted 'Cox Orange Pippin' variety

Legay S, Guerriero G, Leclerc C, Renaut J, Hausman JF, André CM. Integrative analysis of two russeted and non-russeted closely related apple varieties during fruit development provides new insights about the cuticle/suberin interplay.

Patent

Legay S. Suberin production by the use of a MYB93-like transcription factor. 14/04/2016. N°93026

Content

Abstract 3

Acknowledgements 5

Thesis achievements 9

Content 11

List of figures 17

List of tables 21

List of supporting information (SI) tables 23

Abbreviations 25

General introduction 33

I. The apple *33*

A. Apple: genetic origins and domestication 34

B. Breeding, conservation, production and consumption 36

II. Apple russeting *38*

III. Suberin in plants *44*

A. The role of suberin in plants 44

B. Suberin structure and composition 46

C. Suberin-associated waxes 53

IV. Suberin biosynthesis *55*

A. Synthesis of suberin monomer precursors 55

B. Suberin monomers and hydroxycinnamate-conjugates biosynthesis 63

C. Cutin- and suberin-associated triterpene synthesis 65

D. Suberin monomers transport 68

E. Suberin polymerization 71

V. Regulation of russeting and suberin deposition *72*

Objectives 77

References *81*

Chapter I: Apple russeting as seen through the RNA-seq lens: strong alterations in the exocarp cell wall **93**

Abstract *94*

I. Introduction *95*

II. Materials and methods *98*

A. Plant material 98

B. RNA extraction 99

C. Library preparation and sequencing 101

D. Data analysis 101

E. QPCR validation 102

III. Results and discussion *105*

A. Sequencing and mapping 105

B. Overview of the differentially expressed genes between russeted (RAE) and waxy apple exocarp (WAE) 107

C. Primary lipid synthesis and cuticle deposition-related genes were less expressed in russeted apple 110

D. Expression of cell wall loosening-related genes was enhanced in russeted tissues 114

E. Strong differential expression of the suberin deposition-related genes in the russeted apples 120

F. Differential expression of cuticle synthesis- and suberin deposition-related genes goes along with the expression of specific triterpene synthesis gene 125

G. Stress responses signaling cascades and transcription factors were strongly enhanced in russeted apple 126

References *134*

Summary and Perspectives *145*

Chapter II: Differential accumulation of cutin, suberin and their associated waxes in the semi-russeted 'Cox Orange Pippin' variety **151**

Abstract: *152*

I. Introduction *154*

II. Materials and Method *158*

A. Plant material 158

B. RNA extraction 159
C. Targeted gene expression analysis 159
D. Cutin and suberin depolymerization and free lipid analysis 163
III. Results 165
A. Cox Orange Pippin skin phenotype 165
B. Russeted skin displayed a strong decrease in the waxes and triterpene contents 166
C. Cutin and suberin contained embedded wax and triterpenes 174
D. Russeted skin displayed a decreased cutin synthesis associated with an enhanced synthesis of suberin-specific very long chain fatty acid precursors 176
E. Drastic differential expression of cutin, suberin, wax and triterpene biosynthetic genes between russeted and waxy skins of 'Cox Orange Pippin' 181
IV. Discussion 185
References 197
Summary and Perspectives 205

Chapter III: Integrative analysis of two russeted and non-russeted closely related apple varieties during fruit development provides new insights about the cuticle/suberin interplay 211
Abstract 212
I. Introduction 214
II. Materials and methods 220
A. Plant material 220
B. DNA extraction and genetic analysis 220
C. RNA extraction 221
D. Library preparation and sequencing 222
E. Data analysis 222
F. Proteomic analysis 224
G. Triterpene analysis 226
III. Results and discussion 228
A. Phenotypic and genetic characterization 228
1. Fruit growth and phenotype 228
2. Genetic analysis using SSR markers 229
B. Overview of the transcriptomic and proteomic data 232

1. Sequencing, mapping and selection of differentially expressed genes....232
2. Overview of the differentially expressed genes....234
3. Proteome analysis overview....236
C. Integrative analysis....241
1. Cuticle deposition genes displayed inversed expression patterns in CG and CB during fruit growth....241
2. Differential increased expression of the suberin and cell wall metabolism between Canada Blanc and Canada Gris....249
3. Expression of genes for triterpene metabolism in CG and CB strongly differed during fruit growth....265
D. Global outlines and key features....271
References....*277*
Summary and Perspectives....*291*

Chapter IV: MdMyb93 is a regulator of suberin deposition in russeted apple fruit skins....295
Abstract....*297*
I. Introduction....*298*
II. Material and methods....*300*
A. RNA extraction and reverse transcription....300
B. Gene isolation and cloning....301
C. Infiltration by *Agrobacterium tumefaciens*....301
D. Library preparation and sequencing....302
E. Targeted gene expression analysis using RT-qPCR....304
F. Suberin depolymerization and free fatty acid analysis....306
G. Phenylpropanoid analysis....307
III. Results....*309*
A. The MDP0000320772 contig is orthologous to the *Arabidopsis thaliana* AtMYB93 transcription factor....309
B. Whole gene expression profiling of the MDP0000320772-regulated genes in *Nicotiana benthamiana*....312
C. *MdMYB93* triggered the accumulation of suberin monomers and suberin deposition....322
D. *MdMYB93* expression remobilizes phenylpropanoids and influences the lignin precursor accumulation....325
IV. Discussion....*328*

References *336*
Summary and Perspectives *345*

General discussion **349**
A. Synthesis of cutin and suberin and their associated waxes was inversely regulated between russeted and waxy apple skin ... 352
B. The role of α/β-fold hydrolases, GDSL esterase/lipases and BAHD acyltransferases 359
C. Transport of cutin and suberin precursors was likely supported by dedicated ATP-binding cassette subfamily G and lipid transfer protein transporters 360
D. Russeting triggered a cell wall-modification process linked to the suberization process 362
E. The russeting transcriptional regulatory network 365
References *370*

List of figures

Figure 1-1: 'Adam and Eve' by Peter Paul Rubens (1628-1629)……...……..33

Figure 1-2: Evolutionary history of cultivated apples……...……35

Figure 1-3: Examples of apple varieties displaying variable degree of russeting..39

Figure 1-4: Comparison between skin phenotype and cuticle thickness in two progenies obtained from a cross between the non-russeted parents 'Breaburn' and 'Golden delicious'.....41

Figure 1-5: Epicuticular microcracking observed on the skin surface of 'Golden Delicious' at the harvesting date.....42

Figure 1-6: Suberin structure model proposed by Bernards (2002)……..47

Figure 1-7: TEM of an *Arabidopsis* leaf overexpressing *AtMYB41*……..……48

Figure 1-8: Aliphatic precursors of the SPAD found in suberized tissues (adapted from Bernards 2002)……49

Figure 1-9: Model of suberin structure proposed by Graca (2015)…….....…..51

Figure 1-10: Suberin biosynthesis pathway. Lipid biosynthesis part……..…....57

Figure 1-11: Suberin biosynthesis pathway-Phenylpropanoid biosynthesis part.61

Figure 1-12: Biosynthetic pathway of triterpenic acids in apple……..……67

Figure 2-1: Correlation between qPCR and RNA sequencing data……107

Figure 2-2: Distribution of the significant differentially expressed genes across major bins in Mapman 3.6RC1……109

Figure 2-3: Mapman metabolism overview obtained from the significantly regulated genes……..111

Figure 2-4: Gene ontology enrichment analysis performed from a subset of genes in Cytoscape with the ClueGO and CluePedia plugins……..112

Figure 2-5: Hierarchical clustering performed based on qPCR results with correlation similarity metrics and complete linkage……..123

Figure 2-6: Suberin candidate gene interaction matrix performed in STRING...130

Figure 2-7: Schematic overview of the expression patterns observed in waxy and russeted apple exocarps……..132

Figure 3-1: The 'Cox Orange Pippin' skin phenotype…….……...165

Figure 3-2: Distribution of the identified fatty acids (as trimethylsilyl esters) found in the free lipid fraction of the waxy skin and russeted skin……166

Figure 3-3: Distribution of the identified primary fatty alcohols (as trimethylsilyl ethers) and aldehydes found in the free lipid fraction of the waxy skin and russeted skin…..……168

Figure 3-4: Distribution of the identified alkanes found in the free lipid fraction of the waxy skin and russeted skin……..169

Figure 3-5: Distribution of the identified and unidentified trimethyl sylilated triterpenes found in the free lipid fraction of the waxy skin and russeted skin……170

Figure 3-6: Distribution of glycerol (as trimethylsilyl ethers), monoacylglycerol (as trimethylsilyl esters), and β-sitosterol (as trimethylsilyl ethers) found in the free lipid fraction of the waxy skin and russeted skin……..……172

Figure 3-7: Distribution of the alkyl-hydroxycinnamates (as trimethylsilyl ethers) found in the free lipid fraction of the russeted skin……173

Figure 3-8: Distribution of the alkanes and triterpenes (as trimethylsilyl ethers) found in the waxy skin and russeted skin after BF_3/MeOH transesterification...175

Figure 3-9: Distribution of the alkanoic acids (as methyl esters) found in the waxy skin and russeted skin after BF_3/MeOH transesterification……176

Figure 3-10: Distribution of the primary alcohols (as trimethylsilyl ether) and hydroxycinnamic acids (as silylated methyl esters) found in the waxy skin and russeted skin after BF_3/MeOH transesterification……..177

Figure 3-11: Distribution of the α,ω-dicarboxylic acids (as methyl esters) found in the waxy skin and russeted skin after BF_3/MeOH transesterification……179

Figure 3-12: Distribution of the ω-hydroxyacids (as silylated methyl esters) found in the waxy skin and russeted skin after BF_3/MeOH transesterification…….180

Figure 3-13: Normalized relative expression (NRq) of lipid surface biosynthesis genes performed in the waxy skin and russeted skin……..182

Figure 3-14: Overview of the metabolites found in the free lipid and depolymerized fractions obtained from the 'Cox orange Pippin' waxy and russeted skins..……187

Figure 4-1: Skin phenotype and fruit size of 'Canada Gris' (CG) and 'Canada Blanc' (CB) during fruit growth..……...228

Figure 4-2: Phenogram gathering the 27 selected individuals performed with the allelic data obtained from 16 Simple Sequence Repeats (SSR) markers……231

Figure 4-3: Hierarchical clustering of the 1070 differentially expressed genes across the kinetics……..235

Figure 4-4: Distribution of the significantly and differentially expressed proteins according to the MapMan bins classification……238

Figure 4-5: Gene ontology enrichment analysis of the significant differentially expressed genes ordered in the cluster C2 and C3……..244

Figure 4-6: Gene ontology enrichment analysis of the significant differentially expressed genes ordered in the cluster C4 to C7…….……251

Figure 4-7: Subset of the co-expression matrix performed using STRING from the cluster C4 to C7……259

Figure 4-8: Oleanolic acid, ursolic acid, betulinic acid and betulinic acid-3-trans caffeate content in the 'Canada Blanc' (non-russeted) and 'Canada Gris' (russeted) skins……...……...267

Figure 4-9: Principal component analysis performed using differentially expressed genes coding for α/β-fold hydrolases and BAHD acyltransferases...269

Figure 4-10: Trend in expression of genes being involved in the cuticle, suberin, hydroxycinnamic acid, triterpene biosynthesis and cell wall modification, during the fruit growth kinetic of Canada Gris and Canada Blanc…….273

Figure 5-1: Phylogenetic analysis of the apple MYB transcription factors…….310

Figure 5-2: Phyre2 protein modeling of MdMYB93……..311

Figure 5-3: RTqPCR validation of transient expression of MdMYB93 in *Nicotiana benthamiana*……..313

Figure 5-4: Gene ontology enrichment analysis of the MdMYB93 responsive biological processes…….…….315

Figure 5-5: Co-expression matrix performed using STRING from the significantly MdMYB93 up-regulated genes in *N. benthamiana*……317

Figure 5-6: Composition of the free lipid fraction of *N. benthamiana* leaves agro-infiltrated with either MdMYB93/p19 or p19 alone (control)…….……..323

Figure 5-7: Polyester monomer composition of *N. benthamiana* leaves agro-infiltrated with either MdMYB93/p19 or p19 alone (control)……324

Figure 5-8: Ultraviolet microscopy performed on *N. benthamiana* leaves overexpressing MdMYB93 and control leaves after staining with berberine/aniline blue…….325

Figure 5-9: Summary of the biological processes altered by the expression of *MdMYB93* in *N. benthamiana* leaves…….331

Figure 6-1: Schematic representation of the suberin polyaliphatic domain biosynthesis pathway in russeted apple……..355

Figure 6-2: Involvement of BAHD acyltransferase, GDSL-motif esterase/lipase and α/β-fold protein hydrolase in the suberization process……360

Figure 6-3: Hypothetical model of cell wall modification built from gene expression data observed in russeted apple skin and based the model described by Bernards (2002)…….363

Figure 6-4: Tentative regulatory network occurring during apple russeting…..366

List of tables

Table 2-1: Genotype and phenotype data……...…100

Table 2-2: Primers data display qPCR primer sequences, amplicon size, PCR efficiency, melting temperatures…….……...104

Table 2-3: Summary of the sequencing, filtering and mapping in number of sequence reads……...106

Table 2-4: Sub-selection of the differentially expressed genes obtained from the statistical comparison of the RAE against the WAE varieties analysis..……115

Table 3-1: Description of the 28 representative genes involved in the cutin, suberin, wax and triterpene biosynthesis……160

Table 4-1: Overview of the Single Sequence Repeat (SSR) markers used for the phylogenetic analysis of Canada Gris and Canada Blanc ……..230

Table 4-2: Overview of the sequencing, filtering and mapping statistis. The read number is expressed in million……..233

Table 4-3: Subset of the differentially expressed proteins…….……239

Table 4-4: Subset of the significantly differentially expressed genes observed in the cluster C2-C3……..…..……..247

Table 4-5: Gene ontology and KEGG pathway analysis performed from the cluster C4, C5, C6 and C7 performed using the STRING functional analysis tool……..…..……...252

Table 4-6: Subset of the significant differentially expressed genes observed in the cluster C4 to C7…….……254

Table 5-1: Primer data: primer sequences, accession, amplicon size, melting temperature (Tm in °C) and references……...305

Table 5-2: Sub-selection of the differentially expressed genes obtained from comparison of *N. benthamiana* leaves overexpressing MdMYB93 against control infiltrated leaves……319

Table 5-3: List of compounds differentially accumulated in *N. benthamiana* leaf samples after transient overexpression of MdMYB93……..327

List of supporting information (SI) tables

Supporting information tables and figures are available at the following link:

https://drive.google.com/open?id=0B6skBltspH4xZmM3UU40M2V3UDQ

Supporting Information Table 2-1: RTqPCR validation performed on the apple variety panel

Supporting Information Table 2-2: List of the differentially expressed genes observed between russeted and waxy varieties - Mapman gene distribution

Supporting Information Table 3-1: RTqPCR results performed on Cox Orange Pippin - genorm analysis

Supporting Information Table 3-2: GC-MS analysis: fragment Table

Supporting Information Table 3-3: GC-MS analysis: relative contents and statistical analysis

Supporting Information Table 4-1: List of the differentially expressed genes observed between CG and CB skin

Supporting information Table 4-2: List of the differentially expressed proteins observed between CG and CB skin

Supporting information Table 4-3: Mascot identification-protein family report

Supporting information Table 5-1: List of the differentially expressed genes between MdMYB93 agroinfiltrated and control leaves

Supporting information Table 5-2: RT-qPCR results performed on *N. benthamiana* leaves expressing MdMYB93

Abbreviations

35S	Cauliflower mosaic virus 35S promoter
4CL	4-coumarate-CoA ligase
ABA	Abscisic acid
ABCG	ATP-binding cassette subfamily G
ACBP6	Acyl-CoA binding protein 6
ACC	Aminocyclopropanecarboxylate
ACP	NADH-dependent enoyl-acyl carrier protein
AGP	Arabinogalactan protein
AOC4	Allene oxide cyclase 4
AOCS	American Oil Chemists' Society
AP2/EREBP	APELATA2/ethylene-responsive element binding protein
ASFT	*Arabidopsis* suberin feruloyl transferase
ATP	Adenosine triphosphate
ATT1	Fatty acid hydroxylase
BA	Betulinic acid
BA-transC	Betulinic acid-3-trans caffeate
BACC	*Malus baccata*
BAHD	HXXXD-motif acyltransferase family
BAN	BANYULS
BDG	BODYGUARD protein
bHLH	Basic helix-loop-helix
BSATFA	N,O-Bis(trimethylsilyl)trifluoroacetamide
C2H2	Cysteine-2/Histidine-2
C3'H	p-coumaroyl shikimate-3'-hydroxylase
C4H	Cinnamate-4-hydroxylase

CAD	Cinnamyl alcohol dehydrogenase
CASP	Casparian protein
CB	‘Reinette du Canada Blanche’, ‘Canada Blanc’
CCoAOMT	Caffeoyl-CoA 3-O-methyltransferase
CCR	Cinnamoyl-CoA reductase
CD1	GDSL-motif esterase/lipase
cDNA	Complementary DNA
CER	ECERIFERUM
CG	‘Reinette du Canada Grise’, ‘Canada Gris’
CHAPS	3-([3-cholamidopropyl] dimethylammonio)-1-propanesulfonate
CHI	Chalcone isomerase
CID	Collision-induced dissociation
CoA	Coenzyme A
COBRA	COBRA protein
COMT	Caffeic acid/5-hydroxyferulic acid O-methyltransferase
CRA-W	Waloon agronomical research centre
CRRG	Centre Régional de Ressources Phytogénétiques
CTAB	Cetyl trimethylammonium bromide
CUT1	GDSL-motif esterase/lipase
Cx	x carbon
CYP716A175	Cytochrome P450 716A175 monooxygenase
CYP	Cytochrome P450
CYP81D8	Isoflavone 2’-hydroxylase
CYP86A1	Cytochrome P450 86A1 fatty acid hydroxylase
CYP86A2	Cytochrome P450 86A2 fatty acid hydroxylase
CYP86A33	Cytochrome P450 86A33 fatty acid hydroxylase
CYP86A8	Cytochrome P450 86A8

CYP86B1	Cytochrome P450 86B1 very long chain fatty acid hydroxlase
DAFB	Day after full bloom
DCM	Dichloromethane
DCR	Defective in cuticular ridges
DMAPP	Dimethylallyl diphosphate
DOM	*Malus* x *domestica*
DTT	Dithiothreitol
ECH	Echidna
ECPGR	European Cooperative programme for plant genetic ressources
EDA4	Embryo sac development arrest 4
EF1	Elongation factor 1 alpha
EMBL	European Molecular Biology Laboratory
EST	Expressed Sequence Tag
EXP	Expansin
F3'H	Flavonoid-3'-hydrolase
F5H	Ferulate 5-hydroxylase
FACT	Fatty alcohol:caffeoyl-CoA acyltransferase
FAE	Fatty acid elongation complex
FAH1	F5H
FAM	Fluorescein
FAR	Fatty acyl-CoA reductase
FATB	Acyl-ACP thioesterase
FC	Fold change
FDR	False discovery rate
FHT	Feruloyl hydrocinnamoyl transferase
FHT	Fatty hydroxy acid/fatty alcohol hydroxycinnamoyl transferase
FLA	Fasciclin-like arabinogalactan

FNR	National Research Funds - Luxembourg
FPP	Farnesyl diphosphate
GA4+7	Gibberelic acid (4+7)
GAE1	UDP-glucuronate
GC-MS	Gas chromatography-Mass spectrometry
GDSL lipase	GDSL-motif esterase/lipase
GEO	Gene Expression Omnibus
GO	Gene Ontology
GPAT	Glycerol-3-phosphate acyl transferase
GUS	β-glucuronidase
Ha	Hectare
HCALDH	Hydroxycinnamaldehyde dehydrogenase
HCT	Hydroxycinnamoyl-CoA shikimate:quinate hydroxy-cinnamoyl-transferase
HEX	Phosphoramidite
IAA	Indole-3-acetic acid
ILR	IAA-amino acid hydrolase
IMPA9	Importin subunit alpha-9
INRA	National Institute of Agronomical Research
IPP	Isopentenyl diphosphate
IRX	Irregular xylem
KCS	Ketoacyl-CoA synthase
KEGG	Kyoto Encyclopedia of Genes and Genomes
LAC	Laccase
LACS	Long chain acyl-CoA synthetase
LCR	LACERATA
LCR	Fatty acid hydroxylase
LDOX	Lipoxygenase

LTL1	GDSL-motif esterase/lipase
LTP	Lipid transfer protein
LysoPL2	Lysophospholipase 2
M-MuLV	Moloney Murine Leukemia Virus
MAG	Monoacylglycerol
MdSHN3	*Malus* x *domestica* SHINE 3 transcription factor
Me-IAA	Indole-3-acetic acid methyl ester
MES	Methyl esterase
MIQE	Minimum information for publication of qPCR experiments
mRNA	Messenger ribonucleic acid
MVA	Mevalonic acid
MYB	Myeloblastosis transcription factor
NAC	NAC-domain transcription factor
NIST	National Institute of Standards and Technology
NMR	Nuclear magnetic resonance
NSAF	Normalized spectral abundance factor
OA	Oleanolic acid
OR	Malus orientalis
OSC	Oxidosqualene cyclase
p19	Cymbidium ringspot virus silencing inhibitor
PAL	Phenylalanine amonia lyase
PCR	Polymerase chain reaction
PDR4	ABCG32 transporter
PELPK	Pro-Glu-Leu|Ile|Val-Pro-Lys-motif hydroxyproline-rich protein
PME	Pectin methylesterase
PMEI	Pectin methylesterase inhibitor
PR5K	Receptor serine/threonine kinase

PRR	Pattern recognition receptors
PRX	Peroxidase
qPCR	Real-time polymerase chain reaction
QTL	Quantitative trait loci
RAE	Russeted apple exocarp
RD22	RESPONSE TO DEHYDRATION 22
RIN	RNA integrity number
RNA	Ribonucleic acid
RNA-Seq	RNA sequencing
ROX	6-carboxy-X-rhodamine
RPKM	Reads per kilobase transcript per million reads
RubisCO	Ribulose-1,5-bisphosphate carboxylase/oxygenase
RWP1	Reduced levels of wall-bound phenolics 1
SA	Salicylic acid
SI	Supporting information
SAND	Sand family protein
SANT	SANT protein domain
SEM	Scanning Electron Microscopy
SHN	SHINE: APETALA-domain transcription factor
SIEV	*Malus sieversii*
SMT	Cycloartenol-c-24-methyltransferase
SND	Secondary wall–associated NAC domain
SPAD	Suberin polyaliphatic domain
SPPD	Suberin polyphenolic domain
SQS	Squalene synthase
SRG	Senescence-related gene
SYL	*Malus sylvestris*

TAIR	The *Arabidopsis* information ressource
TCA	Trichloroacetic acid
TEM	Transmission electroscopy microscopy
TF	Transcription factor
TMSC	Trimethylchlorosilane
TOF	Time-of-flight
TPX	Thioredoxin peroxidase
TTP	Triterpene
UA	Ursolic acid
UGT	UDP-glucosyl transferase
UK	Uridylate kinase
UPGMA	Unweighted Pair Group method with Arithmetic Mean
UV	Ultraviolet
VLCFA	Very long chain fatty acid
WAE	Waxy apple exocarp
WAK	Wall-associated kinase
WBC11	ABCG11 transporter
WSD1	Wax ester synthase
XET	Xyloglucan endotransglycosylase

General introduction

I. The apple

Malus x *domestica* Borkh. (*M.* x *domestica*) or domesticated apple is one of the most consumed fruit in the world. This false fruit is particularly appreciated for its crunchiness, sweetness, bitterness and acidic taste but also for its easiness to be transported in the everyday life. Over centuries, apple has followed the human civilization through the folklore: Big Apple is the nick name of New York City, William Tell shot an apple on his son's head, etc. (Morgan and Richards 2003, Juniper and Mabberley 2006). The religion also used many times apple as a symbol. The Greek mythology relates on the Heracles hero who picked the golden apples off the Tree of Life in the Hesperides garden. In Biblical tales, apple symbolize the Adam and Eve's sin which was also massively represented in art with the dedicated iconography (Fig. 1-1).



Figure 1-1: 'Adam and Eve' by Peter Paul Rubens (1628-1629)

In addition to this, apple was also widely represented in art through number of still life paintings. More recently, the word 'apple' was heavily associated with the fame and the logo of the well-known computer company. Finally, in the 19th century and before the campaign promoting the benefits of eating five fruits or vegetables per day, apple was already associated with well-being and health with the famous sentence "An apple a day keeps the doctor away" (Juniper and Mabberley 2006).

A. Apple: genetic origins and domestication

M. x *domestica* is a deciduous species belonging to the *Rosaceae* family and the *Malus* genus. A common ancestor, called *Pyrae* gathers other genus such as *Pyrus*, *Sorbus* and *Cydonya*. The *Malus* genus includes four wild species with distinct location in the world. *Malus sieversii* Ledeb. originated from Central Asia, *Malus orientalis* Uglitzk. from the Caucasian regions (Turkey, Armenia, …), *Malus baccata* L. Borkh. from Siberia and South Asia, and finally *Malus sylvestris* L. Mill. 1768 in Western and Central Europe (Fig. 1-2). *Malus sieversii* has been identified as the main contributor of the domesticated apple genpool based on both phenotypic and genetic analysis data (Cornille *et al*. 2014). The first trace of apple domestication has been dated 4000 years ago in the Near Eastern, an era which followed the acquisition of the first grafting methods (3800 years ago, Cornille *et al*. 2012). Wild populations of *Malus sieversii* still occur in central Asia regions displaying strong variations in habit, height, fruit quality with some similarities with the *M. domestica* varieties (Morgan and Richards 2003, Cornille *et al*. 2012). The most important remaining populations are located in China and Kazakhstan, and more sporadically in Uzbekistan, Kirghizstan, Tajikistan, Turkmenistan and Afghanistan (Legay and André, pers. comm. In the frame of a LIST-FNR-FDA project (2012-2016), Cornille *et al*. 2014). Despite the fact that the ancestral *M. sieversii* population has not been clearly identified or disappeared over the years,

domesticated apples seemed to originate from the Tian Shan mountainous forest in China. The first domesticated apples were exported to Europe through the so-called Silk Road trading route, running from Asia to Western Europe (Morgan and Richards 2003, Juniper and Mabberley 2006).

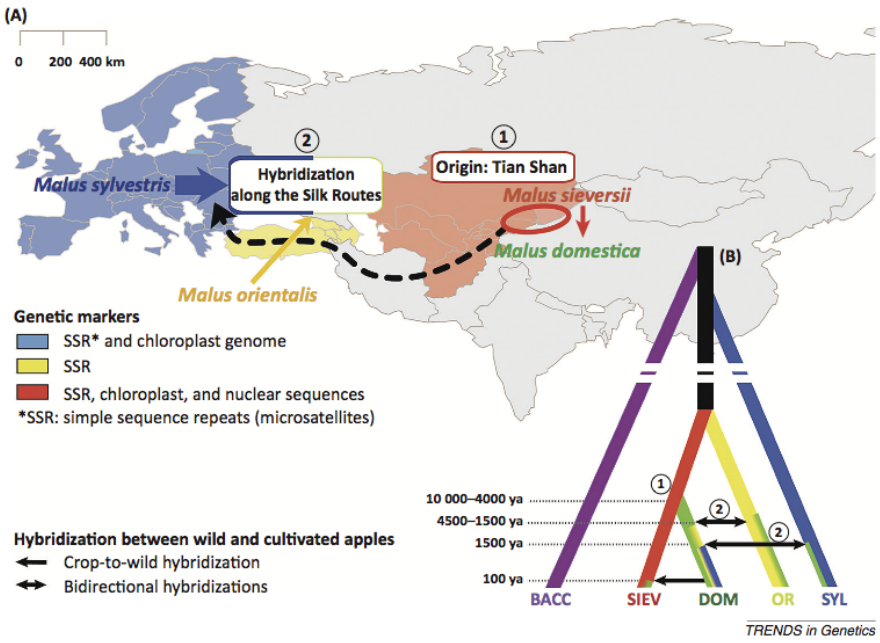

Figure 1-2: Evolutionary history of cultivated apples (from Cornille *et al.* 2014). (A) 1: Recent studies using molecular markers revealed that *Malus* x *domestica* is originated from the *Malus sieversii* forest of the Tian Shan region (China). 2: *M. sieversii* cultivars were dispersed along the Silk Route, favoring hybridizations and introgressions from Caucasian and European crabapples. (B) Genealogical relationship between wild and domesticated apples. Abbreviations: BACC, *Malus baccata*; DOM, *M. domestica*; OR, *Malus orientalis*; SIEV, *M. sieversii*; SYL, *Malus sylvestris*; ya, years ago.

Recent genetic studies showed that the genepool of domesticated apples was slightly modified along these long-way and long-lasting trading road through cross-hybridization with other endemic *Malus* species i.e. *Malus orientalis* or

Malus sylvestris, which are also wild descendent of the *M. sieversii* species. Thus, *M. domestica* can be considered as a domesticated *M. sieversii* with minor introgression of *M. orientalis* and/or *M. sylvestris* (Cornille *et al*. 2012, Cornille *et al*. 2014). Moreover, the recent sequencing of the *M. domestica* cv. Golden Delicious genome revealed more than 60,000 predicted contigs and an estimated size of 742 Mbases (Velasco *et al*. 2010). Pairwise comparison of the 17 chromosome sequences revealed an even more complex structure with an important redundancy between large segments of chromosomes i.e. 3 and 11, 5 and 10, 9 and 17, and 13 and 16 between shorter segments of chromosomes 1 and 7, 2 and 7, 2 and 15, 4 and 12, 12 and 14, 6 and 14, as well as 8 and 15. The haploid chromosome number in the majority of Rosacea species ranged from x=7 to x=9, whereas in the *Malus* ancestor called *Pyrae*, this number is x=17.

A first hypothesis postulated that *Pyrare* was a relevant example of allopolyploidization between species related to extant Spiraeoideae (x=9) and Amygdaleoideae (x=8) (Shulaev *et al*. 2008). However, the recent sequence analysis concluded that *Malus* x *domestica* Borkh. genome results from a duplication with rearrangement of the Pyrae ancestor genome (x=9), leading in 17 haploid chromosomes. For molecular biology analysis, this genome structure is a major concern as a large number of genes share high identity in sequence (97-99%) with their homologous copies and, of course, a high redundancy in the functions (Velasco *et al*. 2010).

B. Breeding, conservation, production and consumption

Domesticated apple cultivation has also improved over years of breeding and cultivation. The majority of the varieties (scion) are grafted on rootstocks which should be selected depending on the soil composition, the desired shape of the tree and blooming date or the variety characteristics (Morgan and Richards 2003, Janick 2005). As an example the rootstock choice alters the agronomical

properties of apple varieties. The M25 or M9 rootstock delays the blooming date by a few days while others are able to modify the alternate bearing phenomenon enabling regulated and optimized fruit production over the years. Depending on the precocity of each variety, apple blooming starts in early spring and is harvested in autumn. *M.* x *domestica* is a self-incompatible pollinator which obliges the use of at least two compatible varieties in an orchard (Janick 2005). The fruit diameter of commercial apples ranges between 8 and 12 cm. Production trees have a human compatible size (1,8- 3 m) with conducted branching and growth leading to an optimized yield, easiness in harvesting (which can be mechanized) and also lowered alternate bearing.

Apple production in 2013 in the world reached 81 million tons from 4.8 million Ha of cultivated area and constitutes one of the most important markets in fruit tree production (FAOSTAT). In 2012, the major apple producer was China followed by the United States, Turkey, Poland and India (FAOSTAT). France, Germany, Belgium and Luxemburg ranking respectively 10th, 14th, 39th and 85th. Apple is consumed in multiple forms i.e. raw, cooked, in beverage or derived alcohols. *M.* x *domestica* gathers over 7000 varieties due to its colossal breeding history (Morgan and Richards 2003, Janick 2005). A large majority of the apple germplasm is diploid (2n=34), but a significant number of triploid varieties and few tetraploids also occur. Old varieties are still produced in dedicated growing farms and maintained through amateur and/or associative collections such as the 'Jardin de Laquenexy in Lorraine, France', governmental institutions (Centre Wallon de Recherches Agronomiques in Belgium, INRA in France) and breeding companies. Over centuries, domesticated apples were selected for (i) higher productivity (i.e. fruit size, weight, number), (ii) fruit quality (i.e flesh firmness, fruit shape, color, acidity, sugar content, polyphenol content and conservation), (iii) easiness of the harvesting (i.e. tree size, growth orientation and more recently

mechanization-compliance), (iv) optimized agricultural practices (i.e. shorter juvenile phase, blooming synchronicity, pest and disease tolerance), (Laurens 1998, Morgan and Richards 2003, Juniper and Mabberley 2006). Despite its immense germplasm, only a few dozens of varieties are currently grown onto several rootstocks (Cornille, 2014). Indeed, since the last decades, marketing promotion and consumer's perception pushed more than ever towards the selection of "good looking" apples with standardized large size, nice-looking color, regular shape and absence of default at the skin surface, one of the best examples being the marketing development of the 'Pink Lady' variety. In order to provide, to consumers, fruits with no apparent defaults, the prevention and the curation of fungal and pest attacks became a crucial priority in fruit tree production. Indeed, major apple pathogens such as the apple scab (*Venturia inaequalis*) and powdery mildew (*Podosphaera leucotricha*) can irreversibly degrade the skin surface and lead to a significant part of the production to be downgraded or used in transformed products reducing its profitability.

II. Apple russeting

Beside the agronomic issues caused by pathogen pressure, a natural and well-known phenomenon called russeting is a major concern in apple fruit production. This rough, brown and corky phenotype, is constituted by multiple layers of dead (on the external side) and living (on the internal side) epidermal cells which have accumulated suberin in their primary cell walls. Russeting occurs in a large majority of the commercial apple varieties with strong variations in the fruit surface coverage. Russeted apples have not always been considered as improper for sale, old varieties such the 'Roxbury Russet' were previously well accepted by consumers (Faust and Shear 1972). But, with the time and changes in the habits of the consumers, the russet phenotype has been progressively considered as a

defect, thus becoming difficult to sale. Russeting can occur under multiple forms in apples. In modern and waxy varieties, a slight russeting area is localized at the calyx and around the stalk cavity (stem-end) of the fruit. Sometimes, little spots of russeting (lenticel) also appear on the whole surface of the fruit as observed in the 'Golden Delicious' variety. In semi-russeted varieties, such as 'Belle de Boskop' or the well-studied 'Cox Orange Pippin', russeting occurred in larger area (russet patch) going from the top to the bottom of the fruit (Fig. 1-3, Skene 1982). Finally, few, and usually old heritage varieties such as the 'Reinette du Canada Gris' or 'Patte de Loup' exhibit a heavier russeted phenotype covering the whole surface of the fruit. In extreme cases, russeting is also associated with skin cracks on the surface of the fruit (Fig. 1-3, Skene 1982).

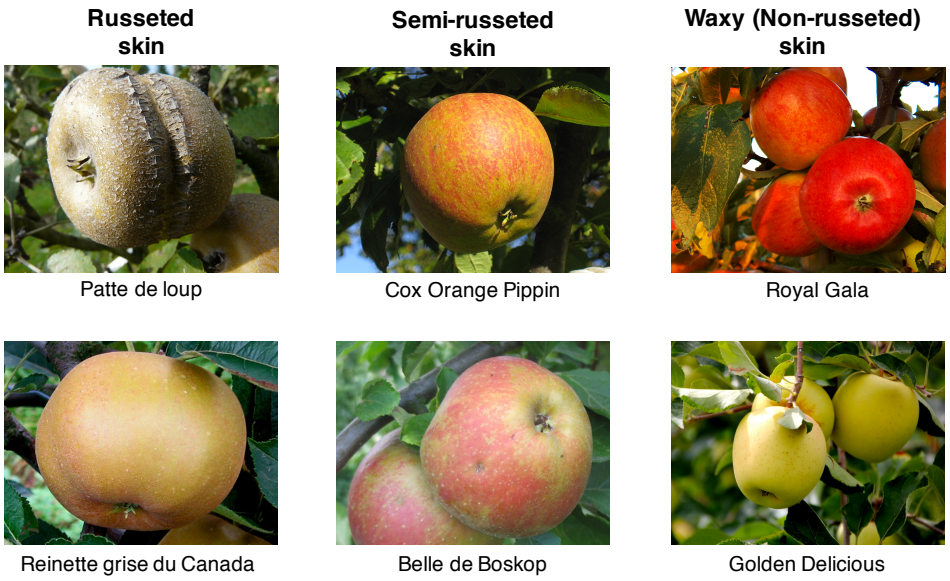

Figure 1-3: Examples of apple varieties displaying variable degree of russeting. Pictures were obtained from private and online collection databases (http://www.pomologie.com, http://croqueurs-national.fr).

The first relevant studies of the russet phenotype were published at the beginning of the 19th century and concluded that russeting starts in the epidermis of fruit (Walter 1967, Skene 1982). The occurrence of russeting in apple fruit has been linked with multiple causes including the genetic background of the variety and/or the biotic and abiotic pressure during fruit growth (Walter 1967). The state and the integrity of the cuticle and/or the viability of epidermal cells seems to be tightly associated with the appearance of russeting. Waxy apple exocarp is constituted by a thick cuticle associated with waxes inclusions covering the epidermal cell layer which protect the epidermal cells from the adverse effects of the environment (Walter 1967, Watanabe 1969). Histological studies revealed that russeted varieties displayed a thinner cuticle layer, compared to waxy varieties, which might result in a favored development of russeting. As an example, a recent study revealed that cuticle deposition, which is controlled by the MdSHN3 transcriptional regulator, was inversely correlated with the development of russeting in apple confirming that the thickness of the cuticle is a crucial factor involved in the occurrence of russeting (Fig. 1-4, Lashbrooke *et al*. 2015). Recently, a QTL mapping study, performed on apple population obtained from a cross between fully russeted and waxy parents, highlighted a transporter from the ATP-binding cassette subfamily G (ABCG11) as a major determinant of russeting occurrence. This gene is involved in the cuticle and waxes transport through the plasma membrane and might be defective or less expressed in russeted apples supporting again the tight relationship between the cuticle deposition and the russeting process (Falginella *et al*. 2015).

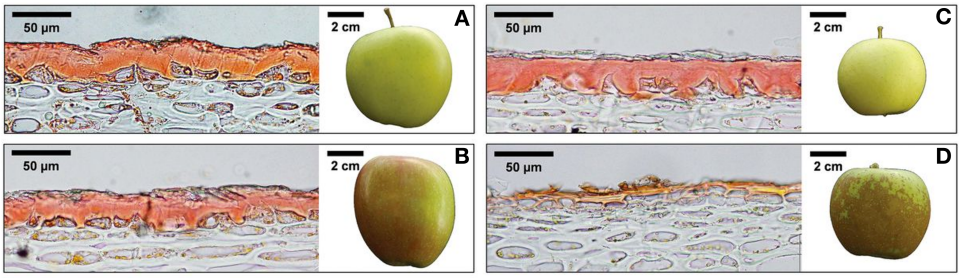

Figure 1-4: Comparison between skin phenotype and cuticle thickness in two progenies (C, D) obtained from a cross between the non-russeted parents 'Breaburn' (B) and 'Golden delicious' (A) (adapted from Lashbrooke *et al*. 2015). Cuticle observation of apple samples was performed with light microscopy with Sudan IV staining (Sudan IV stains cuticle lipids in pink/orange). 'Golden Delicious', 'Breaburn' and progeny C samples displayed the thick cuticle and a waxy skin. Inversely, progeny D displayed a thinner cuticle layer and a heavily russeted phenotype.

In addition, or, due to this thinner cuticle, apple fruits seemed to be particularly sensitive to russeting at the early stage of the fruit development (Faust and Shear 1972, Skene 1982, Knoche *et al*. 2011). The first signs appear after blooming, when the initiation of the fruit development triggers extreme tangential tensions due the massive division of the epidermal cells (Walter 1967, Khanal *et al*. 2013). During this process, microcracking occurs in the cuticle and can reach the epidermal cell walls (Fig. 1-5, Curry 2009). These damages and microcracking might trigger a wounding-like response which enhances the repairing mechanisms such as the initiation of the suberization (Sironval and Clijters 1962, Walter 1967, Faust and Shear 1972, Skene 1982). Moreover, later in the fruit development, some varieties display larger areas with a thinner cuticle layer which also lead to this microcracking phenotype. Recent studies using scanning electron microscopy (SEM) showed that cuticle microcracking can be limited after application of gibberellins (GA_{4+7}) which leads to a decreased russeting in Golden Delicious

(Curry 2012). The GA_{4+7} acts on the epidermal cells by decreasing their size, thus lowering tensions in the cuticle without any change in its chemical or physical properties (Knoche *et al*. 2011, Curry 2012).

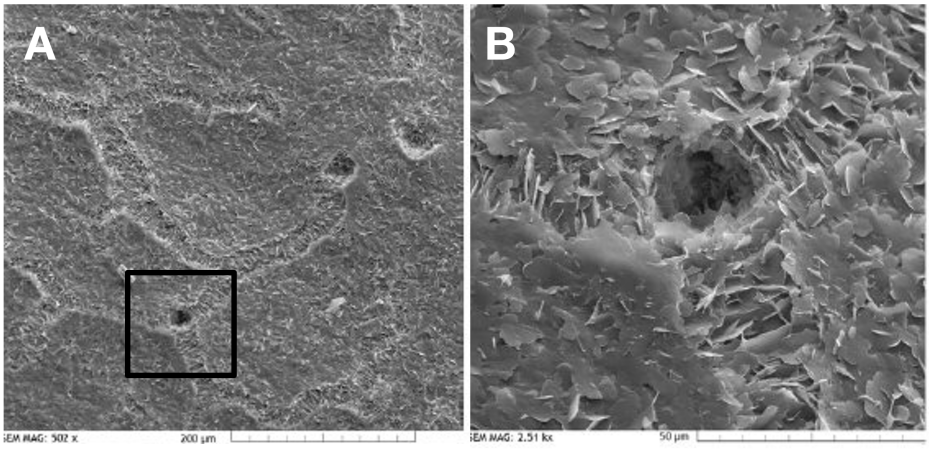

Figure 1-5: Epicuticular microcracking observed on the skin surface of 'Golden Delicious' at the harvesting date. Imaging was performed using SEM, A: 0,5 mm field displayed coverage and depth of the cuticle microcracking, B: enlarged view of a deep microcracking (adapted from Curry 2009).

The apple genetic background, which seems to be linked to the cuticle deposition, plays a crucial role in the occurrence of russeting, particularly in fully russeted apples. However, environmental and developmental factors can also trigger and/or enhanced the russeting appearance in waxy and semi-russeted apples (Sironval and Clijters 1962, Walter 1967, Faust and Shear 1972, Skene 1982, Knoche and Grimm 2008). As an example, biotic stresses such as the powdery mildew infection, are considered as an important cause of russeting. In such a case russeting might act not only as a healing process towards direct damages resulting from the infection, but also as a process limiting the progression of the pathogen (Faust and Shear 1972). Russeting can also occur without any particular biotic pressure. In this case, abiotic stress is usually the cause of russeting. As example,

optimal weather conditions during blooming and the early stage of the fruit development favor regular and shiny skin, whereas heavy rainfalls during the later stages before the harvest leading to an increased russeting in 'Cox Orange Pippin' (Walter 1967 and citations, Faust and Shear 1972). Moreover, the number of rainy days occurring during the fruit growth is correlated with the russeting level. In 'Golden Delicious', chilling temperatures during blooming predispose fruits to russeting. Another well-known russeting facilitating factor is relative humidity (Walter 1967 and citations, Skene 1982, Faust and Shear 1972). Indeed, long exposures to the high relative humidity favors the development of a thinner and/or lacunar cuticle layer which thus does not fulfill its protective role and leads to the initiation of phellogen formation (Tukey 1969, Faust and Shear 1972). Additionally, the controlled and localized moisture application on the apple skin surface also induces microcracking in the cuticle and probably supports the appearance of russeting (Knoche and Grimm 2008). Altogether, these data suggest that the thickness of the cuticle and thus the russeting occurrence might result from a combination of both the genetic background of the variety and the environmental conditions. Other agronomic factors such as the tree vigor and the rootstock also influence the russeting through the abundance of foliage (Faust and Shear 1972, Skene 1982). Solar radiation impacts the polymerization process of the cuticle leading to an abnormal structure which is more sensitive to microcracking. Thus, fruits grown in the shade of leaves are less susceptible to russeting (Faust and Shear 1972, Skene 1982). Mechanical injuries such as wounding trigger the initiation of suberization which can also be considered repairing phenomenon, as observed in response to biotic stresses. As an example, a high fruit number in a cluster increases the abrasion between the young fruits, in turn increasing the risk of russeting appearance. Spraying of phytochemicals also initiates russeting through its direct and indirect consequences on the cuticle

integrity and its toxic effect on epidermal cells (Sironval and Clijters 1962, Walter 1967, Faust and Shear 1972). In the 'Cox Orange pippin' variety, increased periodicity of the spraying leads to a significant increase of russeting occurrence. This phenomenon was induced by particularly aggressive substances; yet adjuvant composition such as detergent should also be considered (Sironval and Clijters 1962, Walter 1967). Altogether, we can assess that any genetic and/or environmental factors that has incidence on the normal fruit surface development, i.e. cuticle deposition and epidermal cell viability, might trigger, to a variable extent, russeting in apple.

III. Suberin in plants

A. The role of suberin in plants

As previously discussed, russeting is mainly caused by the deposition of suberin in the inner part of the primary cell walls of epidermal cells. This polyphenolic and polyaliphatic heteropolymer is able to drastically alter the physical and chemical properties of the plant tissue concurrently conferring new abilities. In plants, suberin is found in multiple tissues and usually acts as a protective barrier against environmental conditions limiting either water, solute and gas exchange, or ion diffusion (Franke and Schreiber 2007). As an example, suberin substantially accumulates in the bark of trees such as *Quercus suber* L. (Graça and Pereira 2000a) or *Betula pendula* as a result of intensive mitotic activity and noticeable production rate of suberized cells from the phellogen. In *Quercus suber* L., it is proposed that cork might result from an adaptation against fires since these trees are usually found in dry area regularly exposed to wildfires (Dantas and Pausas 2013). The suberization of cell walls also occurs after mechanical injuries in wounded tissues, as observed in apple fruits (Skene 1982) and it participates to

the leaf abscission (Graca 2015). Considering the important role of suberin in the physiology of the plant, its deposition has been widely investigated in the *Arabidopsis thaliana* roots but also in the *Solanum tuberosum* L. tubers (Graça and Pereira 2000b, Beisson *et al*. 2007, Baxter *et al*. 2009, Boher *et al*. 2013, Graca 2015). In potato tubers, a russeted skin phenotype, similar to those observed in apple, has been also linked to an enhanced suberin deposition. Suberization of the periderm is closely related to the tuber water content. Silencing of a feruloyl-acyl transferase gene, a key suberin synthesis gene, leads to an abnormal skin phenotype with a concomitant increased water loss (Serra *et al*. 2010). Potato russeting can also appear in response to drought, wounding, high salt stress or improper storage conditions (Ranathunge *et al*. 2011). In *A. thaliana*, suberin is a major component of the seed coat layer and seals off the micropyle region from the vascular tissues during its maturation (Molina *et al*. 2006). Suberin deposition also occurs in endodermal cells of roots where it regulates the water, solute and ion exchange thanks to the formation of suberin lamella and Casparian strips. Casparian strips have a lignin-like structure linked and organized with Casparian (CASP) proteins and suberin. Casparian strips are responsible for the junction between endodermal cells and limit the apoplastic transport together with the suberin lamella which is deposited in the primary cell wall (Schreiber 2010). Suberin deposition in roots increases the tolerance to many abiotic stresses such as waterlogging, heavy metal, drought and salinity exposure: it also reduces the pathogen susceptibility as observed in the russeted apples displaying improved tolerance against oidium (Skene 1982, Ranathunge and Schreiber 2011, Sousa *et al*. 2012, Vishwanath *et al*. 2015). In *A. thaliana* roots, the loss-of-function *horst/CYP86A1* mutant exhibits a reduction of 60% of the suberin content with a concomitant increased NaCl diffusion in the apoplast, suggesting that suberin plays a critical role in the regulation of mineral diffusion in roots (Ranathunge and

Shreiber 2011). Conversely, two mutants with increased suberin deposition in roots exhibited a reduced amounts of Mn, Zn or Ca in shoots (Ranathunge and Schreiber 2011). Overall, the role of suberin might be summarized as a defense mechanism acting as a rescue barrier against multiple stressors. In root, suberin controls the excessive diffusion of solute and minerals, in more external tissues such as periderms of fruits, it appears to act as a protective and/or healing barrier against the environment.

B. Suberin structure and composition

The first model postulated that suberin is an insoluble polyester polymer composed by cross-linked polyaliphatic (suberin polyaliphatic domain: SPAD) and polyphenolic (suberin polyphenolic domain: SPPD) domains (Bernards 2002) anchored in the primary cell wall (Fig. 1-6, Fig. 1-7). As methodologies enabling the direct analysis of the suberin in its polymerized form are not available, the structure and the spatial organization of suberin have been deduced from transmission electronic microscopy (TEM) and suberin monomer composition obtained after depolymerization and/or partial depolymerization coupled with different mass spectrometry techniques or Solid State ^{13}C NMR spectroscopy (Bernards *et al*. 1995, Graca and Pereira 2000a, Graca and Pereira 2000b, Nawrath 2002, Franke *et al*. 2005, Vishwanath *et al*. 2015, Graca 2015). Using transmission electronic microscopy (TEM), the suberin lamella displays a succession of alternated light and dark layers with different thickness, 3 nm and 7-10 nm, respectively. These layers corresponding to the aliphatic (light) and aromatic (dark) domains of the SPAD (Fig. 1-6, Fig. 1-7, Kosma *et al*. 2014).

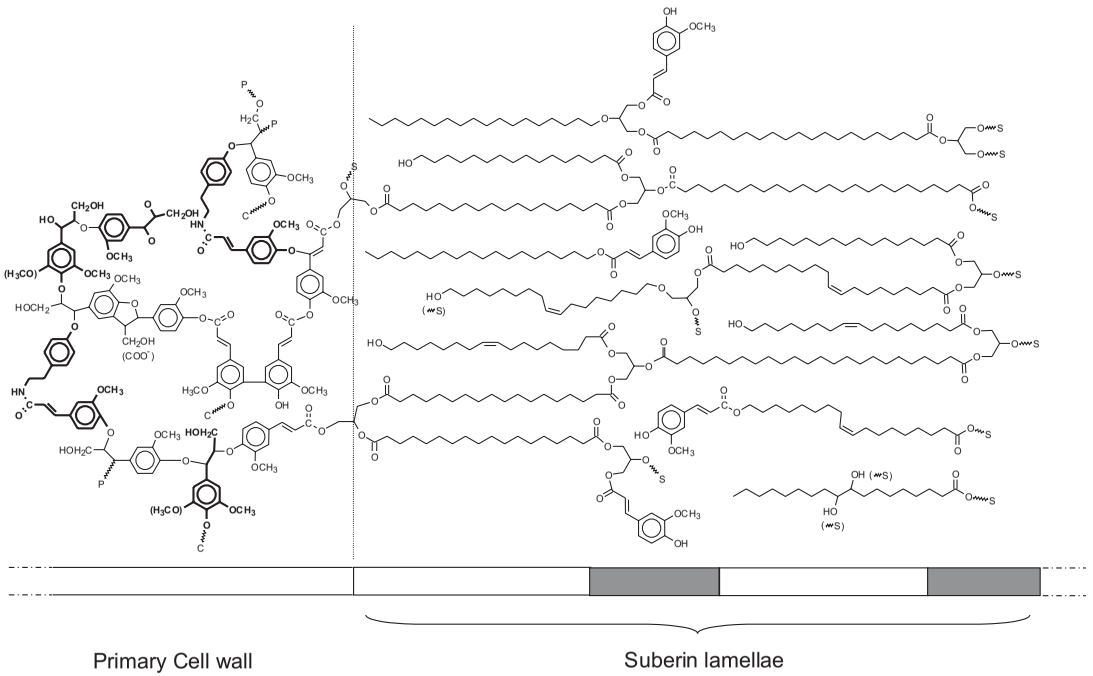

Figure 1-6: Suberin structure model proposed by Bernards (2002). On the left side: the lignin-like suberin polyphenolic domain, anchored in the primary cell wall, is constituted by hydroxycinnamoyl alcohols and hydroxycinnamic acids (ferulic acid). On the right side: the suberin polyaliphatic domain is constituted by ω-hydroxyacids and α,ω-dicarboxylic acids, fatty alcohols, glycerols, and ferulic acids esterified together in reticulated matrix. White and grey section of the suberin lamellae rely on the consecutive aliphatic and phenolic layers of the SPAD.

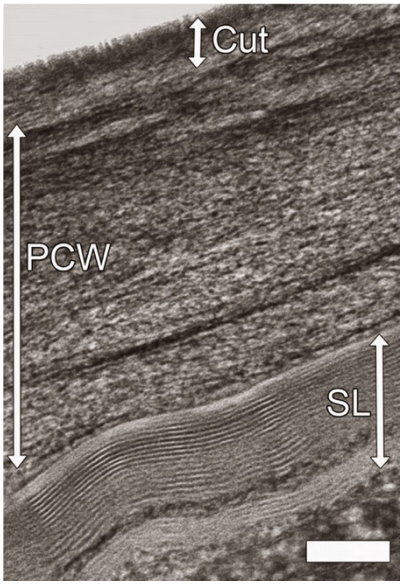

Figure 1-7: TEM of an *Arabidopsis* leaf overexpressing *AtMYB41*. AtMYB41 triggers the ectopic deposition of dark and light suberin layers (SL) in the primary cell wall (PCW). Cutin is deposited on the external side of the cell wall (adapted from Kosma *et al*. 2014).

Total transesterification of the suberin polymer showed that the SPAD is composed of long chain (C16 to C32) ω-hydroxyacids, α,ω-dicarboxylic acids, fatty alcohols, glycerol and ferulic acid (Fig. 1-8, Graça and Peirerra 2000a, Franke *et al*. 2005, Graça and Santos 2006). The ω-hydroxyacids and α,ω-dicarboxylic acids were found in saturated form as well as mid-chain (position 9-10) desaturated or oxygenated forms such as epoxidation or hydroxylation. SPAD is also non-covalently associated with variable amounts of non-polymeric waxes which confer the hydrophobic property to the suberin (Schreiber *et al*. 2005, Graca 2015). Partial depolymerization of the SPAD revealed several oligomeric structures such as (sn-1(-3)) and sn-2 monoacylglycerols of ω-hydroxyacids and α,ω-dicarboxylic acids (Graca and Pereira 2000a, Graca and Santos 2006),

multimeric glycerols esters of ω-hydroxyacids and α,ω-dicarboxylic acids, ω-hydroxyacids linked with ferulic acid and/or glycerol (Graca and Pereira 2000a, Graca and Santos, 2006).

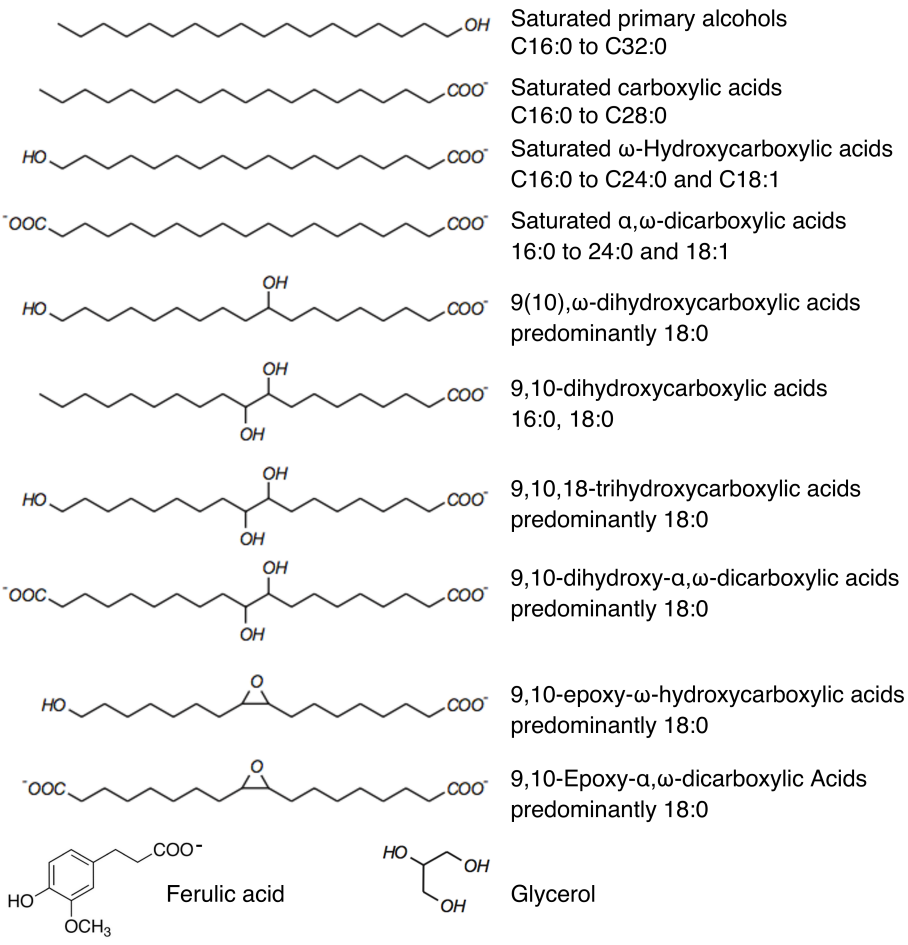

Figure 1-8: Aliphatic precursors of the SPAD found in suberized tissues (adapted from Bernards 2002).

The SPAD is considered as a poly(acylglycerol) polymer with a backbone constituted by α,ω-dicarboxylic acids esterified on both carboxyl groups with glycerols (Graca 2015). Remaining glycerol hydroxyl positions are esterified with ω-hydroxyacids, fatty alcohols with carbon chains organized in an aliphatic layer (Fig. 1-6). This highly hydrophobic layer is sandwiched by aromatic domains whose composition and structure remain unclear and might be ferulic acids esterified on glycerols (Bernards 2002, Molina 2009) or a more complex polyaromatic domain (Graca 2015, Fig. 1-9). It is interesting to notice that the SPAD displays some similarities with the cutin polymer, a major component of the cuticle, but cutin displays ω-hydroxyacids and α,ω-dicarboxylic acids with shorter chain (C16-C18), lower amount in α,ω-dicarboxylic acids and hydroxycinnamic acids (ferulic acid).

Analysis of the suberin phenolic components using solid state ^{13}C NMR spectroscopy reveals that the SPPD is anchored in the primary cell wall and contains a significant amount of monolignols and ferulic acid which appears to be polymerized as a lignin-like polymer structure (Bernards *et al*. 1995, Bernards 2002). In native and wound-induced suberized tissues of potatoes, ferulic acid amides, namely feruloyl tyramine and feruloyl octopamine, were also found but in an even lower amount compared to ferulic acid (Negrel *et al*. 1996). However, evidence of covalent links with the suberin backbone has not been established so far (Graca 2015). It is proposed that the SPPD acts as an interface between the SPAD and the cell wall (Bernards 2002, Graca 2015, Vishwanath *et al*. 2015). On the primary cell wall side, the SPPD is also covalently linked with carbohydrates while on the other side it is linked with the glycerol moiety of the SPAD (Bernard *et al*. 1995, Bernards 2002). However, there is still debate in the scientific community about the structure and the role of the SPPD with on one hand, authors arguing that SPPD can be considered as lignin because of the weak proportion of

hydroxycinnamic acids compared to the monolignols content (Graca 2015), and on the other hand, authors that suspect a real biological meaning of the modified structure of the SPPD compared to lignin (Bernards 2002, Vishwanath *et al*. 2015).

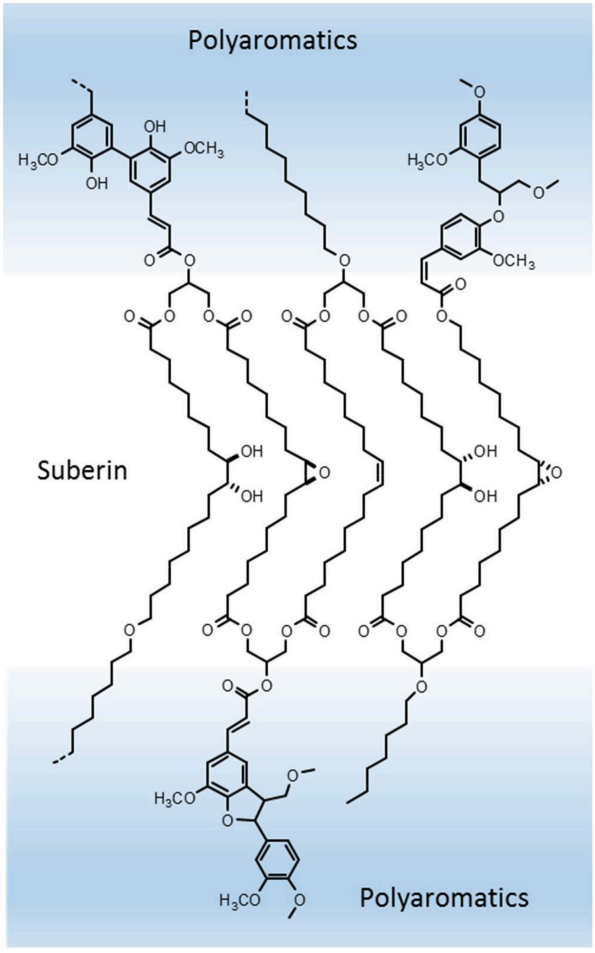

Figure 1-9: Model of suberin structure proposed by Graca (2015). The aliphatic domain of suberin is also composed by a reticular assembly of glycerol and α,ω-dicarboxylic acids, but it is inserted in between layers composed by multiple compounds i.e. tyramine, polymerized ferulate and alcohols.

Although the suberin structure seems to be quite conserved, its composition displays a strong diversity among plant species. This is particularly noticeable for the fatty composition of the SPAD which displays variations in the chain size of the fatty acids (Graça and Pereira 2000a, Franke *et al*. 2005, Ranathunge *et al*. 2011, Vishwanath 2015). In *Quercus suber* C22 and C24 ω-hydroxyacids, α,ω-dicarboxylic acids are predominant while a majority of C16-C18 chains is observed in *Pseudotsuga menziesii* (Graça and Pereira 2000a). In the potato tuber periderm, a large majority of 18:1 derived ω-hydroxyacids, α,ω-dicarboxylic acids was found with long chain alkanoic acids (C24-C28) (Graca and Pereira 2000b). Finally, variations in the fatty acid substitutions at the C9-C10 positions also occurred between species. In *Quercus suber* L., a specific accumulation of 9-epoxy-18-hydroxyocatadecanoic acids was observed (Graça and Pereira 2000a). However, since the identification of these specific forms remains a tough task, and the chemical standards are sorely lacking, care should be taken in the interpretation of the results related to these metabolites. It is noteworthy that, in *A. thaliana*, differential suberin composition has been observed between root and seed coat. Root suberin displayed a large majority of C16, C18:1 and C22 α,ω-dicarboxylic acids, whereas seed coat suberin showed longer chains (C22-C24), suggesting that the suberin monomer composition is also tissue specific and might reflect specific biological functions which have to be determined (Franke *et al*. 2005, Molina *et al*. 2006).

Due to the difficulty to isolate and identify each assembling metabolite, there might be some confusions between the SPPD and the aromatic domain of the SPAD compositions. Some authors considered that (i) the SPAD is suberin on its own and contains a succession of polyaliphatic domain (as described above) and polyaromatic domains mainly composed by ferulic acid, ferulic acid-derived

amines and (ii) the SPPD is a lignin component composed by mainly guaiacyl lignin (G-units) and a small part of ferulic acids (Graca 2015). Inversely, other models considered (i) the SPPD as a lignin-like polyaromatic domain, composed by monolignols and hydroxycinnamic acids (mainly ferulic acid) and (ii) the SPAD as consecutive layers of poly(acylglycerol) and ferulic acids (Bernards 2002). To summarize, the modeling of the suberin structure is a tough task. Different hypothetical models have been drawn from these findings with divergent points of view about the composition and structure of the aromatic domains of suberin (Bernards 2002, Graca 2015).

C. Suberin-associated waxes

As observed in the cuticle, suberized cell walls are non-covalently associated with waxes, which are embedded in the tight suberin network. Suberin-associated waxes have been described in suberized periderm of potato tuber, but also in roots of soybean, *Iris germanica*, *Camelina sativa* and *A. thaliana* (Thomas *et al*. 2007, Li *et al*. 2007, Schreiber 2010, Meyer *et al*. 2011). Suberin associated waxes play a particularly important role in the hydrophobicity of the suberized tissue, the poly(acylglycerol) being considered as the structural skeleton of suberin with lower physical and chemical properties (Schreiber 2010, Kosma *et al*. 2012, Vishwanath *et al*. 2015).

GC-MS analysis of the suberin-associated wax extracts, obtained after lipophilic extraction, displays significant amounts of long chain alkanes, primary alcohols, fatty acids, sterol derivates and alkyl-hydroxycinnamates, the latter reaching, in some cases up to 60% of the whole wax weight. Alkyl-hydroxycinnamates are conjugates synthesized from primary alcohols and hydroxycinnamic acids. They have been described in multiple tissues such as in the bark of *Acacia*, the potato tuber periderm, Arabidopsis mature tap roots, suberized fibers of *Gossypium hirsutum* (Bernards and Lewis 1992, Schmutz *et al*. 1994, Schreiber *et al*. 2005,

Freire *et al*. 2007, Kosma *et al*. 2012). Multiple forms have been observed across species. In *A. thaliana*, alkyl-hydroxycinnamates are mainly composed by alkyl-caffeate and alkyl-coumarate, while in potato a large majority of alkyl-ferulate was observed, reflecting putative differences in their biosynthesis pathway (Schreiber *et al*. 2005, Molina *et al*. 2009, Kosma *et al*. 2012).

In apple, cutin and suberin-associated waxes contain between 32 and 70% of pentacyclic triterpenes. This strongly differs from other model plants such as *A. thaliana,* for which waxes are usually composed by alkanes, ketones, primary and secondary alcohols but no triterpene (Panikashvili 2007, André *et al*. 2012). Pentacyclic triterpenes are secondary metabolites in fruit peel, leaves and bark (Jager *et al*. 2009). They are particularly studied for their anti-inflammatory and anti-tumoral properties (Jager *et al*. 2009, Laszczyk 2009). These C30 terpenes consist of six isoprene units and are produced from the cyclization of the 2,3-oxidosqualene (C30). In plants, up to 20 000 different triterpenes have been reported but three main triterpene series have so far been identified in apple: the oleane (β-amyrin, oleanolic acid), the ursane (α-amyrin, ursolic acid) and the lupane series (lupeol, betulinic acid)(André *et al*. 2016). The analysis of 109 apples varieties revealed that waxy and russet apples differentially accumulated these three triterpene series in fruit skin. In waxy apple skin, the ursane and oleane series were predominant whereas russeted exocaps displayed an increased accumulation of the lupane series of triterpenes (André *et al*. 2012). Furthermore, a recent study, comparing the russeted "Merton Russet" and the "Royal Gala" varieties, showed that russeted tissues also accumulate specific triterpene-hydroxycinnamate conjugates, the most abundant conjugate being the betulinic acid-3-trans-caffeate, followed by the betulinc acid-3-cis caffeate and the oleanolic acid-3-trans caffeate (André *et al*. 2013). Because they accumulate in the same tissues, it is tempting to associate alkyl-hydroxycinamates and

triterpene-caffeate synthesis because some of the enzymatic reactions producing these compounds might be similar (acyl CoA dependent transfer); nevertheless, the scientific community has currently no idea as to whether they share a common synthesis pathway or regulatory networks.

IV. Suberin biosynthesis

A. Synthesis of suberin monomer precursors

To date, in apple, no investigation has been published on the suberin biosynthesis pathway. Hence, suberin synthesis fundamentals are only available from the "model plants" *A. thaliana* and *S. tuberosum* L. for which a large part of the gene identification and functional characterization have been already performed. The first work aiming at unravelling the biosynthesis of suberin started in the end of the 70's with the work of Kolattukkudy and collaborators (Kolattukkudy *et al.* 1975, Espelie *et al.* 1980). Nonetheless, since the last decade, knowledge about the suberin biosynthesis has strongly improved. Enzymes involved in this complex metabolic cascade belong to two distinct metabolic branches, namely the lipid and phenylpropanoid biosynthetic pathways (Millar and Kunst 1997, Beneviste *et al.* 1998, Moire *et al.* 1999, Beisson *et al.* 2007, Molina *et al.* 2009, Serra *et al.* 2009a, Serra *et al.* 2009b, Serra *et al.* 2010).

The synthesis of the suberin lipid precursors is initiated in the plastids (Fig. 1-10). The fatty acid synthase complex produces the C16 and C18:1 fatty acyl-CoA, which are the main suberin monomers precursors. Fatty acyl-CoAs are then exported in the endoplasmic reticulum and their carbon chains are elongated through the action of ketoacyl-CoA synthase of the fatty acid elongation complex (FAE), to produce the typical long chain fatty acids observed in suberin. Few gene isoforms of the ketoacyl-CoA synthase (KCS) family have been identified in

Arabidopsis roots (AtKCS2 and AtKCS20) and potato periderm (StKCS6) which display different product specificity (Lee *et al*. 2009, Serra *et al*. 2009a). The *A. thaliana kcs2* or *kcs20* knock-out mutant leads to a decreased accumulation of C22 and C24 precursors, whereas the *kcs2*/*kcs20* double mutant shows a higher reduction in suberin monomers. Silencing of the *KCS6* exhibits a decreased accumulation of C28 suberin fatty acids while increased in C26 monomers is observed, suggesting that StKCS6 is involved in the elongation of the suberin monomers with aliphatic chain longer than 26 carbons.

The ω-hydroxylation of short (C16-C18) and long chain (>C20) acyl-CoA are processed by cytochromes P450 monoxygenases family 86 (CYP86). Some of these enzymes display affinities which depend on the chain size of their substrates. As an example, in *A. thaliana* roots, the analysis of the *horst* knock-out mutant of a cytochrome P450 CYP86A1 ω-fatty acid hydroxylase, indicates a 60% decreased accumulation of short chain (C16 and 18:1) ω-hydroxyacids with a concomitant decrease of α,ω-dicarboxylic in suberized tissues (Hofer *et al*. 2008). Inversely, in *Arabidopsis* roots and seed coat, the CYP86B1 mutant showed decreased amount of the long chain ω-hydroxyacids chain (>C20) (Compagnon *et al*. 2009). In *S. tuberosum* tuber periderm, silencing of the CYP86A33 gene, a CYP86A1 orthologous gene, leads to a decreased accumulation of C18:1 ω-hydroxyacids and α,ω-dicarboxylic acids (Serra *et al*. 2009b). The step leading to the mid-chain (carbon 9 and 10) modification (desaturation, dehydrogenation, epoxidation) of the ω-hydroxyacids into α,ω-dicarboxylic acids is not fully understood. It is speculated that other cytochrome P450 might be involved in this biological process but no clear evidence has been established yet.

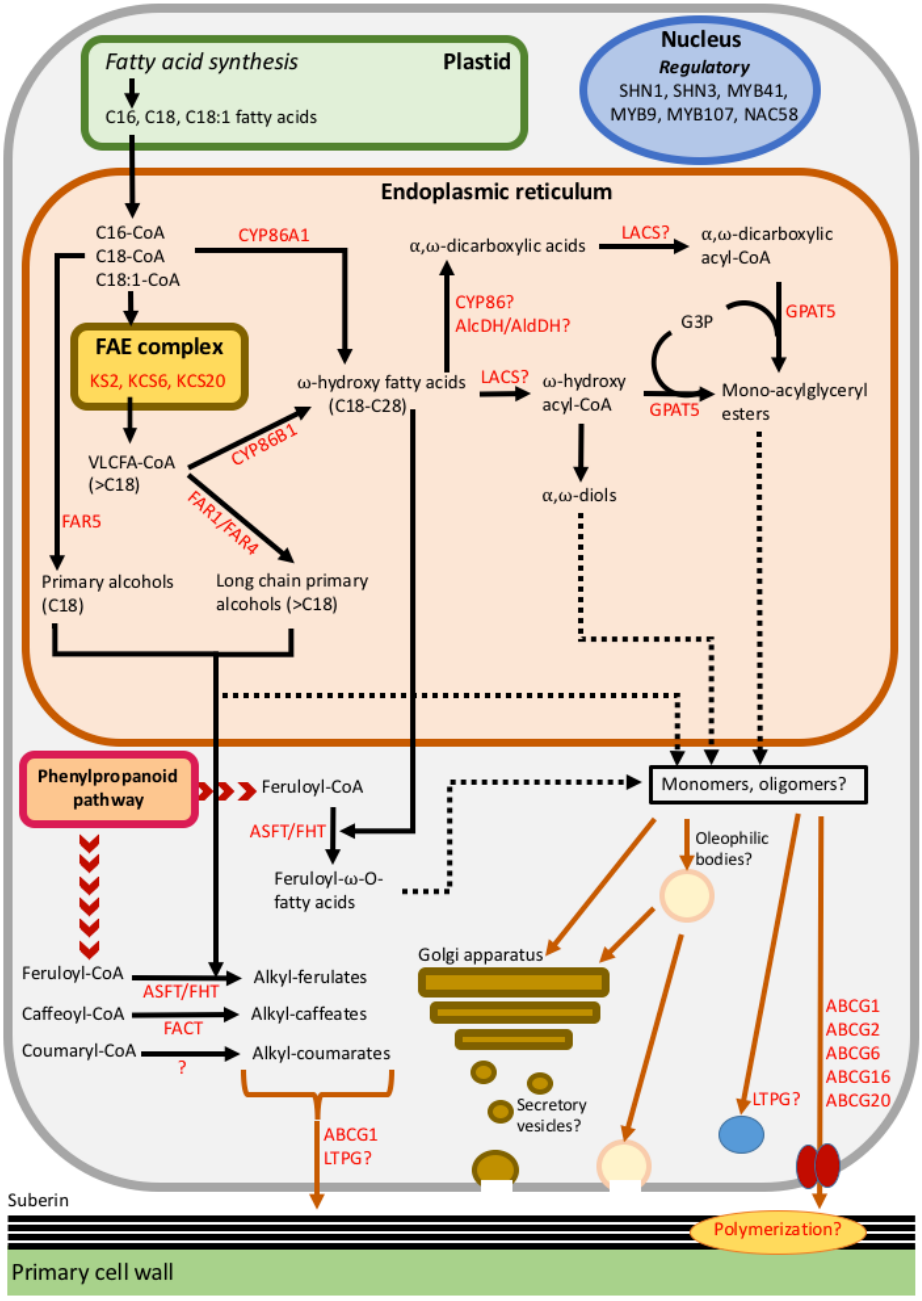

Figure 1-10 : see legend on the next page

Previous page: figure 1-10: Suberin biosynthesis pathway – lipid biosynthesis part (adapted from Franke *et al*. 2007, Li-Beisson *et al*. 2010, Li-Beisson *et al*. 2013, Vishwanath *et al*. 2015, previous page): KCS: 3-ketoacyl-CoA synthase, FAR: fatty acid reductase, CYP86A1: fatty acid hydroxylase, CYP86B1: very long chain fatty acid hydroxylase, AlcDH: alcohol dehydrogenase, AldDH: aldehyde dehydrogenase, LACS: long chain acyl-CoA synthetase, GPAT: glycerol-3-phosphate acyltransferase, ASFT: aliphatic suberin feruloyl transferase, FHT: feruloyl hydroxicinnamoyl transferase, FACT: fatty alcohol:caffeoyl-CoA acyltransferase, ABCG: ATP-binding cassette family G, LTP: lipid transfer protein. VLCFA: very long chain fatty acid.

The conversion of ω-hydroxyacids into α,ω-dicarboxylic acids is also under investigation, some authors proposed that the consecutive action of a ω-hydroxyacid dehydrogenase and ω-oxoacid dehydrogenase, with production of an aldehyde intermediate compound, might fulfil this step but no candidate genes has been found yet (Franke and Schreiber 2007). Another remaining open question is how ω-hydroxyacids and α,ω-dicarboxylic acids are activated prior to any further suberin monomer synthesis steps. Coenzyme A activation of fatty acids are usually performed by long chain acyl-CoA synthetase (LACS), but suberin specific LACS genes have not been identified yet (Vishwanath *et al*. 2015). In *A. thaliana*, the *LACS1* and *LACS2* genes displayed similar functions related to the activation of cutin specific ω-hydroxyacids and α,ω-dicarboxylic acids (Lü *et al*. 2009) and some authors speculate that LACS2 loss-of-function does not only influence the cutin monomer content but might also alter the suberin deposition in *Arabidopsis* roots (Vishwanath *et al*. 2015). Further gene expression profiling investigations might help to find new candidates being able to fulfil these unknown processes acting in the synthesis of ω-hydroxyacids and α,ω-dicarboxylic acids precursors.

Besides, primary alcohols are also important precursors of the suberin monomer (Graca 2015, Vishwanath *et al*. 2015). They are thought to be synthetized from different acyl-CoA precursors which have been synthetized at early or later stages of the ω-hydroxyacids and α,ω-dicarboxylic biosynthetic pathway described above. The reduction of acyl-CoA into primary alcohols is performed by the fatty acyl-coenzyme A reductase (FAR). In *A. thaliana* roots and seed coat, three FAR isoforms, inducible by NaCl exposure and wounding, have been associated with suberin deposition (Domergue *et al*. 2010). These display specific affinity regarding the chain size of the acyl-CoA precursors. Loss-of-function mutants of FAR genes show an altered composition in suberin. As an example, *far1*, *far4* and *far5* mutants exhibit a decreased accumulation of C22, C20 and C18 primary fatty alcohols, respectively. Inversely, in wound-induced suberized leaves, *far1* and *far5* do not shown any increase of C18-OH and C22-OH compared to wild type leaves, respectively. The *far1 far4 far5* triple mutant reduces by 70-80% the amount of primary alcohols in suberin. In addition to this, the *far* single, double and triple mutants also decrease, to a lower extent, the total amount of α,ω-diols, suggesting that other *FAR* genes are probably involved in the synthesis of these latter compounds, although no candidate has been identified yet (Domergue *et al*. 2010, Vishwanath *et al*. 2013, Vishwanath *et al*. 2015). Authors suggested the FAR5 acts on C18:0 acyl-CoA precursor directly after its export out of the plastids while FAR1 and FAR4 preferentially use long chain acyl-CoA as substrate, the latter being produced after the KCS-dependent elongation step. Despite the fact that alteration of the main suberin structure was not observed neither in the *far1*, *far4* and *far5* single mutants nor in the double or triple mutants, the decreased proportion of primary alcohols in the *A. thaliana* seed coat strongly increases the seed germination sensitivity to ABA, suggesting a major role of primary alcohols in the water and solute diffusion resistance of the suberin layer.

The suberin aromatic precursors are mainly represented by hydroxycinnamic acids, monolignols and hydroxycinnamic amide conjugates, which are synthesized via the phenylpropanoid pathway (Bernards 2002, Fraser and Chapple 2011, Graca 2015). Despite the high number of genes involved in the phenylpropanoid pathway already described, their position and involvement in this biosynthetic cascade is still under discussion (Vogt 2010, Fraser and Chapple 2011, Fig. 1-11). Suberin synthesis studies mostly focused on the synthesis of the aliphatic moieties of the suberin; consequently, the aromatic precursor synthesis has been deduced from the general phenylpropanoid biosynthetic pathway data (Bernards 2002, Graca 2015, Vishwanath *et al*. 2015). The phenylalanine is synthetized through the shikimate pathway and converted into *p*-coumaric acid via the consecutive action of the phenylalanine ammonia lyase (PAL) and the cinnamate-4-hydroxylase (C4H). The *p*-coumaric acid is then activated into *p*-coumaroyl-CoA by the 4-coumarate-CoA ligase (4CL). The *p*-coumaroyl-CoA is considered as the central metabolite which is further used as precursor of the synthesis of flavonoids, cutin, suberin, lignin, lignans to name a few (Fraser and Chapple 2011, Vogt 2010). The 4CL has been, for a long time, considered as a multi-substrate enzyme able to CoA activate number of hydroxycinnamic acid family members. However recent studies in *A. thaliana* demonstrated that the 4CL only acts on the *p*-coumaric acid, other hydroxycinnamic acids and monolignols being synthetized through a more complex pathway than previously described. Caffeoyl-CoA is synthesized from the *p*-coumaroyl-CoA via an intermediary shikimate-conjugated form produced by an hydroxycinnamoyl-CoA shikimate:quinate hydroxy-cinnamoyl-transferase (HCT). The *p*-coumaroyl moiety is then hydroxylated by the coumaroyl-shikimate 3'-monooxygenase (C3'H, CYP98A3) and released by the HCT to form the caffeoyl-CoA. The feruloyl-CoA, which the main aromatic suberin monomer precursor, is then

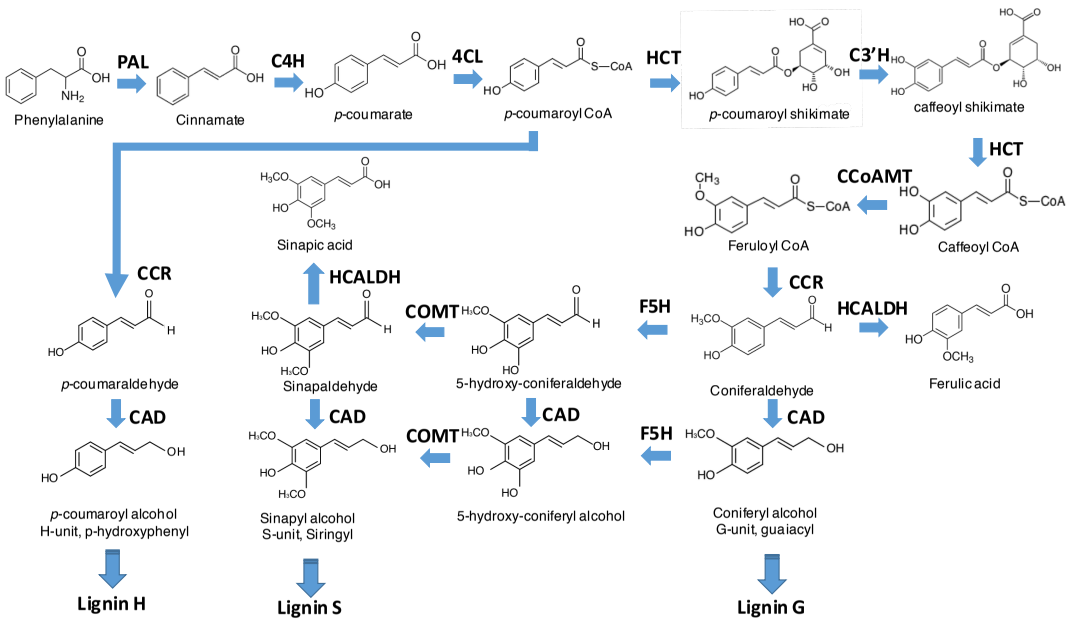

Figure 1-11: Suberin biosynthesis pathway - Phenylpropanoid biosynthesis part (adapted from Frazer and Chapple, 2011). PAL, phenylalanine ammonia-lyase; C4H, cinnamic acid 4-hydroxylase; 4CL, 4-coumarate-CoA ligase; HCT, hydroxycinnamoyl-coenzyme A shikimate:quinate hydroxycinnamoyl-transferase; C3'H, *p*-coumaroyl shikimate 3'-hydroxylase; CCoAOMT, caffeoyl-CoA 3-*O*-methyltransferase; CCR, cinnamoyl-CoA reductase; F5H, ferulate 5-hydroxylase; COMT, caffeic acid/5-hydroxyferulic acid *O*-methyltransferase; CAD, cinnamyl alcohol dehydrogenase; HCALDH, hydroxycinnamaldehyde dehydrogenase.

produced from the caffeoyl-CoA by the caffeoyl-CoA 3-O-methyltransferase (CCoAOMT). Recent researches on this latter enzyme has strongly impacted and revised the whole phenylpropanoid biosynthesis model, which previously restricted the aromatic ring and side-chain modifications to the hydroxycinnamates level (Fraser and Chapple 2011). The cinnamoyl-CoA reductase (CCR), which converts the hydroxycinnamoyl-CoA thioesters into hydrocinnamaldehydes, is the first step of the H, G and S lignin precursor synthesis (Fraser and Chapple 2011, Vogt 2010). This enzyme was first described as a multisubstrate enzyme. However, CCR genes isolated in *A. thaliana* showed a strong affinity for the feruloyl-CoA compared to the sinapoyl-CoA and caffeoyl-CoA, suggesting that feruloyl-CoA is preferentially used for the monolignol biosynthesis (Lauvergeat *et al.* 2001, Baltas *et al.* 2005). The resulting coniferaldehyde is hydroxylated and methylated by the ferulate 5-hydroxylase (F5H) and the caffeic acid *O*-methyl transferase (COMT) to form the 5-OH coniferaldehyde and the sinapaldehyde, respectively. The nomenclature of these two enzymes refers to the hydroxycinnamic acid family as they were previously considered using these substrates, but the very last model updates show that they act preferentially on the hydroxycinnamaldehydes and hydroxycinnamyl alcohols (Fraser and Chapple 2011). The final step of the monolignol synthesis is performed by the NADPH-dependent cinnamyl alcohol dehydrogenase (CAD) producing the coniferyl and sinapyl alcohols, which are G and S lignin precursors, respectively. In suberized pericarp of sand pear, the *CCR* and *CAD* genes display a decreased expression, compared to non russeted tissue, while a significant increase in lignin content can be observed. The authors speculate that a CCR/CAD independent pathway might compensate this decreased expression and explain this lignin accumulation (Wang *et al.* 2014). Another hypothesis might be that the lignin-like polymer, which composes the SPPD, is actually characterized by a

significant amount of hydroxycinnamic acids thus supporting a decrease in expression of the monolignol synthesis (Bernard *et al*. 2002).

B. Suberin monomers and hydroxycinnamate-conjugates biosynthesis

Monoacylglycerols are considered as the main and most abundant building block in suberin. This suberin monomer is synthesized by the glycerol-3-phosphate acyltransferase (GPAT), which catalyzes the transfer of a fatty acyl-CoA to a glycerol-3-phosphate with a concomitant release of phosphate and coenzyme A. In *Arabidopsis*, the GPATs family gathered more than two dozens of members with two main biological activities (Beisson *et al*. 2003, Li-Beisson *et al*. 2013). The sn-1 GPATs are mainly involved in the synthesis of storage and membrane glycerolipids, while the sn-2 glycerolipids are linked with the synthesis of cutin and suberin. As these two polymers share similar structure and precursors, the different sn-2 GPAT isoforms display selectivity against their substrate which determines the part of the polymeric structure, which they are dedicated to. The GPAT 4, 6 and 8 are bifunctional enzymes exhibiting both acyltransferase and phosphatase activity and present a higher affinity for the C16 and 18:1 ω-hydroxyacids compared to longer chain and α,ω-dicarboxylic; these enzymes have been associated with the cutin synthesis (Yang *et al*. 2010, Yang *et al*. 2012, Li-Beisson *et al*. 2013). Inversely, the *A. thaliana* GPAT5 loss-of function mutant shows drastic decreased amount of long chain (C22-C24) ω-hydroxyacids, α,ω-dicarboxylic and unmodified alkanoic acids in the seed coat and roots. In contrast with the cutin-specific GPAT, GPAT5 has no phosphatase activity and transfers acyl moieties on glycerol with a stronger preference for the sn-2 regioselectivity (Beisson *et al*. 2007). An additional GPAT7 isoform displaying similar activities compared to GPAT5, with an sn-2 regioselectivity and no phosphatase activity, was specifically induced by wounding. Overexpression of GPAT7 led to an

accumulation of long chain mono-acyl glycerols suggesting a specific role in suberin synthesis (Yang *et al*. 2012).

Hydroxycinnamoyl-ω-hydroxyacid and hydroxycinnamoyl-alcohol conjugates are also crucial monomers covalently and non-covalently linked to the suberin polymer, respectively (Fig. 1-10, Bernards 2002, Graca 2015, Molina and Kosma 2015). These metabolites are synthesized by enzymes from the BAHD acyltransferase superfamily, which displayed quite low identity in the amino acid sequence of their members but share distinctive consensus motifs, namely HXXXD and DFGWG motifs (D'auria 2006, Molina and Kosma 2015). Phylogenetic analysis of the HXXXD-motif/BAHD acyltransferase reveals five clades implicated in: clade I, the malonylation of phenolic glucosides; clade II, the very-long-chain fatty acid elongation; clades III and V, the volatile esters synthesis; and finally the clade IV, which gathers BAHDs responsible for the acethylation of amino groups to form amides and the transfer hydroxycinnamoyl and benzoyl-CoA (Kosma and Molina 2015). Loss-of-function mutants in *A. thaliana* roots and potato tuber periderm, always displayed an altered suberin structure regarding ferulate, but with variable impacts between species or tissues. This suggests that there might be multiple isoforms or slight variations in the function of these enzymes (Gou *et al*. 2009, Molina *et al*. 2009, Serra *et al*. 2010). An *Arabidopsis* loss-of function mutant of the feruloyl-CoA acyl transferase (*AtASFT*) displayed a significant decrease in ferulate, ω-hydroxyacids content (Fig. 1-10). However, the structure of suberin was not affected, suggesting that (i) ferulate esters are not crucial structural component of suberin compared to the glycerol and α,ω-dicarboxylic acids cross-linked backbone, (ii) other enzymes might be responsible for the covalent linkage of the ferulic acid to the glycerol, which ensures the integrity of the lamellar structure of suberin (Molina *et al*. 2009). In potato, the transfer of feruloyl-CoA onto the ω-hydroxyacid occurs in

the cytoplasm and is catalyzed the fatty ω-hydroxy acid/fatty alcohol hydroxycinnamoyl transferase (StFHT). StFHT displays differences in activity compared the *A. thaliana* orthologous gene. Loss-of-function mutant of the StFHT leads to a decrease of ferulic acid, ω-hydroxyacids and primary alcohols, suggesting that this enzyme is responsible for the formation of both feruloyl-ω-hydroxyacids and feruloyl-alkyls, which are components of the suberin polyester and suberin waxes, respectively (Schreiber *et al*. 2005, Serra *et al*. 2010). In *Populus*, the PtFHT (fatty acid hydroxycinnamoyl transferase) plays a role in the synthesis of feruloyl-ω-hydroxyacyls. Overexpression of the PtFHT increased the load of ferulate in both cutin and suberin and increased by 50% the seed germination rate and seedling establishment, reinforcing the potential role of hydroxycinnamic acids in the hydrophobicity and the permeability of the apoplastic barriers (Cheng *et al*. 2013). Finally, some BAHD acyl transferases do not participate at all in the synthesis of the suberin and cutin backbones. In *A. thaliana*, the fatty alcohol:caffeoyl transferase (FACT) synthesizes preferentially caffeoyl-alkyls from primary alcohols produced by the fatty acyl-CoA reductase (FAR1, FAR4 and FAR5), and caffeoyl-CoA (Fig. 1-10, Kosma *et al*. 2012). This enzyme did not display any acyl transfer activity when ω-hydroxyacids were used as substrates, suggesting it is specifically dedicated to the synthesis of the alkyl-hydroxycinnamates, which compose the suberin waxes (Kosma *et al*. 2012).

C. Cutin- and suberin-associated triterpene synthesis

Knowledge about pentacyclic triterpenes in apple fruit skin recently improved. The differential triterpene accumulation observed between waxy and russeted apples has been supported by functional validation studies of genes being involved in this biosynthetic pathway (Brendolise *et al*. 2011, Sawai and Saito 2011, André *et al*. 2012, André *et al*. 2016, Fig. 1-12). A number of these genes

has been identified these last years and some of them displayed a strong correlation in expression with the russeted trait, suggesting that this pathway might share common regulatory networks with the suberin synthesis pathway (Brendolise *et al*. 2011, André *et al*. 2016). The central precursor of the triterpene synthesis pathway is squalene, which is synthesized through the mevalonate pathway. Squalene is then converted into 2,3-oxidosqualene by the squalene epoxidase which is further ionized into the dammarenyl cation and used as substrate by the oxidosqualene cylase (OSC). According to the recent literature, several *OSC* genes have been already characterized displaying specificity in the series they produce and in their expression. MdOSC1 and MdOSC3 display strong identity in their amino acid sequence due to the genome duplication of the *Pyrae* ancestor and are more expressed in the waxy skin (Brendolise *et al*. 2011, André *et al*. 2016). Transient expression in *Nicotiana benthamiana* showed that MdOSC1 produces α-amyrin and β-amyrin in a 5:1 ratio, suggesting that this isoform is mainly involved in the synthesis of the ursane and oleane series which are predominant in the waxy apples (Brendolise *et al*. 2011, André *et al*. 2012). Recently, two additional OSC enzymes have been characterized in apple. MdOSC4 is able to produce an oleane-like triterpene (probably germanicol), some β-amyrin and lower amount of lupeol (ratio 82:14:4, respectively) whereas MdOSC5 produces lupeol and β-amyrin (ratio 95:5, respectively).

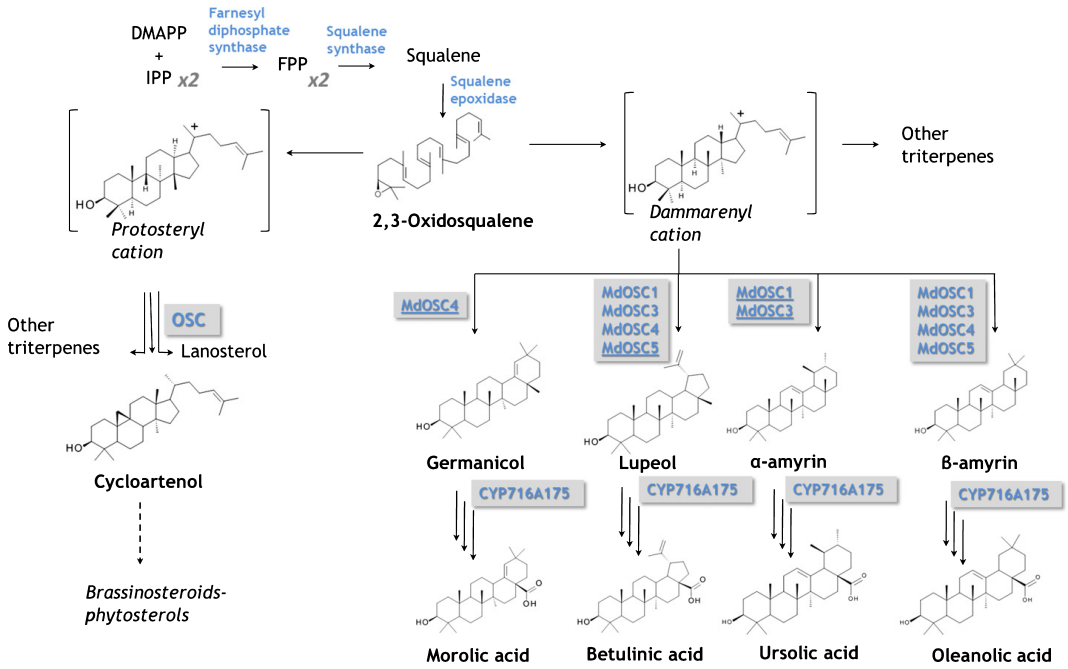

Figure 1-12: Biosynthetic pathway of triterpenic acids in apple (*M.* x *domestica*, adapted from André *et al.* 2016). Triterpenes are synthesized via the mevalonic acid (MVA) pathway. The enzymes that catalyze the various steps are indicated in blue. IPP, isopentenyl diphosphate; DMAPP, dimethylallyl diphosphate; FPP, farnesyl diphosphate; OSC, oxidosqualene cyclase; CYP450, cytochrome P450. MdOSCs are underlined when they catalyze the production of the specific triterpene considered as a major component. CYP716A175 catalyzes the three-step oxidation of triterpene backbones at the C-28 position.

Expression profiling of the genes shows that *MdOSC4* does not exhibit any correlation with the apple fruit skin phenotype whereas *MdOSC5* is highly expressed in the russeted apple suggesting that it might play a critical role in the suberin-associated waxes synthesis (André *et al*. 2016). The hydroxylation of the α-amyrin, β-amyrin, lupeol and germanicol into ursolic, oleanolic, betulinic and morolic acids (respectively) is catalyzed by a cytochrome CYP716 subfamily A175 (André *et al*. 2016). In plants, genes involved in the synthesis of triterpene-caffeate conjugates which accumulate in the suberin associated waxes have not been identified. As observed for the synthesis of alkyl-hydroxycinnamates, the synthesis of triterpene-caffeates might result from a catalytic reaction engaging a BAHD hydroxycinnamoyl-CoA transferase. A deep investigation of genes differentially expressed between russet and waxy skin apple fruits might answer part of this question.

D. Suberin monomers transport

As described above, suberin is anchored in the primary cell wall. The large and heterogeneous amount of metabolites, which is synthesized in the endoplasmic reticulum and the cytosol, has to be exported out of the cell. Despite the recent important progress made in the understanding of the suberin monomer and suberin associated waxes biosynthesis, it remains unclear how they are exported to the primary cell wall. Additionally, we still do not know whether suberin monomers are exported in their original forms, as described in the previous section, or if a preliminary polymerization process occurs before or during the export through the plasma membrane. Different hypothetical transport routes, which might be complementary, are currently envisaged (Fig. 1-10, Vishwanath *et al*. 2015). First, the suberin monomers synthesized in the endoplasmic reticulum might be transported through the secretory pathway via the Golgi derived secretory vesicles and/or oleophilic bodies. A recent study indicates that the export and deposition

of cuticle associated waxes is strongly down-regulated in the *A. thaliana gnl-1* and *ech* mutants. Echidna (ECH) is a crucial component of the secretory vesicle trafficking between the trans Golgi network and the plasma membrane whereas *gln-1* altered the formation of the COAT protein I in the retro-trafficking between the Golgi apparatus and the endoplasmic reticulum. These two mutants strongly decreased the wax load in a large number of metabolites such as primary and secondary alcohols, ketones, free fatty acids, aldehydes and alkanes (McFarlane *et al*. 2014). Despite the fact that suberin-associated waxes are mainly composed of alkyl-hydroxycinnamates, they also share similar compounds with the cutin, suggesting that the Golgi associated vesicles trafficking might also be involved in their transport but no clear evidence has supported this hypothesis so far. The second putative export route of suberin monomers and waxes involves ATP binding cassette family G (ABCG) transporters. Members of this transporter family have been first described to participate in the export of cuticle components. In *A. thaliana*, the *abcg11* loss-of-function mutant shows a significant decrease of alkanes composing the cuticle waxes (Bird *et al*. 2007). Several suberin associated ABCG transporters have already been described in model plants. In *S. tuberosum*, silencing of the ABCG1 transporter results in a drastic reduction in the long chain α,ω-dicarboxylic, ω-hydroxyacids, alkohols and alkanoic acids in the suberin polymer, whereas they increase in the free lipid extract (Landgraf *et al*. 2014). Moreover, suberin monomers such as feruloyl-ω-acyls and feruloyloxy fatty acid glycerol esters, or suberin associated alkyl-ferulates strongly accumulate in this fraction, suggesting that ABCG1 might transport preferentially the suberin monomers and suberin waxes components, the suberin monomers being further polymerized in the cell wall. In *A. thaliana* several *ABCG* genes co-expressed with suberin monomer biosynthetic genes such as *GPAT5* or *CYP86B1*, have been investigated. In roots, the triple mutant of the ABCG2, ABCG6 and ABCG20

transporters displays a similar altered suberin composition compared to ABCG1 in potato periderm. A decrease in C20 and C22 fatty acids, C18:1 ω-hydroxyacid and C22 alcohols was observed, suggesting that they are more specific to the suberin monomer transport (Yadav *et al*. 2014). In addition, a significant decrease of alkyl ferulates and caffeates but not alkyl coumarates was observed. Interestingly, this triple mutant also triggers an enhanced expression of the ABCG16 transporter, which might reflect a compensation process (Yadav *et al*. 2014). The single mutant does not display any phenotype or significant alteration of the suberin layer, suggesting an important redundancy in their function and a low specificity regarding the substrate of these three transporters (Yadav *et al*. 2014). The lipid transfer (LTP) protein constitutes the third hypothetical pathway suspected to be involved in the suberin components exportation trough the plasma membrane. The non-specific LTP (nsLTP), which are only found in plants are classified according to the amino acid sequence similarity of the central cavity which constitutes the binding site. LTP type G transporters are non-specific lipid transfer proteins presenting a GPI-anchor at the C-terminal region, which links the protein to the external side of the plasma membrane. Co-expression pattern analysis of LTPG highlighted three groups which are involved in the synthesis of cuticular waxes, suberin or sporopollenin. Among them, LTPG5, LTPG16 and LTPG20 seem to participate in the phenylpropanoid and suberin metabolism (Edstam *et al*. 2013). Analysis of the available *Arabidopsis* LTPG mutants revealed various phenotypes such as an increased seed coat permeability to many compounds or a decreased ω-hydroxyacid content in suberin, which confirms their putative involvement in suberin deposition. However, the substrate specificity and the transport mechanisms remain ambiguous and further analyses have to be performed to confirm this work (Edstam and Edqvist 2014).

E. Suberin polymerization

The final polymerization of the suberin monomers is still not fully understood. However, recent studies in the field of cuticle development in *Solanum lycopersicum* described a GDSL-motif esterase/lipase (CD1/GDSL1) which is able to perform the transesterification of monoacylglycerol monomers into a multimeric form similar to a polyglyceryl-acyl ester (Girard *et al*. 2012, Yeats *et al*. 2012). The *in vitro* polymerization using the *A. thaliana* orthologous gene of CD1, shows only a linear polymerization of the sn-2 10,16-dihydroxyacyl-glycerol, suggesting that there might be other actors which may be responsible for the reticulated structure of the cutin (Yeats *et al*. 2014). The cell wall-associated α/β-fold hydrolase protein, BODYGUARD (BDG), has been described as a major actor of the cutin synthesis in *Arabidopsis* (Kurdyukov *et al*. 2006). A loss-of-function mutant shows strongly impaired cutin formation in leaves and flowers whereas BDG overexpression leads to an enhanced cutin formation mainly due to an increased incorporation of C18 ω-hydroxyacid. Moreover, suberin deposition in roots is also altered by the BDG loss-of-function mutant, suggesting a shared function which is probably explained by the strong similarity between these two polymers (Jakobson *et al*. 2016).

The polyphenolic domain of suberin, which is anchored in the primary cell wall, has been considered as a lignin-like polymer and it has been for a long time speculated that its assembly might share similar mechanisms as oxidative-mediated processes which engage peroxidases and laccases. In potato, an anionic peroxidase, expressed in wounded suberized tissues, shows an unusual specificity for the hydroxycinnamic acids such as ferulic and caffeic acids compared to their corresponding hydroxycinnamyl alcohols. Inversely, the cationic peroxidase, which is also induced in wounded tissues, uses both families without any substrate specificity. The *in vitro* assay indicates that the anionic peroxidase is able to

synthesize a ferulic acid-based polymer, suggesting a potential involvement in the suberin synthesis (Bernard *et al*. 1999). Laccases have been also proposed to participate in the extracellular coupling of the phenylpropanoids, which leads to lignin synthesis (Ranocha *et al*. 2002). In cork tree (*Q*. *suber*), gene expression profiling of the cork differentiation revealed that a significant number of laccases was co-regulated with the suberin synthesis genes (Soler *et al*. 2007). As the SPPD shares some similarities with lignin, authors claimed that laccases might have a similar function dedicated to the suberin biosynthesis. In maize (*Zea mays* L.) roots, expression of a laccase gene (*ZmLAC1*) is strongly enhanced in response to NaCl stress. Authors suggested that, in response to this salt stress, ZmLAC1 might be involved in the lignification and suberization processes which occur during the Casparian strip formation, enabling the limitation of the diffusion of NaCl in roots (Liang *et al*. 2006).

V. Regulation of russeting and suberin deposition

Suberin deposition can be triggered by multiple stimuli including biotic and abiotic stresses as well as developmental factors, such as those inducing russeting in fruit trees such as apple or pears. To date little is known about the regulatory mechanisms which drive the deposition of suberin in apple and more generally in plants. Causes leading to suberization may cover a large panel of sensing and signaling cascades, nevertheless the early steps which regulate the suberin synthesis remain unclear. However, in the “Golden delicious” apple cultivar, a recent report shows that gibberellins are able to reduce russeting (Barandoozi and Talaie, 2009, Curry 2009, Knoche *et al*. 2011). In potato tubers, feruloyl transferase expression is enhanced by wounding and abscisic acid, whereas a

repression was observed in response to salicylic acid (Boher *et al*. 2013). Furthermore, a recent work showed that suberization of *A. thaliana* roots is regulated by both absissic acid and ethylene. Authors showed that root is able to selectively regulate the degradation of suberin in response to ethylene (Barberon *et al*. 2016). During the last decade, there was some progress in understanding the latest steps of the suberin-related gene regulation, most of them in the *A. thaliana* model plant. Few transcription factors have been described to be more or less closely linked with the suberin deposition. The first candidate transcription factors influencing the suberin deposition were the APETALA-domain transcription factors SHINE (SHN1, SHN2 and SHN3, Fig. 1-10). These transcription factors have been shown to regulate the cuticle deposition in the *A. thaliana* floral organs and have also been associated with the regulation of the suberin synthesis (Shi *et al*. 2011). More recently, QTL mapping performed on a waxy/russet segregating apple population revealed a SHN1-like transcription factor, MdSHN3, which positively regulates cuticle synthesis and prevent fruits from russeting occurrence (Lashbrooke *et al*. 2015). Other non-regulatory candidate genes, such as waxes and cutin synthesis genes have also been found in addition to *MdSHN3* supporting the crucial role of the cuticle state in the regulation of suberin synthesis, but direct suberin biosynthesis regulators have not been highlighted with this approach. The first suberin master regulator, AtMYB41, has been recently identified in *A. thaliana* (Fig 1-10). Overexpression of AtMYB41 in *A. thaliana* (stable transformation) or in *N. benthamiana* (transient expression) triggered the formation of a suberin lamellae in the primary cell wall of leaf cells (Kosma *et al*. 2014). Targeted genes expression profiling revealed that the ectopic accumulation of suberin is supported by the concomitant increased expression of several suberin biosynthetic genes which have been previously functionally characterized. This observation includes *FAR1*, *FAR4*, *FAR5*, *GPAT5*, *ASFT*, *KCS2*, *FACT*, *CYP86A1*

and *CYP86B1*. Few genes from the phenylpropanoid pathway (CAD and some peroxidase) displayed a significant increased expression which was confirmed by an increased total lignin content; yet, it is impossible to conclude whether this increase is associated to normal lignin or to the lignin-like SPPD synthesis. Finally, AtMYB41 does not alter the expression of the cutin and wax biosynthesis genes, suggesting that suberization of the epidermal cell walls does not influence the cuticle integrity. It is unquestionable that AtMYB41 triggers suberin deposition, but the study of its promoter using GUS reporter in *A. thaliana* roots shows that this transcription factor is not expressed under optimal growth conditions but is specifically expressed in the endodermis under NaCl and ABA treatments. In apple, since cuticle microcracking might be perceived as a stress in the fruit, it would be interesting to know if an *AtMYB41* orthologous gene is implicated in the suberization process or if alternative transcription factors are involved in this process under normal developmental conditions.

Additional transcription factors have been found these last months. In *A. thaliana*, MYB9 and MYB107 have been identified as regulators of the suberin deposition during the seed development (Lashbrooke *et al*. 2016). The *myb107* and *myb9* loss-of-function mutants showed decreased levels in both aliphatic and aromatic suberin constituents as well as decreased contents in suberin-associated waxes. Finally, in *S. tuberosum,* silencing of *StNAC103 (A. thaliana NAC58* ortholog*)* resulted in increased contents in wax alkanes and suberin monomers such as ω-hydroxyacids, α,ω-dicarboxylic acids and primary alcohols (Verdaguer *et al*. 2016). This was supported by the enhanced expression of *CYP86A33* (orthologous gene *of AtCYP86A1*), feruloyl-hydroxycinnamoyl transferase (*FHT*) and *ABCG11*. However, the authors explained that further work should be performed to better identify the different targets of StNAC103. Finally, *StNAC103*

expression is triggered by wounding and ABA treatment in roots, tuber flesh and leaves, suggesting that its regulation might be similar to *AtMYB41*.

Objectives

Due to the relative commercial importance of the apple fruit production, apple russeting has been and still is widely studied at the agronomical, histochemical and biomechanical levels. The different environmental causes triggering the suberin deposition have now been well characterized, but the cellular mechanisms, e.g. genes, which are involved in this phenomenon, are still poorly understood. The cuticle integrity has been many times cited as a key factor interacting with the suberin deposition process. After discussions with some apple russeting and cuticle microcracking specialists (Pr Knoche and colleagues, Hannover University), one of the key issues is to understand whether a degraded and/or weak cuticle directly triggers the suberin synthesis or if the cell wall mechanical damages resulting from the extreme surface tensions during the fruit development trigger the suberin synthesis, limiting the cuticle development and increasing the microcracking. The suberin-related data in model plants, such as in *A. thaliana* roots or *S. tuberosum* tubers, provided only few answers on the role of the cutin in the suberization process because of the strong difference existing in the considered tissues and organs. Knowledge about the suberin composition, structure and biosynthetic pathway has widely improved in the last years, providing reliable basis and references enabling an easier design of the apple skin suberization model. Still, some key points remain undetermined. Among them, a strong debate still exists about the suberin structure in plants hindering the interpretation of some results and a proper representation of the suberin model. Knowledge about the enzymes involved in the final polymerization stages is still partial or hypothetical. The complex structure of the suberin and the difficulty to perform *in vitro* assays due the lack of suberin-like precursors available in the

market, increase the difficulties to functionally characterize these candidate enzymes. Finally, the recent discovery of the regulation of the suberin deposition only provides a partial answer and additional key regulators are undoubtedly involved in the suberization process.

From a more applicated and biotechnological point of view, research in the field of suberin is also crucial for the development of new biomaterials. In the next decades, the reduced fossil resources, the growing interest in renewable resources as well as recent legislations on improved waste and carbon footprint management will lead the world to face a drastically expanding demand for plant-based biomaterials and biofuels. Indeed, plants constitute the most promising alternative source of biopolymers in terms of chemical diversity and production capabilities. Numerous products have already been developed based on plant biopolymers such as starch, rubber, proteins, cellulose or pectins and scientific efforts have focused on the structure, the biosynthesis and the alteration of the chemical properties of these compounds to provide advanced biomaterials to the industry. However, despite the drastic progress made in this emerging industrial sector, a significant part of the available plant biopolymers, such as hemicellulose, lignin, and cutin, remains under-used (van Beilen and Poirier, 2007, Gandini 2008, Furtado 2014). Compared to these carbohydrate-based polymers, suberin is particularly interesting for its hydrophobic properties and might be used as a new plastic material or for surface coating applications. Long chain fatty acids and rare epoxydized fatty acids are particularly interesting for the synthesis of new biomaterials such as polyurethanes or polyols (Gandini 2008). Suberin-rich residues can be profusely obtained from the by-products of forest industry. In Portugal, cork production from *Q. suber* represents a potential source of 16 000 tons per year of suberin monomers (Gandini 2008), whereas birch (*Betula pendula*) pulp mills in Nordic countries can generate 28 000 tons/year of suberin-

rich residues (Sousa *et al*. 2011). Nondestructive, environmental friendly and cost effective depolymerization/extraction methods are currently under development to valorize these by-products. Increasing the knowledge on the suberin synthesis will open new perspectives in the field of cork tree breeding, industrial metabolite production using fermenters or new biomaterial engineering using white biotechnologies.

The current project aims at drawing, using an integrative biology approach and bioinformatic analysis, a model including all major players involved in the regulation of russeting and the biosynthesis of suberin in apple. First, in order to determine the genes involved in the russeted phenotype, a bulk-transcriptomic analysis using RNA-Seq was performed between two groups of varieties differing according to their waxy/russet phenotype; the purpose is to lower the genetic specificity of each variety in order to build a clear initial representation of the gene pool involved in the russet phenotype. Second, the suberin, cutin and wax composition of russeted and non-russeted tissues obtained from the 'Cox Orange Pippin' semi-russeted variety was investigated using GC-MS analysis. This was supported by a targeted gene expression profiling of genes being involved in their respective biosynthetic pathways. In a third part, the growth kinetics of two closely related varieties ('Reinette du Canada Grise' and 'Reinette du Canada Blanche') with contrasting phenotypes were investigated. A particular importance was given to the early and late developmental stages of the fruit concerning the expression of lipid metabolism-related genes and to the coordination of the different metabolic processes observed in the previous parts. For this purpose, an integrative biology was performed combining whole transcriptomic and proteomic approaches. Bioinformatic investigations achieved in the three first experiments provided new insights with reference to regulatory networks putatively involved in the russet phenotype. Among the large number of

regulatory elements found in these datasets, the MYB-family transcription factors emerged to play a specific role in our research topic. Finally, a member of this MYB-family, MYB93, was deeply investigated and functionally characterized.

References

Andre CM, Greenwood JM, Walker EG, Rassam M, Sullivan M, Evers D, Perry NB, Laing WA. 2012. Anti-inflammatory procyanidins and triterpenes in 109 apple varieties. *Journal of Agricultural Food Chemistry* **60**: 10546-10554.

Andre CM, Larsen L, Burgess EJ, Jensen DJ, Cooney JM, Evers D, Zhang J, Perry NB, Laing WA. 2013. Unusual immuno-modulatory triterpene-caffeates in the skins of russeted varieties of apples and pears. *Journal of Agricultural Food Chemistry* **61**: 2773-2779.

Andre CM, Legay S, Deleruelle A, Nieuwenhuizen N, Punter M *et al.* 2016. Multifunctional oxidosqualene cyclases and cytochrome P450 involved in the biosynthesis of apple fruit triterpenic acids *New Phytologist* **211**: 1279-1294.

Baltas M, Lapeyre C, Bedos-Belval F, Maturano M, Saint-Aguet P, Roussel L, Duran H, Grima-Pettenati J. 2005. Kinetic and inhibition studies of cinnamoyl-CoA reductase 1 from *Arabidopsis thaliana*. *Plant Physiology and Biochemistry* **43**: 746-753.

Barandoozi FN, Talaie A. 2009. The effect of gibberellins on russeting in golden delicious apples. *Journal of Horticulture and Forestry* **1:** 061-064.

Barberon M, Vermeer JE, De Bellis D, Wang P, Naseer S *et al.* 2016. Adaptation of Root Function by Nutrient-Induced Plasticity of Endodermal Differentiation. *Cell* **164**: 447-459.

Baxter I, Hosmani PS, Rus A, Lahner B, Borevitz JO, Muthukumar B, Mickelbart MV, Schreiber L, Franke RB, Salt DE. 2009. Root suberin forms an extracellular barrier that affects water relations and mineral nutrition in *Arabidopsis*. *PLoS Genetics* **5**: e1000492.

Beisson F, Koo AJK, Ruuska S, Schwender J, Pollard M *et al.* 2003. Arabidopsis genes involved in acyl lipid metabolism. A 2003 census of the candidates, a study of the distribution of expressed sequence tags in organs, and a web-based database. *Plant Physiology* **132**: 681-697.

Beisson F, Li Y, Bonaventure G, Pollard M, Ohlrogge JB. 2007. The acyltransferase GPAT5 is required for the synthesis of suberin in seed coat and root of *Arabidopsis*. The *Plant Cell* **19**: 351-368.

Benveniste I, Tijet N, Adas F, Philipps G, Salaun JP, Durst F. 1998. CYP86A1 from *Arabidopsis thaliana* encodes a cytochrome P450-dependent fatty acid omega-hydroxylase. *Biochemical and Biophysical Research Communications* **243**: 688-693.

Bernards MA. 2002. Demystifying suberin. *Canadian Journal of Botany* **80**: 227-240.

Bernards MA, Fleming WD, Llewellyn DB, Priefer R, Yang X, Sabatino A, Plourde GL. 1999. Biochemical characterization of the suberization-associated anionic peroxidase of potato. *Plant Physiology* **121**: 135-145.

Bernards MA, Lewis NG. 1992. Alkyl ferulates in wound healing potato tubers. *Phytochemistry* **31**: 3409–3412.

Bernards MA, Lopez ML, Zajicek J, Lewis NG. 1995. Hydroxycinnamic acid-derived polymers constitute the polyaromatic domain of suberin. *Journal of Biological Chemistry* **270**: 7382-7386.

Bird D, Beisson F, Brigham A, Shin J, Greer S, Jetter R, Kunst L, Wu X, Yephremov A, Samuels L. 2007. Characterization of Arabidopsis ABCG11/WBC11, an ATP binding cassette (ABC) transporter that is required for cuticular lipid secretion. *Plant Journal* **52**: 485-498.

Boher P, Serra O, Soler M, Molinas M, Figueras M. 2013. The potato suberin feruloyl transferase FHT which accumulates in the phellogen is induced by wounding and regulated by abscisic and salicylic acids. *Journal of Experimental Botany* **64**: 3225-3236.

Brendolise C, Yauk YK, Eberhard ED, Wang M, Chagne D, Andre C, Greenwood DR, Beuning LL. 2011. An unusual plant triterpene synthase with predominant alpha-amyrin-producing activity identified by characterizing oxidosqualene cyclases from *Malus* x *domestica*. *The FEBS Journal* **278**: 2485-2499.

Cheng AX, Gou JY, Yu XH, Yang H, Fang X, Chen XY, Liu CJ. 2013. Characterization and ectopic expression of a Populus hydroxyacid hydroxycinnamoyltransferase. *Molecular Plant* **6**: 1889-1903.

Compagnon V, Diehl P, Benveniste I, Meyer D, Schaller H, Schreiber L, Franke R, Pinot F. 2009. CYP86B1 is required for very long chain omega-hydroxyacid and alpha, omega-dicarboxylic acid synthesis in root and seed suberin polyester. *Plant Physiology* **150**:1831-1843.

Cornille A, Gladieux P, Smulders MJM, Roldán-Ruiz I, Laurens F, *et al.* 2012. New insight into the history of domesticated apple: secondary contribution of the european wild apple to the genome of cultivated varieties. *PLoS Genetics* **8**: e1002703.

Cornille A, Giraud T, Smulders MJ, Roldán-Ruiz I, Gladieux P. 2014. The domestication and evolutionary ecology of apples. *Trends in Genetics*. **30**: 57-65.

Curry EA. 2009. Growth-induced microcracking and repair mechanisms of fruit cuticles. *Proceedings of the SEM annual conference*.

Curry EA. 2012. Increase in epidermal planar cell density accompanies decreased russeting of 'Golden Delicious' apples treated with Gibberellin A_{4+7}. *Hortscience* **47**: 232-237.

D'Auria JC. 2006. Acyltransferases in plants: a good time to be BAHD. *Current Opinion in Plant Biology* **9**: 331-340.

Dantas VD, Pausas JG. 2013. The lanky and the corky: fire-escape strategies in savanna woody species. *Journal of Ecology* **101**: 1265-1272.

Domergue F, Vishwanath SJ, Joubes J, Ono J, Lee J *et al.* 2010. Three Arabidopsis fatty acyl-CoA reductases, FAR1, FAR4, and FAR5, generate primary fatty alcohols associated with suberin deposition. *Plant Physiology* **153**:1539-1554.

Edstam MM, Blomqvist K, Eklöf A, Wennergren U, Edqvist J. 2013. Coexpression patterns indicate that GPI-anchored non-specific lipid transfer

proteins are involved in accumulation of cuticular wax, suberin and sporopollenin. *Plant Molecular Biology* **83**: 625-649.

Edstam MM, Edqvist J. 2014. Involvement of GPI-anchored lipid transfer proteins in the development of seed coats and pollen in *Arabidopsis thaliana*. *Physiologia Plantarum* 152: 32-42.

Espelie KE, Sadek NZ, Kolattukudy PE. 1980. Composition of suberin-associated waxes from the subterranean storage organs of seven plants, parsnip, carrot, rutabaga, turnip, red beet, sweet potato and potato. *Planta* **148**: 468-476.

FAOSTAT: faostat.foa.org

Falginella L, Cipriani G, Monte C, Gregori R, Testolin R, Velasco R, Troggio M, Tartarini S. 2015. A major QTL controlling apple skin russeting maps on the linkage group 12 of 'Renetta Grigia di Torriana'. *BMC Plant Biology* **15**: 150.

Faust M, Shear C. 1972. Russeting of apples, an interpretative review. *HortScience* **7**: 233-235.

Franke R, Briesen I, Wojciechowski T, Faust A, Yephremov A, Nawrath C, Schreiber L. 2005. Apoplastic polyesters in *Arabidopsis* surface tissues - a typical suberin and a particular cutin. *Phytochemistry* **66**: 2643-2658.

Franke R, Schreiber L. 2007. Suberin - a biopolyester forming apoplastic plant interfaces. *Current Opinion in Plant Biology* **10**: 252-259.

Fraser CM, Chapple C. 2011. The phenylpropanoid pathway in Arabidopsis. *Arabidopsis Book* **9**: e0152.

Freire CSR, Silvestre AJD, Neto CP. 2007. Demonstration of long-chain n-alkyl caffeates and delta7-steryl glucosides in the bark of Acacia species by gas chromatography-mass spectrometry. *Phytochemical Analysis* **18**: 151–156.

Furtado A, Lupoi JS, Hoang NV, Healey A, Singh S, Simmons BA, Henry RJ. 2014. Modifying plants for biofuel and biomaterial production. *Plant Biotechnology Journal* **12**: 1246-1258.

Gandini A. 2008. Polymers from renewable resources: a challenge for the future of macromolecular materials. *Macromolecules* **41**: 9491–9504.

Girard AL, Mounet F, Lemaire-Chamley M, Gaillard C, Elmorjani K *et al.* 2012. Tomato GDSL1 is required for cutin deposition in the fruit cuticle. *The Plant Cell* **24**: 3119-3134.

Gou JY, Yu XH, Liu CJ. 2009. A hydroxycinnamoyltransferase responsible for synthesizing suberin aromatics in *Arabidopsis*. *Proceedings of the National Academy of Science USA* **106**: 18855-18860.

Graça J. 2015. Suberin: the biopolyester at the frontier of plants. *Frontiers in Chemistry* **3**: 62

Graca J, Pereira H. 2000a. Methanolysis of bark suberins: analysis of glycerol and acid monomers. *Phytochemical Analysis* **11**: 45-51.

Graça J, Pereira H. 2000b. Suberin structure in potato periderm: glycerol, long-chain monomers, and glyceryl and feruloyl dimers. *Journal of Agricultural and Food Chemistry* **48**: 5476-5483.

Graca J, Santos S. 2006. Glycerol-derived ester oligomers from cork suberin. *Chemistry and Physics of Lipids* **144**: 96–107

Höfer R, Briesen I, Beck M, Pinot F, Schreiber L, Franke R. 2008. The *Arabidopsis* cytochrome P450 CYP86A1 encodes a fatty acid omega-hydroxylase involved in suberin monomer biosynthesis. *Journal of Experimental Botany* **59**: 2347-2360.

Jäger S, Trojan H, Kopp T, Laszczyk MN, Scheffler A. 2009. Pentacyclic triterpene distribution in various plants - rich sources for a new group of multi-potent plant extracts. *Molecules* **14**: 2016-2031.

Jakobson L, Lindgren LO, Verdier G, Laanemets K, Brosché M, Beisson F, Kollist H. 2016. BODYGUARD is required for the biosynthesis of cutin in Arabidopsis. *New Phytologist* Epub ahead of print.

Janick J. 2005. The origins of fruits, fruit growing, and fruit breeding. *Plant*

Breeding Review. **25**: 255–321.

Juniper BE, Mabberley DJ. 2006. *The Story of the Apple*, Imber Press

Khanal BP, Grimm E, Knoche M. 2013. Russeting in apple and pear: a plastic periderm replaces a stiff cuticle. *Annals of Botany – Plants* **5**: ls048.

Knoche M, Grimm E. 2008. Surface moisture induces microcracks in the cuticle of 'Golden Delicious' apple. *Hortscience* **43**: 1929–1931

Knoche M, Khanal BP, Stopar M. 2011. Russeting and microcracking of 'Golden Delicious' apple fruit concomitantly decline due to Gibberellin A4+7 application. *Journal of the American Society for Horticultural Science* **136**: 159-164.

Kolattukudy PE, Kronman K, Poulose AJ. 1975. Determination of structure and composition of suberin from roots of carrot, parsnip, rutabaga, turnip, red beet, and sweet-potato by combined gas-liquid- chromatography and mass-spectrometry. *Plant Physiology*. **55**: 567-573.

Kosma DK, Molina I, Ohlrogge JB, Pollard M. 2012. Identification of an Arabidopsis fatty alcohol:caffeoyl-Coenzyme A acyltransferase required for the synthesis of alkyl hydroxycinnamates in root waxes. *Plant Physiology* **160**: 237–248.

Kosma DK, Murmu J, Razeq FM, Santos P, Bourgault R, Molina I, Rowland O. 2014. AtMYB41 activates ectopic suberin synthesis and assembly in multiple plant species and cell types. *Plant Journal* **80**: 216-229.

Kurdyukov S, Faust A, Nawrath C, Bar S, Voisin D *et al.* 2006. The epidermis-specific extracellular BODYGUARD controls cuticle development and morphogenesis in *Arabidopsis*. *The Plant Cell* **18**: 321-339.

Landgraf R, Smolka U, Altmann S, Eschen-Lippold L, Senning M *et al.* 2014. The ABC transporter ABCG1 is required for suberin formation in potato tuber periderm. *The Plant Cell* **26**: 3403-3415.

Lashbrooke J, Aharoni A, Costa F. 2015. Genome investigation suggests MdSHN3, an APETALA2-domain transcription factor gene, to be a positive regulator of apple fruit cuticle formation and an inhibitor of russet development. *Journal of Agricultural Food Chemistry*. **63**: 185-191.

Lashbrooke J, Cohen H, Levy-Samocha D, Tzfadia O, Panizel I *et al.* 2016. MYB107 and MYB9 Homologs Regulate Suberin Deposition in Angiosperms. *Plant Cell* (Epub ahead of print).

Laszczyk MN. 2009. Pentacyclic triterpenes of the lupane, oleanane and ursane group as tools in cancer therapy. *Planta Medica* **75**: 1549-1560.

Laurens F. 1998. Review of the current apple breeding programmes in the world. *ISHS Acta Horticulturae* **484**: 163-170.

Lauvergeat V, Lacomme C, Lacombe E, Lasserre E, Roby D, Grima-Pettenati J. 2001. Two cinnamoyl-CoA reductase (CCR) genes from *Arabidopsis thaliana* are differentially expressed during development and in response to infection with pathogenic bacteria. *Phytochemistry* **57**: 1187-1195.

Lee SB, Jung SJ, Go YS, Kim HU, Kim JK, Cho HJ, Park OK, Suh MC. 2009. Two Arabidopsis 3-ketoacyl CoA synthase genes, KCS20 and KCS2/DAISY, are functionally redundant in cuticular wax and root suberin biosynthesis, but differentially controlled by osmotic stress. *Plant Journal* **60**: 462-475.

Li Y, Beisson F, Ohlrogge J, Pollard M. 2007. Monoacylglycerols are components of root waxes and can be produced in the aerial cuticle by ectopic expression of a suberin-associated acyltransferase. *Plant Physiology* 144: 1267-1277.

Li-Beisson Y, Shorrosh B, Beisson F, Andersson MX, Arondel V *et al.* 2010. Acyl-lipid metabolism. *The Arabidopsis Book* **8**: e0133.

Li-Beisson Y, Shorrosh B, Beisson F, Andersson MX, Arondel V *et al.* 2013. Acyl- lipid metabolism. *Arabidopsis Book* **11**: e0161.

Liang M, Haroldsen V, Cai X, Wu Y. 2006. Expression of a putative laccase gene, ZmLAC1, in maize primary roots under stress. *Plant Cell and Environment* **29**: 746-753.

Lü S, Song T, Kosma DK, Parsons EP, Rowland O, Jenks MA. 2009. *Arabidopsis* CER8 encodes LONG-CHAIN ACYL-COA SYNTHETASE 1 (LACS1) that has overlapping functions with LACS2 in plant wax and cutin synthesis. *Plant Journal* **59**: 553-564.

McFarlane HE, Watanabe Y, Yang W, Huang Y, Ohlrogge J, Samuels AL. 2014. Golgi- and trans-Golgi network-mediated vesicle trafficking is required for wax secretion from epidermal cells. *Plant Physiology* **164**: 1250-1260.

Meyer CJ, Peterson CA, Bernards MA. 2011. A comparison of suberin monomers from the multiseriate exodermis of *Iris germanica* during maturation under differing growth conditions. *Planta* **233**: 773-786.

Millar AA, Kunst L. 1997. Very-long-chain fatty acid biosynthesis is controlled through the expression and specificity of the condensing enzyme. *Plant Journal* **12**: 121-131.

Moire L, Schmutz A, Buchala A, Yan B, Stark RE, Ryser U. 1999. Glycerol is a suberin monomer. New experimental evidence for an old hypothesis. *Plant Physiology* **119**: 1137-1146.

Molina I, Bonaventure G, Ohlrogge J, Pollard M. 2006. The lipid polyester composition of *Arabidopsis thaliana* and *Brassica napus* seeds. *Phytochemistry* **67**: 2597-2610.

Molina I, Kosma D. 2015. Role of HXXXD-motif/BAHD acyltransferases in the biosynthesis of extracellular lipids. *Plant Cell Reports* **34**: 587-601.

Molina I, Li-Beisson Y, Beisson F, Ohlrogge JB, Pollard M. 2009. Identification of an Arabidopsis feruloyl-coenzyme A transferase required for suberin synthesis. *Plant Physiology* **151**: 1317-1328.

Morgan J, Richards A. 2003. *The New Book of Apples*, Brogdale Horticultural Trust, Ebury Press.

Nawrath C. 2002. The biopolymers cutin and suberin. *Arabidopsis Book* **1**: e0021.

Negrel J, Pollet B, Lapierre C. 1996. Ether-linked ferulic acid amides in natural and wound periderms of potato tuber. *Phytochemistry* **43**: 1195–1199.

Panikashvili D, Savaldi-Goldstein S, Mandel T, Yifhar T, Franke RB, Höfer R, Schreiber L, Chory J, Aharoni A. 2007. The Arabidopsis DESPERADO/AtWBC11 transporter is required for cutin and wax secretion. *Plant Physiology* **145**: 1345-1360.

Ranathunge K, Schreiber L. 2011. Water and solute permeabilities of Arabidopsis roots in relation to the amount and composition of aliphatic suberin. *Journal of Experimental Botany* **62**: 1961–1974.

Ranathunge K, Schreiber L, Franke R. 2011. Suberin research in the genomics era - new interest for an old polymer. *Plant Science* **180**: 399-413.

Ranocha P, Chabannes M, Chamayou S, Danoun S, Jauneau A, Boudet AM, Goffner D. 2002. Laccase down-regulation causes alterations in phenolic metabolism and cell wall structure in poplar. *Plant Physiology* **129**: 145-155.

Sawai S, Saito K. 2011. Triterpenoid biosynthesis and engineering in plants. *Frontiers in Plant Science* **30**: 25.

Schmutz A, Jenny T, Ryser U. 1994. A caffeoyl fatty-acid glycerol ester from wax associated with green cotton fiber suberin. *Phytochemistry* **36**: 1343-1346.

Schreiber L. 2010. Transport barriers made of cutin, suberin and associated waxes. *Trends in Plant Sciences* **15**: 546–553.

Schreiber L, Franke R, Hartmann K. 2005. Wax and suberin development of native and wound periderm of potato (*Solanum tuberosum L.*) and its relation to peridermal transpiration. *Planta* **220**: 520–530.

Serra O, Hohn C, Franke R, Prat S, Molinas M, Figueras M. 2010. A feruloyl transferase involved in the biosynthesis of suberin and suberin-associated wax is

required for maturation and sealing properties of potato periderm. *The Plant Journal* **62**: 277-290.

Serra O, Soler M, Hohn C, Franke R, Schreiber L, Prat S, Molinas M, Figueras M. 2009a. Silencing of StKCS6 in potato periderm leads to reduced chain lengths of suberin and wax compounds and increased peridermal transpiration. *Journal of Experimental Botany* **60**: 697-707.

Serra O, Soler M, Hohn C, Sauveplane V, Pinot F, Franke R, Schreiber L, Prat S, Molinas M, Figueras M. 2009b. CYP86A33-targeted gene silencing in potato tuber alters suberin composition, distorts suberin lamellae, and impairs the periderm's water barrier function. *Plant Physiology* **149**: 1050-1060.

Sironval C, Clijsters H. 1962. Sur la nature de la rugosité chez la pomme Cox's Orange. *Bulletin de la société royale de botanique de Belgique* **94**: 35-44.

Shi JX, Malitsky S, De Oliveira S, Branigan C, Franke RB, Schreiber L, Aharoni A. 2011. SHINE transcription factors act redundantly to pattern the archetypal surface of *Arabidopsis* flower organs. *PLoS Genetics* **7**: e1001388.

Shulaev V, Korban SS, Sosinski B, Abbott AG, Aldwinckle HS *et al.* 2008. Multiple models for Rosaceae genomics. *Plant Physiology* 147: 985-1003.

Soler M, Serra O, Molinas M, Huguet G, Fluch S, Figueras M. 2007. A genomic approach to suberin biosynthesis and cork differentiation. *Plant Physiology* **144**: 419-431.

Skene DS. 1982. The development of russet, rough russet and craks on the fruit of the apple Cox's Orange Pippin during the course of the season. *Journal of Horticultural Science* **57**: 165-174.

Sousa AF, Gandini A, Silvestre AJD, Neto CP, Cruz Pinto JJC, Eckerman C, Holmbom B 2011. Novel suberin-based biopolyesters: from synthesis to properties. *Journal of Polymer Science Part A-Polymer Chemistry* **49**: 2281-2291.

Sousa AF, Silvestre AJ, Gandini A, Neto CP. 2012. Synthesis of aliphatic suberin-like polyesters by ecofriendly catalytic systems. *High Performance Polymers* **24**: 4-8.

Thomas R, Fang X, Ranathunge K, Anderson TR, Peterson CA, Bernards MA. 2007. Soybean root suberin: anatomical distribution, chemical composition, and relationship to partial resistance to *Phytophthora sojae*. *Plant Physiology* **144**: 299-311.

Tukey LD. 1969. Observations on the russeting of apples growing in plastic bags. *Proceedings of the American Society for Horticultural Science* **74**: 30-39.

van Beilen JB1, Poirier Y. 2007. Prospects for biopolymer production in plants. *Advances in biochemical engineering/Biotechnology* **107**: 133-151.

Velasco R, Zharkikh A, Affourtit J, Dhingra A, Cestaro A, Kalyanaraman A, Fontana P *et al.* 2010. The genome of the domesticated apple (*Malus* x *domestica* Borkh.). *Nature Genetics* **42**:833-839.

Verdaguer R, Soler M, Serra O, Garrote A, Fernández S, Company-Arumí D, Anticó E, Molinas M, Figueras M. 2016. Silencing of the potato StNAC103 gene enhances the accumulation of suberin polyester and associated wax in tuber skin. *Journal of Experimental Botany* **67**: 5415-5427.

Vishwanath SJ, Delude C, Domergue F, Rowland O. 2015. Suberin: biosynthesis, regulation, and polymer assembly of a protective extracellular barrier. *Plant Cell Reports* **34**: 573-86.

Vishwanath SJ, Kosma DK, Pulsifer IP, Scandola S, Pascal S, Joubes J, Dittrich-Domergue F, Lessire R, Rowland O, Domergue F. 2013. Suberin-associated fatty alcohols in *Arabidopsis thaliana*: distributions in roots and contributions to seed coat barrier properties. *Plant Physiology* **163**: 1118-1132.

Vogt T. 2010. Phenylpropanoid biosynthesis. *Molecular Plant* **3**: 2-20.

Walter TE. 1967. Russeting and cracking in apples. A review of world literature. *Report of East Mailing Research Station* **1966**: 83-95.

Wang YZ, Zhang S, Dai MS, Shi ZB. 2014. Pigmentation in sand pear (*Pyrus pyrifolia*) fruit: biochemical characterization, gene discovery and expression

analysis with exocarp pigmentation mutant. *Plant Molecular Biology* **85**: 123-134.

Watanabe S. 1969. Historical studies on the cause of apple russeting. *Bulletin of the Yamagata University* **5**: 205-267.

Yadav V, Molina I, Ranathunge K, Castillo IQ, Rothstein SJ, Reed JW. 2014. ABCG transporters are required for suberin and pollen wall extracellular barriers in Arabidopsis. *The Plant Cell* **26**: 3569–3588.

Yang W, Pollard M, Li-Beisson Y, Beisson F, Feig M, Ohlrogge J. 2010. A distinct type of glycerol-3-phosphate acyltransferase with sn-2 preference and phosphatase activity producing 2-monoacylglycerol. *Proceedings of the National Academy of Science USA* **107**: 12040-12045.

Yang W, Simpson JP, Li-Beisson Y, Beisson F, Pollard M, Ohlrogge JB. 2012. A land-plant-specific glycerol-3-phosphate acyltransferase family in *Arabidopsis*: substrate specificity, sn-2 preference, and evolution. *Plant Physiology* **160**: 638–652.

Yeats TH, Huang W, Chatterjee S, Viart HM, Clausen MH, Stark RE, Rose JK. 2014. Tomato Cutin Deficient 1 (CD1) and putative orthologs comprise an ancient family of cutin synthase-like (CUS) proteins that are conserved among land plants. *Plant Journal* **77**: 667-675.

Yeats TH, Laetitia BB, Martin Viart HMF, Isaacson T, He Y, Zhao L *et al.* 2012. The identification of cutin synthase: formation of the plant polyester cutin. *Nature Chemical Biology* **8**: 609-611.

Chapter I: Apple russeting as seen through the RNA-seq lens: strong alterations in the exocarp cell wall

Adapted from the published article:

Legay S, Guerriero G, Deleruelle A, Lateur M, Evers D, André CM, Hausman, J-F. 2015. Apple russeting as seen through the RNA-seq lens: strong alterations in the exocarp cell wall. *Plant Molecular Biology* **88**: 21-40.

Contributions:

S. Legay designed the experimental setup, performed the laboratory work (RNA extraction, RT-qPCR, library preparation and sequencing). He performed the bioinformatic work, statistical analysis and wrote the present article.

G. Guerriero was involved in the library preparation and sequencing. She also provided her expertise in the interpretation of results related to the cell wall modification.

A. Deleruelle involved in the apple fruit sampling and the RNA extraction.

M. Lateur provided the sample material.

D. Evers initiated the project.

C. André and J.-F. Hausman participated in the manuscript refinement.

Abstract

Russeting, a commercially important defect in the exocarp of apple (*Malus* x *domestica*), is mainly characterized by the accumulation of suberin on the inner part of the cell wall of the outer epidermal cell layers. However, knowledge on the underlying genetic components triggering this trait remains sketchy. Bulk transcriptomic profiling was performed on the exocarps of three russeted and three waxy apple varieties. This experimental design was chosen to lower the impact of genotype on the obtained results. Validation by qPCR was carried out on representative genes and additional varieties. Gene ontology enrichment revealed a repression of lignin and cuticle biosynthesis genes in russeted exocarps, concomitantly with an enhanced expression of suberin deposition, stress responsive, primary sensing, NAC and MYB-family transcription factors, and specific triterpene biosynthetic genes. Notably, a strong correlation (R^2=0.976) between the expression of a *MYB93*-like transcription factor and key suberin biosynthetic genes was found. Our results suggest that russeting is induced by a decreased expression of cuticle biosynthetic genes, leading to a stress response which not only affects suberin deposition, but also the entire structure of the cell wall. The large number of candidate genes identified in this study provides a solid foundation for further functional studies.

Keywords: *Malus* x *domestica,* exocarp, russeting, cell wall, suberin, cuticle, triterpene, gene expression

I. Introduction

Apple is one of the most important fruit crops in the world with more than 80 million tons produced worldwide in 2013 (FAOSTAT data). Since the 60's, traits such as yield, biotic stress tolerance, fruit shape, taste or storage properties have been improved. Despite the rich diversity of apple varieties, consumer's choice clearly favors waxy and glossy apples, restricting apple commercial germplasm to a majority of waxy skin varieties. Some old heritage varieties such as 'Reinette Parmentier', 'St Edmund Pippin' or 'Patte de loup' may, however, present a contrasting phenotype, displaying a russeted (rough and brown) skin. Waxy apples can also be affected by russeting, which, in this case, is perceived as a major defect by consumers and leads to quality and price downgrading, considerably reducing the profitability of fruit production (Curry 2009). Despite significant improvements in apple commercial germplasm, appearance of this non-desirable phenotype can appear in a large number of glossy commercial varieties, including well-studied varieties such as 'Golden Delicious' and 'Cox Orange Pippin'. To date, few treatments, including phytohormones and fungicides, are able to limit its occurrence (Gildemacher *et al*. 2006, Barabdoozi and Talaie 2009).

Russeting occurrence has been linked to lacks and defects in the cuticular and epidermal layers (Watanabe 1969, Skene 1982, Khanal *et al*. 2013). Cuticle is a lipophilic barrier composed of many different components, such as cutin and waxes, which covers the epidermal layer, limits gas exchange or water loss, and protects plants from environmental injuries (Suh *et al*. 2005). A broad range of environmental factors that cause epidermal and cuticular defects have been identified. Among them, pathogen attacks, non-optimal environmental conditions, such as heavy rainfalls, temperature stress, humidity, or the application of plant

protection agents are the most predominant cause of russeting (Faust and Shear 1972, Skene 1982, Khanal *et al*. 2013). As a representative example, extended exposure to a humid environment results in a thinner or complete absence of the cuticle. Apples are particularly sensitive to russeting during early stages of fruit development, at which time extreme tangential tensions of the epidermis occur because of the high pressure exerted on the skin by the growing fruit, which consequently results in microscopic cracks in the cuticle (Walter 1967, Watanabe 1969, Faust and Shear 1972, Skene 1982, Khanal *et al*. 2013).

Apple russeting is an accumulation of suberin on the inner side of the cell wall where it plays a role as global barrier between plants and the environment, thus limiting water, solute, gas, and ion exchanges, as well as decreasing pathogen susceptibility (Sousa *et al*. 2012). Its deposition has been mainly investigated in *Arabidopsis thaliana* roots (Beisson *et al*. 2007, Franke and Schreiber 2007, Li and Beisson 2009, Beisson *et al*. 2012, Kosma *et al*. 2014) and the tuber skin of potato (*Solanum tuberosum* L.) (Lulai and Corsini 1998, Graca and Pereira 2000b, Serra *et al*. 2009b, Serra *et al*. 2010, Boher *et al*. 2013). In *Arabidopsis*, suberin and Casparian strips control the apoplastic transport of water and minerals (Zimmermann *et al*. 2000, Franke *et al*. 2005, Baxter *et al*. 2009), while reduced suberin deposition, observed in the fatty acid hydroxylase *horst* mutant, increased root permeability (Hofer *et al*. 2008). Conversely, two mutants with increased amounts of suberin in the roots exhibited reduced levels of Mn, Zn and Ca in their shoots (Ranathunge and Schreiber 2011).

Suberin is a ubiquitous insoluble biopolyester composed of two polyphenolic and one polyaliphatic domain (SPPD, for Suberin Poly-Phenolic Domain, and SPAD, for Suberin Poly-Aliphatic Domain, respectively) (Bernards 2002). The SPAD is composed of cross-linked saturated and substituted ω-hydroxyacid or α,ω-dicarboxylic acid monomers, esterified with glycerol and ferulic acid (Graca and

Pereira 2000a, Franke *et al*. 2005, Graca and Santos 2007), while SPPD displays a lignin-like structure with a higher hydroxycinnamic acid content (Bernards 2002). Despite commercial and scientific interest, knowledge of the genetic components responsible for suberin synthesis in apple remains limited. Available data on the suberization process mainly originate from model plants. In *A. thaliana*, a number of gene families involved in suberin synthesis have been described (Ranathunge *et al*. 2011, Beisson *et al*. 2012), providing an initial, precursory overview of the complexity of the suberin biosynthetic process. The SPAD monomers are synthesized in plastids and the endoplasmic reticulum. C16-C18 acyl precursors are elongated by the fatty acid elongation complex and activated by fatty acid long chain acyl-CoA synthetases. Cytochrome P450 proteins, belonging to the CYP86 and CYP94 subfamilies, are involved in the multiple modifications of C16 and C18 acyl precursors resulting in α,ω-dicarboxylic acid and hydroxyacyls precursors. The resulting suberin precursors are then esterified with glycerol by a glycerol phosphate acyltransferase (Moire *et al*. 1999, Beisson *et al*. 2007, Li *et al*. 2007, Hofer *et al*. 2008), or reduced by a fatty acid reductase and conjugated with ferulic acid (Molina *et al*. 2009). The SPPD anchored in the cell wall is considered as a hydroxycinnamic acids polymer comparable to lignin (Pollard *et al*. 2008). Suberin monomers may be exported out of the cell by ABC transporters and lipid transfer proteins, but few genes have been identified so far (Panikashvili *et al*. 2010). How these SPPD and SPAD are finally polymerized is not known, although the existence of a polyester synthase function has been proposed (Soler *et al*. 2007). Recent studies suggest that some oxidizing enzymes, such as peroxidases, are involved in the polymerization of the SPPD, whereas lipase/esterase may play a role in the final step of the SPAD synthesis (Beisson *et al*. 2012).

Few studies related to the regulation of suberin deposition are available. Plant growth regulators influence suberin synthesis-related genes. The application of gibberellins can reduce russeting in 'Golden Delicious' (Barabdoozi and Talaie 2009). In potato tubers, feruloyl transferase expression is enhanced by wounding and abscisic acid, whereas a repression was observed in response to salicylic acid (Boher *et al*. 2013). Finally, in *A. thaliana* roots, AtMYB41 has been recently identified to trigger the expression of a large number of suberin synthesis genes under abiotic stress condition (Kosma *et al*. 2014).

To identify genes and pathways associated with apple russeting, gene expression profiling using RNA sequencing (Illumina) was performed. In order to draw a consistent picture of the gene expression profiles specific to both russeted and waxy apples and at the same time to highlight and interpret the mechanism leading to the russeted phenotype, a bulk RNA-sequencing was performed on the exocarp of a group of three distinct fully-russeted apple varieties ('Patte de loup', 'Reinette Parmentier', 'St Edmund's Pippin') and a second one including 3 fully waxy varieties ('Gala', 'CRAW/Ma/AF42', and 'CRAW/Ma/AG94'). This specific design was chosen to decrease the effect of genotype on the obtained results and consequently to gain a more specific overview of the suberization process occurring in apples during the development of russeting.

II. Materials and methods

A. Plant material

For the preparation of the RNA-sequencing library, 6 apple varieties presenting 3 fully-waxy ('CRAW/Ma/AF42', 'CRAW/ma/AG94', 'Gala') and 3 fully-russeted phenotypes ('Patte de loup', 'Reinette Parmentier', 'St Edmund's Pippin') were harvested in October 2012 at commercial maturity (150 days after full bloom) in

the orchards of the Walloon Agronomic Research Centre (CRA-W, Gembloux, Belgium). qPCR experiments were performed using additional apple fruit, sampled in October 2013, including the waxy cultivar 'CRAW/Ma/AG94', the russeted 'Patte de loup', 'Reinette du Canada Grise', 'Court Pendu Gris' and semi-russeted apple 'Cox Orange Pippin' varieties, the latter being collected separately in two different locations (CRA-W and a Luxemburgish commercial orchard). The phenotypes, pedigree and origins of each variety were displayed in the Table 2-1. For each variety, 6 fruit were sampled and each fruit was split into quarters. A 5 millimeter (large) longitudinal slice was peeled with scalpels from each quarter, taking care to remove the remaining flesh from the exocarp. For the semi-russeted variety 'Cox Orange Pippin', waxy and russeted exocarpic areas were carefully excised from 6 fruit. For the RNA-sequencing experiment each biological replicate was constituted by a pool of 6 fruits (1 biological replicate per variety = 3 biological replicates per trait). For the qPCR experiment, each variety was tested on 3 distinct pools (biological replicates) of 6 fruits. The resulting exocarp samples were directly flash-frozen in liquid nitrogen, roughly ground to homogenize the sample and stored at -80°C until RNA extraction.

B. RNA extraction

Samples (250 mg) were ground to a fine powder with mortar and pestle in liquid nitrogen. Total RNA was extracted using an adapted CTAB buffer extraction protocol (Gasic *et al*. 2004). Total RNAs were cleaned and treated with DNase I using the RNeasy plant mini kit (QIAGEN, Leusden, The Netherlands), following the manufacturer's guidelines. Total RNA integrity was assessed using the RNA Nano 6000 assay (Agilent Technologies, Diegem, Belgium) and a 2100 Bioanalyzer with quality parameters adapted to plant RNA profiles (Agilent Technologies, Santa Clara, CA, USA). Samples, with RINs (RNA integrity number) lower than 8, were excluded from the experiment.

Table 2-1: Genotype and phenotype data: russeting and waxiness index set according to the ECPGR guidelines (http://www.ecpgr.cgiar.org), pedigree, origin and obtention date where given when available.

Variety	Phenotype	ECPGR Global russetir index (1=no russeting-9=fully russeted)	ECPGR Global waxyness index (1=low,3=high) (ECPGR)	Pedigree	Comment
St Edmund's Pippin	Fully russeted	8	1	Unknown	Amateur bred old variety from UK, 1875
Reinette Parmentier	Fully russeted	7	1	Unknown	Amateur bred old variety from France, ~1830
Patte de Loup	Fully russeted	9	1	Unknown	Old variety from france, ~1790
CRA-W/Ma/AG 94	Waxy	1	3	Vf hybr x Mme Collard	CRA-W breeding programm, 2010
CRA-W/Ma/AF 42	Waxy	3	2	Vanda x Golden Delicio	CRA-W breeding programm, 2010
Gala	Waxy	2	2	Kidds Orange Red X Gc	Old variety from New zealand, ~1920
Canada Gris	Fully russeted	8	1	Mutation of 'Canada Bla	Old variety from France, 1803
Court pendu Gris	Fully russeted	9	1	Unknown	Really old variety from Belgium, before 1500
Cox orange pippin	Semi-russeted	5	1 to 2	Unknown, claimed to be	Amateur bred old English cv. raised in 1825

RNA purity was assessed measuring the absorbance at 230 nm, 260 nm and 280 nm using a Nanodrop ND1000 spectrophotometer (Thermo scientific, Villebon-sur-Yvette, France). Total RNA was quantified using a Qubit RNA assay kit (Life technologies, Carlsbad, CA, USA).

C. Library preparation and sequencing

Libraries were prepared from 3 μg total RNA using the TruSeq RNA Sample Preparation v2 kit according to the manufacturer's guidelines (Illumina, San Diego, CA, USA). After mRNA purification, cDNA synthesis, shearing, Illumina adapters/barcodes ligation and 15-cycles of PCR amplification, libraries were controlled using the Agilent 2100 bioanalyzer and the DNA-1000 kit. Libraries were quantified using the Library Quantification Kit - Illumina/ROX Low (Kapa Biosystems, Boston, MA, USA) on a Viia7 96-well real-time-qPCR instrument (Life Technologies). The pooled libraries were sequenced on an Illumina MiSeq using 4 consecutive runs (Illumina MiSeq reagent V2 and V3) to generate 76 base-pairs paired-end reads. Raw sequences have been deposited at the NCBI Gene Expression Omnibus website (GEO, http://www.ncbi.nlm.nih.gov/geo, accession number: GSE61040).

D. Data analysis

MiSeq generated FASTQ files were imported in CLC genomics workbench v6.5 discarding reads with poor quality (<Q30). For each library, read duplicates (23 to 32%) were removed from each sample independently using the duplicate read removal plugin, Illumina adapter residues were then trimmed using the TruSeq adaptor sequence and finally filtered (~2% removed) using the following criteria: low sequence quality <0.01, maximum of 2 ambiguous nucleotides, read length between 35 and 80 nucleotides. The remaining reads were mapped to the predicted apple transcriptome (Velasco *et al*. 2010) with annotations obtained from

Phytozome v.10 beta (http://phytozome.jgi.doe.gov) with the following criteria: mapped reads having multiple hits lower than 5, 90% identity and 50% of coverage with the reference. Expression values were calculated using the RPKM (Reads per kilobase transcript per million reads) method (Mortazavi *et al*. 2008). Genes with no mapped reads, with no specifically mapped reads and/or with a RPKM value lower than 0.1 in at least one of the libraries were removed from the dataset.

Differentially expressed genes between the russeted exocarp group ('Patte de loup', 'Reinette Parmentier', 'St Edmund's Pippin') and the waxy group ('CRAW/Ma/AF42', 'CRAW/ma/AG94', 'Gala') were statistically determined using a Baggerley's 'on proportions' weighted test (Baggerly *et al*. 2003), a false discovery rate (Benjamini-Hotchberg correction) was set at 0.2 and a fold-change cut-off value at -1>log2 ratio (Russet group/Waxy group))>1. The Gene ontology enrichment analysis was performed from a subset of genes (-2>log2 ratio (Russet group/Waxy group)>2, FDR<0.2) in Cytoscape (v3.1.0) with the ClueGO v2.1.1 and CluePedia v1.1.1 plugins (Bindea *et al*. 2009, Bindea *et al*. 2013) to highlight significantly regulated biological processes (Benjamini-Hotchberg corrected P-value<0.05) following these criteria: gene ontology from level 3 to level 10, kappa score set at 0.9. A suberin-related functional association network was built using STRING (http://string-db.org) from the TAIR code obtained from the significantly expressed gene, which were more expressed in the russeted exocarps.

E. QPCR validation

Gene expression results were validated on a subset of 8 representative genes using qPCR. Reverse transcription was carried out using the M-MuLV Reverse Transcriptase (RNase H-), the Murine RNase Inhibitor (New England Biolabs, Ipswich, MA, USA) and random hexamers (Invitrogen, Carlsbad, NM, USA) following the manufacturers' guidelines. qPCR primers were designed using the

Primer3 software (http://frodo.wi.mit.edu/) with the following criteria: primer size between 18 and 25 base pairs, GC content between 30 and 70%, amplicon size from 80 to 200 base pairs, primer annealing temperatures in the 57-61°C range. Matching primer sets were checked using NetPrimer (http://www.premierbiosoft.com/netprimer/index.html) for unexpected secondary structures. In order to test the specificity of the primers, a BLAST search against the *M*. x *domestica* genome sequence was carried out. qPCR runs were carried out, using technical triplicates and 3 to 4 biological replicates (SI Table 2-1), on a Viia7 384-well real-time PCR instrument (Life Technologies) with Takyon SYBR Green low ROX (Eurogentec) following the manufacturer's guidelines. Experiments were carried out following the MIQE guidelines (Bustin *et al*. 2009) and a melting curve was performed at the end of all the runs to assess the specificity of the primers. Primers information and melting curves are available on the Table 2-2. The relative expression of a gene of interest and the Pearson correlation between them was calculated using the Biogazelle Qbase+ V2.5 software (Hellemans *et al*. 2007), taking into account multiple reference gene normalization and specific PCR efficiencies. For the present experiment, the GeNorm+ analysis described the MdEF1 and MdActin gene couple as the most suitable for optimal normalization of the data (Vandesompele *et al*. 2002). A hierarchical clustering of the results was performed using the Cluster 3.0 software with un-centered correlation and complete linkage metrics. The resulting heatmap was built using Treeview. Statistical analysis of the $\log_2$ transformed normalized relative quantities was performed using SPSS 19.0. Normal distribution was assessed and a general linear mixed model using a Tukey Post-Hoc test was applied (α=0.05). Results of the Post-Hoc test are displayed on the SI Table 2-1 using different letters indicating significantly different data points.

Table 2-2: Primers data display qPCR primer sequences, amplicon size, PCR efficiency, melting temperatures.

Gene Code	Targeted contig/EST	Sense	Primer sequence (5'-3')	Amplicon size (bp)	PCR efficiency	Melting temperature (°C)
KCS10	MDP0000235280	F	GTGTACCAAGAGGAAGATGAACAAA	123	1.98	82
		R	GAAAGGCAGCACTAACGGC			
CYP86B1	MDP0000306273	F	CGCTTTGTGACCCCATCC	114	2.03	82.5
		R	AATGACGTCTTCCGCAAACT			
GPAT6	MDP0000479163	F	CCCAATAGTTGCCCTTCTGA	154	1.94	82.5
		R	AGGAGGGGTGCCCTTAACTA			
CYP86A1	MDP0000923760	F	GCGCCTCCTCTATCCTTCC	89	1.96	84
		R	CGACTTCGAGGCTCTTCTCC			
MYB42	MDP0000787808	F	GACCCGTTGGTGAGTTTCAT	104	1.96	79.5
		R	TCCTCCGTTGGATTATCAGC			
WSD-1	MDP0000701887	F	AGAAATGGTCAAACCCGACA	107	2.00	82
		R	AGACGAAGTCAAGCGCATTT			
MYB93	MDP0000320772	F	TATCCAACACCACCAAGCAA	145	1.98	80.5
		R	CCACCGAAGTAGGAGATGGA			
GPAT5	MDP0000150502	F	GAACAAATCCACCCACCACT	131	1.97	85
		R	ATTAAGAGGGCGGTTGAAGG			
eF-1alpha	AJ223969.1	F	ACTGTTCCTGTTGGACGTGTTG	208	2.01	84
		R	TGGAGTTGGAAGCAACGTACCC			
ACTIN	EB127077	F	ACCATCTGCAACTCATCCGAACCT	185	2.02	83.5
		R	ACAATGCTAGGGAACACGGCTCTT			

III. Results and discussion

A. Sequencing and mapping

The direct interest of our study is to draw a picture of the suberization process in apple. Whole gene expression profiling using RNA-seq is the method of choice to identify genes linked to a trait of interest. For this purpose, six cDNA libraries were built from mRNA extracted from the skin of six apple varieties with either a russet or waxy phenotype. A total of 156,914,224 76-base pairs-sequence reads, ranging from 17 to 36 million reads per library, were generated from four consecutive MiSeq runs (Table 2-3). About 69 to 73% of the reads were mapped to the reference transcriptome with a consistent part (18-19%) matching to multiple contigs with a large majority of reads mapped to 2 contigs (Table 2-3). This non negligible part of multi-hit mapped reads may be probably due to the specific structure of the *M.* x *domestica* genome which results from a genome-wide duplication of a *Pyreae* ancestor (Velasco *et al.* 2010). Indeed, chromosomes 3, 5, 9 and 13 have a high nucleotide sequence identity with chromosomes 11, 10, 17 and 16 respectively and many shorter segments from other chromosomes also present high identities between each other. QPCR validation (Fig. 2-1) was performed on eight suberin-related genes and displayed a strong correlation RNA-Seq data ($y=1.0038x+0.4639$, $R^2=0.9941$).

Table 2-3: Summary of the sequencing, filtering and mapping in number of sequence reads. Sequence with low quality score (<Q30) were removed when imported in CLC genomics workbench v6.5. Then sequences were trimmed using Illumina adaptor sequences. PCR duplicates were then removed using the Duplicate reads removal v1.0 beta 6 plugin. Remaining sequences were then mapped to the predicted transcriptome sequence using the RNA-seq analysis tool.

Libraries	Raw reads	Duplicated reads	Trimming removed reads	Post filtering remaining reads	Total read mapped	Reads mapped with unique hit	Reads mapped with multiple hits	Un-mapped reads
St Edmund's Pippin	21 224 536	5 396 872	391 773	15 435 891	11 325 509	8 452 829	2 872 680	4 110 382
Reinette Parmentier	36 334 042	9 614 801	866 794	25 852 447	19 050 437	14 263 520	4 786 917	6 802 010
Patte de Loup	30 987 212	7 159 173	731 404	23 096 635	17 183 311	12 833 668	4 349 643	5 913 324
Gala	17 942 430	5 351 026	236 925	12 354 479	9 441 893	7 048 200	2 393 693	2 912 586
CRAW/Ma/AF42	18 169 644	4 145 737	285 605	13 738 302	10 487 469	7 942 611	2 544 858	3 250 833
CRAW/Ma/AG94	32 256 360	10 450 008	507 161	21 299 191	16 757 229	12 619 754	4 137 475	4 541 962

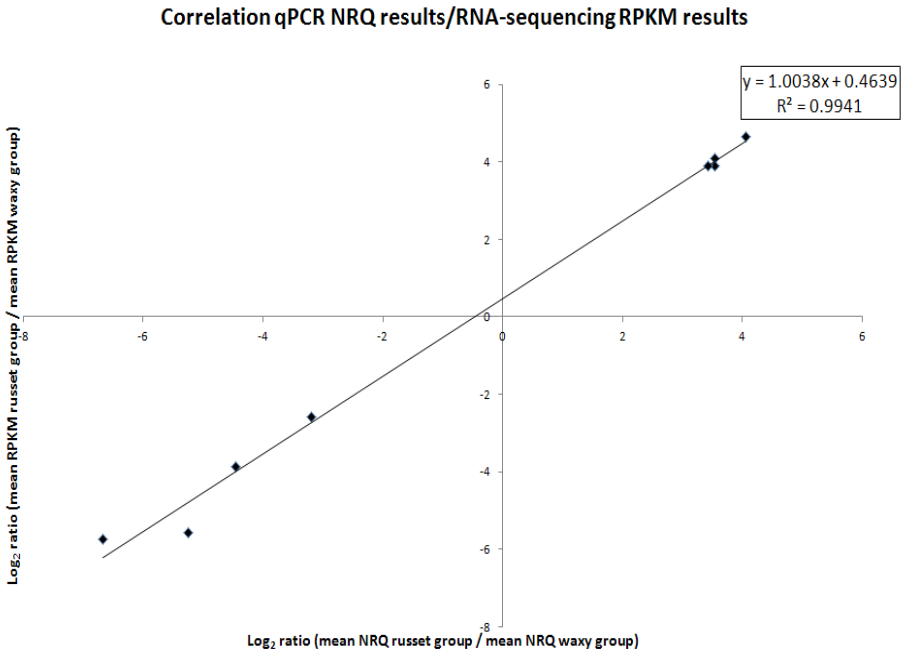

Figure 2-1: Correlation between qPCR and RNA sequencing data performed on eight suberin-related genes described in the Table 2-2: GPAT5 (MDP0000150502), GPAT6 (MDP0000479163), MYB93 (MDP0000320772), MYB42 (MDP0000787808), WSD-1 (MDP0000701887), CYP86A1 (MDP0000923760), CYP86B1 (MDP0000306273), KCS10 (MDP0000235280). qPCR data is expressed in Log_2 ratio(mean NRQ russeted group/mean NRQ waxy group) versus Log_2 ratio (mean RPKM russeted group/mean RPKM waxy group).

B. Overview of the differentially expressed genes between russeted (RAE) and waxy apple exocarp (WAE)

In order to highlight genes involved in the russet trait and to minimize noise due to genotypic specificities of each cultivar, a Baggerley's "on proportion" statistical test was performed on the gene expression results obtained between russeted and waxy varieties. A total of 1261 genes were differentially regulated between russet and waxy apple exocarps. The first interesting key result was related to the number of up-regulated genes, which was nearly three times higher

than the number of down-regulated genes. The same trend has been already described in *Quercus suber* (cork tree) where the authors compared gene expression profiles of the phellem with wood tissues (Soler *et al*. 2007) and when comparing *Pyrus pyrifolia* green and russeted pericarp (Wang *et al*. 2014b). Given this distribution of the significantly regulated genes, russeting occurrence can be considered as an additive trait.

In order to extract general trends from this dataset, the differentially expressed genes were first classified using the MapMan tool (Thimm *et al*. 2004). The most represented genes belonged to the protein metabolism bin and are in majority composed of protein turnover and protein kinase-related genes reflecting putative differences in the protein pool and the protein regulation processes between russeted and waxy skin (Fig. 2-2). The RNA processing bin is also largely represented and the stress-related bin contains a large number of genes implicated in biotic stress (Fig. 2-2). Concerning transcription factors, the signaling and phytohormone metabolism-related bins contain a relatively large number of differentially expressed genes including many receptor kinases, as well as genes involves in auxin and ethylene metabolism. Not unexpectedly lipid and secondary metabolite synthesis appears to be important in the waxy/russet skin phenotype compared to carbohydrate, glycolysis and gluconeogenesis, where only a small number of genes were differentially regulated (Fig. 2-2). The results also indicated that cell and cell wall development are tightly linked with the appearance of the russeting in apple skin. Finally, a significant number of transporters were found including ABC transporters and multidrug resistance systems.

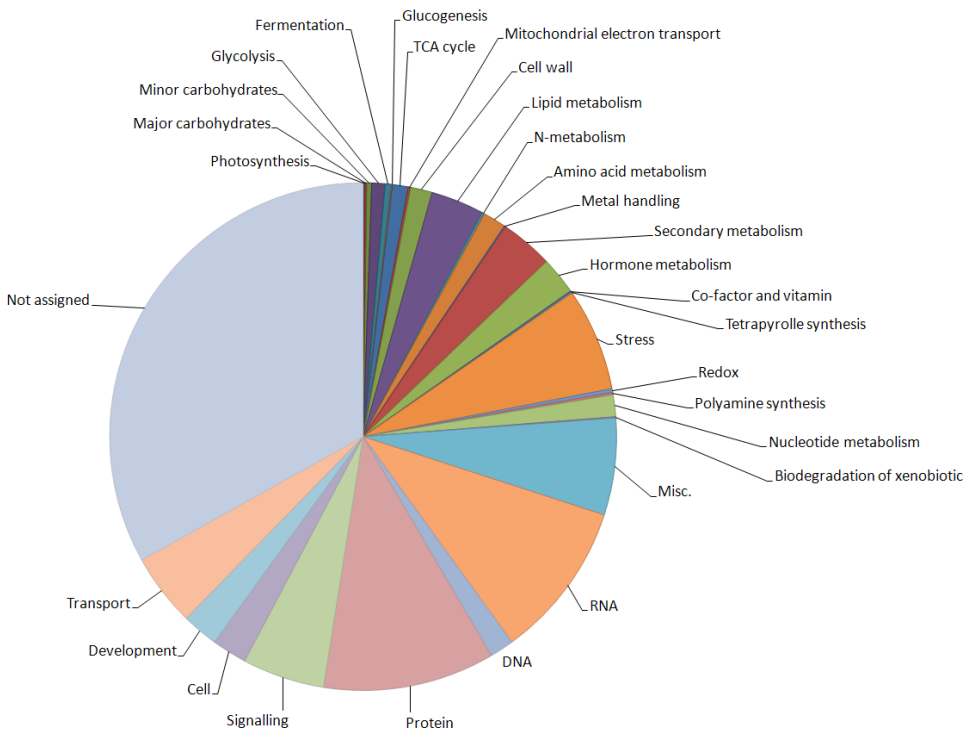

Figure 2-2: Distribution of the significant differentially expressed genes (-1>$\log_2$(ratio RAE group/WAE group)>1, p-Value<0.05, FDR<0.2) across major bins in Mapman 3.6RC1. Data obtained from the statistical analysis performed in CLC genomics workbench were imported in MapMan and sorted according to their biological processes.

Overall, the russet phenotype had an altered expression of genes with roles spanning from the cell wall primary sensing to the end point metabolic and cell structure level. In the following sections, the most remarkable observations will be discussed. To facilitate the description of the results, gene expression data will hereafter always be described as how genes were expressed in the RAE in relation to WAE.

C. Primary lipid synthesis and cuticle deposition-related genes were less expressed in russeted apple

As mentioned above, comparison between RAE and WAE resulted in a large number of differentially expressed genes belonging to the lipid metabolism (Fig. 2-2, Fig. 2-3). Indeed, the whole primary fatty acid elongase (FAE) complex, from acetyl-CoA carboxylase to NADH-dependent enoyl-acyl carrier protein (ACP) reductase-like gene (Fig. 2-3), was less expressed in the RAE suggesting a lower C16-ACP synthesis rate compared to the WAE. Gene Ontology (GO) enrichment performed on the highly significant genes using Cluepedia/ClueGO plugins (p-Value<0,05, FDR<0.2 correction, $-2<\log_2(\text{Russeted/waxy})<2$) confirmed this trend showing a majority of down regulated biological processes being involved in the alkanes, unsaturated and long-chain fatty acid, phosphatidylglycerol biosynthetic process, cutin and wax metabolism, as well as cuticle development (Fig. 2-4). Other genes involved in cuticle development, cutin and wax biosynthetic process, such as the 3-ketoacyl-CoA synthase genes (*KCS*) 1, 3, 6, and 10, are less expressed in RAE (Table 2-4, Fig. 2-4, Fig. 2-5). *KCS* genes, which encode very-long-chain fatty acid condensing enzymes, have been shown to play a crucial role in the synthesis of epicuticular wax (Serra *et al*. 2009a) and were also less expressed in russeted sand pear pericarps (Wang *et al*. 2014a, Wang *et al*. 2014b).

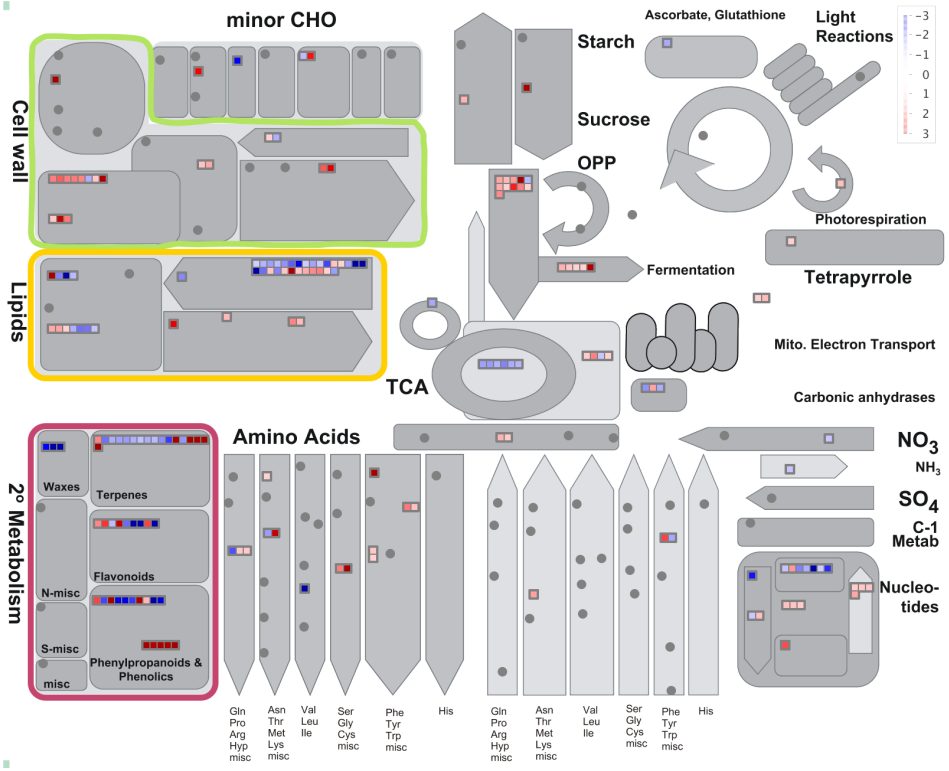

Figure 2-3: Metabolism overview map obtained from the significantly regulated genes using MapMan V3.6 RC1. Squares represent differentially expressed genes. In red, the genes more expressed in the RAE. In blue, the genes less expressed in the RAE. The darker the colors, the higher the fold changes (Log_2 expression ratio (RAE/WAE). A majority of genes were grouped into the 'cell wall', 'lipids' and 'secondary metabolism' bins, highlighted in green, yellow and dark purple, respectively.

The gene coding for a wax ester synthase/acyl-coenzyme A: diacylglycerolacyltransferase (WSD1), which involved in the final step of the wax esters synthesis (Li *et al*. 2008), is also less expressed in russeted skin (Table 2-4, Fig. 2-5). Following the same trend, RNA-seq and qPCR data showed that the glycerol-3-phosphate acyl transferase 6-like gene (*GPAT6*-like) was also less

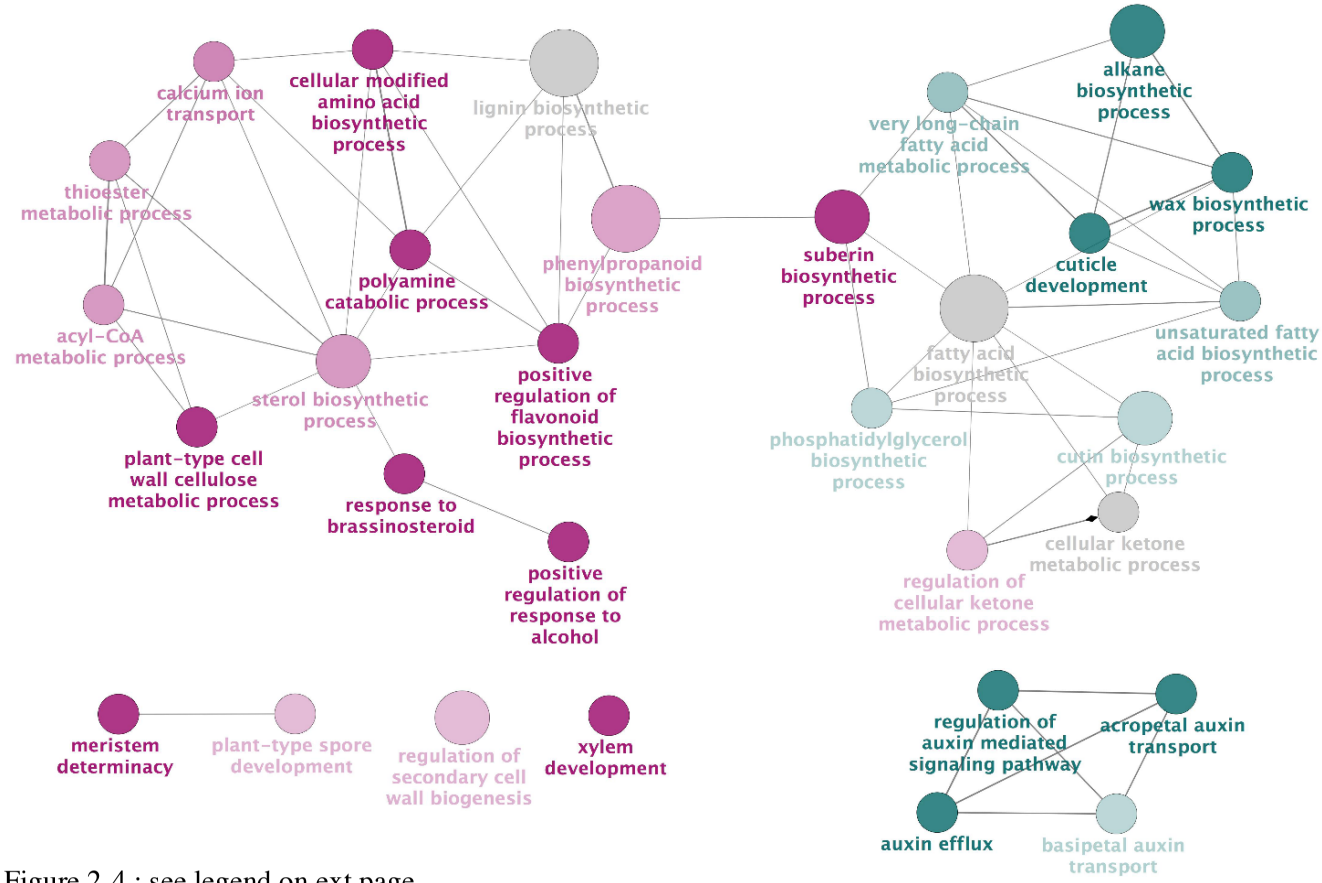

Figure 2-4 : see legend on ext page

Figure 2-4: Gene ontology enrichment analysis performed from a subset of genes (-2>log2 ratio (Russet group/Waxy group)>2, p-Value<0.05, FDR<0.2) in Cytoscape (v3.1.0) with the ClueGO v2.1.1 and CluePedia v1.1.1 plugins, highlight the significantly regulated biological processes (Benjamini-Hotchberg corrected p-Value<0.05, gene ontology from level 3 to level 10, kappa score set at 0.09). Biological processes (nodes) with genes overrepresented in the russeted and waxy groups are highlighted in red and blue, respectively. The larger the circles, the higher the statistical significance (smaller circles display corrected p-Value< 0.05) of the enrichment is. Lines between nodes display the shared genes between the corresponding biological processes.

expressed in RAE compared to the WAE (Table 2-4, Fig. 2-5). GPATs, which are responsible for the linkage of acyls to glycerol-3-phosphate, are the key regulators of both cutin and suberin synthesis (Fig. 2-4). Eight GPAT isoforms with diverse functions have been identified in *A. thaliana* with localized expression and isoform-specific functional characterization (Beisson *et al*. 2012). AtGPAT6 is a crucial enzyme in the synthesis of palmitate-based cutin monomers in flowers (Li and Beisson 2009), suggesting that russeted apple fruits have a lower cuticle deposition. Among the large number of differentially expressed transporter genes, two, which encode ABCG11 (Table 2-4), implicated in the excretion of the cuticular (cutin and wax) monomers through the epidermal cell (McFarlane *et al*. 2010), were also down-regulated in RAE. These observations are in accordance with the literature arguing that the thickness and the structure of the cuticle play a central role in the appearance of russeting (Faust and Shear 1972, Skene 1982, Khanal *et al*. 2013).

Since the cuticle is a critical protective barrier against environmental stresses (Beisson *et al*. 2012), the decreased expression of cuticle biosynthetic genes and the resulting weakening of the exocarp may trigger additional defense responses such as the deposition of the suberized layer. Additionally, a recent study also showed that the phellem is more plastic than the cuticle layer, which might suggest

that the RAE is able to expand more during the early fruit growth phase (Khanal *et al*. 2013), a hypothesis that may fit with the results observed for cell wall-related genes.

D. Expression of cell wall loosening-related genes was enhanced in russeted tissues

In RAE the expression of a large number of genes implicated in the modification of the main components of primary cell walls, i.e. cellulose, hemicellulose and pectin, was enhanced (Fig. 2-3, Table 2-4). A careful analysis of the results obtained revealed that differences in cellulose synthesis/cellulose microfibrils organization exist between RAE and WAE. Genes coding for a cellulose synthase 6, a fasciclin-like arabinogalactan protein, two other arabinogalactan proteins (AGP) family and a COBRA-like protein were up-regulated. Fasciclin-like AGPs and COBRA proteins are thought to have roles in cell expansion and cellulose microfibrils orientation, and this last aspect is crucial for the modulation of the cell wall stiffness and mechanical properties (Roudier *et al*. 2005, Liepman *et al*. 2010, MacMillan *et al*. 2010). Two xyloglucan endotransglycosylase (*XET*) genes were also found to be up-regulated. Xyloglucan is one of the most abundant hemicelluloses in primary plant walls and is cross-linked with cellulose microfribrils. XETs are considered as the major regulator of cell wall expansion and are able to cleave and elongate xyloglucan (Bourquin *et al*. 2002). Another up-regulated gene involved in cell wall modification codes for an expansin EXLB3-like protein, which is a non-enzymatic protein able to rapidly disrupt hydrogen bonds between cellulose and hemicellulose and thus to participate in cell wall expansion allowing the rapid increase of cell growth (Cosgrove 2005, Sampedro and Cosgrove 2005). Pectin is another major component of primary walls and middle lamellas. Pectin methylesterase (PME) is usually associated with cell wall modifications, in response to biotic and abiotic stimuli, by catalyzing the

Table 2-4: Sub-selection of the differentially expressed genes disccussed in the results part and obtained from the statistical comparison of the RAE against the WAE varieties. Fold changes (-1>$\log_2$ ratio (Russeted apple exocarp group (RAE)/Waxy apple exocarp group (WAE))>1, p-Value<0.05, FDR<0.2) display the difference between the mean expression of genes (RPKM) in RAE divided by the mean expression genes in WAE. Functionnal annotations were obtained from the apple genome consortium and the *Malus* x *domestica* MapMan annotation file.

Biological Process	Feature ID	TAIR name	Gene symbol	Annotation description	Log2 fold change (russet/waxy)
Suberin synthesis					
	mdp0000150502	AT3G11430.1	GPAT5	glycerol-3-phosphate acyltransferase 5	4.23
	mdp0000879217	AT5G58860.1	CYP86A1	cytochrome P450, family 86, subfamily A, polypeptide 1	3.38
	mdp0000923760	AT5G58860.1	CYP86A1	cytochrome P450, family 86, subfamily A, polypeptide 1	3.97
	mdp0000306273	AT5G23190.1	CYP86B1	cytochrome P450, family 86, subfamily B, polypeptide 1	4.75
	mdp0000234292	AT5G23190.1	CYP86B1	cytochrome P450, family 86, subfamily B, polypeptide 1	2.97
	mdp0000312405	AT5G41040.1		Feruloyl-CoA acyl-transferase family protein	3.08
	mdp0000233110	AT4G28570.1		Long-chain fatty alcohol dehydrogenase family protein	2.05
Cutin and wax synthesis					
	mdp0000479163	AT2G38110.1	GPAT6	glycerol-3-phosphate acyltransferase 6	-3.74
	mdp0000200335	AT1G17840.1	ABCG11	ABCG11, white-brown complex homolog protein 11	-4.71
	mdp0000248808	AT1G17840.1	ABCG11	ABCG11, white-brown complex homolog protein 11	-4.49
	mdp0000461409	AT1G02205.2	CER1	Fatty acid hydroxylase superfamily	-4.18
	mdp0000625646	AT1G04220.1	KCS2	3-ketoacyl-CoA synthase 2	-1.50
	mdp0000165547	AT5G57800.1	CER3	Fatty acid hydroxylase superfamily	-2.41
	mdp0000392495	AT1G68530.1	CER6	3-ketoacyl-CoA synthase 6	-4.45
	mdp0000134273	AT2G26250.1	FDH,KCS10	3-ketoacyl-CoA synthase 10	-4.22
	mdp0000235280	AT2G26250.1	FDH,KCS10	3-ketoacyl-CoA synthase 10	-5.62
	mdp0000195926	AT5G53390.1	WSD1	O-acyltransferase (WSD1-like) family protein	-4.94
	mdp0000701887	AT3G49190.1	WSD1	O-acyltransferase (WSD1-like) family protein	-5.45
Terpene synthesis					
	mdp0000207731	AT1G78950.1		Terpenoid cyclases family protein	4.04
	mdp0000951949	AT1G78955.1		Terpenoid cyclases family protein	3.93
	mdp0000205224	AT1G78950.1		Terpenoid cyclases family protein	3.88
	mdp0000194935	AT1G78950.1		Terpenoid cyclases family protein	3.76
	mdp0000553490	AT1G78955.1		Terpenoid cyclases family protein	3.68
	mdp0000227287	AT1G78950.1		Terpenoid cyclases family protein	-1.55
	mdp0000440922	AT5G36110.1	CYP716A1	cytochrome P450, family 716, subfamily A, polypeptide 1	-2.65

Table 2-4 continued…

Biological Process	Feature ID	TAIR name	Gene symbol	Annotation description	Log2 fold change (mock/trans)
Lipid misc.					
	mdp0000233546	AT1G43800.1		Plant stearoyl-acyl-carrier-protein desaturase family protein	3.24
	mdp0000223597	AT2G15230.1	LIP1	Lipase 1, LIP1	2.13
	mdp0000253113	AT3G26040.1		BAHD/HXXXD-type acyl-transferase family protein	5.10
	mdp0000674537	AT3G29670.1		BAHD/HXXXD-type acyl-transferase family protein	2.18
	mdp0000637737	AT5G17540.1		BAHD/HXXXD-type acyl-transferase family protein	-2.06
	mdp0000120595	AT1G24430.1		BAHD/HXXXD-type acyl-transferase family protein	-2.09
	mdp0000120594	AT1G24430.1		BAHD/HXXXD-type acyl-transferase family protein	-2.14
	mdp0000272499	AT1G24430.1		BAHD/HXXXD-type acyl-transferase family protein	-2.61
	mdp0000242697	AT4G29250.1		BAHD/HXXXD-type acyl-transferase family protein	-4.62
	mdp0000146006	AT1G75900.1		GDSL-like Lipase/Acylhydrolase superfamily protein	3.86
	mdp0000136589	AT5G03610.1		GDSL-like Lipase/Acylhydrolase superfamily protein	3.21
	mdp0000660239	AT1G74460.1		GDSL-like Lipase/Acylhydrolase superfamily protein	3.14
	mdp0000928830	AT3G16370.1		GDSL-like Lipase/Acylhydrolase superfamily protein	-3.12
	mdp0000208936	AT3G23410.1	FAO3	fatty alcohol oxidase 3	2.66
	mdp0000951278	AT1G08510.1	FATB	fatty acyl-ACP thioesterases B	1.15
	mdp0000322556	AT5G51290.1		Diacylglycerol kinase family protein	1.31
	mdp0000131182	AT3G51520.1		Diacylglycerol acyltransferase family	1.13
Cell Wall modification					
	mdp0000145104	AT5G64310.1	AGP1	arabinogalactan protein 1	1.62
	mdp0000211411	AT2G46330.1	AGP16	arabinogalactan protein 16	1.13
	mdp0000320017	AT4G25810.1	XTH6	xyloglucan endotransglycosylase 6	1.13
	mdp0000842877	AT5G57560.1	XTH22	Xyloglucan endotransglucosylase/hydrolase family protein	2.82
	mdp0000253802	AT4G15560.1	CLA1	Deoxyxylulose-5-phosphate synthase	1.68
	mdp0000282305	AT4G12730.1	FLA2	FASCICLIN-like arabinogalactan 2	3.03
	mdp0000480237	AT5G64740.1	CESA6	cellulose synthase 6	1.17
	mdp0000120592	AT3G02210.1	COBL1	COBRA-like protein 1 precursor	1.43
	mdp0000756536	AT3G05910.1		Pectinacetylesterase family protein	2.95
	mdp0000129387	AT1G53840.1	PME1	pectin methylesterase 1	1.73
	mdp0000168682	AT1G53840.1	PME1	pectin methylesterase 1	1.68
	mdp0000621927	AT1G53840.1	PME1	pectin methylesterase 1	1.13
	mdp0000223235	AT2G18660.1	EXLB3	EXPANSIN-LIKE B3 PRECURSOR	1.76
Hydroxycinnamic acid synthesis					
	mdp0000602841	AT2G30490.1	C4H	cinnamate-4-hydroxylase	1.98
	mdp0000245663	AT2G30490.1	C4H	cinnamate-4-hydroxylase	1.14
	mdp0000274409	AT5G54160.1	OMT1	O-methyltransferase 1	2.42
	mdp0000310987	AT4G26220.1	CCoAMT	Caffeoyl-CoA methyl-transferase	1.29

Table 2-4 continued…

Biological Process	Feature ID	TAIR name	Gene symbol	Annotation description	Log2 fold change (mock/drought)
	mdp0000123993	AT3G19450.1	CAD4	cinnamyl alcohol dehydrogenase 4	-2.68
	mdp0000322755	AT1G15950.1	CCR1	cinnamoyl coa reductase 1	-1.24
Oxidase					
	mdp0000244884	AT1G65980.1	TPX1	thioredoxin-dependent peroxidase 1	2.20
	mdp0000202801	AT5G48100.1	LAC15	laccase 15	3.02
	mdp0000655646	AT5G48100.1	LAC15	laccase 15	2.99
	mdp0000302838	AT5G09360.1	LAC14	laccase 14	3.22
	mdp0000211955	AT5G09360.1	LAC14	laccase 14	2.91
	mdp0000148967	AT5G09360.1	LAC14	laccase 14	3.89
Transport Misc.					
	mdp0000246150	AT3G22600.1		Bifunctional inhibitor/lipid-transfer protein	2.80
	mdp0000942052	AT2G28070.1		ABC-2 type transporter family protein	1.47
	mdp0000241976	AT5G13580.1		ABC-2 type transporter family protein	3.29
	mdp0000265619	AT2G37360.1		ABC-2 type transporter family protein	2.37
Phytohormone/signaling					
	mdp0000278380	AT5G38280.1	PR5K	PR5-like receptor kinase	1.98
	mdp0000574183	AT5G38280.1	PR5K	PR5-like receptor kinase	1.92
	mdp0000742228	AT3G14460.1		LRR and NB-ARC domains-containing disease resistance protein	3.33
	mdp0000207438	AT3G14460.1		LRR and NB-ARC domains-containing disease resistance protein	1.80
	mdp0000190654	AT3G14460.1		LRR and NB-ARC domains-containing disease resistance protein	1.30
	mdp0000514599	AT5G36930.1		Disease resistance protein (TIR-NBS-LRR class) family	2.72
	mdp0000468499	AT5G36930.2		Disease resistance protein (TIR-NBS-LRR class) family	2.68
	mdp0000289517	AT4G12010.1		Disease resistance protein (TIR-NBS-LRR class) family	2.45
	mdp0000589425	AT1G69550.1		disease resistance protein (TIR-NBS-LRR class)	2.20
	mdp0000310094	AT5G66900.1		Disease resistance protein (CC-NBS-LRR class) family	2.18
	mdp0000570102	AT1G17020.1	SRG1	senescence-related gene 1	1.99
	mdp0000113336	AT1G17020.1	SRG1	senescence-related gene 1	2.01
	mdp0000586656	AT5G47530.1		Auxin-responsive family protein	1.75
	mdp0000283197	AT3G20770.1	EIN3	Ethylene insensitive 3 family protein	2.06
	mdp0000250876	AT4G28640.3	IAA11	indole-3-acetic acid inducible 11	1.10

Table 2-4 end

Biological Process	Feature ID	TAIR name	Gene symbol	Annotation description	Log2 fold change
NAC transcription factor					
	mdp0000282616	AT1G33060.2	NAC014	NAC domain containing protein 14	1.50
	mdp0000232008	AT2G24430.1	NAC038	NAC domain containing protein 38	3.88
	mdp0000128461	AT2G43000.1	NAC042	NAC domain containing protein 42	1.84
	mdp0000130785	AT3G18400.1	NAC058	NAC domain containing protein 58	2.83
	mdp0000276278	AT4G28500.1	NAC073,SND2	NAC domain containing protein 73	2.19
	mdp0000124509	AT4G29230.1	NAC075	NAC domain containing protein 75	3.47
	mdp0000723762	AT4G29230.1	NAC075	NAC domain containing protein 75	3.96
	mdp0000618650	AT4G29230.1	NAC075	NAC domain containing protein 75	3.83
MYB transcription factor					
	mdp0000655330	AT3G13540.1	MYB5	myb domain protein 5	1.09
	mdp0000787808	AT4G12350.1	MYB42	myb domain protein 42	-2.45
	mdp0000291518	AT1G17950.1	MYB52	myb domain protein 52	2.51
	mdp0000852158	AT1G17950.1	MYB52	myb domain protein 52	3.16
	mdp0000157506	AT3G12720.1	MYB67	myb domain protein 67	3.77
	mdp0000322479	AT3G49690.1	MYB84	myb domain protein 84	2.51
	mdp0000320772	AT1G34670.1	MYB93	myb domain protein 93	3.97
	mdp0000228252	AT1G34670.1	MYB93	myb domain protein 93	3.61
	mdp0000149535	AT3G47600.1	MYB94	myb domain protein 94	-3.12
	mdp0000197283	AT4G21440.1	MYB102	myb domain protein 102	2.00
Misc.					
	mdp0000921896	AT5G09530.1		hydroxyproline-rich glycoprotein family protein	3.73
	mdp0000128733	AT4G31940.1	CYP82C4	cytochrome P450, family 82, subfamily C, polypeptide 4	2.87
	mdp0000323033	AT4G37370.1	CYP81D8	cytochrome P450, family 81, subfamily D, polypeptide 8	2.58

de-esterification of pectin with the resulting severing of the bonds with cellulose (Pelloux *et al*. 2007). A large number of *PME*s were found up-regulated in RAE (Table 2-4), together with a gene involved in the synthesis of UDP-glucuronate (*GAE1*), which is the major precursor of pectin (Molhoj *et al*. 2004). Taken altogether, differentially expressed genes related to the cell wall followed a common trend suggesting that enhanced cell wall loosening occurred in RAE compared to WAE. The whole cell wall polysaccharide matrix composed of cellulose, hemicellulose and pectin might be impacted by the differential expression of the above-mentioned genes, thereby modifying the relative abundance of the different polysaccharides and severing the interchain bonds connecting them. Peroxidases might be involved in a wall loosening mechanism (Passardi *et al*. 2004) and in this respect it is tempting to speculate that they could contribute to the differences observed between RAE and WAE. However, it should be noted that in our results only very few peroxidases showed significant differences in expression levels, therefore further studies are needed to validate this hypothesis.

During apple fruit growth, the increase of fruit size is mainly limited by the expansion of the epidermis (Curry 2009, Khanal *et al*. 2013). The sigmoidal increase of fruit size induced the cell enlargment triggers extreme biaxial tangential tensions and these mechanical stresses lead, in certain cases, to tissue disruption and microcracks in the primary fruit skin *i.e*. cuticle, epidermis and hypodermis (Watanabe 1969, Skene 1982, Curry 2009, Khanal *et al*. 2013). The development of fleshy fruit is characterized by stages of significant expansion which must necessarily be accompanied by deep modifications of the cell walls. The expansion phase experienced by the growing fruit implies an active synthesis and deposition of cuticular membrane constituents which contribute to the overall strength of the skin surface. Hence, it is clear that a fine cross-talk exists and is

activated during fleshy fruit development and expansion and delicate regulatory mechanisms must coordinate these crucial events. It is already described that critical cell wall-related factors control the onset of cracking susceptibility in fruit: the activities of wall-modifying enzymes, for instance β-galactosidases, can have important effects in cracking tolerance (Balbontin *et al*. 2014). Overexpression of a pectin methylesterase inhibitor (PMEI5) in *A. thaliana* triggers dramatic changes in stems, which appear curly and display altered biomechanical properties and failure of organ separation (Müller *et al*. 2013). Notably these overexpressing lines also show defects associated with an altered cuticle development: the cuticle indeed appears discontinuous (Müller *et al*. 2013).

E. Strong differential expression of the suberin deposition-related genes in the russeted apples

As expected, the RAE tissues displayed several strongly expressed key genes related to suberin synthesis and deposition compared to the waxy group (Fig. 2-4, Fig. 2-6, Table 2-4). Comparison of RAE to WAE revealed differences in the expression of genes of the phenylpropanoid biosynthetic pathway (Fig. 2-4). This family of secondary metabolites, which includes ferulic acid, *p*-coumaric acid and caffeic acid, are partly involved in determining the structure of both suberin SPAD and SPPD (Pollard *et al*. 2008, Beisson *et al*. 2012). Two cinnamate-4-hydroxylases (*C4H*), a caffeoyl-CoA-O-methyltransferase (*CCoAOMT*) and a caffeate-O-methyltransferase (*COMT*) genes were strongly expressed, suggesting that the hydroxycinnamic acid and especially ferulic acid synthesis was enhanced in RAE. A feruloyl-CoA acyltransferase gene was also found among the large number of differentially regulated BAHD family acyltransferase genes (Table 2-4). This gene has been already described in *A. thaliana* and *S. tuberosum* to be a key player of the ω-hydroxyacyl- ferulate synthesis, which are suberin monomers found in the suberin aliphatic domain (Gou *et al*. 2009, Molina *et al*. 2009, Boher

et al. 2013). Conversely, some monolignol synthesis genes, encoding a cinnamoyl-CoA reductase (*CCR*) and cinnamyl alcohol dehydrogenases (*CAD4* and *CAD9*-like genes) were less expressed in russeted apples (Table 2-4). In russeted Sand Pear, a repression of the *CCR* and *CAD* genes was also observed and may contribute to the russet pigmentation of the exocarp (Wang *et al*. 2014a, Wang *et al*. 2014b). Previous experiments also showed a reduced activity and expression of the *CCR* and *CAD* in the suberized tissues with concomitant decreased lignin precursor content (Bernards *et al*. 2000, Bernards 2002). Indeed, the SPPD shares a similar structure and localization in the cell wall with lignin, but displays a contrasting composition. As previously mentioned, the amount of monolignols in the SPPD is lower than in lignin, whereas hydroxycinnamic acids are more abundant (Bernards *et al*. 1995, Bernards 2002). This decreased expression of lignin precursor's synthesis genes in the SPPD may further favor the cell wall loosening and expansion as suggested earlier (Moura *et al*. 2010).

The SPPD assembly is still not fully understood. However, in *S. tuberosum*, *S. lycopersicum* and *A. thaliana*, hypotheses involving the participation of oxidizing enzymes such as oxidase/peroxidase couples and/or laccases, have been proposed (Quiroga *et al*. 2000, Bernards and Razem 2001, Soler *et al*. 2007, Pollard *et al*. 2008). Based on the data from the present study these two hypotheses seem to be conceivable. Increased expression of amine oxidase and peroxidase genes, including a thioredoxin peroxidase (*TPX1*)-like gene, was found in RAE (Table 2-4, SI Table 2-2). In tomato, expression of the TPX1 cell wall basic peroxidase is enhanced in lignified/suberized roots, but the involvement of other peroxidases is also suspected (Quiroga *et al*. 2000). Additionally, a higher expression of several laccase genes was noted in the russeted tissues (*LAC14* and *LAC15*, Table 2-4). Although laccases seem to be involved in lignin metabolism in the secondary cell wall, their role is not clearly understood. The *LAC15* gene has been linked

with the synthesis of lignin in seeds and roots during elongation (Liang *et al*. 2006), but the involvement of laccases in suberin synthesis is so far only suspected (Soler *et al*. 2007, Pollard *et al*. 2008). Nevertheless, the similar structure of lignin and the SPAD, together with the enhanced expression of laccase genes observed in the russeted apple tissues, as well as in the cork of *Q. suber* (Soler *et al*. 2007) and the russeted exocarp of *Pyrus pyrifolia* (Wang *et al*. 2014a), lead to speculate about the implication of laccases in suberin metabolism.

Gene ontology enrichment and the qPCR analysis highlight the importance of a group of genes implicated in the synthesis of SPAD monomers (Table 2-4, Fig. 2-4, Fig. 2-5). The most differentially expressed genes included the well-known *CYP86A1* and *CYP86B1*, which encode fatty acid hydroxylase and a very long-chain fatty acid hydroxylase, respectively. These genes code for proteins involved in the early synthesis steps of ω-hydroxyacid suberin monomer precursors (Benveniste *et al*. 1998, Kurdyukov *et al*. 2006, Compagnon *et al*. 2009, Hofer *et al*. 2008, Pinot and Beisson 2011). In contrast to the behavior of the cutin-related GPAT6, the GPAT5-like is an alternative isoform of the GPAT enzyme family, which was also strongly expressed in the RAE (Fig. 2-4, Fig. 2-5). In *A. thaliana* roots, this enzyme is considered as the key regulator of the suberin monomer synthesis, linking ω-hydroxyacyl and α,ω-dicarboxylicacyl-CoA precursors to glycerol (Beisson *et al*. 2007). To date, it is not clearly understood how acyls are supplied for the synthesis of these monomers (Pollard *et al*. 2008). In the present experiment, despite the lower expression of the primary fatty acid synthesis genes (FAE complex) observed in the RAE, a significant number of glycolysis-related genes, including many pyruvate kinase genes, were significantly more expressed, reflecting a potential remobilization of sugar for acetyl-CoA synthesis (Fig. 2-3, SI Table 2-2). Moreover, higher expression of genes for acyl-ACP thioesterase (*FATB*) and desaturase, which are responsible for the final fatty acid elongation

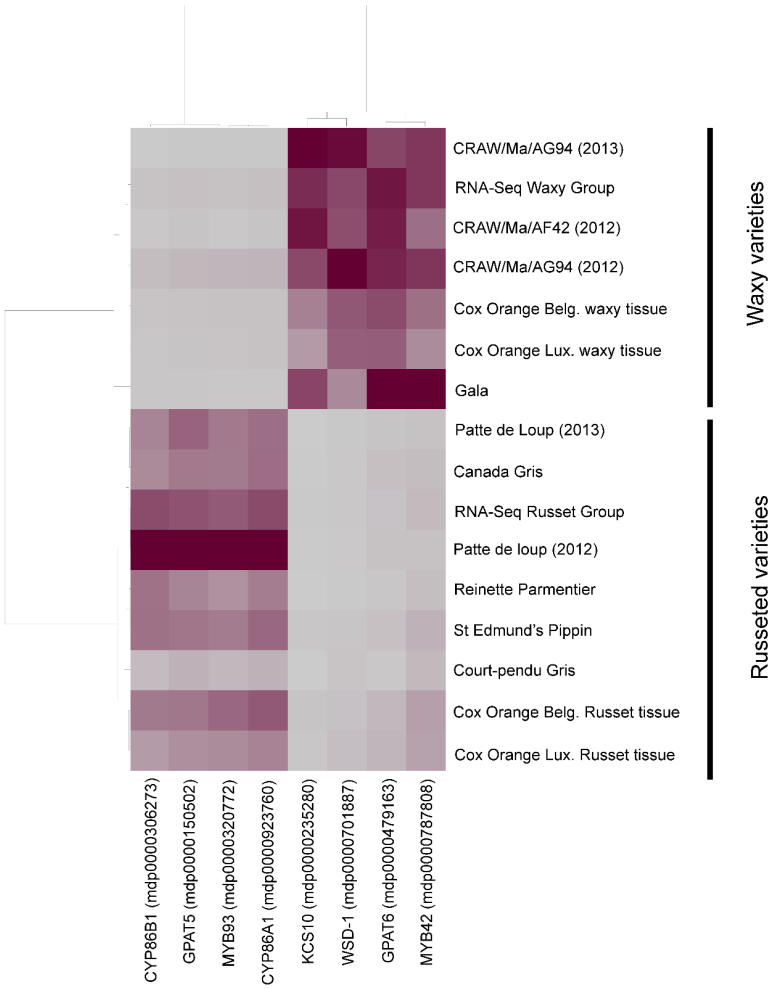

Figure 2-5: Hierarchical clustering performed based on qPCR results with correlation similarity metrics and complete linkage. Eight suberin-related genes described in the Table 2-2: suberin biosynthesis: GPAT5 (MDP0000150502), CYP86A1 (MDP0000923760), CYP86B1 (MDP0000306273); cuticle biosynthesis: GPAT6 (MDP0000479163), WSD-1 (MDP0000701887), KCS10 (MDP0000235280); transcription factors: MYB93 (MDP0000320772), MYB42 (MDP0000787808). For each gene, normalized relative quantities were rescaled to the most expressed sample (max NRQ=1 in dark purple, min NRQ=0 in grey). Full data and statistical analysis is available in the SI Table 2-1.

and desaturation, was observed in RAE (Table 2-4) and seems to be associated with the expression of the *GPAT5* gene (Fig. 2-6).

FATB plays an essential role in saturated fatty acid synthesis, suggesting an increased synthesis of C16:0, C18:0 in the RAE (Bonaventure *et al*. 2003). Alternative sources of acyl precursors might also be considered. Indeed, some triacylglycerol and fatty acid degradation genes were also more expressed, *i.e*. triacylglycerol lipase 3, lipase LIP1, glycerophosphodiester phosphodiesterase and acyl-CoA oxidase, and might provide an alternative source of acyls and glycerol (Table 2-4, SI Table 2-2). The mechanisms for final suberin polymerization and its localization remain unclear, recent reviews and experiments showed that suberin monomers might be localized in the apoplast and hypotheses about the mechanism involved in the exportation of these monomers have been proposed (Graca and Santos 2007, Pollard *et al*. 2008, Beisson *et al*. 2012). Among the large number of differentially expressed transport-related genes, a number of ABCG-like transporters, lipid transfer proteins and vesicles-associated proteins were up-regulated in RAE (Table 2-4, SI Table 2-2). Interestingly, genes for a lipid-transfer protein and an ABCG (ABC-2) type transporter present multiple interactions with some of the key suberin synthesis genes, suggesting a functional link in the transport of suberin monomers (Fig. 2-6). As mentioned above, ABCG11 which is implicated in cutin monomer transport was down-regulated in RAE, suggesting that specific isoforms are implicated in the transport of cutin or the suberin monomers. Further functional analyses have to be performed to unravel the involvement of these transporters in the suberin deposition process. To date, GDSL-motif lipases/esterases are considered as the best candidates for cutin and suberin polymerization (Mahapatro *et al*. 2004, Olsson *et al*. 2007, Pollard *et al*. 2008, Beisson *et al*. 2012). In the present data,

three GDSL-motif lipase/esterase genes were strongly up-regulated and one was strongly down-regulated, suggesting that the final assembly of cutin and suberin is performed using polymer-specific esterases (Table 2-4). The protein association network analysis (Fig. 2-6) shows a relatively weak correlation between one of these GDSL-motif lipases and suberin monomer key synthesis genes i.e. GPAT5, CYP86A1, CYP86B1, FATB and the ABCG type transporter mentioned above, suggesting that this gene may be part of a co-regulated network of genes in this process. Nevertheless, further analyses have to be carried out to validate whether it plays a role in the polymerization process.

F. Differential expression of cuticle synthesis- and suberin deposition-related genes goes along with the expression of specific triterpene synthesis gene

In addition to the strong enhancement of the suberin synthesis-related genes observed in russeted apples, a significant number of triterpene biosynthetic genes were differentially regulated (Fig. 4, Table 2-4). Pentacyclic triterpenes are particularly interesting for their pharmacological properties including anti-inflammatory, antitumor, and anti-HIV activities. They belong to a large family of 30-carbon terpenes that are embedded in the leaf, fruit skin cuticle and tree bark (Watanabe 1969, Brendolise *et al*. 2011, Andre *et al*. 2013). In the apple skin, three major families of pentacyclic triterpenes are highly abundant: ursane-, oleane- and lupane-series (Andre *et al*. 2012). The respective precursors of these triterpene families, α-amyrin, β-amyrin and lupeol, are produced by cyclization of the 2,3-oxidosqualene precursor by multifunctional oxidosqualene cyclases (OSCs). Remarkably, waxy apples have a higher content of ursolic (ursane) and oleanolic acid (oleane), whereas russeted apples have a higher betulinic acid (lupane) content, as well as some specific triterpene-caffeate conjugates (Andre *et al*. 2013). However, only a few genes involved in the triterpene synthesis have

been identified so far. In the present data (Table 2-4), many *OSC* genes were differentially regulated. Only one *OSC* gene sharing more than 99% identity with the *MdOSC1* gene, was less expressed in the RAE (Brendolise *et al*. 2011). MdOSC1 is responsible for the synthesis of both α- and β-amyrin with a 5:1 ratio, confirming the lower amount of ursolic and oleanolic acid generally found in russeted apple (Brendolise *et al*. 2011). Five *OSC* genes, which were strongly expressed in the russeted tissues, might be implicated in lupeol synthesis, but the genes responsible for this biosynthetic step have not yet been identified. Therefore, further functional analysis needs to be performed to validate this hypothesis. Gene(s) implicated in the oxygenation of the α-amyrin, β-amyrin and lupeol have not yet been identified in apple, but a *CYP716A* family gene (Table 2-4), highly similar to a gene for the triterpene synthesis multifunctional oxidase identified in *M. truncatula*, was strongly down-regulated in the RAE (Fukushima *et al*. 2011). Interestingly, the concomitant higher amount of both lupeol and betulinic acid observed in the 'Merton Russet' variety compared to waxy ones such as 'Royal Gala' might be explained by a similar regulation of the *CYP716A* gene (Andre *et al*. 2013). Finally, the recent observation of the betulinic acid-3-trans caffeate conjugate in the 'Merton Russet' variety and earlier in *Q. suber*, suggests that shared enzymes with the suberin synthesis pathway might result in the synthesis of these compounds. As an example, some hydroxycinnamoyl transferase such as the feruloyl-CoA acyl transferase candidate genes found in the present experiment might be involved in this reaction.

G. Stress responses signaling cascades and transcription factors were strongly enhanced in russeted apple

The lower expression of cuticle synthesis genes may result in micro-cracks in the cuticle observed in many studies. As the cuticle plays a critical role as a hydrophobic barrier against the environment and limits water loss or gas

exchange, we hypothesize that the relative lack of efficient protection triggers a boosted stress response signaling cascade and transcription factors expression in russeted apple. This postulate is substantiated by the activation in RAE of a large set of genes related to the stress response machinery, like genes related to the signal transduction, stress, hormone metabolism or RNA processing (Fig. 2-2). Genes for transmembrane pattern recognition receptors (*PRR*), such as *PR5K*, lectin, LRR-motif and wall-associated kinases (*WAK1*) are highly expressed, which is usually observed during biotic and to a lower extent abiotic stress exposure. A similar expression pattern was also observed in *Pyrus pyrifolia*, where a large number of disease resistance response proteins were more expressed in the russeted pericarps (Wang *et al*. 2014a). Expression of many TIR-NBS-LRR-motif disease genes (intracellular PRR) is also increased (Table 2-4, SI Table 2-2). PRR proteins are involved in the recognition and transduction of biotic stress signals, e.g. microbial and damage stimuli, and trigger defense responses and cell apoptosis through the hypersensitive response mechanism (Belkhadir *et al*. 2004, Tor *et al*. 2009). The increased expression of the gene for wall associated kinase WAK1, which is implicated in cell wall loosening and expansion, and the cell wall-related expression pattern discussed above, support the hypothesis that enhanced cell wall expansion and loosening occur in RAE.

The downstream phytohormonal regulation is slightly different between the two apple groups and although the primary sensing implicated some biotic stress-like responsive genes, only a few genes related to salicylic and jasmonic acid degradation were differentially expressed, suggesting that the supposed "stress state" of russeted apple is more particular and may not involve the common wounding and biotic stress response. Conversely, a number of genes implicated in auxin and ethylene signaling pathways are more expressed in russeted apple (Table 2-4, SI Table 2-2). To our knowledge, the involvement of auxin regulatory

pathways in the suberization process has not been investigated and ethylene seems to have no effect on wound-induced suberization in *S. tuberosum* (Lulai and Suttle 2004). But, due to the major roles of auxin and ethylene in fruit development, growth and ripening and their strong implication in the present data, some involvement in the russeted phenotype may be expected. Indeed, specific senescence-related gene 1 (*SRG1*) ACC oxidase and flavonol synthase genes displayed an increased expression, whereas other non-SRG1 ACC oxidase genes were less expressed (SI Table 2-2). Multiple auxin-induced growth regulators and an IAA-amino acid conjugate hydrolase (ILR) were also found. Recent studies demonstrate the tight crosstalk between these two phytohormones, which are able to regulate each other i.e. accumulation of auxin and ethylene down-regulation, through flavonol accumulation and auxin efflux (Lewis *et al*. 2011). This is in accordance with the decreased expression of genes classified in the auxin efflux and basipetal transport GO process (Fig. 2-4). In apple fruit, increased auxin content is able to trigger cell expansion (Devoghalaere *et al*. 2012). As previously discussed, the present data suggests that an accumulation of auxin, through the *ILR* gene and the lower efflux, might occur and lead to enhanced cell expansion in RAE.

A large number of transcription factor genes were differentially expressed, including members of families such as the bHLH, AP2/EREBP, C2H2, NAC-domain and R2R3-MYB and MYB-related (Table 2-4, SI Table 2-2). Although some of these families are suspected to be involved in the regulation of the suberization process, to date few candidates have been identified *in planta* and none in apple. A significant number of transcription factor genes belonging to the NAC-domain family such as *NAC038*, *NAC058*, *NAC073*, *NAC075*, were strongly expressed in RAE (Table 2-4). NAC family transcription factors participate in the regulation of a broad spectrum of biological processes in plants. In rice,

OsNAC075 is responsive to abiotic stress such as salt and cold stress (Jung *et al*. 2011). Interestingly, *NAC058* displayed a slight interaction (confidence=0.534) association with the *CYP86A1* gene, but no clear evidence of the involvement of NAC transcription factor has been found yet (Fig. 2-6). The R2R3-MYB transcription factor family is implicated in many biological processes such as metabolism, plant development or defense and displayed the most significant differences (Table 2-4, SI Table 2-2). In the present study *MYB93*, *MYB67*, *MYB68*, *MYB52*, *MYB5* and *MYB102*-like transcription factor genes were strongly expressed in russeted apple, whereas *MYB94* and *MYB42* were less expressed (Table 2-4). *MYB52* and *MYB42* were classified in the GO "regulation of the secondary cell wall biogenesis", together with *ANAC073/SND2*, which is also up-regulated in russeted apple skin (Fig. 2-4). Their functions are not fully understood, but they are part of the second regulatory layer of secondary cell wall biogenesis, which is driven by the master *SND1* regulatory gene, and involved in the regulation of secondary cell wall thickening (Zhong *et al*. 2008). Recent investigations showed that MYB52, which is co-expressed with SND2, may be a repressor of the lignin biosynthesis and secondary cell wall formation (Cassan-Wang *et al*. 2013). SND2 regulates cellulose, xylan and mannan synthesis as well as lignin polymerization (laccase), but is not involved in the regulation of monolignol synthesis (Hussey *et al*. 2011). In maize, *MYB42* is responsive to wounding and represses *COMT* and to a lower extent the *C4H*, *4CL* and *CAD6* genes, which leads to a decreased lignin deposition (Fornale *et al*. 2006). In the present study, the expression of MYB42 seemed to be associated with the RAE (Table 2-4, Fig. 2-5) and a concomitant increase in the expression of *COMT* and *C4H* genes was observed (Table 2-4), while *CAD4* and *CAD9* remained less expressed suggesting that additional regulatory processes occur. The stronger expression of the cell wall loosening-related genes observed in the present study

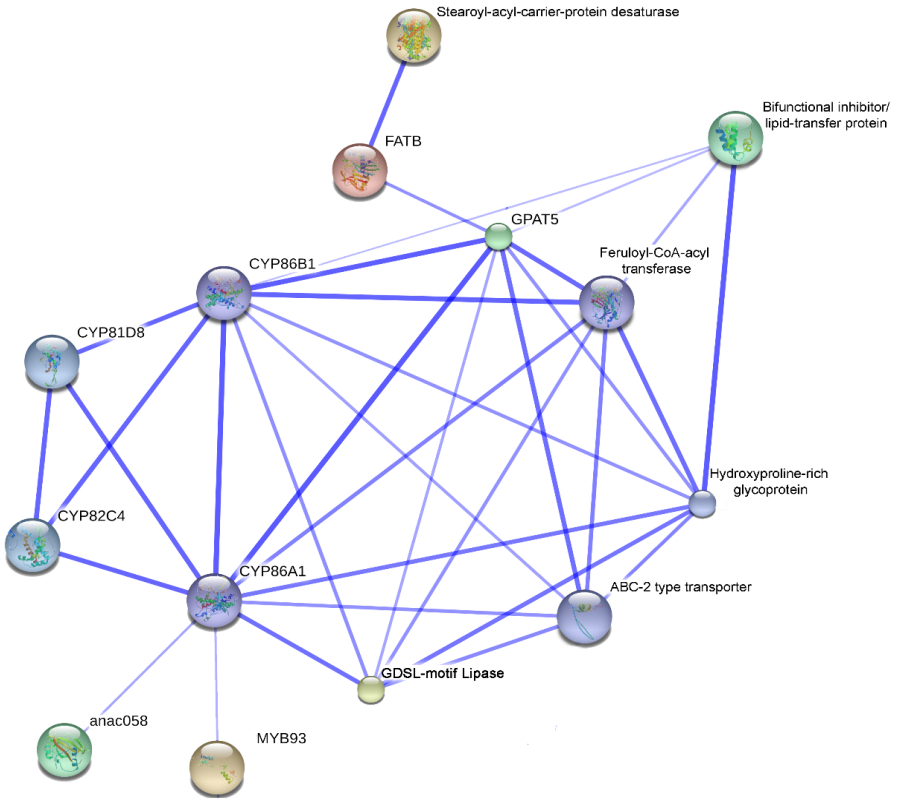

Figure 2-6: Suberin candidate gene interaction matrix performed in STRING using the TAIR accessions of glycerol-3-phosphate acyl transferase 5 (GPAT5, accession number mdp0000150502), CYP86A1 fatty acid hydroxylase (mdp0000879217, mdp0000923760), CYP86B1 very long-chain fatty acid hydroxylase (mdp0000306273, mdp0000234292), CYP81D8 isoflavone 2'-hydroxylase (mdp0000323033), CYP78C4 (mdp0000128733), anac058-like transcription factor (mdp0000130785), MYB93-like (mdp0000320772, mdp0000228252), GDSL-motif lipase (mdp0000660239), ABC-2 type transporter (mdp0000241976), hydroxyproline-rich glycoprotein (mdp0000921896), feruloyl-CoA-acyl transferase (mdp0000312405), bifunctional inhibitor/lipid-transfer protein (mdp0000246150), fatty acyl-ACP thioesterases B (FATB, mdp0000951278), stearoyl-acyl-carrier-protein desaturase (mdp0000233546). Blue lines represent the gene interaction confidence (ranged from 0 to 1): thickest lines display confidence scores higher than 0.9, thinnest lines display confidence scores between 0.4 and 0.7.

might be linked to the increased expression of MYB102, which enhances the expression of expansin, *XET* or pectin esterase genes in response to wounding in *A. thaliana* (De Vos *et al*. 2006). As these R2R3-MYB transcription factors play a role in secondary cell wall modification, we can speculate that they might also be involved in the suberization process. Moreover, the function of *MYB93*, *MYB67* and *MYB94* transcription factor genes, which displayed the largest differences in expression, is not known. Particular interest should be given to the MYB93 transcription factor, which displays a weak interaction with the CYP86A1 fatty acid ω-hydroxylase in the STRING analysis (Fig. 2-6). However, qPCR data (Fig. 2-5) shows a high Pearson correlation coefficient between MYB93 and GAPT5, CYP86A1, CYP86B1, with R^2=0.987, 0.976 and 0.976 respectively (p-Value<0.0001). In *A. thaliana*, AtMYB93 is induced by auxin and acts as a repressor of lateral root development (Gibbs *et al*. 2014), but no studies related to the involvement of MYB93 in suberization are available. Further investigations have to be done to clarify whether these regulators play any role in the russeted phenotype.

In plants, russeting occurs in response to various stimuli. However, in russeted and semi-russeted apple varieties, this phenotype can be observed without any direct external stress exposure. Previous studies showed that the tensions caused by the growing fruit on the periderm can lead to cracks in the cuticle, which in turn leads to suberin deposition. The present study provides a comprehensive picture of the causes, consequences and actors of russeting. An unexpected result is the differential expression of numerous cell wall-related genes, which suggests a stronger loosening of the cell wall in russeted apple skin concomitantly with a lower expression of cuticle deposition-related genes, i.e.

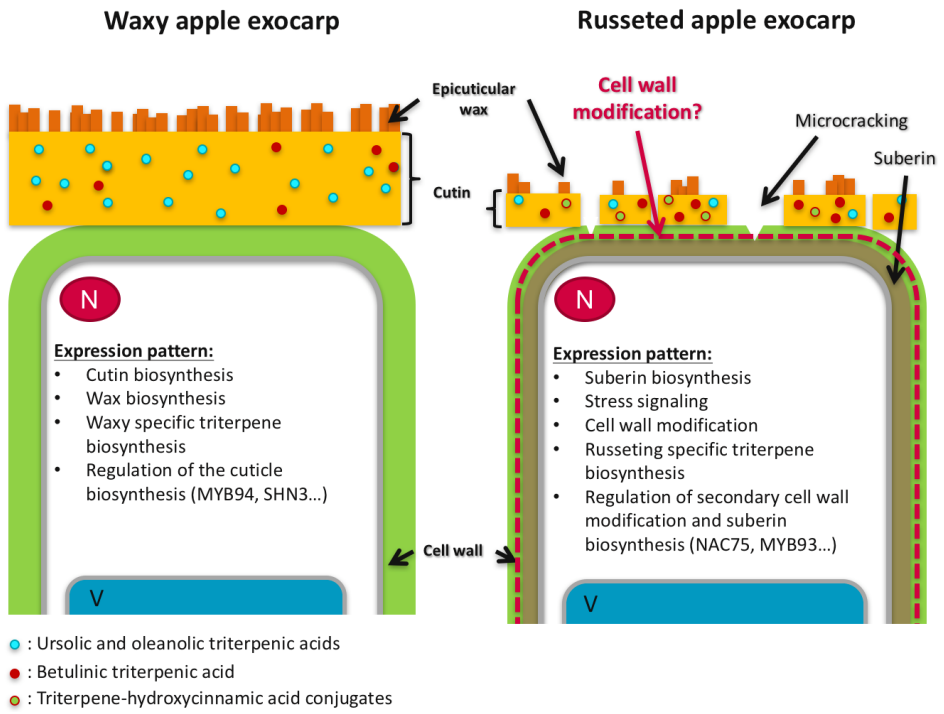

Figure 2-7: Schematic overview of the expression patterns observed in waxy and russeted apple exocarps based on the RNA-Seq data. The exocarpic structure and the representation of the triterpene content are based on the current knowledge of waxy and russeted apple skin (André *et al*. 2013, Lashbrooke *et al*. 2015). N: nucleus, V: vacuole.

genes involved in cutin and wax synthesis (Fig. 2-7). The alterations of the peridermal composition and the weakening of the protective barrier due to the mechanical stress may explain the increased expression of numerous genes involved in stress responsive signaling and regulatory machinery, which probably initiates the synthesis and deposition of suberin as well as the synthesis of specific triterpenes (Fig. 2-7).

Taken altogether, these data confirm previous hypotheses, which postulate that suberin occurrence is tightly linked to the integrity of the cuticle layer.

Additionally, this particular experimental design provides a large coverage of orthologous genes implicated in apple skin russeting and unveils new players related to suberin synthesis and its regulation.

Aknowledgements: The authors thank the 'Centre Régional de Ressources Phytogénétiques' (CRRG) for providing the delivery 'Reinette Parmentier' and 'Patte de Loup' varieties to the CRA-W. Sylvain and Jean-Francois Hausman are grateful to the National Research Funds (FNR, Luxembourg) for partial funding (AFR ID: 9208308). The authors also acknowledge Pr. Lucien Hoffmann, Pr. Marc Boutry and Dr. Kjell Sergeant for their critical reading and Aude Corvisy for her precious technical support.

References

Andre CM, Greenwood JM, Walker EG, Rassam M, Sullivan M, Evers D, Perry NB, Laing WA. 2012. Anti-inflammatory procyanidins and triterpenes in 109 apple varieties. *Journal of Agricultural Food Chemistry* **60**:10546-10554.

Andre CM, Larsen L, Burgess EJ, Jensen DJ, Cooney JM, Evers D, Zhang J, Perry NB, Laing WA. 2013. Unusual immuno-modulatory triterpene-caffeates in the skins of russeted varieties of apples and pears. *Journal of Agricultural Food Chemistry* **61**: 2773-2779.

Baggerly KA, Deng L, Morris JS, Aldaz CM. 2003. Differential expression in SAGE: accounting for normal between-library variation. *Bioinformatics* **19**: 1477-1483.

Balbontin C, Ayala H, Rubilar J, Cote J, Figueroa CR. 2014. Transcriptional analysis of cell wall and cuticle related genes during fruit development of two sweet cherry cultivars with contrasting levels of cracking tolerance. *Chilean Journal of Agricultural Research* **74**

Barabdoozi FN, Talaie A. 2009. The effect of gibberellins on russeting in Golden Delicious apples. *Journal of horticulture and forestry* **1**:061-064.

Baxter I, Hosmani PS, Rus A, Lahner B, Borevitz JO, Muthukumar B, Mickelbart MV, Schreiber L, Franke RB, Salt DE. 2009. Root suberin forms an extracellular barrier that affects water relations and mineral nutrition in *Arabidopsis*. *PLoS Genetics* **5**: e1000492.

Beisson F, Li Y, Bonaventure G, Pollard M, Ohlrogge JB. 2007. The acyltransferase GPAT5 is required for the synthesis of suberin in seed coat and root of *Arabidopsis*. *The Plant Cell* **19**:351-368.

Beisson F, Li-Beisson Y, Pollard M. 2012. Solving the puzzles of cutin and suberin polymer biosynthesis. *Current opinion in plant biology* **15**:329-337.

Belkhadir Y, Subramaniam R, Dangl JL. 2004. Plant disease resistance protein signaling: NBS-LRR proteins and their partners. *Current opinion in plant biology* **7**:391-399.

Benveniste I, Tijet N, Adas F, Philipps G, Salaun JP, Durst F. 1998. CYP86A1 from *Arabidopsis thaliana* encodes a cytochrome P450-dependent fatty acid

omega-hydroxylase. *Biochemical and Biophysical Research Communications* **243**: 688-693.

Bernards MA. 2002. Demystifying suberin. *Canadian Journal of Botany* **80**: 227-240.

Bernards MA, Lopez ML, Zajicek J, Lewis NG. 1995. Hydroxycinnamic acid-derived polymers constitute the polyaromatic domain of suberin. *The journal of Biological Chemistry* **270**: 7382-7386.

Bernards MA, Razem FA. 2001. The poly(phenolic) domain of potato suberin: a non-lignin cell wall bio-polymer. *Phytochemistry* **57**: 1115-1122.

Bernards MA, Susag LM, Bedgar DL, Anterola AM, Lewis NG. 2000. Induced phenylpropanoid metabolism during suberization and lignification: a comparative analysis. *Journal of Plant Physiology* **157**: 601-607.

Bindea G, Galon J, Mlecnik B 2013. CluePedia Cytoscape plugin: pathway insights using integrated experimental and *in silico* data. *Bioinformatics* **29**: 661-663.

Bindea G, Mlecnik B, Hackl H, Charoentong P, Tosolini M, Kirilovsky A, Fridman WH, Pages F, Trajanoski Z, Galon J. 2009. ClueGO: a Cytoscape plug-in to decipher functionally grouped gene ontology and pathway annotation networks. *Bioinformatics* **25**:1091-1093.

Boher P, Serra O, Soler M, Molinas M, Figueras M. 2013. The potato suberin feruloyl transferase FHT which accumulates in the phellogen is induced by wounding and regulated by abscisic and salicylic acids. *Journal of Experimental Botany* **64**: 3225-3236.

Bonaventure G, Salas JJ, Pollard MR, Ohlrogge JB. 2003. Disruption of the FATB gene in *Arabidopsis* demonstrates an essential role of saturated fatty acids in plant growth. *The Plant Cell* **15**: 1020-1033.

Bourquin V, Nishikubo N, Abe H, Brumer H, Denman S, Eklund M, Christiernin M, Teeri TT, Sundberg B, Mellerowicz EJ. 2002. Xyloglucan endotransglycosylases have a function during the formation of secondary cell walls of vascular tissues. *The Plant Cell* **14**: 3073-3088.

Brendolise C, Yauk YK, Eberhard ED, Wang M, Chagne D, Andre C, Greenwood DR, Beuning LL. 2011. An unusual plant triterpene synthase with

predominant alpha-amyrin-producing activity identified by characterizing oxidosqualene cyclases from *Malus* x *domestica*. *FEBS Journal* **278**: 2485-2499.

Bustin SA, Benes V, Garson JA, Hellemans J, Huggett J, Kubista M, Mueller R, Nolan T, Pfaffl MW, Shipley GL, Vandesompele J, Wittwer CT. 2009. The MIQE guidelines: minimum information for publication of quantitative real-time PCR experiments. *Clinical Chemistry* **55**: 611-622.

Cassan-Wang H, Goue N, Saidi MN, Legay S, Sivadon P, Goffner D, Grima-Pettenati J. 2013. Identification of novel transcription factors regulating secondary cell wall formation in *Arabidopsis*. *Frontiers in Plant Science* **4:** 189.

Compagnon V, Diehl P, Benveniste I, Meyer D, Schaller H, Schreiber L, Franke R, Pinot F. 2009. CYP86B1 is required for very long chain omega-hydroxyacid and alpha, omega-dicarboxylic acid synthesis in root and seed suberin polyester. *Plant Physiology* **150**: 1831-1843.

Cosgrove DJ 2005. Growth of the plant cell wall. *Nature Reviews. Molecular Cell Biology* **6**: 850-861.

Curry EA 2009. Growth-induced microcracking and repair mechanisms of fruit cuticles. Proceedings of the SEM annual conference.

De Vos M, Denekamp M, Dicke M, Vuylsteke M, Van Loon LC, Smeekens SC, Pieterse CM. 2006. The *Arabidopsis thaliana* transcription factor AtMYB102 functions in defense against the insect herbivore *Pieris rapae*. *Plant Signal and Behaviour* **1**: 305-311.

Devoghalaere F, Doucen T, Guitton B, Keeling J, Payne W, Ling TJ, Ross JJ, Hallett IC, Gunaseelan K, Dayatilake GA, Diak R, Breen KC, Tustin DS, Costes E, Chagne D, Schaffer RJ, David KM. 2012. A genomics approach to understanding the role of auxin in apple (*Malus* x *domestica*) fruit size control. *BMC Plant Biology* **12**: 7.

Faust M, Shear C. 1972. Russeting of apples, an interpretative review. *HortScience* **7**: 233-235.

Fornale S, Sonbol FM, Maes T, Capellades M, Puigdomenech P, Rigau J, Caparros-Ruiz D. 2006. Down-regulation of the maize and *Arabidopsis thaliana* caffeic acid O-methyl-transferase genes by two new maize R2R3-MYB transcription factors. *Plant Molecular Biology* **62**: 809-823.

Franke R, Briesen I, Wojciechowski T, Faust A, Yephremov A, Nawrath C, Schreiber L. 2005. Apoplastic polyesters in *Arabidopsis* surface tissues - a typical suberin and a particular cutin. *Phytochemistry* **66**: 2643-2658.

Franke R, Schreiber L. 2007. Suberin - a biopolyester forming apoplastic plant interfaces. *Current Opinion Plant Biological* **10**: 252-259.

Fukushima EO, Seki H, Ohyama K, Ono E, Umemoto N, Mizutani M, Saito K, Muranaka T. 2011. CYP716A subfamily members are multifunctional oxidases in triterpenoid biosynthesis. *Plant Cell Physiology* **52**: 2050-2061.

Gasic K, Hernandez A, Korban S. 2004. RNA extraction from different apple tissues rich in polyphenols and polysaccharides for cDNA library construction. Plant Molecular Biological Report **22**: 437a-437g.

Gibbs DJ, Voß U, Harding SA, Fannon J, Moody LA, Yamada E, Swarup K, Nibau C, Bassel GW, Choudhary A *et al.* 2014. AtMYB93 is a novel negative regulator of lateral root development in Arabidopsis. *New Phytologist* **203**: 1194-1207.

Gildemacher P, Heijne B, Silvestri M, Houbraken J, Hoekstra E, Theelen B, Boekhout T. 2006. Interactions between yeasts, fungicides and apple fruit russeting. *FEMS Yeast Research* **6**: 1149-1156.

Gou JY, Yu XH, Liu CJ. 2009. A hydroxycinnamoyltransferase responsible for synthesizing suberin aromatics in *Arabidopsis*. *Proceedings of National Academy of Science USA* **106**:18855-18860.

Graca J, Pereira H. 2000a. Methanolysis of bark suberins: analysis of glycerol and acid monomers. *Phytochemical Analysis* **11**: 45-51.

Graca J, Pereira H. 2000b. Suberin structure in potato periderm: glycerol, long-chain monomers, and glyceryl and feruloyl dimers. *Journal Agricultural Food Chemical* **48**: 5476-5483.

Graca J, Santos S. 2007. Suberin: a biopolyester of plants' skin. *Macromolecular Bioscience* **7**: 128-135.

Hellemans J, Mortier G, De Paepe A, Speleman F, Vandesompele J. 2007. qBase relative quantification framework and software for management and automated analysis of real-time quantitative PCR data. *Genome Biology* **8**: R19.

Hofer R, Briesen I, Beck M, Pinot F, Schreiber L, Franke R. 2008. The *Arabidopsis* cytochrome P450 CYP86A1 encodes a fatty acid omega-hydroxylase involved in suberin monomer biosynthesis. *Journal of Experimental Botany* **59**: 2347-2360.

Hussey SG, Mizrachi E, Spokevicius AV, Bossinger G, Berger DK, Myburg AA. 2011. SND2, a NAC transcription factor gene, regulates genes involved in secondary cell wall development in Arabidopsis fibres and increases fibre cell area in *Eucalyptus*. *BMC Plant Biology* **11**: 173.

Jung YJ, Lee MC, Kang KK. 2011. A transcription factor "OsNAC075" is essential for salt resistance in rice (*Oryza sativa* L.). *Journal of Plant Biotechnology* **38**: 94-104.

Khanal BP, Grimm E, Knoche M. 2013. Russeting in apple and pear: a plastic periderm replaces a stiff cuticle. *Annals of Botany - Plants* **5**: ls048.

Kosma DK, Murmu J, Razeq FM, Santos P, Bourgault R, Molina I, Rowland O. 2014. AtMYB41 activates ectopic suberin synthesis and assembly in multiple plant species and cell types. *Plant Journal* **80**: 216-229.

Kurdyukov S, Faust A, Trenkamp S, Bar S, Franke R, Efremova N, Tietjen K, Schreiber L, Saedler H, Yephremov A. 2006. Genetic and biochemical evidence for involvement of HOTHEAD in the biosynthesis of long-chain α-,ω-dicarboxylic fatty acids and formation of extracellular matrix. *Planta* **224**: 315-329.

Lewis DR, Ramirez MV, Miller ND, Vallabhaneni P, Ray WK, Helm RF, Winkel BS, Muday GK. 2011. Auxin and ethylene induce flavonol accumulation through distinct transcriptional networks. *Plant Physiology* **156**: 144-164.

Li F, Wu X, Lam P, Bird D, Zheng H, Samuels L, Jetter R, Kunst L. 2008. Identification of the wax ester synthase/acyl-coenzyme A: diacylglycerol acyltransferase WSD1 required for stem wax ester biosynthesis in Arabidopsis. *Plant Physiology* **148**: 97-107.

Li Y, Beisson F. 2009. The biosynthesis of cutin and suberin as an alternative source of enzymes for the production of bio-based chemicals and materials. *Biochimie* **91**: 685-691.

Li Y, Beisson F, Koo AJ, Molina I, Pollard M, Ohlrogge J. 2007. Identification of acyltransferases required for cutin biosynthesis and production of cutin with suberin-like monomers. *Proceedings of National Academy of Science USA* **104**: 18339-18344.

Li-Beisson Y, Pollard M, Sauveplane V, Pinot F, Ohlrogge J, Beisson F. 2009. Nanoridges that characterize the surface morphology of flowers require the synthesis of cutin polyester. *Proceedings of National Academy of Science USA* **106**: 22008-22013.

Liang M, Davis E, Gardner D, Cai X, Wu Y. 2006. Involvement of AtLAC15 in lignin synthesis in seeds and in root elongation of Arabidopsis. *Planta* **224**: 1185-1196.

Liepman AH, Wightman R, Geshi N, Turner SR, Scheller HV. 2010. Arabidopsis - a powerful model system for plant cell wall research. *Plant Journal* **61**: 1107-1121.

Lulai EC, Corsini DL.1998. Differential deposition of suberin phenolic and aliphatic domains and their roles in resistance to infection during potato tuber (*Solanum tuberosum* L.) wound-healing. *Physiological and Molecular Plant Pathology* **53**: 209-222.

Lulai EC, Suttle JC. 2004. The involvement of ethylene in wound-induced suberization of potato tuber (*Solanum tuberosum* L.): a critical assessment. *Postharvest Biology and Technology* **34**:105-112.

MacMillan CP, Mansfield SD, Stachurski ZH, Evans R, Southerton SG. 2010. Fasciclin-like arabinogalactan proteins: specialization for stem biomechanics and cell wall architecture in *Arabidopsis* and Eucalyptus. *Plant Journal* **62**: 689-703.

Mahapatro A, Kumar A, Gross RA. 2004. Mild, solvent-free ω-hydroxy acid polycondensations catalyzed by *Candida antarctica* lipase B. *Biomacromolecules* **5**: 62-68.

McFarlane HE, Shin JJ, Bird DA, Samuels AL. 2010. *Arabidopsis* ABCG transporters, which are required for export of diverse cuticular lipids, dimerize in different combinations. *The Plant Cell* **22**: 3066-3075.

Moire L, Schmutz A, Buchala A, Yan B, Stark RE, Ryser U. 1999. Glycerol is a suberin monomer. New experimental evidence for an old hypothesis. *Plant Physiology* **119**: 1137-1146.

Molhoj M, Verma R, Reiter WD. 2004. The biosynthesis of D-Galacturonate in plants. Functional cloning and characterization of a membrane-anchored UDP-D-Glucuronate 4-epimerase from *Arabidopsis*. *Plant Physiology* **135**:1221-1230.

Molina I, Li-Beisson Y, Beisson F, Ohlrogge JB, Pollard M. 2009. Identification of an Arabidopsis feruloyl-coenzyme A transferase required for suberin synthesis. *Plant Physiology* **151**: 1317-1328.

Mortazavi A, Williams BA, McCue K, Schaeffer L, Wold B. 2008. Mapping and quantifying mammalian transcriptomes by RNA-Seq. *Nature Methods* **5**: 621-628.

Moura JC, Bonine CA, de Oliviera Fernandes Viana J, Dornelas MC, Mazzafera P. 2010. Abiotic and biotic stresses and changes in the lignin content and composition in plants. *Journal of integrative Plant Biology* **52**: 360-376.

Müller K, Levesque-Tremblay G, Bartels S, Weitbrecht K, Wormit A, Usadel B, Haughn G, Kermode AR. 2013. Demethylesterification of cell wall pectins in Arabidopsis plays a role in seed germination. *Plant Physiology* **161**: 305-16.

Olsson A, Lindstrom M, Iversen. 2007. Lipase-catalyzed synthesis of an epoxy-functionalized polyester from the suberin monomer cis-9,10-epoxy-18-hydroxyoctadecanoic acid. *Biomacromolecules* **8**: 757-760.

Panikashvili D, Shi JX, Bocobza S, Franke RB, Schreiber L, Aharoni A. 2010. The Arabidopsis DSO/ABCG11 transporter affects cutin metabolism in reproductive organs and suberin in roots. *Molecular Plant* **3**:563-575.

Passardi F, Penel C, Dunand C. 2004. Performing the paradoxical: how plant peroxidases modify the cell wall. *Trends in Plant Science* **9**: 534-540.

Pelloux J, Rusterucci C, Mellerowicz EJ. 2007. New insights into pectin methylesterase structure and function. *Trends in plant Plant Science* **12**: 267-277.

Pinot F, Beisson F. 2011. Cytochrome P450 metabolizing fatty acids in plants: characterization and physiological roles. *FEBS Journal* **278**: 195-205.

Pollard M, Beisson F, Li Y, Ohlrogge JB. 2008. Building lipid barriers: biosynthesis of cutin and suberin. *Trends Plant Science* **13**: 236-246.

Quiroga M, Guerrero C, Botella MA, Barcelo A, Amaya I, Medina MI, Alonso FJ, de Forchetti SM, Tigier H, Valpuesta V. 2000. A tomato peroxidase involved in the synthesis of lignin and suberin. *Plant Physiology* **122**: 1119-1127.

Ranathunge K, Schreiber L. 2011. Water and solute permeabilities of Arabidopsis roots in relation to the amount and composition of aliphatic suberin. *Journal Experimental Botany* **62**: 1961-1974.

Ranathunge K, Schreiber L, Franke R. 2011. Suberin research in the genomics era - new interest for an old polymer. *Plant Science* **180**: 399-413.

Roudier F, Fernandez AG, Fujita M, Himmelspach R, Borner GH, Schindelman G, Song S, Baskin TI, Dupree P, Wasteneys GO, Benfey PN. 2005. COBRA, an *Arabidopsis* extracellular glycosyl-phosphatidyl inositol-anchored protein, specifically controls highly anisotropic expansion through its involvement in cellulose microfibril orientation. *The Plant Cell* **17**: 1749-1763.

Sampedro J, Cosgrove DJ. 2005. The expansin superfamily. *Genome Biology* **6**: 242.

Serra O, Hohn C, Franke R, Prat S, Molinas M, Figueras M. 2010. A feruloyl transferase involved in the biosynthesis of suberin and suberin-associated wax is required for maturation and sealing properties of potato periderm. *Plant Journal* **62**: 277-290.

Serra O, Soler M, Hohn C, Franke R, Schreiber L, Prat S, Molinas M, Figueras M, 2009a Silencing of StKCS6 in potato periderm leads to reduced chain lengths of suberin and wax compounds and increased peridermal transpiration. *Journal of Experimental Botany* **60**: 697-707.

Serra O, Soler M, Hohn C, Sauveplane V, Pinot F, Franke R, Schreiber L, Prat S, Molinas M, Figueras M. 2009b. CYP86A33-targeted gene silencing in potato tuber alters suberin composition, distorts suberin lamellae, and impairs the periderm's water barrier function. *Plant Physiology* **149**:1050-1060.

Skene DS. 1982. The development of russet, rough russet and craks on the fruit of the apple Cox's Orange Pippin during the course of the season. *Journal of Horticultural Science* **57**:165-174.

Soler M, Serra O, Molinas M, Huguet G, Fluch S, Figueras M. 2007. A genomic approach to suberin biosynthesis and cork differentiation. *Plant Physiology* **144**: 419-431.

Sousa AF, Silvestre AJ, Gandini A, Neto CP. 2012. Synthesis of aliphatic suberin-like polyesters by ecofriendly catalytic systems. *High Performance Polymer* **24**: 4-8.

Suh MC, Samuels AL, Jetter R, Kunst L, Pollard M, Ohlrogge J, Beisson F. 2005. Cuticular lipid composition, surface structure, and gene expression in Arabidopsis stem epidermis. *Plant Physiology* **139**: 1649-1665.

Thimm O, Blasing O, Gibon Y, Nagel A, Meyer S, Kruger P, Selbig J, Muller LA, Rhee SY, Stitt M. 2004. MAPMAN: a user-driven tool to display genomics data sets onto diagrams of metabolic pathways and other biological processes. *Plant Journal* **37**: 914-939.

Tor M, Lotze MT, Holton N. 2009. Receptor-mediated signalling in plants: molecular patterns and programmes. *Journal of Experimental Botany* **60**: 3645-3654.

Vandesompele J, De Preter K, Pattyn F, Poppe B, Van Roy N, De Paepe A, Speleman F. 2002. Accurate normalization of real-time quantitative RT-PCR data by geometric averaging of multiple internal control genes. *Genome Biology* **3**: RESEARCH0034.

Velasco R, Zharkikh A, Affourtit J, Dhingra A, Cestaro A, Kalyanaraman A, Fontana P *et al*. 2010. The genome of the domesticated apple (*Malus* x *domestica* Borkh.). *Nature Genetics* **42**: 833-839.

Walter TE. 1967. Russeting and cracking in apples. A review of world literature. *Report of East Mailing Research Station for 1966*: 83-95.

Wang YZ, Dai MS, Zhang SJ, Shi ZB. 2014a. Exploring candidate genes for pericarp russet pigmentation of sand pear (*Pyrus pyrifolia*) via RNA-Seq data in two genotypes contrasting for pericarp color. *PLoS One* **9**: e83675.

Wang, YZ, Zhang S, Dai MS, Shi ZB. 2014b. Pigmentation in sand pear (*Pyrus pyrifolia*) fruit: biochemical characterization, gene discovery and expression analysis with exocarp pigmentation mutant. *Plant Molecular Biology* 85: 123-134.

Watanabe S. 1969. Historical studies on the cause of apple russeting. *Bulletin of the Yamagata University* **5**: 205-267.

Zhong R, Lee C, Zhou J, McCarthy RL, Ye ZH. 2008. A battery of transcription factors involved in the regulation of secondary cell wall biosynthesis in *Arabidopsis*. *The Plant Cell* **20**: 2763-2782.

Zimmermann HM, Hartmann K, Schreiber L, Steudle E. 2000. Chemical composition of apoplastic transport barriers in relation to radial hydraulic conductivity of corn roots (*Zea mays* L.). *Planta* **210**: 302-311.

Chapter I

Apple russeting as seen through the RNA-seq lens: strong alterations in the exocarp cell wall

Summary and Perspectives

Apple is a particularly interesting model to study russeting. This undesired phenotype occurs as a response to environmental conditions in non-russeted varieties, such as the common commercial apples found in the market, but also in old varieties displaying russeted skins from the earliest stages of the fruit development to the commercial harvest without any explicit biotic or abiotic stress exposure. In Chapter I, we used a bulk transcriptomic analysis, in order to compared two groups of apple fruits: fully russeted vs non-russeted apples. This let us draw, for the first time, a preliminary picture of the complex gene network involved in the russeting trait in apple based on the *Malus* x *domestica* draft genome.

Histological, mechanical and rheological studies previously revealed that apple russeting is often associated with a defect of the cuticle layer. This section of our study allows the observation of a strong repression of genes being involved in the cutin and wax synthesis in russeted varieties. This decreased expression was associated with a concomitant enhanced expression of the suberin biosynthesis pathway, the latter being the main component of russeting in apple. Interestingly, part of these two biosynthetic pathways shared strong similarities with model plants such as *S. tuberosum* (skin) or *A. thaliana* (roots), the major difference

being triggered by the high gene redundancy observed in the *M.* x *domestica* genome. Several genes were identified in these two pathways in association with the current knowledge coming from model plant studies, new candidate genes or metabolic pathways involved in russeting were also highlighted. Among these, the cell wall metabolism appeared to be strongly altered in the russeted varieties. Indeed, a significant number of genes associated with cell wall loosening displayed an increased expression in the russeted apple skin. Recent advances in the field of apple skin biomechanics and biophysics described that the stiffer cuticle observed in russeted apple and the extreme tensions on the fruit surface during the fruit development might be a major cause of cuticle microcracking. The increased expression of genes involved in cell wall loosening might also be a response to this lower cuticle elasticity, but further work should clarity this point. Triterpenes are major components of the apple skin reaching up to 60% of the total waxes amount. The differential triterpene accumulation in the non-russeted and russeted apple skin has been deeply investigated in the last five years. In the present work, we identified several original candidate genes putatively involved in this pathway. Among these, some oxidosqualene cyclases and cytochrome P450 monooxygenase were specifically expressed in the non-russeted or russeted apple skin. Some of them have been recently investigated and characterized, but others request further experiment to assess their involvement in the triterpene synthesis pathway. To date, no gene responsible for the synthesis of triterpene conjugates in the russeted apple skin has been identified. However, in *S. tuberosum* and *A. thaliana*, some BAHD acyl transferases participate in the synthesis of alkyl-hydroxycinnamates, which also accumulated in the suberin associated waxes. We found some alkyl-hydroxycinnamates in russeted apple skin and speculate that some enzymes belonging to the same family might participate in the synthesis of triterpene-caffeate conjugates. Moreover, the relation between

the differential accumulation of triterpene and the russeting process is particularly interesting. To date, we could not identify any common regulatory network nor putative metabolic routes shared between these two pathways.

One of the aims of the present project was to identify regulatory elements implicated in the russeting and specifically in the suberin deposition process. To date, the knowledge of the regulation of the suberin deposition remains fragmentary in *planta*. Few regulatory elements have been identified in model plants such as *A. thaliana* (AtMYB41) and apple (MdSHN3). A major achievement of the present chapter lies in the description of a large number of transcription factor genes, which are differentially regulated between russeted and non-russeted apples. Some of them have been recently associated with the cutin biosynthetic process (MYB94) or in the cell wall modification (NAC75, NAC73). Among the uncharacterized or poorly characterized transcription factors, a gene coding for a MYB93 transcriptional regulator displays a tightly correlated expression pattern with the suberin synthesis core cluster (GPAT5, CYP86A1, CYP86B1, etc…). We argue that this *MdMYB93* represents a valuable candidate gene putatively implicated in the regulation of the suberin deposition process. However, co-expression is not enough to conclude about the role of this transcription factor and further functional validation is needed to clarify this point. The present chapter depicts a global snapshot of the pathways and differentially regulated genes between russeted and non-russeted apple skin at the commercial harvest. However, it remains difficult to draw conclusions about the chronological events and the complex interactions between pathways, which drive the apple skin to russet. As an example, in russeted apple skins, we can't conclude whether the decreased expression of the cutin biosynthetic genes is the cause or the consequence of the enhanced activation of the suberin biosynthesis pathway. There are also some remaining questions about the role of the altered expression

of cell wall modification genes. This enhanced loosening process might occur before, concomitantly or in response to the suberin deposition process. The inferred conclusions might be quite different regarding the chronological occurrence of these processes. As suggested before, cell wall loosening might be linked to the growth of the fruit. However, as suberin is anchored in the primary cell wall, this modification might also be an intrinsic part of the suberin deposition process. The bulk transcriptomic approach used in the present work provides a first overview of those genes implicated in the biosynthesis of the cuticle, the wax and the suberin in apple. By using multiple varieties within each group, we lowered the genotypic specificity of each variety and focused on the russet/waxy traits. Indeed, gene expression profiling performed between two varieties might centre the results to genes and pathways which are not directly linked with the trait of interest. Inversely, bulk transcriptomic experimental designs might also result in the statistical loss of interesting genes due to a higher variability in the gene expression levels between varieties. As an example, in the present work, although the russeted varieties were selected from phenotypic data which were gathered over years of field observations, the 'Patte de loup' variety displayed a higher expression of the suberin biosynthesis gene compared to 'St Edmund Pippin' or 'Reinette Parmentier'. This might have hidden some relevant genes implicated in our trait of interest.

In order to assess how these concomitant decreased expression of cuticle deposition-related genes and increase expression of the suberin synthesis genes affect the apple fruit skin, we investigated the lipid composition of both free and polymerized fraction of the 'Cox Orange Pippin' skin (see next chapter). This semi-russeted variety has been extensively studied as a model for russeting because it displays a waxy skin, which is randomly covered by russeted patches. Compared to the old heritage fully russeted varieties previously used in our

transcriptomic study, 'Cox Orange Pippin' is genetically closer to commercial apples, as it has been widely used as parent in multiple crosses. Moreover, 'Cox Orange Pippin' develops a slight to medium russeting and constitutes a relevant model, which might be more comparable to the russeting cases observed in commercial varieties. A targeted gene expression analysis was also performed with genes involved in the cutin, suberin, wax and triterpene biosynthesis, selected from our previous transcriptomic analysis, as well as from some works in our lab focusing on triterpenes and from the literature.

Chapter I highlights:

Outcome:

- The transcriptomic data provide a first picture of the genes and pathways probably involved in the russeting trait linked to the *Malus* x *domestica* genome database.
- These data suggest that russeted apples display an impaired cuticle biosynthesis associated with an increased suberin deposition and cell wall modification process.
- Some candidate transcription factors likely implicated in the regulation of the russeting are uncovered.
- Genes with unknown functions involved in the pentacyclic triterpene biosynthesis are identified.

Questions raised:

- What is the chemical structure and composition of the waxy and russeted skin?

- How do cuticle formation, suberin deposition and cell wall modification interact during the growth of russeted apples?
- Is MdMYB93 regulating the suberin deposition in apple skin and what is the function of other uncharacterized transcription factors?

Chapter II: Differential accumulation of cutin, suberin and their associated waxes in the semi-russeted 'Cox Orange Pippin' variety

Adapted from the draft article in preparation

Contributions:

S. Legay designed the experimental setup, performed the sampling and the laboratory work (sample preparation, RNA extraction, RT-qPCR, analytical chemistry). He also adapted the depolymerisation method, performed the GC-MS data extraction, metabolite identification, statistical analysis and wrote the article.

E. Cocco adapted the depolymerisation method and was involved in the GC-MS data extraction. She also participated in the manuscript refinement.

C. Guignard supervised the analytical chemistry work.

C. André and J.-F. Hausman participated in the manuscript refinement.

Abstract:

Russeting is one of the most important defects on apple fruit surface causing part of the production to be redirected to the industrially processed products with a concomitant price downgrading and economical loss for actors of the apple production sector. This particular rough and brown phenotype is mainly due to the accumulation of suberin in the inner part of the epidermal cell walls. Previous studies showed that the occurrence of russeting is tightly linked with the development and the integrity of the cuticle. Indeed, during the fruit growth development, the appearance of russeting is associated to an increased cuticle microcracking, which results from the extreme tensions occurring on the fruit surface. Our previous bulk transcriptomic analysis, comparing fully russeted and waxy apple varieties, showed a massive decreased expression of cutin, wax and some pentacyclic triterpene biosynthesis genes in the russeted varieties, with an expected concomitant enhanced expession of the suberin biosynthesis genes. In the present work, we performed a deep investigation of the aliphatic composition of the cutin, suberin, their associated waxes and triterpenes in the waxy and russeted patches of the semi-russeted apple variety 'Cox Orange Pippin'. A targeted gene expression profiling was performed to validate candidate genes which were identified in our previous work and that might be involved in these metabolic pathways. Our results show that a decreased of cuticular waxes, ursolic acid and oleanolic acid, accompanied by an accumulation of alkyl-hydroxycinamates and betulinic acid, occurs in the russeted patches. The suberin monomer composition is characterized by specific contents in 20, 22 and 24 carbon aliphatic chains whereas the cutin is mainly represented by common C16 and C18 aliphatic chains. This work depicts, for the first time in apple, the complex composition of suberin, cutin and their associated waxes and confirms the strong interplay between these epidermal polymers in apple fruit skin.

Key words: Cox Orange Pippin, suberin, cutin, russeting, composition, *Malus* x *domestica*

I. Introduction

Apple is among the most consumed fruits worldwide with approximately 81 million tons produced in 2013 (FAOSTAT). The *Malus* x *domestica* species have a long history of breeding and cross hybridization which started by the import of the first *Malus sieversii* cultivars in Europe, through the Silk Route (Cornille *et al*. 2012, Cornille *et al*. 2014). Later, breeding efforts aimed at improving yield, tolerance to pathogens and fruit quality traits such as flesh firmness, juiciness, sugar and polyphenol contents, to name a few (Laurens 1998, Morgan and Richards 2003, Juniper and Mabberley 2006). Since the last decades, consumers and breeders have been more and more attentive to the skin phenotype, favoring the development of no-default glossy and colored skin varieties. The recent commercial apple varieties were developed to fulfil this goal, the best example being the 'Pink Lady' variety. However, the production of fruits with no default is extremely dependent on environmental pressures and compels farmers to use more and more pesticides and fertilizers (Faust and Shear 1972). Despite their efforts, some defects on the fruit surface can still occur. Among these, russeting is one of the most important causes of economical loss in the apple production sector. Fruits exhibiting this rough brown phenotype on the surface are usually redirected to the transformed product sector with a concomitant price downgrading, compared to the consumers market.

Russeting is mainly due to the accumulation of suberin in the inner part of the primary cell wall. This complex biopolymer has been widely studied in other plant models such as *Arabidopsis thaliana*, *Solanum tuberosum* L. and *Quercus suber* L. (Graca and Pereira 2000a, Graca and Pereira 2000b, Franke *et al*. 2005, Molina *et al*. 2006). Although recent advances strongly improved the knowledge of the complex metabolic cascade resulting in the deposition of suberin in the primary cell wall, factors driving its biosynthesis remains unclear in apple and more

generally in plants (Vishwanath *et al*. 2015, Graca *et al*. 2015, Legay *et al*. 2015). Since the 60's, russeting has been extensively studied at the agronomical and histological levels and key factors favoring the development of russeted skin in apple have been identified (Sironval and Clijters 1962, Walter 1967, Tukey 1969, Faust and Shear 1972, Skene 1982, Knoche and Grimm 2008, Lashbrooke *et al*. 2015). Among these, the development and the integrity of the cuticle layer seems to be one of the most critical points in the regulation of russeting (Lashbrooke *et al*. 2015). Indeed, the development a thinner cuticle layer is correlated with the occurrence of skin russeting. This altered cuticle layer appears to be linked with the appearance of cuticle microcracking on the apple fruit surface and is thought to be one of the major causes of russeting in apple (Knoche *et al*. 2011, Curry 2012). The cuticle is particularly sensitive to microcracking during the early stage of fruit development, due to the extreme tangential tensions on the surface generated by the expansive growth (Khanal *et al*. 2013). Moreover, rheological studies showed that the skin of the non-russeted apple is less elastic compared to the russeted periderm, suggesting that the cuticle might be more sensitive to microcracking compared to the suberized tissue (Khanal *et al*. 2013). Scanning electron microscopy (SEM) analyses performed on the 'Golden Delicious' variety showed that gibberellins (GA_{4+7}) application during the early stage of fruit development decreases the epidermal cell surface and fruit surface tensions, leading to a lower cuticle microcracking rate and russeting (Curry 2012). In addition to the developmental factors, environmental factors strongly impact russeting in apple. As an example, the long term moisture exposure has been also associated with cuticle microcracking and russeting, suggesting that the causes leading to russeting are multifactorial (Tukey 1969).

In our previous bulk transcriptomic analysis comparing russeted and waxy apples, a large number of genes involved in the cutin, wax and suberin biosynthesis

pathway have been identified and new putative candidate genes implicated in these metabolic processes have been highlighted too (Legay *et al*. 2015). Interestingly, a strong decreased expression of the cutin and their associated wax synthesis genes with a concomitant increased expression of suberin biosynthesis and cell modifications genes, was observed in russeted skin. Cutin and suberin share a similar backbone composed of α,ω-dicarboxylic acids and ω-hydroxyacids esterified with glycerol (Bernards 2002). However, strong differences occur between these biopolymers, which might explain their differential rheological properties observed in apple (Khanal *et al*. 2013). As an example, cutin displays higher relative content in ω-hydroxyacids, which are composed by a majority of C16 and C18 aliphatic chains. Conversely, suberin is constituted by two polyphenolic and polyaliphatic domains, which contains significant amount of hydroxycinnamic acids, mainly ferulic acid, which are esterified within the suberin structure (Bernards 2002, Graca and Pereira 2000b). The suberin polyaliphatic domain also displays characteristic very long chains ω-hydroxyacids and α,ω-dicarboxylic acids and a higher content in these compounds (Franke *et al*. 2005, Molina *et al*. 2006, Graca and Pereira 2000a, Graca and Pereira 2000b).

Interestingly, the suberin composition displays variable distribution of these suberin precursors among plant species (Graça and Pereira 2000a, Franke *et al*. 2005, Ranathunge and Schreiber 2011, Vishwanath 2015). In *Q. suber*, C22 and C24 ω-hydroxyacids and α,ω-dicarboxylic acids are predominant, while a majority of C16-C18 chains is observed in *Pseudotsuga menziesii* (Graça and Pereira 2000a). In the potato tuber periderm, in addition to the long chain alkanoic acids (C24-C28), a majority of 18:1 derived ω-hydroxyacids and α,ω-dicarboxylic acids is found (Graca and Pereira 2000b). Moreover, variable composition of suberin is also observed between tissues of the same species. As

an example, a differential suberin composition has been observed between *Arabidopsis* root and seed coat. Root suberin displays a large majority of C16, C18:1 and C22 α,ω-dicarboxylic acids, whereas seed coat suberin shows longer chains (Franke *et al*. 2005, Molina *et al*. 2006).

In plants, cutin and suberin are associated with non-covalently linked waxes which differ between these two type of polymers (Millar *et al*. 1999, Rowland *et al*. 2007, Von Wettstein-Knowles 2012, Schreiber *et al*. 2005, Kosma *et al*. 2012). The cutin-associated waxes are composed by very long chain fatty acids, primary and secondary alcohols, aldehydes and ketones, alkanes and wax esters, which are deposited on the cutin surface (epicuticular waxes) or embedded within the polymer matrix (Aarts *et al*. 1995, Rowland *et al*. 2007, Lü *et al*. 2009). Conversely, the suberin-associated waxes comprise very long chain alkanes, primary alcohols, fatty acids, some sterol derivates and alkyl-hydroxycinnamates. Alkyl-hydroxycinnamates, which are composed by hydroxycinnamic acid esterified with primary alcohols, can reach 60% of the total waxes weight in *A. thaliana* (Kosma *et al*. 2012). Moreover, in *A. thaliana*, a recent study showed that the large majority of the primary alcohols non covalently linked to suberin is in the form of these alkyl-hydroxycinnamates (Delude *et al*. 2016).

The apple waxy and russeted (suberized) skins present some important specificities in their wax composition compared to *A. thaliana*. Indeed, in the waxy apples, massive contents of the pentacyclic triterpenes, ursolic and oleanolic acids, are found and can reach 30 to 60% of the total content depending on the variety (André *et al*. 2012, André *et al*. 2013). Conversely, russeted skins contain a lower amount of these compounds but accumulate betulinic acid and lupeol (André *et al*. 2012, André *et al*. 2013). Moreover, betulinic acid-3-*trans*-caffeate also specifically accumulates in this suberized tissue (André *et al*. 2013). This

suggests that, in apple, there might be a close interplay between the suberin, cutin and triterpene biosynthesis pathways, but no evidence has been established yet.

The purpose of this study is to characterize for the first time, in apple, the differential distribution of the cutin, suberin and their associated waxes, which occur between waxy and russeted tissues. For this, a deep investigation of the lipid surface composition was performed from normal waxy skin and russeted patches sampled from the semi-russeted fruits of the 'Cox Orange Pippin' variety. 'Cox Orange Pippin' is a famous and well-studied apple variety, which has been used as parent in a large number of the available commercial varieties (Sironval and Clijters 1962, Knee 1972, Skene 1981, Skene 1982, Irving and Drost 1987, Evans *et al*. 2011, Chagné *et al*. 2012, Legay *et al*. 2015). The comparison of the russeted and waxy areas of the same variety provides a first picture of the differential accumulation of cutin, suberin and their associated waxes, discarding genotypic factors that might occur when such a comparison on different russeted/waxy varieties is done. The composition of these polymers and associated compounds was also compared with previous works performed in suberin model plants, such as *A. thaliana, S. tuberosum* and *Q. suber* (Graca and Pereira 2000a, Graca and Pereira 2000b, Franke *et al*. 2005, Molina *et al*. 2006). Finally, a targeted gene expression profiling of biosynthetic genes previously identified in apple has been performed using RT-qPCR. These results will be merged in order to pinpoint the key players involved in the differentiation of these two contrasting tissue types.

II. Materials and Method

A. Plant material

For the lipid and the qPCR experiments, four trees of the 'Cox Orange Pippin' variety (four biological replicates) were randomly sampled from the orchard of

the Walloon Agronomic Research Center of Gembloux (CRA-W) in 2014. From each tree, 10 apples were sampled from the south side of the tree at a height ranging from 1,20 to 2,20 m and constituted a biological replicate. For each biological replicate, the russeted and waxy patches (areas) were carefully excised with scalpels taking care to remove the flesh as much as possible. The resulting exocarp samples were directly flash-frozen in liquid nitrogen and stored at -80°C until RNA extraction.

B. RNA extraction

Samples (250 mg) were ground to a fine powder with a mortar and pestle in liquid nitrogen. Total RNA was extracted using an adapted CTAB buffer extraction protocol (Gasic *et al*. 2004). Total RNAs were cleaned and treated with DNase I using the RNeasy Plant Mini Kit (QIAGEN, Leusden, The Netherlands), following the manufacturer's guidelines. Total RNA integrity was assessed using the RNA Nano 6000 assay and a 2100 Bioanalyzer with quality parameters adapted to plant RNA profiles (Agilent Technologies, Santa Clara, CA, USA). Samples, with RINs (RNA integrity number) lower than 7, were excluded from the experiment. RNA purity was assessed measuring the absorbance at 230 nm, 260 nm and 280 nm using a Nanodrop ND1000 spectrophotometer (Thermo Fisher Scientific, Waltham, MA, USA). Total RNA was quantified using a Qubit RNA assay kit (Life technologies, Carlsbad, CA, USA).

C. Targeted gene expression analysis

The targeted gene expression analysis was performed on 28 representative genes being involved in the cutin, suberin, wax and triterpene biosynthesis, using RT-qPCR (Table 3-1). Reverse transcription was carried out using the M-MuLV Reverse Transcriptase (RNase H), the Murine RNase Inhibitor (New England

Table 3-1: Description of the 28 representative genes involved in the cutin, suberin, wax and triterpene biosynthesis. Primer sequences were obtained from previous studies or designed from the differentially expressed genes observed in our previous transcriptomic data.

Gene Code	Description	Targeted contig/EST	Primer sequence (5'-3')	Amplicon size (bp)	PCR efficiency	Reference
ASFT	Arabidopsis suberin feruloyl transferase	MDP0000312405	F: GAGCCACCAGTACCAGAAGG	105	2.07	
			R: ACCCAACTGCAAATGAAAGC			
FAR5	Fatty acid reductase 5	MDP0000138841	F: CCGGGAGACGTAGTTTCTGA	105	2.00	
			R: GTTGGTGGTTCCTGCAGAGT			
KSC4	3-ketaoacyl-CoA Synthetase 4	MDP0000922301	F: GAACTATGTTCCGCCAAGGA	83	1.87	
			R: ACAGATCATCCAATGCACCA			
FARx	Fatty acid reductase x	MDP0000185343	F: AAATCATACGGATGGCCAAA	112	2.01	
			R: TAACTACCGTTGGGCGTAGG			
CER1	Eceriferum 1	MDP0000461409	F: TTCCAAATTGGCTCTTCACC	81	1.99	
			R: GTGTGTGGTGCAAAGAATGG			
KCS2	3-ketaoacyl-CoA Synthetase 2	MDP0000625646	F: GGTGCAGACGACAGAGCATA	134	1.93	
			R: GGGCCAAGAGTTGTGATGTT			
CER3	Eceriferum 3	MDP0000165547	F: CCAATGTTGAGGTCGTTCCT	117	1.88	
			R: GGCAGAAGTTGGTGTCCATT			
CER6	3-ketaoacyl-CoA Synthetase 6/Eceriferum 6	MDP0000392495	F: CTTCAAACCTCCGGTCATGT	99	1.88	
			R: GACGCTCTTAGGGTTGTTGC			
C4H	Coumarate 4-hydroxylase	MDP0000602841	F: GGCTAATGGGAACGACTTCA	85	1.97	
			R: CATGATTGGAAGGGCTAGGA			
CER8/LACS1	Long chain acyl-CoA synthetase 1	MDP0000465035	F: CCGCGTGATTGAGGAGTATT	88	2.02	
			R: CACCATGTCATCCCTCAGTG			
CYP86A2	Fatty acid hydroxylase	MDP0000858983	F: TTCCAAATGGGTGAAAGAGC	104	2.00	
			R: GTGGCACAGAAGGGTAAAGC			
LCR/CYP86A8	LACERATA/Fatty acid hydroxylase	MDP0000941955	F: AGCTTGAACCATAGCCTCCA	102	1.97	
			R: CCCATTGCAAAGACCTTGTT			
MYB52	MYB domain transcription factor 52	MDP0000852158	F: TTGTAGCTGCAACCCTCCAC	122	2.01	
			R: ACCACCAACACCTATGAATGCT			

KCS10	3-ketaoacyl-CoA Synthetase 10	MDP0000235280	F: GTGTACCAAGAGGAAGATGAACAAA R: GAAAGGCAGCACTAACGGC	123	1.92	Legay *et al.* 2015
CYP86B1	Very long chain fatty acid hydroxylase	MDP0000306273	F: CGCTTTGTGACCCCATCC R: AATGACGTCTTCCGCAAACT	114	1.98	Legay *et al.* 2015
GPAT6	Glycerol-3-phosphate acyltransferase 6	MDP0000479163	F: CCCAATAGTTGCCCTTCTGA R: AGGAGGGGTGCCCTTAACTA	154	1.98	Legay *et al.* 2015
CYP86A1	Fatty acid hydroxylase	MDP0000923760	F: GCGCCTCCTCTATCCTTCC R: CGACTTCGAGGCTCTTCTCC	89	1.94	Legay *et al.* 2015
MYB42	MYB domain transcription factor 42	MDP0000787808	F: GACCCGTTGGTGAGTTTCAT R: TCCTCCGTTGGATTATCAGC	104	2.00	Legay *et al.* 2015
WSD-1	O-acyltransferase	MDP0000701887	F: AGAAATGGTCAAACCCGACA R: AGACGAAGTCAAGCGCATTT	107	1.91	Legay *et al.* 2015
MYB93	MYB domain transcription factor 93	MDP0000320772	F: TATCCAACACCACCAAGCAA R: CCACCGAAGTAGGAGATGGA	145	1.96	Legay *et al.* 2015
GPAT5	Glycerol-3-phosphate acyltransferase 5	MDP0000150502	F: GAACAAATCCACCCACCACT R: ATTAAGAGGGCGGTTGAAGG	131	1.97	Legay *et al.* 2015
MdOSC1	Oxidosqualene cyclase 1	FJ032006.1	F: TTGTACTACTAATCCAGTGATCAAGATGTGG R: CTCTCTTAGTATCTGAAAACGCCATAGGAG	238	1.86	Brendolise *et al.* 2011
MdOSC3	Oxidosqualene cyclase 3	FJ032008.1	F: GCAATCGTGATCAAAGAAGATGTGGAGG R: TTCTCTTAAAATCTGAAAACGCCATAGG	232	1.82	Brendolise *et al.* 2011
MdOSC4	Oxidosqualene cyclase 4	MDP0000034165	F: TATGCATCCAGCAAAAATGTTT R: TCCAATTAATTTCGCCATAAGGT	124	1.94	André *et al.* 2016
MdOSC5	Oxidosqualene cyclase 5	KT383436	F: CTCTCGAAGTAACAATGAAGCACA R: TAATCACCATTTGGGTCTTCAG	152	1.97	André *et al.* 2016
CYP716A145	Cytochrome P450 monooxygenase	MDP0000478473	F: AGGCACGTTCCTCGCTTC R: CAAACCCTAAGAGGAGGGTCA	70	2.04	André *et al.* 2016
SQS	Squalene synthase	CN880837.1	F: GTTTTGGCCACGTCAAATCT R: CATTGCACTGCCTTCTCTGA	87	2.12	André *et al.* 2016
eF-1alpha	Elongation factor 1 alpha	AJ223969.1	F: ACTGTTCCTGTTGGACGTGTTG R: TGGAGTTGGAAGCAACGTACCC	208	1.95	Giorno *et al.* 2012
ACTIN	Actin	EB127077	F: ACCATCTGCAACTCATCCGAACCT R: ACAATGCTAGGGAACACGGCTCTT	185	1.94	Giorno *et al.* 2012
IMPA-9	imortin subunit alpha-9	CN909679	F: TCGTGAACTCAGGCGCTTACTG R: AAGCAACGGTAAAGCGGGCAAC	205	1.92	Giorno *et al.* 2012
GAPDH	glyceraldehyde 3-phosphate dehydrogenase	EB146750	F: TGAGGGCAAGCTGAAGGGTATCTT R: TCAAGTCAACCACACGGGTACTGT	185	1.91	Giorno *et al.* 2012

Biolabs, Ipswich, MA, USA) and random hexamers (Invitrogen, Carlsbad, NM, USA) following the manufacturers' guidelines. qPCR primers were designed using the Primer3 software (http://frodo.wi.mit.edu/) with the following criteria: primer size between 18 and 25 base pairs, GC content between 30 and 70%, amplicon size from 80 to 200 base pairs, primer annealing temperatures in the 57-61°C range. Matching primer sets were checked for unexpected secondary structures using NetPrimer (http://www.premierbiosoft.com/netprimer). In order to test the specificity of the primers, a BLAST search against the *M*. x *domestica* genome sequence was performed (www.rosaceae.org). qPCR runs were carried out, using technical triplicates and four biological replicates on a Viia7 384-well real-time PCR instrument (Thermo Fisher, Waltham, MA, USA) with Takyon SYBR Green low ROX (Eurogentec, Liege, Belgium) following the manufacturer's guidelines. Experiments were carried out following the MIQE guidelines (Bustin *et al*. 2009) and a melting curve was performed at the end of all the runs to assess the specificity of the primers. Primers information are available in the Table 3-1 and SI Table 3-1. The relative expression of a gene of interest was calculated using the Biogazelle qBase+ V3 software (Hellemans *et al*. 2007), taking into account multiple reference gene normalization and specific PCR efficiencies. For the present experiment, the geNorm+ analysis described the *MdIMPA9* and *MdActin* gene couple as the most suitable for optimal normalization of the data (Giorno *et al*. 2012, Vandesompele *et al*. 2002). A statistical analysis of the $\log_2$ transformed normalized relative quantities was performed between both groups (Russeted and Waxy skins) using a Mann-Whitney test in Biogazelle qBase+ V3.

D. Cutin and suberin depolymerization and free lipid analysis

Sample cleaning

For each biological replicate, the total apple peel surface was measured and transferred into a 50 mL polypropylene tube. Cell wall and flesh residues were removed using 12 mL of a solution of pectinase and cellulase (250 U/mL, Novozymes, Bagsvaerd, Denmark) in a 0.1 M sodium citrate/critic acid buffer pH=4.2 for 3 days on a rolling table at 60 Hz at room temperature. After 3 days, the solution was removed and the samples were washed using 12 mL sodium borate/boric acid buffer (0.01 M, pH=9) and 12 mL of a fresh cellulose/pectinase digestion solution in sodium citrate/critic acid buffer was added. Seven consecutive digestion/washing cycles were performed. After a final wash with 12 mL sodium borate/boric acid buffer buffer (0.01 M, pH=9) and 12 mL mQ water, samples were dried in an oven at 35°C for 48 hours and transferred into a 2 mL centrifuge tube. Samples were then ground using 2 steel beads (4,5 mm) and a Retsch MM400 cryogenic grinder at 25Hz for 5min (Retsch, Aartselaar, Belgium).

Extraction and transesterification

To extract the soluble lipid fraction, three consecutive extractions were performed with 1 mL of dichloromethane by shaking at 25 Hz for 10 min. The extracts were then evaporated under vaccum (CentriVap, Labconco, Kansas City, MO, USA) and recovered in 1 mL of dichloromethane. The remaining material was then oven-dried for 48 h at 35°C. Suberin depolymerization was performed according to the protocol described by Franke et al. (2005). Six mL of boron trifluoride methanolic solution (10% BF_3/MeOH, Sigma Aldrich) was added to the powder in a glass tube sealed with a Teflon cap. After 16 h at 70°C, the transesterification reaction was stopped using 10 mL aqueous $NaHCO_3$ saturated solution. An internal standard, i.e. nonadecanoic acid (4 μg), was added to the solution. The

methylesters were then extracted 3 times (3 mL dichloromethane, 25 Hz for 10 min), evaporated, and resuspended in 1 mL dichloromethane. A 200 μL aliquot of the soluble lipid and suberin depolymerization extract in dichloromethane was placed in a GC-MS vial and dried under a gentle nitrogen flow, then 50 μL of a Bis-Trimethylsilyl-trifluoroacetamide: Trimethylchlorosilane mixture (BSTFA:TMCS 99:1) was added. The reaction was carried out for 60 min at 60 °C, then the derivatized extract was directly analyzed by GC-MS.

GC-MS Analysis

The identification and quantification of derivatized compounds in both extracts were achieved on an Agilent 7890B/5977A GC-MS coupled to a Gerstel Multipurpose Sampler (Santa Clara, CA, USA). The injection was performed at 280°C in splitless mode (1 μL). The carrier gas was He at a constant flow of 1.2 mL/min. The column was an Agilent HP5-MS (30 m x 0.25 mm i.d. x 0.25 μm film thickness) and the oven temperature was programmed as follows: 80°C (2 min) to 210°C (8°C/min), then 280°C (3°C/min) and 320°C (15°C/min, 15 min isotherm). The MS transfer line was kept at 280°C. MS spectra were recorded in Full-Scan mode between 50 and 900 amu. The identification of compounds in the soluble lipid and polymerized polyester fractions and the determination of their relative peak areas were performed using the Agilent MassHunter Software suite. The identification of the different metabolites was performed from comparison of the mass spectra with data from the National Institute of Standards and Technology (NIST) database (http://www.nist.gov), the American Oil Chemists' Society (AOCS) lipid library (http://lipidlibrary.aocs.org) and fragmentation patterns described in the literature (Bento *et al*. 1998, Graca and Pereira 2000b, Graca *et al*. 2002, Franke *et al*. 2005, Molina *et al*. 2006, Molina *et al*. 2009, Kosma *et al*. 2012). GC-MS fragment tables are available in the SI Table 3-2. For each compound, the relative peak area was normalized the C19 internal standard

and the skin surface. The statistical significance was assessed using a Mann-Whitney test comparing the four biological replicates of the waxy and the russeted skin, respectively (SI Table 3-3).

III. Results

A. Cox Orange Pippin skin phenotype

The 'Cox Orange Pippin' variety harvested in 2014, in the orchards of the CRA-W, showed a quite high coverage of russeting on the fruit surface (Fig. 3-1). The calyx and stem ends were heavily russeted as observed in a majority of commercial apple varieties. Some russeted patches were also present on the rest of the fruit surface with no evident relation with the fruit orientation in the tree. In addition, some characteristic russeted spots (lenticels) were observed on the whole surface of the fruit including the waxy areas. Sampling of the tissues was performed by carefully excising the russeted patches and the remaining waxy areas.



Figure 3-1: The Cox Orange Pippin skin phenotype. On the left: side view, on the right: top view. The majority of the fruit surface was covered by a waxy skin with small lenticels (russeting spots). Russeting was systematically found on the calyx and stalk ends of the fruit and russeted patches occurred aleatory on the fruit surface.

B. Russeted skin displayed a strong decrease in the waxes and triterpene contents

Analysis of the free lipid fraction of the russeted and waxy skin of the 'Cox Orange Pippin' variety showed a large diversity in metabolites composing the cutin-associated waxes. These were represented by common fatty acids, primary fatty alcohols, alkanes, aldehydes, triterpenes, which displayed drastic decreased contents in the russeted skin. Fatty acids displayed a large diversity of chain length, which ranged from 16 carbons (C16) to thirty carbons (C30) (Fig. 3-2).

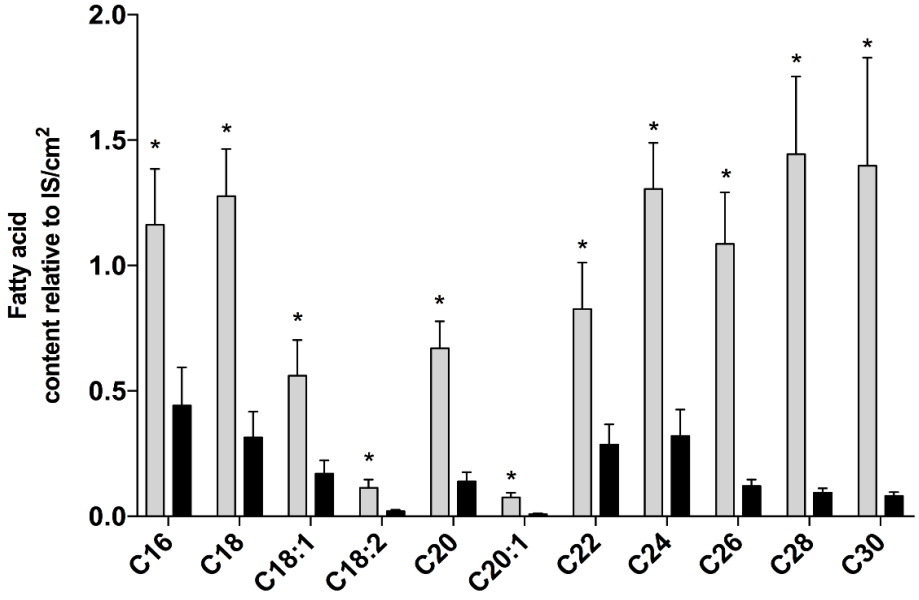

Figure 3-2: Distribution of the identified fatty acids (as trimethylsilyl esters) found in the free lipid fraction of the waxy skin (in grey) and russeted skin (in dark). Relative quantities are normalized to the nonadecanoic acid internal standard and the skin surface in cm^2. Stars display statistically significant differences between waxy and russeted 'Cox Orange Pippin' skins (Mann-Whitney test, *p*-value<0,05). Error bars represent the standard deviation obtained from four biological replicates.

The C16, C18, C18:1 and C18:2 fatty acid precursors, which are synthesized in the plastids, displayed a higher accumulation in the waxy skin with fold changes equal to 2.6, 4.1, 3.2 and 4.1, respectively. This suggests that a decreased fatty acid biosynthesis might occur in these russeted areas. Very long chain fatty acids (VLCFA), with carbon chain number higher than 18, are synthesized in the endoplasmic reticulum from the C16, C18 and C18:1 acyl-CoA precursors. Elongation of the aliphatic chain is catalyzed by the fatty acid elongation complex (FAE), which is composed of the 3-ketocyl-CoA synthase (KCS), the 3-hydroxyacyl-CoA reductase, the 3-ketoacyl-CoA dehydratase and the enoyl-CoA reductase (Todd *et al*. 1999). Among these four enzymes, only KCSs shows a substrate specificity (Millar and Kunst, 1997). In the present work, C26, C28 and C30 VLCFAs, which are commonly found in the cutin-associated waxes, displayed the highest content in the waxy skin with fold changes ranging from 9 to 17 compared to russeted skin. Interestingly, russeted patches showed a slightly higher accumulation of the C22 and C24 VLCFAs compared to the C26, C28 and C30, suggesting that these two VLCFAs groups might be synthesized by different KCS genes (Millar and Kunst 1997).

In *A. thaliana*, primary alcohols are synthesized by alcohol-forming fatty acyl CoA reductase (FAR) such as the FAR1, FAR4 and FAR5 (Domergue *et al*. 2010). Members of this family of compounds, which comprise C18 to C30 aliphatic chains, were found in both russeted and waxy skin. These also displayed a similar distribution compared to fatty acids, with an expected prevalence of even carbon chains (Fig. 3-3). In the waxy skins, the most abundant primary alcohols were composed by 26 and 28 carbons chains which represented 34% and 35% of the total primary alcohol content. The C24 and C30 chains primary alcohols also accumulated, to a lower extent, in the waxy tissues and showed lower amount in russeted tissues as observed for the C26 and C28 primary alcohols. Other odd-

carbon chain primary alcohols displayed lower content in both tissues and a slight decreased accumulation in the russeted tissues. Finally, small octadecanol and eicosanol contents were detected and can be considered as trace. Only two aldehydes were found in the free lipid extract. Aldehydes were mostly represented by C26 and C28 chains, which accumulated 49 and 28 times more in the waxy skin, respectively. Interestingly, the carbon chain length of these aldehydes matched with the most abundant primary alcohols, supporting a link between these two families in the metabolic cascade of waxes biosynthesis (See discussion).

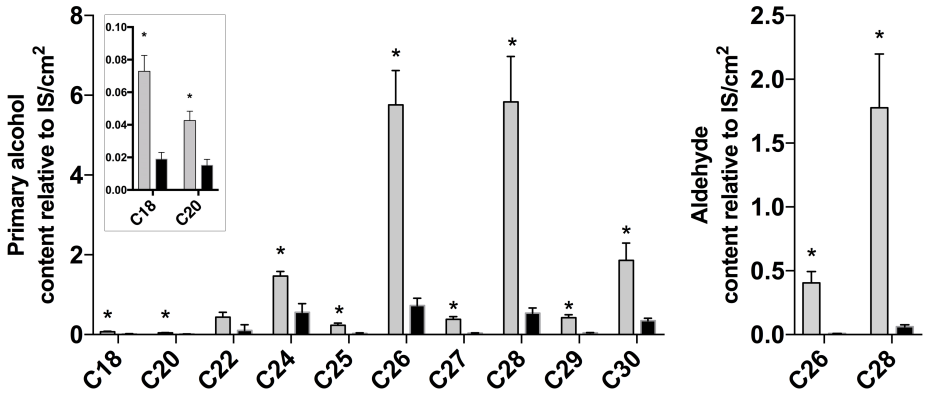

Figure 3-3: Distribution of the identified primary fatty alcohols (as trimethylsilyl ethers, on the left) and aldehydes (on the right) found in the free lipid fraction of the waxy skin (in grey) and russeted skin (in dark). Relative quantities are normalized to the nonadecanoic acid internal standard and the skin surface in cm^2. Stars display statistically significant differences between waxy and russeted 'Cox Orange Pippin' skins (Mann-Whitney test, *p*-value<0,05). Error bars represent the standard deviation obtained from four biological replicates.

Alkanes were among the most abundant metabolites found in the free lipid fraction (Fig. 3-4). The C27 and C29 n-alkanes were the most represented forms with 19% and 75% of the total alkanes in the waxy skin, respectively, and 22% and 70% in the russeted skin, respectively. Although their relative abundance was similar between both skin types, the C27 and C29 n-alkanes accumulated 10 and 8 times more in the waxy skin, respectively, suggesting that the alkane biosynthesis was also impaired in russeted skins. Other alkanes such as the even number chain length and the C31 accumulated to a much lower extent.

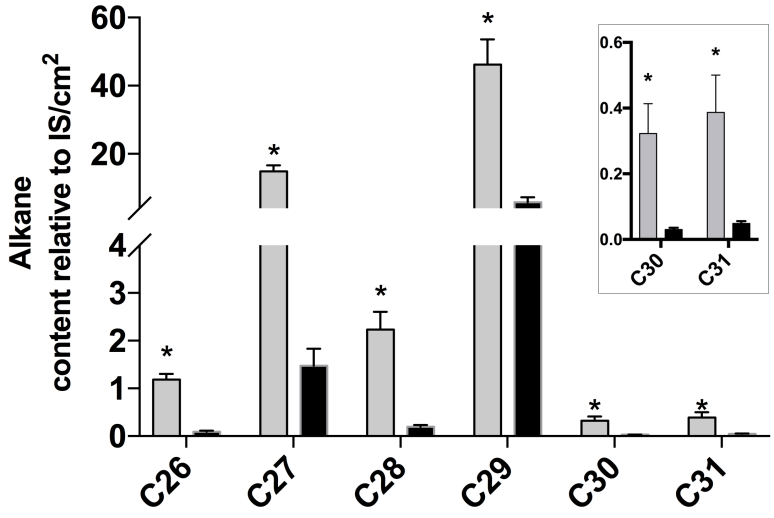

Figure 3-4: Distribution of the identified alkanes found in the free lipid fraction of the waxy skin (in grey) and russeted skin (in dark). Relative quantities are normalized to the nonadecanoic acid internal standard and the skin surface in cm^2. Stars display statistically significant differences between waxy and russeted 'Cox Orange Pippin' skins (Mann-Whitney test, *p*-value<0,05). Error bars represent the standard deviation obtained from four biological replicates.

Pentacyclic triterpene content can represent up to 60% of the total wax content in apple (André *et al*. 2012). Three main triterpene series, namely the ursane, oleane and lupane series, have been identified in the apple skin, so far. Recent studies showed that the ursane and oleane series strongly accumulate in the waxy tissues, whereas the lupane series seems to be specifically synthesized in the russet skin (André *et al*. 2012, Brendolise *et al*. 2011). A significant number of identified and unidentified pentacyclic triterpenes were found in the free lipid extract of 'Cox Orange Pippin'. As expected, ursolic and oleanolic acids represented 45% and 27% of the total triterpene content in the waxy skin, respectively (Fig. 3-5).

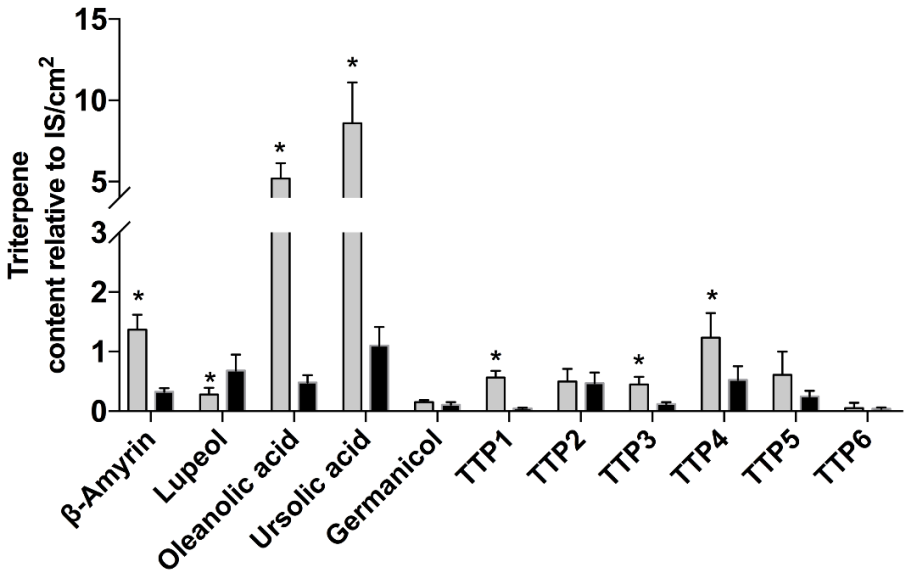

Figure 3-5: Distribution of the identified and unidentified trimethyl sylilated triterpenes found in the free lipid fraction of the waxy skin (in grey) and russeted skin (in dark). Relative quantities are normalized to the nonadecanoic acid internal standard and the skin surface in cm^2. Stars display statistically significant differences between waxy and russeted 'Cox Orange Pippin' skins (Mann-Whitney test, *p*-value<0,05). Error bars represent the standard deviation obtained from four biological replicates. TTPx: undetermined triterpene.

A significant decrease of these two metabolites was observed in the russeted skin, oleanolic and ursolic acid display 10-fold and 7.8-fold decrease compared to the waxy tissues, respectively. β-amyrin, which is further converted into oleanolic acid by the multifunctional CYP716A145 (André *et al*. 2016), was present in a larger extent in the waxy tissues with a fold change equal to 4.2. Interestingly, lupeol, which is also converted to betulinic acid by CYP716A145 displayed a slightly increased content (FC=2.4) in the russeted tissues. Surprisingly, betulinic acid, which has been previously shown to accumulate specifically in the russeted apple skin (André *et al*. 2012), was not detected in this fraction. Finally, germanicol was also identified from the NIST database, but no significant difference in content was observed between skin tissues (Fig. 3-5). According to their mass spectra and retention time, other metabolites were suspected to be part of pentacyclic triterpene family. Although they showed lower contents compared to the triterpenes discussed above, some of them also displayed a decreased accumulation in the russeted tissues.

Other metabolites from different classes were also identified (Fig. 3-6). As an example, glycerol displayed a strong decreased accumulation in the russeted skin of 'Cox Orange Pippin' (FC=3.8). Glycerol is a crucial component of the cutin and suberin building blocks (Moire *et al*. 1999, Yang *et al*. 2010, Beisson *et al*. 2007). Cutin and suberin share a similar structure which is composed, in part, by middle position bound (sn-2) monoacylglycerol (MAG) which are further polymerized within these polymers (Bernard 2002, Vishwanath *et al*. 2015, Graca 2015). The glycerol-3-phosphate acyltransferase, namely GPAT5 and GPAT6, are responsible for the synthesis of suberin and cutin MAGs, respectively (Beisson *et al*. 2007, Li *et al*. 2012). Moreover, in *A. thaliana* roots, free MAGs were also detected in the suberin-associated waxes (Li *et al*. 2007). Two MAGs with C16 and C18:1 aliphatic chains were detected in the free lipid extract of both tissues.

Only the C18:1-MAG displayed a significant difference as it was only detected in the russeted tissue. Finally, the β-sitosterol was also more abundant in the waxy skin of 'Cox Orange Pippin'. β-sitosterol has previously been reported in the apple peel of the 'Florina' variety, but its role in the cuticle-associated waxes remains unclear (Verardo et al. 2003).

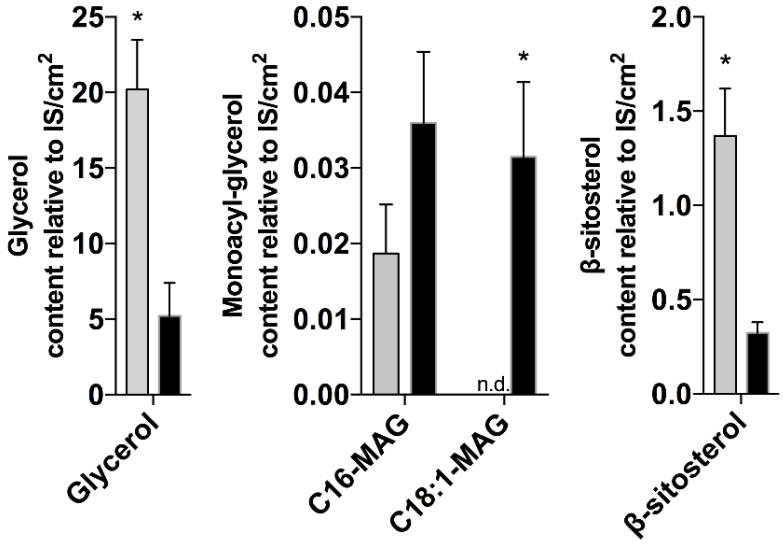

Figure 3-6: Distribution of glycerol (as trimethylsilyl ethers, on the left), monoacylglycerol (as trimethylsilyl esters in the middle), and β-sitosterol (as trimethylsilyl ethers, on the right) found in the free lipid fraction of the waxy skin (in grey) and russeted skin (in dark). Relative quantities are normalized to the nonadecanoic acid internal standard and the skin surface in cm^2. Stars display statistically significant differences between waxy and russeted 'Cox Orange Pippin' skins (Mann-Whitney test, *p*-value<0,05). Error bars represent the standard deviation obtained from four biological replicates. n.d.: not detected.

As shown in the graphs above, a large majority of the well-known cuticle-associated waxes component identified in this work displayed a drastic decrease in the russeted patches of the 'Cox Orange Pippin'. However, one metabolite class, namely the alkyl-hydroxicinnamates showed an inversed trend. These compounds were not detectable in the waxy skin whereas they accumulated in the suberized tissues (Fig. 3-7).

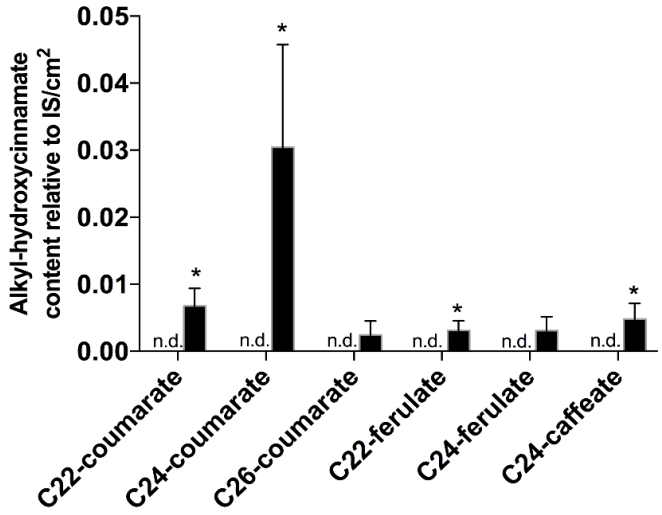

Figure 3-7: Distribution of the alkyl-hydroxycinnamates (as trimethylsilyl ethers, in dark) found in the free lipid fraction of the russeted skin. Relative quantities are normalized to the nonadecanoic acid internal standard and the skin surface in cm^2. Stars display statistically significant differences between waxy and russeted 'Cox Orange Pippin' skins (Mann-Whitney test, *p*-value<0,05). Error bars represent the standard deviation obtained from four biological replicates. n.d.: not detected in the waxy skin).

Alkyl-hydroxycinnamates are synthesized by enzymes belonging to the BAHD acyltransferase family and composed by hydroxycinnamic acids conjugated with primary alcohols (Kosma and Molina 2015, Delude *et al*. 2016). In *A. thaliana*

and *S. tuberosum* alkyl-hydroxycinnamates specifically accumulated in suberized tissues and their contents seem to differ from species to species (Schreiber *et al*. 2005, Serra *et al*. 2010, Kosma *et al*. 2012). In the present study, a majority of alkyl-hydroxycinnamates were composed by coumarate esters followed by ferulate and caffeate esters. Primary alcohols were mostly represented by C22 and C24 chain except for the C26-coumarate ester.

C. Cutin and suberin contained embedded wax and triterpenes

The boron trifluoride-methanol (BF_3/MeOH) transesterification method is commonly used to depolymerize either cutin or suberin (Franke *et al*. 2005, Gou *et al*. 2009, Panikashvili *et al*. 2009). It is worth noting that in the present experimental design, these two polymers are likely to be present in the russeted skin of the 'Cox Orange Pippin' variety, whereas a large majority of cutin monomers are expected in the waxy tissue. The BF_3/MeOH transesterification produced methyl ester from carboxylated fatty acids such as the α,ω-dicarboxylic acids and ω-hydroxyacids composing the cutin and suberin polymers. This makes the distinction easier between compounds which are esterified in the polymer matrix or conjugated with other metabolites from the free metabolites, which were detected as trimethylsilyl compounds.

First, some alkane traces were found in the depolymerized extract (Fig. 3-8). These metabolites, which are neither covalently linked with cutin nor with suberin, might have been confined in the polymer matrix (probably in the cutin, see discussion) and released during the depolymerization process. This hypothesis was supported by the predominance of the C29 alkane which was more abundant in the waxy skin (FC=3.1). Other n-alkanes with longer chains were identified but these did not show any significant differences between the two tissues. Triterpenes were also found in the depolymerized fraction. To our knowledge, triterpenes are not covalently linked to the cutin and suberin polymers (André *et al*. 2012, André

et al. 2016). Their occurrence in this fraction suggests that they might be also captured during the polymer assembly. Interestingly, the distribution of the different members of this class is similar to that in the free lipid extract. Ursolic and oleanolic acids are overrepresented in the waxy tissues, whereas a strong decrease is observed in the russeted skin. Moreover, a slight accumulation of betulinic acid was also observed (Fig. 3-8). Other unidentified triterpenes, which were more abundant in the waxy tissues were found.

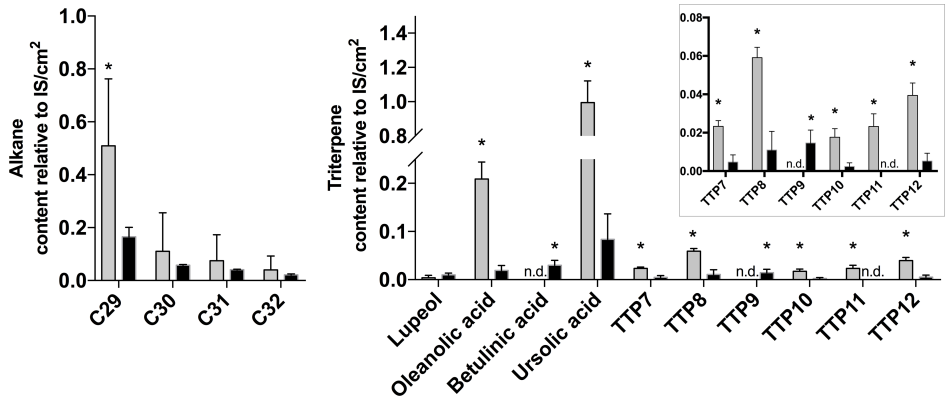

Figure 3-8: Distribution of the alkanes (on the left) and triterpenes (as trimethylsilyl ethers, on the right) found in the waxy skin (in grey) and russeted skin (in dark) after BF_3/MeOH transesterification. Relative quantities are normalized to the nonadecanoic acid internal standard and the skin surface in cm^2. Stars display statistically significant differences between waxy and russeted 'Cox Orange Pippin' skins (Mann-Whitney test, *p*-value<0,05). Error bars represent the standard deviation obtained from four biological replicates. n.d.: not detected. TTPx: undetermined triterpenes.

D. Russeted skin displayed a decreased cutin synthesis associated with an enhanced synthesis of suberin-specific very long chain fatty acid precursors

Analysis of the fatty acid (methyl esters) showed significant differences in content between the russeted and waxy skin (Fig. 3-9). The C16, C18:1, C18:2, C28 and C30 fatty acids were slightly, but significantly more abundant in the waxy skin. As an example, the C16, C18:1 and C18:2 fatty acids accumulated 1.6, 3.1 and 4.3 times more in the waxy tissues, respectively (Fig. 3-9). However, the most abundant fatty acids were found in the russeted tissues, which strongly accumulated C20, C22 and C24 fatty acids, with respective 2,96-, 7.1- and 5.2-fold increase.

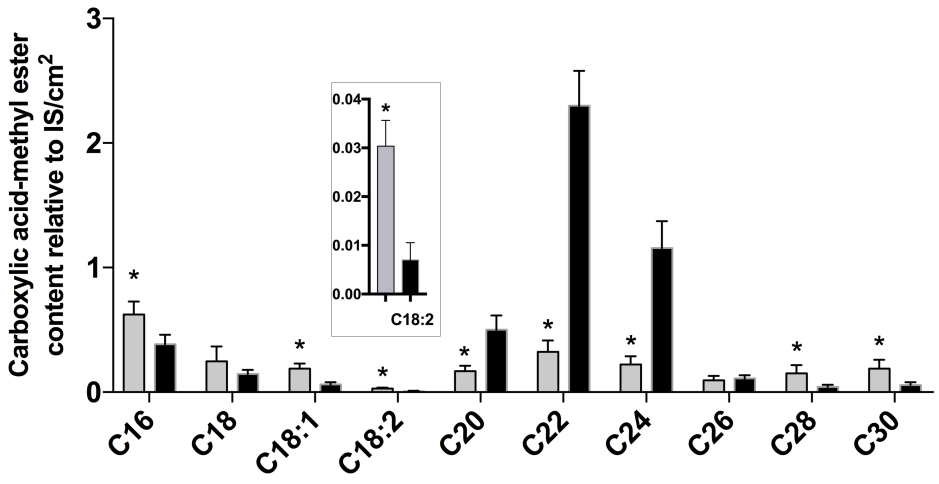

Figure 3-9: Distribution of the alkanoic acids (as methyl esters) found in the waxy skin (in grey) and russeted skin (in dark) after BF_3/MeOH transesterification. Relative quantities are normalized to the nonadecanoic acid internal standard and the skin surface in cm^2. Stars display statistically significant differences between waxy and russeted 'Cox Orange Pippin' skins (Mann-Whitney test, *p*-value<0,05). Error bars represent the standard deviation obtained from four biological replicates.

This VLCFAs accumulation in the depolymerized fraction of the russeted tissues suggests that they might be part of the suberin polymer matrix. Conversely, their slight contents observed in the waxy skin, might be attributed to the russeted spots (lenticels), which are spread on the whole fruit surface.

The analysis of the depolymerized extracts, showed a significant increase of C22 and C24 chain length trimetylsilylated primary alcohols in the russeted skin with 7.7- and 1.8- fold increase, respectively (Fig. 3-10). Conversely, the C28 and C30 chain primary alcohols were more abundant in the waxy skin with 3.1- and 2.3-fold increase compared to russeted skin.

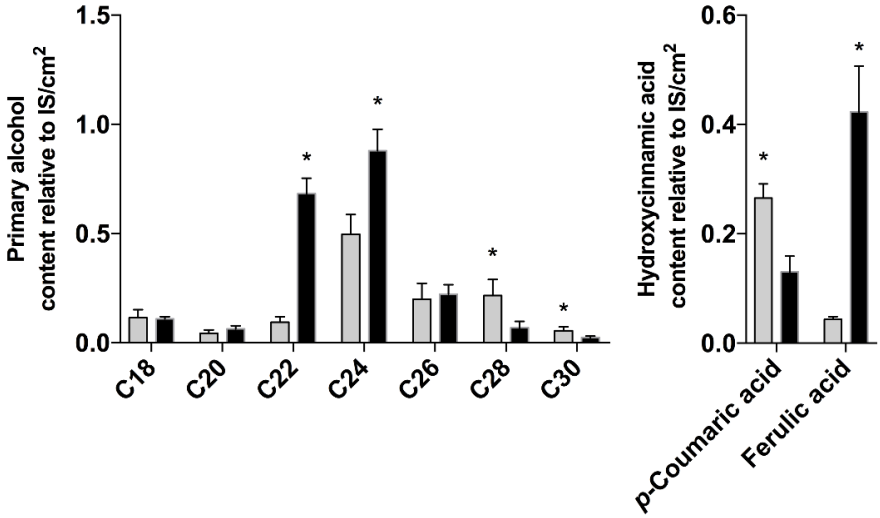

Figure 3-10: Distribution of the primary alcohols (as trimethylsilyl ether, on the left) and hydroxycinnamic acids (as silylated methyl esters, on the right) found in the waxy skin (in grey) and russeted skin (in dark) after BF_3/MeOH transesterification. Relative quantities are normalized to the nonadecanoic acid internal standard and the skin surface in cm^2. Stars display statistically significant differences between waxy and russeted 'Cox Orange Pippin' skins (Mann-Whitney test, *p*-value<0,05). Error bars represent the standard deviation obtained from four biological replicates.

As transesterification of the conjugated primary alcohols results in a free hydroxyl group, these data reflect a merged quantification of the free and conjugated primary alcohols *i.e.* alkyl-hydroxycinnamates. However, the differential accumulation of, on one hand C22 and C24 primary alcohols and, on the other hand, C28 and C30 ones, suggests that these two groups might have been synthesized for a different purpose. Interestingly, significant amounts of *p*-coumaroyl and feruloyl-methyl esters were found in the depolymerized fraction. These two compounds displayed an inverse accumulation pattern. The waxy skin presented a higher amount of *p*-coumaroyl-methyl ester and a lower amount of feruloyl-methyl ester compared to the russeted skin. It is noteworthy that the feruloyl methyl ester displayed the largest difference between both tissue types (FC=9.7), which might be explained by the crucial role of ferulic acid in the suberin structure and its associated waxes (Bernards 2002, Graca 2015, Molina and Kosma 2015).

The α,ω-dicarboxylic acids are major components of cutin and suberin. These precursors are esterified with glycerols on both carboxyl groups resulting in a reticular structure which constitutes the core backbone of these polymers (Bernards 2002, Graca 2015). The analysis of BF_3/MeOH depolymerized extract showed that α,ω-dicarboxylic acids contents were higher in the suberized (russeted) tissues (Fig. 3-11). This observation is in agreement with a previous work performed on *A. thaliana,* which also showed higher proportions of these diacids in suberin compared to cutin (Franke *et al.* 2005). As an example, in russeted tissues, C16 and C18 α,ω-dicarboxylic acids displayed 2.4 and 3.1 fold increase compared to the waxy tissues, respectively. The 9,10 dihydroxy-α,ω-dicarboxylic acid showed the strongest increase among this metabolite family (FC=6.5). Finally, three saturated very long chain α,ω-dicarboxylic acids comprising 20, 22 and 24 carbon chains also displayed, to a lower extent, a

significant increase in the russeted skin (FC=5 for the C20 and C22, presence for the C24). On the contrary, the C18:1 and C18:2 α,ω-dicarboxylic acid-dimethyl esters slightly decreased in the russeted tissues.

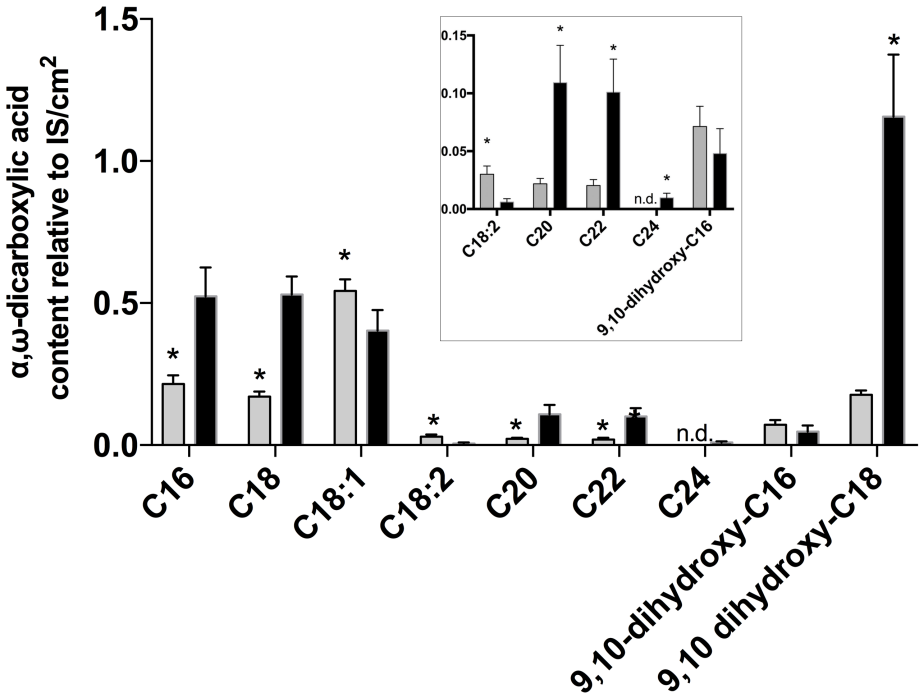

Figure 3-11: Distribution of the α,ω-dicarboxylic acids (as methyl esters) found in the waxy skin (in grey) and russeted skin (in dark) after BF_3/MeOH transesterification. Relative quantities are normalized to the nonadecanoic acid internal standard and the skin surface in cm^2. Stars display statistically significant differences between waxy and russeted 'Cox Orange Pippin' skins (Mann-Whitney test, *p*-value<0,05). Error bars represent the standard deviation obtained from four biological replicates. n.d.: not detected.

As the α,ω-dicarboxylic acids, ω-hydroxyacids are considered as characteristic elements of cutin and suberin. These hydroxylated fatty acids are esterified with glycerol within the α,ω-dicarboxylic acid reticular structure and display multiple

forms with various carbon chain numbers and multiple mid- and side-chain modifications such as desaturation, hydroxylation and epoxidation (Bernards 2002, Graça 2015). In the waxy skin of 'Cox Orange Pippin', higher contents in 16-hydroxydecanoic acid; 18-hydroxydecanoic acid, 18-hydroxy-9,12-octadecenoic acid, 10,16-dihydroxyhexadecanoic acid and 9,10,18-trihydroxy-12-octadecenoic acid were observed (Fig. 3-12).

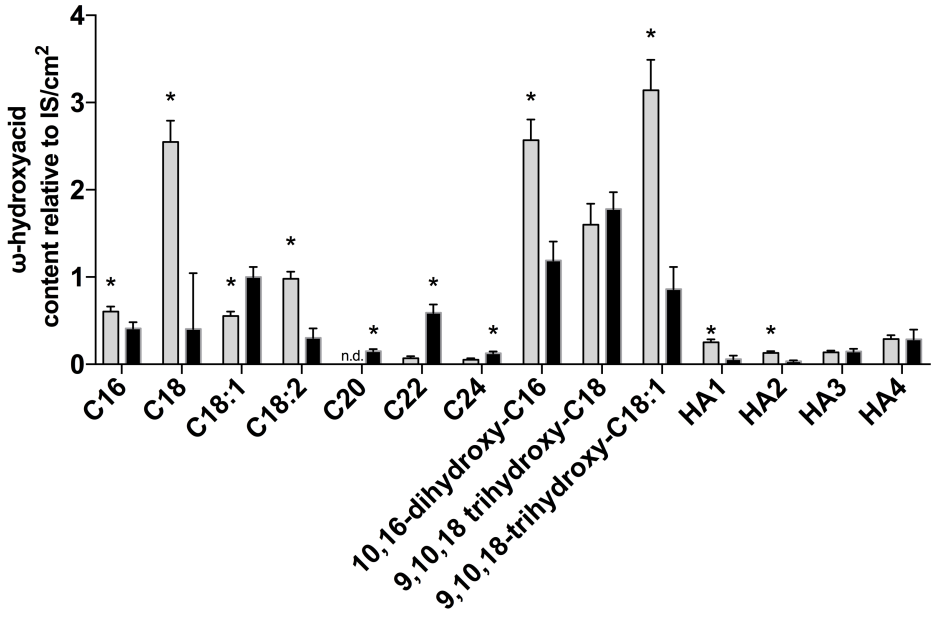

Figure 3-12: Distribution of the ω-hydroxyacids (as silylated methyl esters) found in the waxy skin (in grey) and russeted skin (in dark) after BF_3/MeOH transesterification. Relative quantities are normalized to the nonadecanoic acid internal standard and the skin surface in cm^2. Stars display statistically significant differences between waxy and russeted 'Cox Orange Pippin' skins (Mann-Whitney test, *p*-value<0,05). Error bars represent the standard deviation obtained from four biological replicates. n.d.: not detected. HAx: undetermined hydroxyacid-methyl esters.

The 18-hydroxydecanoic acid, 18-hydroxy-9,12-octadecenoic acid and the 9,10,18-trihydroxy-12-octadecenoic acid showed remarkable differences in content with FC equal to 6.3, 3.2 and 3.6, respectively (*p*-value<0,05). In addition, some putative ω-hydroxyacids with mid-chain modifications also displayed a slight increase in the waxy skin. Conversely, suberized skin presented a higher amount of 18-hydrodecanoic acid and, as observed for the previous classes, some members with longer chain, including the 20-hydroxyeicosanoic acid, 22-hydroxydocosanoic acid and 24-hydroxytetracosanoic acid, the highest increased being observed for the 22-hydroxydocosanoic acid (FC=2.4).

E. Drastic differential expression of cutin, suberin, wax and triterpene biosynthetic genes between russeted and waxy skins of 'Cox Orange Pippin'

In order to support the results obtained from the free lipid and BF_3/MeOH extracts, the expression of the apple orthologs of *A. thaliana* genes involved in the cutin, suberin, wax and triterpene biosynthesis, selected from our previous transcriptomic works and other published studies, was also investigated in the semi-russeted 'Cox Orange Pippin' variety (Fig. 3-13, Brendolise *et al*. 2011, Legay *et al*. 2015, André *et al*. 2016). As observed in our previous work, the data displayed drastic changes in the expression of genes involved in these pathways between the russeted and waxy skin of 'Cox Orange Pippin'.

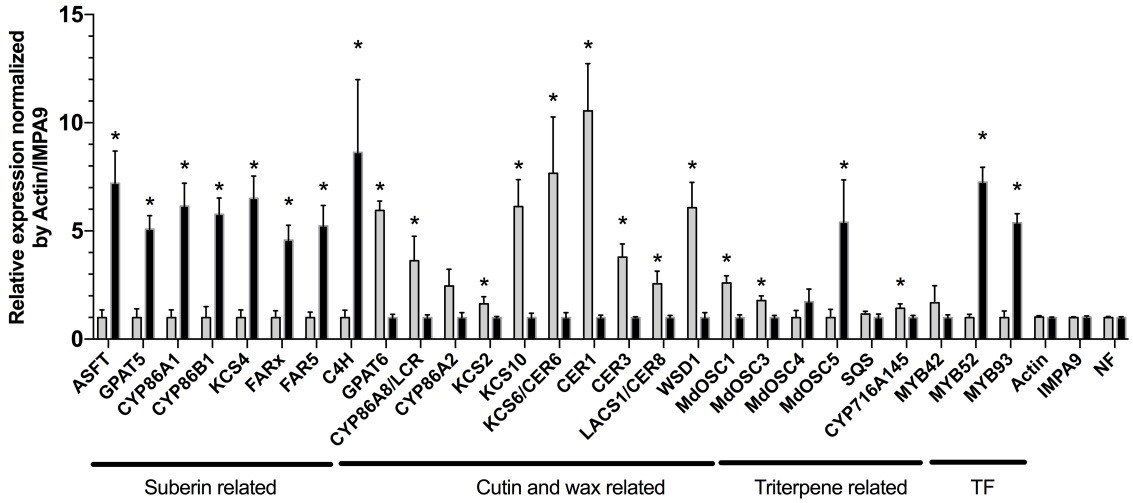

Figure 3-13: Normalized relative expression (NRq) of lipid surface biosynthesis genes performed in the waxy skin (in grey) and russeted skin (in dark). Relative quantities (Rq) are normalized by Md_Actin and Md_IMPA9 (showed as control (not normalized), NF: normalization factor). Stars highlight genes displaying a statistically significant difference between waxy and russeted 'Cox Orange Pippin' skin obtained from a Mann-Whitney test in qbase+ v3 (*p*-value<0,05). Normalized relative quantities were rescaled to the less expressed group (waxy or russet skin) to better visualize fold changes. Error bars display the standard deviation obtained from four biological replicates for each groups. ASFT: Arabidopsis suberin feruloyl transferase-like, GPAT: Glycerol-3-phosphate acyl transferase, CYP: cytochrome P450, 'CYP86A1': fatty acid hydroxylase, 'CYP86B1': very long chain fatty acid hydroxylase, FAR: fatty acid reductase, C4H: cinnamate-4-hydroxylase, CYP86A2: putative fatty acid hydroxylase, CYP86A8/LCR, CER: ECERIFERUM, LACS: long chain acyl-CoA synthetase, KCS: 3-ketoacyl-CoA synthase, WSD1: bifunctional wax ester synthase/diacylglycerol acyltransferase, SQS: Squalene synthase, OSC: oxidosqualene cyclase, CYP716A145: pentacyclic triterpene oxidase. TF: transcription factors, MYB: MYB transcription factor.

Cutin biosynthesis genes globally showed a decreased expression in the russeted tissues. First, a gene coding for a long chain acyl-CoA synthetase 1 (*LACS1/CER8*), which is responsible for the CoA activation of the fatty acid precursors, was downregulated (Lü *et al*. 2009). In *A. thaliana*, C16, C18 and C18:1 acyl-CoA precursors are further hydroxylated into ω-hydroxyacids by fatty acid hydroxylases such as the CYP86A2 or/and CYP86A8 (LACERTA, LCR) (Voisin *et al*. 2009, Wellesen *et al*. 2001). In the present study, a significant decreased expression (FC=3.6) of the *LCR* gene was observed in the russeted skin, suggesting that synthesis of the cutin monomer precursors was impaired in these tissues. This decreased cutin biosynthesis was also supported by the lower expression of the *GPAT6* gene (FC=5.9). In *Solanum lycopersicum*, the GPAT6 displays a strong specificity for C16 and C18 carbon chain and plays a crucial role in the formation of ω-hydroxyacyl- and α,ω-dicarboxyl-glycerol monomers, which are further used as cutin building blocks (Petit *et al*. 2016). The expression of genes belonging to the wax biosynthesis seemed to be altered in the russeted area of the 'Cox Orange Pippin' skin. Three 3-ketoacyl-CoA synthase genes (*KCS2, 6* and *10*), responsible for the conversion of fatty acyl-CoA into very long chain acyl-CoA, which are further used for the wax biosynthesis, also displayed a decreased expression (Millar *et al*. 1999, Voisin *et al*. 2009, Yeats and Rose 2013). The Eceriferum *CER1* and *CER3* genes, which are also involved in the wax biosynthesis displayed a similar expression pattern with fold changes equal to 10 and 3.8, respectively. Finally, the bifunctional wax ester synthase/diacylglycerol acyltransferase (*WSD1*) gene found in our previous bulk transcriptomic analysis was also tested and showed a similar trend (FC=6.1).

On the other hand, the expression of suberin biosynthetic genes seemed to be enhanced in the russeted skin. A *KCS4* gene displayed an increased expression in

the russeted tissues (FC=6.5). In *A. thaliana*, the KCS2/DAISY and KCS20 display a redundant function in cuticle waxes and root suberin biosynthesis (Lee et al. 2009). A *KCS2* gene was also induced in the russeted varieties, in our previous work (Legay *et al.* 2015), but the involvement of the KCS4 in the suberization process is still unclear. In *A. thaliana*, a KCS4 enzyme expressed in flowers and old siliques was unable to use the C16 and C18:1 fatty acid precursor as substrate, suggesting that this enzyme might process acyl-CoAs with longer carbon chains (Blacklock and Jaworski 2006, Joubès *et al.* 2008). The expression of the *FARx* and *FAR5*, which encodes fatty acyl-CoA reductases and produce primary alcohols, was also significantly induced with fold changes equal to 4.6 and 5.2, respectively. FAR5 has been previously associated with the production of suberin-associated fatty alcohols (Domergue *et al.* 2010). The FARx seems to be close to FAR1, which is also involved in the suberin-associated primary alcohols synthesis. Genes for well-known CYP86A1 fatty acid hydroxylase and CYP86B1 VLCFA hydroxylase displayed a significant increased expression in the russeted tissues (Höfer *et al.* 2008, Compagnon *et al.* 2009). Gene for GPAT5, which is responsible for the suberin specific biosynthesis of ω-hydroxyacyl- and α,ω-dicarboxyl-glycerols showed a similar expression pattern (FC=5.1). The expression of the *MYB52* and *MYB93* transcription factors was also induced in the russeted tissues, with FC=7.2 and 5.4, respectively. The *MYB93* gene previously showed a highly correlated expression with *GPAT5*, *CYP86A1* and *CYP86B1*, suggesting that it might be involved in the regulation of the suberin synthesis (Legay *et al.* 2015). The orthologous gene of the *A. thaliana* suberin feruloyl-CoA acyl transferase (ASFT), which is crucial for the incorporation of ferulic acid in the suberin matrix was also significantly induced (FC=7.2; Molina *et al.* 2009, Legay *et al.* 2015). Finally, the cinnamate-4-hydroxylase (C4H) involved in the

hydroxycinnamic acid biosynthesis, was also strongly induced in the russeted skin (FC=8.3).

Genes belonging to the pentacyclic triterpene biosynthesis pathway were also investigated (Brendolise *et al*. 2011, André *et al*. 2016). To date, three main triterpene series, namely the ursane, oleane and lupane series, have been identified in apple (André *et al*. 2012). MdOSC1, which synthesizes predominantly the α-amyrin, the ursane series precursor further converted into ursolic acid, was more expressed in the waxy skin (FC=2.6). A similar trend was observed for the *MdOSC3* gene, which is highly similar to *MdOSC1* and might share a similar function (Brendolise *et al*. 2011, André *et al*. 2016). Inversely, the *MdOSC5* gene was significantly up-regulated in the russeted skin. MdOSC5 has been recently described as a crucial enzyme involved in the synthesis of lupeol, which is further converted to betulinic acid by the CYP716A145 monooxygenase (André *et al*. 2016). Interestingly, the *CYP716A145* gene displays a slight increase (43%) in the waxy skin. This multifunctional enzyme is responsible for the conversion of α-amyrin, β-amyrin and lupeol into ursolic, oleanolic and betulinic acids, respectively (André *et al*. 2016). Genes for the squalene synthase, which is involved in the early steps of the triterpene synthesis, and MdOSC4, which synthesizes germanicol, β-amyrin and lupeol in the proportion 84: 14: 4, were not differentially expressed between these two tissues.

IV. Discussion

Russeting is a major concern for the apple fruit production. Since the 60's, the complex relationship occurring between the cuticle deposition and russeting has been extensively reported as a crucial point by multiple teams. The current model postulates that russeting occurrence is tightly linked with defects and/or lower

deposition of the cuticle on the fruit surface (Sironval and Clijters 1962, Walter 1967, Faust and Shear 1972, Skene 1982, Knoche and Grimm 2008, Lashbrooke *et al*. 2015). Our previous bulk transcriptomic analysis showed that genes involved in cutin and waxes biosynthesis displayed a decreased expression in russeted apple skin, with a concomitant increased expression of the suberin biosynthetic genes (Legay *et al*. 2015). Compared to the fully russeted varieties, which represent an extreme case of russeting, the use of the semi-russeted 'Cox Orange Pippin' provided a model which is closer to the genetic and phenotypic germplasm used in the apple production. Indeed, russeting in commercial varieties usually appears as patches, as those observed in 'Cox Orange Pippin', which gradually appear during the fruit development, whereas old heirloom fully russeted apples exhibit this strong phenotype at the very early stage of the fruit growth (Sironval and Clijters 1962, Walter 1967, Faust and Shear 1972).

The analysis of the lipids of the apple fruit surface showed a massive decreased accumulation of the cuticle-associated waxes. These include the very long chain primary alcohols, aldehydes, fatty acids and alkanes, with carbon chains longer than 24 carbons (Fig. 3-14). This observation was reinforced by the decreased expression of genes coding for *KCS2*, *KCS6* and *KCS10*, which are implicated in the elongation of C16 and C18 acyl-CoA into very long chain acyl-CoA, the latter being used as precursors for the different classes of metabolites comprised in these cuticle waxes (Millar *et al*. 1999, Lee *et al*. 2009, Lee and Suh 2013). The following steps of the cuticular wax biosynthesis are still under investigation. However, it is suggested that the wax biosynthesis pathway follows two distinct branches (Millar *et al*. 1999, Von Wettstein-Knowles 2012). The reductive pathway produces even number carbon chain numbers as found in aldehydes and primary alcohols. Aldehydes are considered as intermediate compounds between the acyl-CoAs and

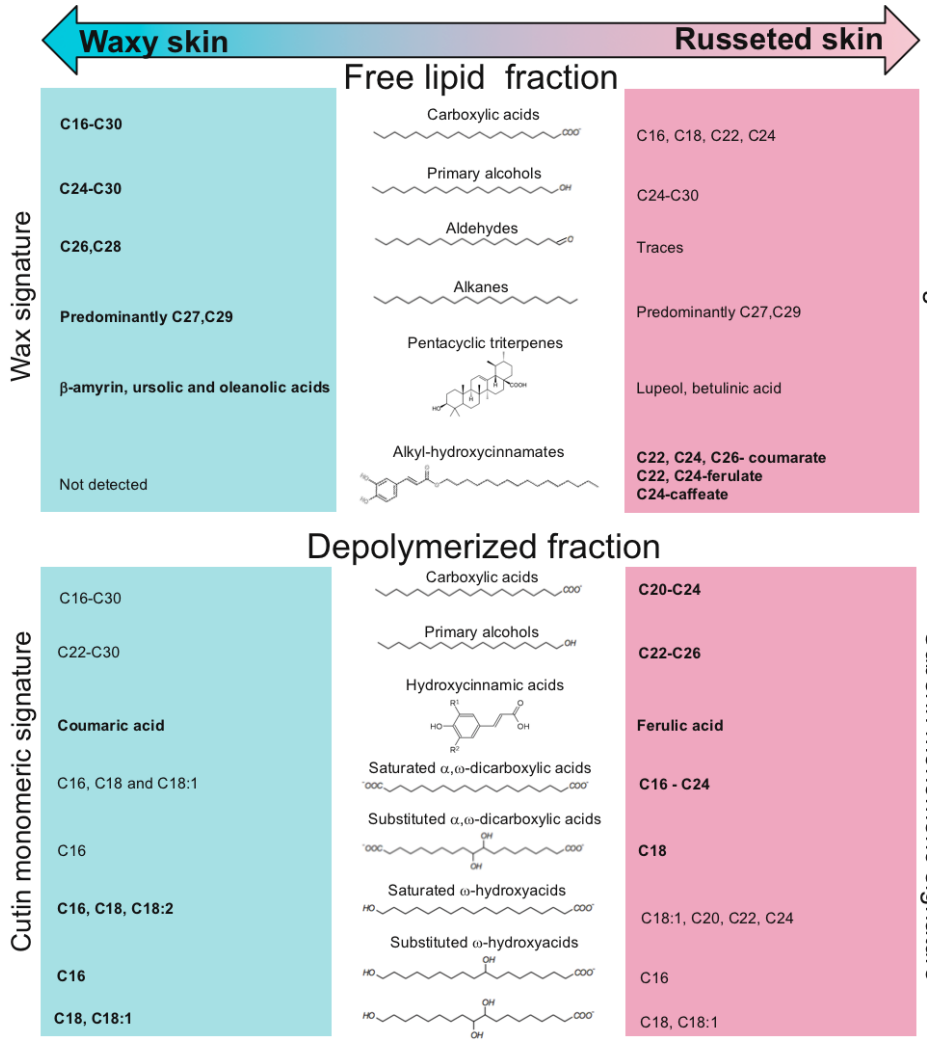

Figure 3-14: Overview of the metabolites found in the free lipid and depolymerized fractions of the 'Cox orange Pippin' waxy and russeted skins. Compounds highlighted in bold indicate the global higher content of their respective family in the tissue.

primary alcohols (Von Wettstein-Knowles 2012). On the other side, the decarbonylation of fatty acyl-CoAs might be involved in the biosynthesis of classes sharing odd carbon chain number, as observed for the alkanes. These latter compounds are further hydroxylated into secondary alcohols and ketones. In the present work, it is noteworthy that the major primary alcohols and aldehydes were composed of 26- and 28-carbon chains whereas alkanes showed C27- and C29-carbon chains. Thirty-carbon chains were only observed for the free fatty acids, which strongly accumulated in the waxy skin of 'Cox Orange Pippin' (Fig. 3-14). As VLCFAs are synthesized from very long chain acyl-CoA, the C29 n-alkanes biosynthesis might result from the decarbonylation of a C30 acyl-CoA common precursor. CER1, CER3 and CER8 are also involved in the alkanes biosynthesis (Aarts *et al*. 1995, Rowland *et al*. 2007, Lü *et al*. 2009). Apple orthologous genes of *CER1* and *CER3*, which have been found in our previous RNA-Seq data, were more expressed in the waxy tissues of 'Cox orange Pippin', suggesting that they might indeed have a role in the biosynthesis of apple skin waxes.

As opposed to the cutin-associated waxes described above, the 'Cox orange Pippin' russeted skin specifically accumulated some alkyl-hydroxycinnamates (Fig. 3-14). These metabolites, which are constituted of hydroxycinnamic acids conjugated with primary alcohols, have been previously associated with the suberization process in *A. thaliana* and *S. tuberosum* to name a few (Schreiber *et al*. 2005, Serra *et al*. 2010, Kosma *et al*. 2012, Kosma *et al*. 2015, Molina and Kosma 2015, Delude *et al*. 2016). In our work, a majority of coumarate conjugates have been found, followed by ferulates and caffeates. Primary alcohols esterified with these hydroxycinnamic acids are mostly represented by 22- and 24-carbon chains length (Fig. 3-14). This was not in accordance with the primary alcohols distribution observed in the free lipids extract, which displayed predominantly 26- and 28- carbon chains. However, primary alcohols found in the depolymerized

extract showed a completely different pattern with an enhanced accumulation of C22 and C24 chains in the russeted skin (Fig. 3-14). In *A. thaliana* roots, the large majority of the primary alcohols found in the suberized tissues are in the form of alkyl-hydroxycinnamates (Delude *et al*. 2016). In apple, it might be conceivable that a similar process occurred and explains the concordant distribution of primary alcohols observed in the alkyl-hydroxycinnamates and those identified in the depolymerized extract. This suggests that the differentially expressed *KCS2 and KCS4* genes, observed in this work and in our previous transcriptomic data, might be responsible for the specific synthesis of these C22 and C24 acyl-CoA, which are further partly converted into primary alcohols by FARx and FAR5 (Legay *et al*. 2015). In *A. thaliana*, the *kcs2* loss-of-function mutant displayed a significant decreased content in C22 and C24 VLCFAs (Lee *et al*. 2009). The suberin biosynthetic process occurring in the russeted skin might induce *KCS2* genes which produce essentially C22 and C24 chains for further synthesis of these alkyl-hydroxycinamates. Inversely, the *KCS2*, *KCS6*/*CER6*/*CUT1* and *KCS10* genes, which are up-regulated in the waxy skin, might produce longer carbon chain acyl-CoA, which are further used for the cutin wax, including the C26 and C28 primary alcohols observed in the present work. As an example, the *cut1*-loss of function mutant led to an over-accumulation of C24 chain-length wax components, suggesting that KCS6 is responsible for the elongation of the C24 acyl-CoA into longer precursors (Millar *et al*. 1999).

Pentacyclic triterpenes are major components of the fruit skin waxes in apple (André *et al*. 2012). In waxy varieties, the total triterpene content can reach up to 70% of the total waxes content depending on the genetic background of the variety and the environmental factors (André *et al*. 2012). The distribution of the different series of triterpene seems to be tightly linked with the degree of skin russeting (Brendolise *et al*. 2011, André *et al*. 2012, André *et al*. 2016). As observed for the

other wax component described above, our data showed that ursolic and oleanolic acids displayed severe decreased contents in the russeted skin, suggesting that the whole wax deposition process, which includes these triterpenes, is impaired in these tissues (Fig. 3-14). This observation was supported by the decreased expression of the *MdOSC1* and *MdOSC3* genes in the russeted skin. MdOSC1 produces mainly α-amyrin, which is further converted into ursolic acid by the CYP716A145 oxidase. *MdOSC3*, which is highly homologous to *MdOSC1*, probably because of the ancestral genome duplication of the *Pyrae* ancestor, has a similar function (Brendolise *et al*. 2011, André *et al*. 2016). Conversely, previous works showed that betulinic acid predominantly accumulates in the russeted tissues (André *et al*. 2012). Surprisingly, betulinic acid was only detected in the depolymerized fraction. To date there is no evidence that betulinic acid might be covalently linked to the suberin matrix. Thus, we can speculate that it might be embedded in this polymeric matrix. Finally, it is noteworthy that other minor unidentified pentacyclic triterpenes, which display differential accumulations, have been detected in both fractions. However, standards are currently lacking to identify them properly and it is not yet possible to identify them. Altogether, these observations strengthened the present knowledge about the tight relationship between the suberization process and the pentacyclic triterpenes synthesis. As ursolic and oleanolic acids are major component of the non-russeted skin waxes, their decreased accumulation might also have an impact on the integrity of the cuticle. Thus, it would be interesting, in further works, to evaluate their role in the development of cuticle microcracking.

The analysis of the depolymerized extract showed strong differences between the metabolic profiles obtained from the russeted and waxy skin of 'Cox Orange Pippin'. The distribution of fatty acids was particularly interesting and differed from the results obtained in the free lipid extract. Suberized tissues displayed

increased content of VLCFAs ranging from C20 to C24 chains, whereas a decreased accumulation of C16, C18, C18:1 and C18:2 was observed (Fig. 3-14). In plants, the composition of suberin-associated fatty acids seems to vary among species and tissues. In *A. thaliana* roots, the analysis of the suberin monomers revealed a majority of C20 and C22 fatty acids whereas the *S. tuberosum* suberin displayed longer carbon chains with a majority of C24 to C28 fatty acids (Franke *et al*. 2005, Graca and Pereira 2000b). *A. thaliana* seed coat suberin is composed of a majority of C16, C20 and C24 chains (Molina *et al*. 2006). Finally, the bark suberin monomeric contents of *P. menziesii* and *Q. suber* display higher proportions of the C20 to C24 fatty acids as observed in our work (Graca and Pereira 2000a). Caution should be taken with the present results because these fatty acids are probably issued from both cutin and suberin. However, as observed for the alkyl-hydroxycinnamate-associated primary alcohols, our results suggest a suberin specific biosynthesis of C20 to C24 (predominantly C22) very long chain acyl-CoA precursors in the russeted tissues (Legay *et al*. 2015, Lee *et al*. 2009). In *A. thaliana*, the analysis of the cutin composition indicated a quasi-exclusive occurrence of C16 and C18 monomers, suggesting that the shorter carbon chain fatty acids, found in a higher amount in the waxy apple skin, might be part of the cutin polymer and that their synthesis is impaired in the russeted tissue (Bonaventure *et al*. 2004).

The composition of the ω-hydroxyacids is more complex but seemed to follow a similar trend compared to fatty acids. Indeed, waxy skin displayed increased amount of C16, C18, C18:2 whereas a specific accumulation of C18:1, C20, C22 and C24 ω-hydroxyacids was observed in the suberized skin (Fig. 3-14). In *A. thaliana* roots, ω-hydroxyacids are mainly composed of C16, C18, C20 and C22 aliphatic chains with a strong predominance of the 18-hydroxyoctadec-9-enoic acid (C18:1 ω-hydroxyacid, Franke *et al*. 2005), whereas C18:1, C18:2, C22 and

C24 ω-hydroxyacids are mostly represented in the *A. thaliana* seed coat suberin (Molina *et al*. 2006). In the potato periderm, a massive amount of C18:1 ω-hydroxyacid has been also found and, to a lower extent, some C16, C22, C24, C26 and C28 ω-hydroxyacids (Graca and Pereira 2000b). Finally, the bark of *Q. suber* displays a majority of C22, C24 ω-hydroxyacids (Graca and Pereira 2000a). In our study, the specific accumulation of these very long chain ω-hydroxyacids in the apple suberized skin was supported by the increased expression of the VLCFA hydroxylase (CYP86B1) gene (Compagnon *et al*. 2009). Moreover, an increased expression of *GPAT5* was observed in the russeted tissues. In *A. thaliana*, GPAT5, which synthetizes the suberin ω-hydroxyacyl- and α,ω-diacyl-glycerol building blocks, displays a strong affinity for the very long chain (>C18) ω-hydroxyacids and α,ω-dicarboxylic acids (Beisson *et al*. 2007). Altogether, these data support the idea that C20, C22 and C24 ω-hydroxyacids might constitute specific precursor of suberin in apple.

Furthermore, the C18:1 ω-hydroxyacid, which strongly accumulates in the *A. thaliana* roots (Franke *et al*. 2005) and the russeted potato periderm (Graca and Pereira 2000b) is the only short chain ω-hydroxyacid displaying an increased content in the russeted apple skin. We might speculate that this compound might be produced by the CYP86A1 fatty acid hydroxylase (Höfer *et al*. 2008), which displayed a significant increased expression in our RT-qPCR results. Some mid-chain hydroxylated ω-hydroxyacids showed a higher content in the waxy skin, suggesting that they might be part of the cutin polymer. These might be synthesized by the preliminary action of some cutin specific epoxidase such as the *A. thaliana* CYP77A4 (Sauveplane *et al*. 2009), which was also more expressed in the waxy skin in a previous work (Legay *et al*. 2015). Epoxidized fatty acids

might be further hydroxylated by some epoxide hydrolase to yield mid-chain hydroxylated fatty acids, but no candidate has been found yet (Yeats *et al*. 2012). The core structural backbone of both cutin and suberin is constituted of α,ω-dicarboxylic acids esterified to glycerols. Previous studies showed that suberin exhibits high content in this compound family compared to cutin (Franke *et al*. 2005). A similar tendency was observed in apple, which showed an increased accumulation in the majority of the identified α,ω-dicarboxylic acids. Interestingly, the highest contents were observed for the shorter carbon chains α,ω-dicarboxylic acids, such as hexadecanedioic, octadecanedioic and 9,10-dihydroxyoctadecanedioic acids, whereas eiocosanedioic, docosanedioic and tetracosanedioic acids were less abundant. Again, the apple suberization process seemed to specifically produce C20, C22 and C24 α,ω-dicarboxylic acids, whereas shorter carbon chains α,ω-dicarboxylic acids were predominant in the waxy apple skin (Fig. 3-14). The same trend is observed in *S. tuberosum*, *A. thaliana* roots and *P. menziesii* (Franke *et al*. 2005, Graca and Pereira 2000a, Graca and Pereira 2000b). Only suberin monomers obtained from the *Quercus suber* bark and *A. thaliana* seed coats displayed predominant or large amount of very long chain α,ω-dicarboxylic acids (Graca and Pereira 2000a, Molina *et al*. 2006). The synthesis of these α,ω-dicarboxylic acids remains unclear, some authors argue that the consecutive action of alcohol dehydrogenase and aldehyde dehydrogenase on ω-hydroxyacids precursors might support the synthesis of these crucial compounds but no candidates have been found yet (Franke and Schreiber 2007).

Finally, coumarate and ferulate methyl esters were detected in both russeted and waxy tissues, suggesting that they were covalently linked within the cutin and/or suberin polymeric matrix, or conjugated into other compounds such as alkyl-

hydroxycinnamates or triterpene conjugates (Kosma *et al*. 2012, André *et al*. 2013, Fig. 3-14). Higher content of ferulic acid in the russeted skin is obvious as it is one of the major suberin structure signature (Bernard 2002, Franke *et al*. 2005, Molina *et al*. 2006, Graca 2015, Vishwanath *et al*. 2015). Hydroxycinnamic acids are thought to be part of the suberin polyphenolic domain of suberin which is anchored in the cell wall (Bernard *et al*. 1995, Bernard 2002). Moreover, ASFT is responsible for the linkage of ferulic acid with ω-hydroxyacids resulting in feruloyl-acyl esters, which are considered as crucial suberin building blocks (Molina *et al*. 2009). An apple orthologous gene of *ASFT*, which has been found in our previous transcriptomic profiling of the russet trait, displayed a strong increased expression in the russeted tissues of 'Cox Orange Pippin' (Legay *et al*. 2015). Covalently linked coumaric acid, possibly to cutin, has been already described in apple, but not ferulic acid (Riley and Kolattukudy 1975); this might be explained by the fact that this study did not comprise russeted varieties. Conversely, a fairly detectable amount of coumaric acid was found in the russeted skin and even more in the waxy skin, suggesting that coumaric acid might be more related to the cuticle development but its exact involvement in this matrix remains unclear (Riley and Kolattukudy 1975).

The present data depict for the first time the complex structure of the waxy and russeted apple skins. Our previous transcriptomic profiling study showed an impaired expression of genes involved in the cuticle deposition in the russeted varieties with a concomitant increased expression of genes involved in the suberin biosynthetic pathway. Recent studies postulated that an efficient cuticle is crucial to prevent any occurrence of suberization on the fruit surface (Knoche and Grimm 2011, Khanal *et al*. 2013, Lashbrooke *et al*. 2015). Our data clearly support this hypothesis. In the russeted skin patches of the 'Cox Orange Pippin', a massive decrease of the cuticle waxes was observed. These included primary alcohols,

alkanes, fatty acids and aldehydes, along with the pentacyclic triterpenes ursolic and oleanolic acids. This decrease in the wax content is also accompanied by a decreased synthesis of cutin which is composed by a majority of 16- and 18-carbon chain ω-hydroxyacids and α,ω-dicarboxylic acids. The concomitant decreased content of cutin and wax components together with the expression pattern of their biosynthetic genes, suggest that a common regulatory network might orchestrate these pathways. It would be interesting to investigate whether some cuticle deposition master regulators such as *MdSHN3* and/or a *AtMYB94* apple orthologous genes, are able to alter the triterpenic acid contents in the apple fruit skin (Lashbrooke *et al*. 2015, Lee and Suh 2015).

Suberin, which accumulates in russeted patches, was similar to the previously reported composition investigated in other species (Franke *et al*. 2005, Graca and Pereira 2000a, Graca and Pereira 2000b, Molina *et al*. 2006). In addition to the characteristic ferulic acid, C20, C22 and C24 very long chain backbone precursors, which are further used for the synthesis of primary alcohols, fatty acids, ω-hydroxyacids, α,ω-dicarboxylic and possibly the suberin specific non-covalently linked alkyl-hydroxycinnamates, constituted the main characteristic of the apple suberin. Notably, the small amount of C20, C22 and C24 precursors observed in the waxy tissues might be due to the presence of suberized lenticels on the whole surface of the fruit.

The tight interplay between the decreased cuticle synthesis and suberin deposition is evident and the central remaining question now relates to the causes leading part of the fruit epidermis to a decreased cuticle deposition. To date, we still do not know whether the cuticle deficiency induces russeting through mechanical stress responses generated by a higher development of cuticle microcracking, or if the suberization process directly triggers a repression of the cuticle deposition. Further works aiming at better understanding the chronology of the different

events, leading to russeting in apple, might provide an answer to this crucial question. This might be achieved by studies focusing on the effect of a provoked cuticle degradation (humidity, solvent wash, scratching, etc).

References

Aarts MG, Keijzer CJ, Stiekema WJ, Pereira A. 1995. Molecular characterization of the CER1 gene of arabidopsis involved in epicuticular wax biosynthesis and pollen fertility. *The Plant Cell* **7**: 2115-2127.

Andre CM, Greenwood JM, Walker EG, Rassam M, Sullivan M, Evers D, Perry NB, Laing WA. 2012. Anti-inflammatory procyanidins and triterpenes in 109 apple varieties. *Journal of Agricultural Food Chemistry* **60**: 10546-10554.

Andre CM, Larsen L, Burgess EJ, Jensen DJ, Cooney JM, Evers D, Zhang J, Perry NB, Laing WA. 2013. Unusual immuno-modulatory triterpene-caffeates in the skins of russeted varieties of apples and pears. *Journal of Agricultural Food Chemistry* **61**: 2773-2779.

Andre CM, Legay S, Deleruelle A, Nieuwenhuizen N, Punter M *et al.* 2016. Multifunctional oxidosqualene cyclases and cytochrome P450 involved in the biosynthesis of apple fruit triterpenic acids *New Phytologist* **211**: 1279-1291.

Bento MF, Pereira H, Cunha MÁ, Moutinho AMC, van den Berg KJ, Boon JJ. 1998. Thermally assisted transmethylation gas chromatography–mass spectrometry of suberin components in cork from *Quercus suber* L. *Phytochemical Analysis* **9**: 75-87.

Beisson F, Li Y, Bonaventure G, Pollard M, Ohlrogge JB. 2007. The acyltransferase GPAT5 is required for the synthesis of suberin in seed coat and root of *Arabidopsis*. The *Plant Cell* **19**: 351-368.

Bernards MA. 2002. Demystifying suberin. *Canadian Journal of Botany* **80**: 227-240.

Bernards MA, Lopez ML, Zajicek J, Lewis NG. 1995. Hydroxycinnamic acid-derived polymers constitute the polyaromatic domain of suberin. *The journal of Biological Chemistry* **270**: 7382-7386.

Blacklock BJ, Jaworski JG. 2006. Substrate specificity of *Arabidopsis* 3-ketoacyl-CoA synthases. *Biochemical and Biophysical Research Communications* **346**: 583-590.

Bonaventure G, Beisson F, Ohlrogge J, Pollard M. 2004. Analysis of the aliphatic monomer composition of polyesters associated with *Arabidopsis* epidermis: occurrence of octadeca-cis-6, cis-9-diene-1,18-dioate as the major component. *Plant Journal* **40**: 920-930.

Brendolise C, Yauk YK, Eberhard ED, Wang M, Chagne D, Andre C, Greenwood DR, Beuning LL. 2011. An unusual plant triterpene synthase with predominant alpha-amyrin-producing activity identified by characterizing oxidosqualene cyclases from *Malus* x *domestica*. *The FEBS Journal* **278**: 2485-2499.

Bustin SA, Benes V, Garson JA, Hellemans J, Huggett J *et al.* 2009. The MIQE guidelines: minimum information for publication of quantitative real-time PCR experiments. *Clinical Chemistry* **55**: 611-622.

Chagné D, Crowhurst RN, Troggio M, Davey MW, Gilmore B *et al.* 2012. Genome-wide SNP detection, validation, and development of an 8K SNP array for apple. *PLoS One*. **7**: e31745.

Compagnon V, Diehl P, Benveniste I, Meyer D, Schaller H, Schreiber L, Franke R, Pinot F. 2009. CYP86B1 is required for very long chain omega-hydroxyacid and alpha, omega -dicarboxylic acid synthesis in root and seed suberin polyester. *Plant Physiology* **150**: 1831-1843.

Cornille A, Gladieux P, Smulders MJM, Roldán-Ruiz I, Laurens F, *et al.* 2012. New insight into the history of domesticated apple: secondary contribution of the european wild apple to the genome of cultivated varieties. *PLoS Genetics* **8**: e1002703.

Cornille A, Giraud T, Smulders MJ, Roldán-Ruiz I, Gladieux P. 2014. The domestication and evolutionary ecology of apples. *Trends in Genetics*. **30**: 57-65.

Curry EA. 2012. Increase in epidermal planar cell density accompanies decreased russeting of 'Golden Delicious' apples treated with Gibberellin A_{4+7}. *Hortscience* **47**: 232-237.

Delude C, Fouillen L, Bhar P, Cardinal MJ, Pascal S, Santos P, Kosma DK, Joubès J, Rowland O, Domergue F. 2016. Primary fatty alcohols are major components of suberized root tissues of *Arabidopsis* in the form of alkyl-hydroxycinnamates. *Plant Physiology* **171**: 1934-1950.

Domergue F, Vishwanath SJ, Joubes J, Ono J, Lee J *et al.* 2010. Three *Arabidopsis* fatty acyl-CoA reductases, FAR1, FAR4, and FAR5, generate primary fatty alcohols associated with suberin deposition. *Plant Physiology* **153**: 1539-1554.

Evans KM, Patocchi A, Rezzonico F, Mathis F, Durel CE *et al.* 2011. Genotyping of pedigreed apple breeding material with a genome-covering set of SSRs: trueness-to-type of cultivars and their parentages *Molecular Breeding* **28**: 535–547.

Faust M, Shear C. 1972. Russeting of apples, an interpretative review. *HortScience* **7**: 233-235.

Franke R, Briesen I, Wojciechowski T, Faust A, Yephremov A, Nawrath C, Schreiber L. 2005. Apoplastic polyesters in *Arabidopsis* surface tissues - a typical suberin and a particular cutin. *Phytochemistry* **66**: 2643-2658.

Gasic K, Hernandez A, Korban S. 2004. RNA extraction from different apple tissues rich in polyphenols and polysaccharides for cDNA library construction. Plant Molecular Biological Report **22**: 437a-437g.

Giorno F, Guerriero G, Baric S, Mariani C. 2012. Heat shock transcriptional factors in *Malus domestica*: identification, classification and expression analysis. *BMC Genomics* **13**: 639.

Gou JY, Yu XH, Liu CJ. 2009. A hydroxycinnamoyltransferase responsible for synthesizing suberin aromatics in *Arabidopsis*. *Proceedings of the National Academy of Science USA* **106**: 18855-18860.

Graça J. 2015. Suberin: the biopolyester at the frontier of plants. *Frontiers in Chemistry* **3**: 62.

Graca J, Pereira H. 2000a. Methanolysis of bark suberins: analysis of glycerol and acid monomers. *Phytochemical Analysis* **11**: 45-51.

Graca J, Pereira H. 2000b. Suberin structure in potato periderm: glycerol, long-chain monomers, and glyceryl and feruloyl dimers. *Journal Agricultural Food Chemical* **48**: 5476-5483.

Graça J, Schreiber L, Rodrigues J, Pereira H. 2002. Glycerol and glyceryl esters of omega-hydroxyacids in cutins. *Phytochemistry* **61**: 205-215.

Hofer R, Briesen I, Beck M, Pinot F, Schreiber L, Franke R. 2008. The *Arabidopsis* cytochrome P450 CYP86A1 encodes a fatty acid omega-hydroxylase involved in suberin monomer biosynthesis. *Journal of Experimental Botany* **59**: 2347-2360.

Irving DE, Drost JH. 1987. Effects of water deficit on vegetative growth, fruit growth and fruit quality in Cox's Orange Pippin apple. *Journal of Horticultural Science* **62**: 427-432.

Joubès J, Raffaele S, Bourdenx B, Garcia C, Laroche-Traineau J, Moreau P, Domergue F, Lessire R. 2008. The VLCFA elongase gene family in *Arabidopsis thaliana:* phylogenetic analysis, 3D modelling and expression profiling. *Plant Molecular Biology* **67**: 547-566.

Juniper BE, Mabberley DJ. 2006. *The Story of the Apple*, Imber Press

Khanal BP, Grimm E, Knoche M. 2013. Russeting in apple and pear: a plastic periderm replaces a stiff cuticle. *Annals of Botany – Plants* **5**: ls048.

Knee M. 1972. Anthocyanin, carotenoid, and chlorophyll changes in the peel of Cox's Orange Pippin apples during ripening on and off the tree. *Journal of Experimental Botany* **23**: 184-196.

Knoche M, Grimm E. 2008. Surface moisture induces microcracks in the cuticle of 'Golden Delicious' apple. *Hortscience* **43**: 1929–1931.

Knoche M, Khanal BP, Stopar M. 2011. Russeting and microcracking of 'Golden Delicious' apple fruit concomitantly decline due to Gibberellin A4+7 application. *Journal of the American Society for Horticultural Science* **136**: 159-164.

Kosma DK, Molina I, Ohlrogge JB, Pollard M. 2012. Identification of an Arabidopsis fatty alcohol:caffeoyl-Coenzyme A acyltransferase required for the synthesis of alkyl hydroxycinnamates in root waxes. *Plant Physiology* **160**: 237–248.

Kosma DK, Rice A, Pollard M. 2015. Analysis of aliphatic waxes associated with root periderm or exodermis from eleven plant species. *Phytochemistry* **117**: 351-62.

Laurens F. 1998. Review of the current apple breeding programmes in the world. *ISHS Acta Horticulturae* **484**: 163-170.

Lashbrooke J, Aharoni A, Costa F. 2015. Genome investigation suggests MdSHN3, an APETALA2-domain transcription factor gene, to be a positive regulator of apple fruit cuticle formation and an inhibitor of russet development. *Journal of Agricultural Food Chemistry*. **63**: 185-91.

Lee SB, Jung SJ, Go YS, Kim HU, Kim JK, Cho HJ, Park OK, Suh MC. 2009. Two Arabidopsis 3-ketoacyl CoA synthase genes, KCS20 and KCS2/DAISY, are functionally redundant in cuticular wax and root suberin biosynthesis, but differentially controlled by osmotic stress. *Plant Journal* **60**: 462-475.

Lee SB, Suh MC. 2013. Recent Advances in Cuticular Wax Biosynthesis and Its Regulation in Arabidopsis. *Molecular Plant* **6**: 246-249.

Lee SB, Suh MC. 2015. Cuticular wax biosynthesis is up-regulated by the MYB94 transcription factor in Arabidopsis. *Plant Cell Physiology* **56**: 48-60.

Legay S, Guerriero G, Deleruelle A, Lateur M, Evers D, André CM, Hausman, J-F. 2015. Apple russeting as seen through the RNA-seq lens: strong alterations in the exocarp cell wall. *Plant Molecular Biology* **88**: 21-40.

Li Y, Beisson F, Ohlrogge J, Pollard M. 2007. Monoacylglycerols are components of root waxes and can be produced in the aerial cuticle by ectopic expression of a suberin associated acyltransferase. *Plant Physiology* 144: 1267-1277.

Lü S, Song T, Kosma DK, Parsons EP, Rowland O, Jenks MA. 2009. Arabidopsis CER8 encodes LONG-CHAIN ACYL-COA SYNTHETASE 1 (LACS1) that has overlapping functions with LACS2 in plant wax and cutin synthesis. *Plant Journal* **59**: 553-564.

Millar AA, Clemens S, Zachgo S, Giblin EM, Taylor DC, Kunst L. 1999. CUT1, an *Arabidopsis* gene required for cuticular wax biosynthesis and pollen

fertility, encodes a very-long-chain fatty acid condensing enzyme. *The Plant Cell* **11**: 825-838.

Millar AA, Kunst L. 1997. Very-long-chain fatty acid biosynthesis is controlled through the expression and specificity of the con- densing enzyme. *Plant Journal* **12**: 121-131.

Moire L, Schmutz A, Buchala A, Yan B, Stark RE, Ryser U. 1999. Glycerol is a suberin monomer. New experimental evidence for an old hypothesis. *Plant Physiology* **119**: 1137-1146.

Molina I, Bonaventure G, Ohlrogge J, Pollard M. 2006. The lipid polyester composition of *Arabidopsis thaliana* and *Brassica napus* seeds. *Phytochemistry* **67**: 2597-2610.

Molina I, Kosma D. 2015. Role of HXXXD-motif/BAHD acyltransferases in the biosynthesis of extracellular lipids. *Plant Cell Reports* **34**: 587-601.

Molina I, Li-Beisson Y, Beisson F, Ohlrogge JB, Pollard M. 2009. Identification of an Arabidopsis feruloyl-coenzyme A transferase required for suberin synthesis. *Plant Physiology* **151**: 1317-1328.

Morgan J, Richards A. 2003. *The New Book of Apples*, Brogdale Horticultural Trust, Ebury Press.

Panikashvili D, Shi JX, Schreiber L, Aharoni A. 2009. The Arabidopsis DCR encoding a soluble BAHD acyltransferase is required for cutin polyester formation and seed hydration properties. *Plant Physiology* **151**: 1773-1789.

Petit J, Bres C, Mauxion JP, Tai FW, Martin LB, Fich EA, Joubès J, Rose JK, Domergue F, Rothan C. 2016. The glycerol-3-phosphate acyltransferase GPAT6 from tomato plays a central role in fruit cutin biosynthesis. *Plant Physiology* **171**: 894-913.

Ranathunge K, Schreiber L. 2011. Water and solute permeabilities of Arabidopsis roots in relation to the amount and composition of aliphatic suberin. *Journal of Experimental Botany* **62**: 1961–1974.

Riley RG, Kolattukudy PE. 1975. Evidence for covalently attached *p*-coumaric acid and ferulic acid in cutins and suberins. *Plant Physiology* **56**: 650-654.

Rowland O, Lee R, Franke R, Schreiber L, Kunst L. 2007. The CER3 wax biosynthetic gene from Arabidopsis thaliana is allelic to WAX2/YRE/FLP1. *FEBS Letters* **581**: 3538-3544.

Sauveplane V, Kandel S, Kastner PE, Ehlting J, Compagnon V, Werck-Reichhart D, Pinot F. 2009. Arabidopsis thaliana CYP77A4 is the first cytochrome P450 able to catalyze the epoxidation of free fatty acids in plants. *FEBS Journal* **276**: 719-735.

Schreiber L, Franke R, Hartmann K. 2005. Wax and suberin development of native and wound periderm of potato (*Solanum tuberosum L.*) and its relation to peridermal transpiration. *Planta* **220**: 520–530.

Serra O, Hohn C, Franke R, Prat S, Molinas M, Figueras M. 2010. A feruloyl transferase involved in the biosynthesis of suberin and suberin-associated wax is required for maturation and sealing properties of potato periderm. *The Plant Journal* **62**: 277-290.

Sironval C, Clijsters H. 1962. Sur la nature de la rugosité chez la pomme Cox's Orange. *Bulletin de la société royale de botanique de Belgique* **94**: 35-44.

Skene DS. 1981. Wound healing in apple fruits: the anatomical response of Cox's Orange pippin at different stages of development. *Journal of Horticultural Science* **56**: 145-153.
Skene DS. 1982. The development of russet, rough russet and craks on the fruit of the apple Cox's Orange Pippin during the course of the season. *Journal of Horticultural Science* **57**: 165-174.

Todd J, Post-Beittenmiller D, Jaworski JG. 1999. KCS1 encodes a fatty acid elongase 3-ketoacyl-CoA synthase affecting wax biosynthesis in *Arabidopsis thaliana*. *Plant Journal* **17**: 119-130.

Tukey LD. 1969. Observations on the russeting of apples growing in plastic bags. *Proceedings of the American Society for Horticultural Science* **74**: 30-39.

Vandesompele J, De Preter K, Pattyn F, Poppe B, Van Roy N, De Paepe A, Speleman F. 2002. Accurate normalization of real-time quantitative RT-PCR data by geometric averaging of multiple internal control genes. *Genome Biology* **3**: RESEARCH0034.

Verardo G, Pagani E, Geatti P, Martinuzzi P. 2003. A thorough study of the surface wax of apple fruits. *Analytical and bioanalytical chemistry* **376**: 659-667.

Vishwanath SJ, Delude C, Domergue F, Rowland O. 2015. Suberin: biosynthesis, regulation, and polymer assembly of a protective extracellular barrier. *Plant Cell Reports* **34**: 573-86.

Voisin D, Nawrath C, Kurdyukov S, Franke RB, Reina-Pinto JJ, Efremova N, Will I, Schreiber L, Yephremov A. 2009. Dissection of the complex phenotype in cuticular mutants of Arabidopsis reveals a role of SERRATE as a mediator. *PLoS Genetics* **5**: e1000703.

von Wettstein PM 2012. Plant waxes. *eLS: citable reviews in the life sciences*. Wiley
press.

Walter TE. 1967. Russeting and cracking in apples. A review of world literature. *Report of East Mailing Research Station* **1966**: 83-95.

Wellesen K, Durst F, Pinot F, Benveniste I, Nettesheim K, Wisman E, Steiner-Lange S, Saedler H, Yephremov A. 2001. Functional analysis of the LACERATA gene of *Arabidopsis* provides evidence for different roles of fatty acid ω-hydroxylation in development. *Proceedings of the national Academy of of Sciences of USA* **98**: 9694-9699.

Yang W, Pollard M, Li-Beisson Y, Beisson F, Feig M, Ohlrogge J. 2010. A distinct type of glycerol-3-phosphate acyltransferase with sn-2 preference and phosphatase activity producing 2-monoacylglycerol. *Proceedings of the National Academy of Sciences of USA* **107**: 12040-12045.

Yeats TH, Gregory GJ, Wang Z, Chehanovsky N, Moyle LC, Jetter R, Schaffer AA, Rose JKC. 2012. The fruit cuticles of wild tomato species exhibit architectural and chemical diversity, providing a new model for studying the evolution of cuticle function. *Plant Journal* **69**: 655-666.

Yeats TH, Rose JKC. 2013. The formation and function of plant cuticles. *Plant Physiology* **163**: 5–20.

Chapter II

Differential accumulation of cutin, suberin and their associated waxes in the semi-russeted 'Cox Orange Pippin' variety

Summary and Perspectives

Our previous bulk transcriptomic work (Chapter I) showed that fully russeted apples displayed a decreased expression of genes involved in the cuticle synthesis. This supports the current hypothesis that the thickness and the integrity of cuticle are the most important factors influencing the apple skin suberization (russeting). A large number of differentially expressed genes putatively implicated in the synthesis of the cutin, the wax and the suberin has been identified from the current knowledge gathered these last years in suberin model plants such as *A. thaliana*, *S. tuberosum* L., *Q. suber* L.. The investigation of the cutin and suberin composition showed a strong variability in the monomer distribution between species and tissues, suggesting that the apple fruit skin might also exhibit specificities. To our knowledge, only non-russeted apple skin waxes have been investigated in apple and these already showed major differences with *A. thaliana*. In addition to the well-known long chain alkanes, primary and secondary alcohols, aldehydes and ketones, and wax esters, the apple skin wax massively accumulates ursolic acid and, to a lesser extent, oleanolic acid. These compounds, which belong to the pentacyclic triterpene family, have been extensively studied in apple

and other plant species, for their anti-inflammatory and anti-cancer properties. No data related to the cutin and suberin polymer are currently available for apple.

The present work aimed at depicting for the first time the composition of these polymers and to assess their differential accumulation in russeted and non-russeted tissues. In our previous transcriptomic analysis, a comparison of old heritage fully russeted varieties and waxy commercial varieties was performed to identify key metabolic genes and regulatory elements involved in the waxy and russet traits. However, for the apple production sector, russeting is a major concern for commercial varieties which have to display a perfect waxy phenotype. To investigate a close-to-reality case, the 'Cox Orange Pippin' variety was chosen for the present work. This variety displays a slight to medium russeting degree depending on the environmental conditions. In this variety, russeting appears as patches randomly placed on the fruit surface. Compared to the fully russeted varieties, which represent an extreme case, this model is closer to the genetic and phenotypic germplasm used in the apple production sector. Russeted and waxy areas of the semi-russeted fruits were carefully excised and the remaining flesh was removed with consecutive cell wall digestion cycles using a mixed pectinase and cellulase solution. The free lipids were then extracted and the remaining lipid matrix composed by either or both suberin and cutin was then *trans*-esterified using the BF_3/MeOH methodology. The free lipid and depolymerized fractions obtained from russeted and waxy patches were analyzed by GC-MS and compared to each other. Additionally, the expression of a selection of genes involved in the cutin, suberin, wax and triterpene biosynthesis pathways was also investigated and coupled to the GC-MS analysis results.

The free lipid extract showed a massive decrease of the cuticular waxes in russeted tissues. These include very long chain fatty acids, aldehydes, primary alcohols and alkanes, with carbon chains ranging between 26 and 29. These results were

supported by the decreased expression of wax biosynthetic genes in the russeted skin of 'Cox Orange Pippin'. Moreover, ursolic acid and oleanolic acid, which predominantly accumulate in the waxy tissues, also showed a drastic decrease in the russeted patches. This observation was in accordance with the gene expression pattern of the *MdOSC1* gene, which displayed a higher expression in the waxy skin and suggests that synthesis of ursolic and oleanolic acids and the wax biosynthesis pathway might be driven by common regulatory pathways. Conversely, an increase in alkyl-hydroxycinnamate contents, which are considered as suberin-associated waxes, was observed in these tissues. Primary alcohols composing these alkyl-hydroxycinnamates displayed shorter chains (C22 and C24) compared to the free primary alcohols discussed above. Our previous transcriptomic data and the present work showed differentially regulated 3-ketoacyl-CoA synthetase, which might be responsible for this chain length difference.

Analysis of the depolymerized extracts suggests that a lower cutin biosynthesis occurs in the russeted tissues. As an example, lower contents in C16 and C18 fatty acids, ω-hydroxyacids and mid-chain hydroxylated ω-hydroxyacids, which are characteristic of cutin, were observed in the suberized tissues. Conversely, increased contents of the α,ω-dicarboxylic acids and ferulic acid were observed in the russeted skin. This increase, which constitutes a characteristic signature of the suberin polymer, was accompanied by the associated increased expression of suberin biosynthetic genes in these tissues. As observed for the non-covalently linked alkyl-hydroxycinnamates, suberin deposition was also associated with the specific increase of C20, C22 and C24 precursors, which were absent or present as traces in the waxy skin. These specific very long aliphatic chains were observed in the fatty acids, primary alcohols, α,ω-dicarboxylic and ω-hydroxyacids. VLCFAs have been already described as a characteristic component of suberin,

but a strong variability in their distribution has been observed in other suberin plant models. In apple, although these very long chain precursors do not represent the major part of suberin, they might be considered as a characteristic of the apple suberin. It is noteworthy that the small accumulation of these compounds, observed in the waxy tissues, might be due to the presence of suberized lenticels which covered the fruit surface.

Finally, the depolymerization of suberin also released some triterpenes and alkanes, which were probably embedded in the suberin and cutin matrix during their synthesis. Remarkably, the betulinic acid, which was not detectable in the free lipid fraction, was detectable in the depolymerized fraction of the russeted skin. This suggests that betulinic acid can be considered as a suberin wax component which might be embedded within the suberin matrix during its synthesis.

Altogether, the transcriptomic and biochemical analysis of the russeted and waxy apple skin supports previous hypotheses which correlated the decreased cuticle deposition with the occurrence of russeting in apple. However, it is still difficult to conclude about the causal effects and events leading to the alteration of the biosynthesis of these two major components of the fruit skin. A first hypothesis might be that the lower cuticle deposition results in higher cuticle microcracking rate and the resulting stress response might activate the suberin biosynthesis. A second hypothesis might be that mechanical stress, generated by environmental and developmental factors, triggers directly the biosynthesis of suberin, which further represses the cuticle biosynthesis.

To date, there is no evidence that one of these hypotheses is more relevant than the other. In order to answer to this point, we decided to perform a second gene expression profiling study, coupled with a proteome analysis, during the fruit development of two closely related varieties collected in the orchard of the

Walloon Agronomic Research Centre of Gembloux (CRA-W, Belgium) (see next chapter). The 'Reinette du Canada Grise' (or 'Canada Gris') is a well-known fully russeted variety, particularly appreciated for cooking whereas the 'Reinette du Canada Blanche' (or 'Canada Blanc') is a slightly russeted variety. These varieties have been first considered as distinct, however a genotyping analysis using simple sequence repeats (SSR) markers showed that these were genetically extremely close and can be considered as extremely closely related varieties. Thus, it is expected that a differential display analysis performed during the fruit growth of these two varieties will provide a clear picture of causes and events leading to this cuticle synthesis repression and to the suberin biosynthesis. The aim of this work is to (i) validate for a second time the candidate genes identified in our first transcriptomic work including transcriptional regulators and metabolic genes, (ii) highlight new candidate genes which did not appear in the previous dataset, (iii) compare for the first time transcriptomic and proteomic data in this particular case, (iv) better understand the complex interactions which might occur between the cutin and wax biosynthesis, the suberin deposition, the cell wall modification and the triterpene biosynthesis pathways.

Chapter II highlights:

Outcome:

- A general chemically detailed characterization of the cutin, suberin and associated waxes composition of waxy and russeted sections in *Malus* x *domestica*.
- A confirmation of gene expression data obtained in our transcriptomic data (Chapter I).

Questions raised:

- Is there a tight/common regulatory pathway that connects, on the one side, synthesis of the triterpene composing the russeted and non-russeted apple skin waxes and, on the other side, the suberin biosynthetic pathway?
- Why are cutin and wax biosyntheses down-regulated in the suberized tissues?

Chapter III: Integrative analysis of two russeted and non-russeted closely related apple varieties during fruit development provides new insights about the cuticle/suberin interplay

---

Adapted from the article draft (in preparation)

Contributions:

S. Legay designed the experimental setup, performed the sampling, the fruit size measurement and the laboratory work (sample preparation, RNA and DNA extraction and genotyping). He performed the bioinformatic work, statistical analysis and wrote the article.

A. Deleruelle was involved in the triterpene analysis laboratory work.

M. Lateur provided the sample material.

C. André performed the triterpene analysis (data extraction).

Gea Guerriero, Christelle André and J.-F. Hausman were involved in the manuscript refinement.

Abstract

Russeting is a major concern for the apple fruit production leading part of the production to important price devaluation. This rough brown is characterized by the deposition of suberin in the inner part of the epidermal cell walls. Causes, which lead apple skin to develop this polymer on the fruit surface are multiple. However the thickness and the integrity of the cuticle have been associated with russeting, in multiple studies. Indeed, in a previous bulk transcriptomic study performed on mature fruits, russeted tissues displayed a massive decreased expression of cuticle biosynthesis-related genes, whereas an increased expression of cell wall modification, phenylpropanoid and suberin synthesis-related genes was observed. Additionally, genes being involved in the triterpene biosynthesis displayed variable expression pattern in the waxy and russeted skin. Despite the fact that number of genes being involved in these pathways have been identified, it is still difficult to understand the chronological events leading a waxy skin to trigger this suberization process. In the present work, the fruit growth development of two closely related varieties, Canada Gris and Canada Blanc, which display russeted and waxy skin phenotypes, respectively, was investigated using combined transcriptomic and proteomic approaches. A particular interest was given to the triterpene synthesis pathway and to candidate genes being putatively involved in the synthesis of the triterpene-hydroxycinnamic acid conjugate specifically found in russeted skins. Our results suggest that the decreased synthesis of the cuticle, observed in the russeted apple skin, has to be considered as an aggravating factor of russeting more than a main cause. Moreover, some interesting candidates being involved in the regulation and the synthesis of suberin specific triterpenic acids were also found.

Key words: russeting, transcriptomics, proteomics, triterpene, suberin, cutin, wax, apple skin.

I. Introduction

Russeting is a major concern in the apple fruit production, strongly affecting the benefits of professionals acting in this major agricultural sector (81 million tons produced in 2013, FAOSTAT). Apple russeting appears as a brownish rough corky texture on the fruit surface (Curry 2009). Although apple skin russeting is totally harmless in terms of health safety, consumers' preference usually goes for sound apple fruits with a nice color and perfect shape. This leads to flawed fruits (such as the russeted ones) being discarded from the market. There is hence a major interest to better understand the complex network of environmental sensing, cell signaling, as well as to decipher the regulatory cascade and metabolic alterations leading to this undesired trait. Since the last century, noteworthy progresses have been made in the identification of factors triggering russeting in commercial waxy apple varieties. Environmental stresses have been the first characterized causes associated with russeting in apple. As an example, heavy rainfalls and extended periods of humidity on the surface of the fruit have been shown to favor the development of russeted skin (Walter 1967, Faust and Shear 1972, Skene 1982, Knoche and Grimm 2008). Russeting is also observed in response to pathogen infection and has been considered as both a wounding response and a process limiting the pathogen spread in the epidermal cells (Faust and Shear, 1972). In addition to environmental factors, histological studies performed on apple revealed the crucial role of the cuticle in the development of russeting (Skene 1982, Lashbrooke *et al*. 2015). Indeed, the cuticle thickness seemed to be inversely correlated with the occurrence of russeting in apple. A recent study showed that heirloom fully russeted apple varieties displayed a lower expression level of the *MdSHN3* transcription factor, a cuticle master regulator, which was associated with a thinner cuticle layer (Lashbrooke *et al*. 2015). Moreover, this thinner cuticle layer seemed to be stiffer and more prone (or

susceptible) to microcracking (Khanal *et al*. 2013). Interestingly, the apple fruit skin seemed to be more sensitive to cuticle microcracking at early stages of fruit development (Khanal *et al*. 2013, Walter 1967). During this window of time, fruit development triggers extreme mechanical tensions on the fruit surface, which in turn play a major role in the occurrence of microcracking. Indeed, the application of Gibberellin A_{4+7} on apple fruits at an early stage of development leads to a decreased epidermal cell surface and a concomitant decrease in microcracking and russeting, suggesting a tight relationship between cuticle deposition, fruit growth and russeting (Knoche *et al*. 2011, Curry 2012).

Russeting is mainly associated with the deposition of suberin in the primary cell wall of epidermal cells. A bulk transcriptomic analysis performed between russeted and non-russeted (waxy) apple varieties collected at the commercial harvest stage enabled the identification of a number of genes involved in the suberin, cutin and triterpene synthesis pathways, and revealed a strong alteration in processes related to the cell wall modification processes (Legay *et al*. 2015). Interestingly, russeted varieties exhibited a lower expression of the genes involved in cutin and wax synthesis with a concomitant increased expression of those related to the suberin synthesis pathway. These crucial results confirmed previous observations, which postulated that fruit skins with a thinner cuticle layer were more susceptible to develop russeting (Skene 1982, Lashbrooke *et al*. 2015). Moreover, an altered expression of a significant number of genes implicated in cell wall modification was also observed in russeted varieties. These were more particularly associated with hemicellulose modification and cell wall loosening, suggesting the existence of a mechanism specifically releasing the extreme surface tension occurring during the fruit development (Khanal *et al*. 2013). This work provided a broad snapshot of the different actors participating in the russet trait. The identification of orthologous genes involved in the cutin, wax and

suberin synthesis pathway have been already identified in model species such as *Arabidopsis thaliana* or *Solanum tuberosum* (Graca 2015, Vishwanath *et al*. 2015). Notably, a particular interest has been given to the suberin biosynthesis pathway. As an example, multiple genes coding for the 3-ketoacyl-CoA synthase (KCS) responsible for the synthesis of very long chain fatty acids, which are characteristic of the suberin biopolyester, were found in *A. thaliana* (Blacklock and Jarowski 2006, Joubès *et al*. 2008, Lee *et al*. 2009). Orthologous genes of the cytochrome P450 family 86 members A1 and B1(*CYP86A1* and *CYP86B1*) fatty acid hydroxylase have been also identified (Hofer *et al*. 2008, Compagnon *et al*. 2009). Finally, the distinctive glycerol-3-phosphate acyltransferase 5 (GPAT5, Beisson *et al*. 2007), which is specific to the suberin monomer synthesis, was also found in our previous study (Legay *et al*. 2015). Although the knowledge on suberin synthesis greatly progressed this last decade, a part of the last steps of the polymerization process remains still unclear. A recent review trying to transpose the latest advances in the field of cutin synthesis, which shares similarities with suberin, argued that these final steps might involve some GDSL-motif lipase/esterase (GDSL lipase) and α/β-fold hydrolase (Kurdyukov *et al*. 2006, Girard *et al*. 2012, Yeats *et al*. 2012, Yeats *et al*. 2014, Vishwanath *et al*. 2015). Interestingly, members of these families were found in our previous work to be differentially expressed between russeted and non-russeted varieties (Legay *et al*. 2015). However, due to the broad diversity in function of these two families, their selection as candidate genes remains a difficult task.

One particular interest of the apple model related to the suberization process is the massive and differential accumulation of pentacyclic triterpenes in russeted and non-russeted varieties (André *et al*. 2012). In apple, pentacyclic triterpenes, in the form of triterpenic acids, are major components of the skin waxes accounting for up to 60% of the total mass. This feature distinguishes apples from other plant

models such as *A. thaliana* which does not exhibit detectable quantities of triterpenenic acids neither in the cuticle not in suberized tissues (Buschhaus and Jetter, 2012, André *et al*. 2012). According to the recent literature, apple pentacyclic triterpenes belong to three distinctive series namely the oleane, ursane and lupane series (Brendolise *et al*. 2011, André *et al*. 2013). Interestingly, a differential accumulation of these three series was observed when comparing russeted to non-russeted varieties (André *et al*. 2013). This crucial point was also supported by gene expression profiling and functional studies, which highlighted differentially expressed genes such as oxidosqualene cyclases (OSC), involved in the synthesis of the different triterpene series (Brendolise *et al*. 2011, André et al. 2016). As an example, *MdOSC1* is more expressed in the non-russeted tissue and produces predominantly α-amyrin and β-amyrin, the precursors of the ursolic and oleanolic acid, respectively, whereas *MdOSC5* is more expressed in the russeted skin and mainly produces lupeol, which is further converted to betulinic acid. Furthermore, a betulinic acid-3-trans caffeate specifically accumulated in the russeted skin (André *et al*. 2013). This ester has been already described in the bark of trees, but its production pathway remains unclear (Pan *et al*. 1994, Jiang *et al*. 1995). In *A. thaliana*, suberin-associated waxes comprise a large amount of alkyl-hydroxycinnamate esters and suberin is composed by feruloyl-ω-hydroxycarboxilic esters. These compounds are produced by enzymes belonging to the BAHD (HXXXD-motif) acyltransferase family (Kosma *et al*. 2012). It is tempting to speculate that the specific accumulation of these esters in suberized tissues might be produced by common or similar members of this family, but there are also several other proteins which might catalyze this condensation step. Altogether, these results suggest that (i) pentacyclic triterpenes should be considered as a crucial component of the apple skin structure (cuticle and suberized tissues), which should not be dissociated from the analysis of the

russeting process, and (ii) some metabolic and regulatory actors might interact transversally between these different pathways.

One of the most interesting but maybe most challenging topics in the field of suberin deposition relates to the early exogenous sensing, to the resulting cell signaling cascade and finally to the key transcriptional regulators triggering its deposition (Vishwanath *et al*. 2015). As mentioned above, cuticle microcracking seems to play a major role in the russeting occurrence. The primary sensing and signaling cascade triggering the suberization are not fully understood, but previous studies relate these processes to an increased expression of genes associated with stress signaling and stress responses (Soler *et al*. 2007, Legay *et al*. 2015). One hypothesis could be that damages resulting from cuticle microcracking act as wounding stimuli which in their turn activate a healing response, including the suberization process (Legay *et al*. 2015). Recent improvements have been made in the knowledge of the downstream regulation of the suberization process. In apple, the transcription factor MdSHN3 positively and negatively regulates the cuticle and the suberin deposition, respectively (Lashbrooke *et al*. 2015). This study corroborates the current postulate suggesting that a thicker cuticle deposition is associated with the deposition of less suberin, but the authors did not show whether MdSHN3 is a direct negative regulator of suberin biosynthesis. In *A. thaliana*, the overexpression of *AtMYB41* results in an increased expression of the key suberin synthesis genes and a massive accumulation of suberin (Kosma *et al*. 2014). Interestingly, this transcriptional regulator was only expressed under stress conditions. This was confirmed by the gene expression profiling study performed in apples where the orthologous gene of *AtMYB41* was expressed at a low level in both russeted and non-russeted varieties (Legay *et al*. 2015). This suggests that other actors might also play this role during development. Remarkably, the same study also showed that a large

number of transcription factors belonging to the NAC and MYB-domain family displayed a differential expression between russeted and non-russeted varieties (Legay *et al*. 2015). Some of them, such as NAC75 or MYB52, were previously associated with secondary cell wall biogenesis, but their involvement in russeting is not fully understood (Zhong *et al*. 2008). Interestingly, the expression of a MYB93-like transcription factor seemed to be correlated with the expression of some suberin core synthesis node genes (*GAPT5*, *CYP86A1*, *CYP86B1*). In *A. thaliana,* AtMYB93 has been described as a negative regulator of the lateral root formation, but no evidences of its participation of the suberization process have been provided (Gibbs and Coates 2014, Gibbs *et al*. 2014).

In order to go further in the hunt/discovery of genes playing a major role in apple russeting and to try to answer the multiple questions raised by the recent advances in this field, we performed an integrative analysis comparing two closely related varieties, *i.e*. Reinette du Canada Blanche (also named Canada Blanc, CB) and Reinette du Canada Grise (also named Canada Gris, CG). Canada Blanc is a non-russeted or slightly russeted apple variety whereas Canada Gris is a well-known russeted apple, appreciated for cooking. These varieties were investigated using transcriptomic, proteomic and targeted metabolite analysis approaches during the developmental kinetics of the fruit growth. This study aimed at better understanding the interplay occurring between the different pathways participating in the regulation of russeting, as well as their connections and coordination during fruit growth. A particular interest will be given to the pentacyclic triterpene synthesis pathway and its putative interaction with the onset of russeting.

II. Materials and methods

A. Plant material

During the spring-autumn 2013 (May-October), 27 apple varieties including 'Reinette du Canada Grise' (CG) and 'Reinette du Canada Blanche' (CB), were collected in the orchards of the Walloon Agronomic Research Center in Gembloux (CRAW, Gembloux, Belgium). For CB and CG, five time points were selected: 57, 78, 99, 120 days after full bloom (DAFB) and at the commercial maturity (Harvest, 150 DAFB). For each time point and variety, three biological replicates were chosen and each fruit was randomly chosen in the south exposed part (height: 1,20 m-2,2 m). For each biological replicate, six fruits were sampled and each fruit was split into quarters. A 5-millimeter (width) longitudinal slice was peeled with sterile scalpels from each quarter, taking care to remove the remaining flesh from the exocarp. The resulting exocarp samples were directly flash-frozen in liquid nitrogen, roughly ground to homogenize the sample and stored at -80°C until RNA extraction.

B. DNA extraction and genetic analysis

Twenty-five apple varieties were used in addition to CG and CB to perform the genetic analysis. Two additional samples corresponding to a *Malus sieboldii* individual and *Malus floribunda* cv. 824 were also added as control. Two hundred mg apple skin were frozen in liquid nitrogen and ground with mortar and pestle. DNA extraction was performed using the Nucleospin Plant II DNA extraction Kit (Macherey-Nagel, Düren, Germany). Quantification and purity checks were performed using a Nanodrop ND-1000 (Thermo scientific, Waltham, MA, USA). Sixteen Single Sequence Repeats (SSR) markers spread over the *Malus* x *domestica* genome were selected for their reliability and polymorphism (Guilford *et al*. 1997, Gianfransceschi *et al*. 1998, Liebhard *et al*. 2002, Table 4-1). SSR

primers were ordered with FAM and HEX labeling. PCR were performed using the Q5 hot start high-fidelity 2X master mix according to the manufacturer's guidelines with a 55°C annealing temperature. SSR markers were then multiplexed, diluted 25 fold and mixed with a formamide/400 HD-ROX ladder according to the manufacturer guidelines (Thermo scientific, Waltham, MA, USA). Samples were then denatured at 95°C and run on a ABI 3500 Genetic Analyzer (Thermo scientific, Waltham, MA, USA). The allele calling was performed using Genemapper v5 (Thermo scientific, Waltham, MA, USA). In order to deal with diploid and triploid varieties, the alleles were formatted as binary data. Distance matrix was calculated using Pearson correlation distance and the phenogram was performed using the Unweighted Pair Group method with Arithmetic Mean (UPGMA) method and 100 bootstraps using the DendroUPGMA online tool (http://genomes.urv.cat/UPGMA). The tree was built using the Phylodendron online tool (http://iubio.bio.indiana.edu/treeapp/treeprint-form.html).

C. RNA extraction

Samples (250 mg) were ground to a fine powder with mortar and pestle in liquid nitrogen. Total RNA was extracted using an adapted CTAB buffer extraction protocol (Gasic *et al*. 2004). Total RNAs were cleaned and treated with DNase I using the RNeasy plant mini kit (QIAGEN, Leusden, The Netherlands), following the manufacturer's guidelines. Total RNA integrity was assessed using the RNA Nano 6000 assay (Agilent Technologies, Diegem, Belgium) and a 2100 Bioanalyzer with quality parameters adapted to plant RNA profiles (Agilent Technologies, Santa Clara, CA, USA). Samples, with RNA integrity numbers (RINs) lower than 8, were excluded from the experiment. RNA purity was assessed measuring the absorbance at 230 nm, 260 nm and 280 nm using a Nanodrop ND1000 spectrophotometer (Thermo scientific, Villebon-sur-Yvette,

France). Total RNA was quantified using a Qubit RNA assay kit (Life technologies, Carlsbad, CA, USA). Samples were sent to the EMBL Genecore sequencing platform.

D. Library preparation and sequencing

Library preparation and sequencing was performed at the GeneCore platform (EMBL). Libraries were prepared from 1 μg total RNA using the TruSeq Stranded RNA library Preparation kit according to the manufacturer's guidelines (Illumina, San Diego, CA, USA). After mRNA purification, cDNA synthesis, shearing, Illumina adapters/barcodes ligation and 8-cycles of PCR amplication, libraries were controlled using the Agilent 2100 bioanalyser and the DNA-1000 kit (Agilent Techonolgies, Santa Clara, CA,USA). Libraries were quantified using qPCR at the EMBL gene core platform. The pooled libraries were sequenced on an Illumina NextSeq 500 (Illumina, San Diego, CA, USA) using 4 runs (NextSeq 500 High Output Kit 150 cycles) to generate 75 base-pairs paired-end reads.

E. Data analysis

NextSeq 500 generated FASTQ files were imported in CLC genomics workbench v8.5 discarding reads with poor quality (<Q30). Reads with nucleotide ambiguity (N) and CLC quality index above 0,01 (default parameter = 0,05) were then filtered from the remaining sequences. Two trimming procedures were then applied. First, a TrueSeq Illumina adaptor trimming was performed to ensure that no technical sequences (adaptors and indexes) remained in the reads. Second, in order to remove conserved sequences generated by the hybridization and amplification of the random hexamers, which are commonly found in the stranded libraries, sequences were trimmed by a "hard trim" of 14 base pairs at the 5' end of the reads. Finally, sequences with sizes below 35 base pairs were removed from the data. The remaining reads were mapped to the predicted apple transcriptome

V1 (Velasco *et al*. 2010) with annotations obtained from Phytozome v.10 beta (http://phytozome.jgi.doe.gov) with the following criteria: mapped reads must have multiple hits lower than 10, a minimum of 80% identity and 80% coverage with the reference. Mismatch cost was set at 2 (medium) and a deletion/insertion cost at 3 (highest stringency). Expression values were calculated using the Reads per Kilobase transcript per Million reads (RPKM) method (Mortazavi *et al*. 2008). Genes, with less than 10 specifically mapped reads and/or with a mean RPKM value of the biological replicates lower than 0.1 in at least one of the libraries, were also removed from the dataset.

Genes displaying a significant and differential expression were determined using a Baggerley's 'on proportion' weighted t-test at each time point (57, 78, 99 120 and 150 DAFB, Baggerly *et al*. 2003). A false discovery rate correction was then applied to the *p*-values and a stringent cut-off was set at 0,05 (Benjamini-Hotchberg correction). Genes which displayed a significant difference in expression (-2>log2 ratio (Russet group/Waxy group)>2, FDR *p*-value<0.05) in, at least, one time-point were retained for the analysis. To structure the dataset and group genes displaying similar expression profiles, a hierarchical clustering based on Pearson correlation distances and a complete linkage method was performed from the $\log_2$ transformed data of the expression results (RPKM CB, RPKM CG and ratio CG/CB) using the Cluster v3.0 software (http://bonsai.hgc.jp/~mdehoon/software/cluster/software.htm). Output files were then imported and treated using Treeview v1.1.6r4 (http://taxonomy.zoology.gla.ac.uk/rod/treeview.html).

A gene ontology enrichment analysis was performed using ClueGO v2.1.1 and CluePedia v1.1.1 (Bindea *et al*. 2009; Bindea *et al*. 2013) plugins from two subsets of genes chosen from the hierarchical clustering results gathering the C2 to C3 and the C4 to C7 clusters, respectively. The significantly regulated biological

processes (Benjamini-Hotchberg corrected *p*-value<0.05) were selected following these criteria: gene ontology level from 3 to level 8, kappa score set at 0.1. New candidate genes implicated in the suberin synthesis were identified using the gene association network tool 'STRING' (http://string-db.org) from the C4, C5, C6 and C7 clusters.

F. Proteomic analysis

Total soluble proteins were extracted by trichloroacetic acid (TCA)/acetone precipitation method as described in Renaut *et al*. (2004) with some modifications: 500 mg of leaves were ground with mortar and pestle in liquid nitrogen and then resuspended in 20% w/v TCA in acetone with 0.1% w/v dithiothreitol (DTT) and kept at −20°C overnight. Samples were centrifuged for 45 min at 35,000×*g* and 4°C. The pellets were washed with ice-cold acetone and centrifuged again at 4°C. This step was repeated twice, and the pellets were freeze-dried. Dried samples were solubilized in labeling buffer (7 M urea, 2 M thiourea, 2% w/v 3-([3-cholamidopropyl] dimethylammonio)-1-propanesulfonate (CHAPS), and 30 mM Tris) and incubated for 1 h at room temperature. Before the quantification, the pH of the solution was adjusted at 8.5 with sodium hydroxide 0.05 M. The protein concentration was determined with the RC DC™ protein assay (reducing agent and detergent compatible protein assay, Bio-Rad) according to the manufacturer's instructions with bovine serum albumin (2 mg/ml) as standard.

After quantification of the extracted proteins, 10 µg total proteins were loaded in a precast gel according to the manufacturer's instructions. Electrophoresis was performed with Criterion™ XT precast 1D gel 4-12% Bis-Tris (1.0mm X 12 wells, Bio-Rad) on a short migration. The gel was stained with Instant Blue (Gentaur BVBA, Kampenhout, Belgium) and ready for band excision. The bands were excised and cut into 1-2 mm cubes. Each band was reduced, alkylated and de-

stained separately then digested by trypsin enzyme (sequencing mass grade, Promega, Mannheim, Germany). The extracted peptides were desalted using a C18 pre-column (C18 PepMap™, 5 µm, 5 mm * 300 µm i.d., Thermo scientific, Bremen, Germany). The peptides were loaded and separated on a NanoLC-2D System (Eksigent, AB Sciex, Belgium) using a C18 reverse phase column (PepMap™ 100, 3 µm, 100 Å, 75 µm id x 15 cm, Thermo scientific) using a linear binary gradient (solvent A: 0.1% formic acid; solvent B: 80% acetonitrile 0.1% formic acid). Peptides were eluted from 5%B to 55% over 40 min, risen to 100% to wash the column then re-equilibrated for the next injection 18 min at 5%B at flow rate of 300 nl/min.

The peptides were injected into the TripleTOF 5600+ mass spectrometer (AB Sciex, Concord, Ontario, Canada) with a NanoSpray III source using a 10 µm i.d. picotip (New Objective, Woburn, MA). The values were for gas1= 1-6, gas2=0, curtain gas=20-30, the ion spray voltage around 2.6kV. CID fragmentations for MS/MS spectra acquisitions used the automatically adjusted system of rolling collision energy voltage. The instrument cycle consisted of a full MS scan (scan range: 300–1250 m/z, accumulation time: 250 ms) and a set of 20 most intense product ion scans in the high sensitivity mode with a 2+ to 5+ charge state covering the mass range of 100–1250 *m/z*. The dynamic exclusion for MS/MS was set at 10s. Each sample was processed in three technical replicates. The systems were controlled by Analyst software (version TF1.7, Framingham, MA, USA). An automatic mass recalibration was performed using a beta-galactosidase during the sequence of samples. CID spectra were processed by Mascot (version 2.4.2, Matrix Science Ltd, London, UK) using Mascot Daemon (version 2.4.2, Matrix Science) by searching against the *Malus* x *domestica* transcriptome V1.0 (Velasco *et al*. 2010). The searches were performed with the following parameters: enzyme: trypsin, 2 missed cleavages, mass accuracy precursor: 20

ppm, mass accuracy fragments: 0.3 Da, fixed modifications: carbamidomethyl (C), dynamic modifications: Oxidation (M), Acetyl (protein N-term). An average number of the spectral counts of a protein across technical repeats within a biological sample was done by Mascot Daemon with merging MS/MS files into a single search.

On the protein family report of Mascot results, supplemental filters were applied: peptide confidence (p-value<0.05), a minimum of five spectra per peptide and a minimum of two or more significant peptides per protein. Only features, displaying spectra in at least two replicates were retained. The proteins accepted were selected from the following filters: an average number of the spectral counts of a protein across technical repeats within a biological sample was done by Mascot Daemon; a protein's abundance was considered significantly different if its p-value was <0.05. Abundance was calculated using the normalized spectral abundance factors (NSAF). NSAF takes into account the number of spectral counts divided by the protein's length normalized to the sum of these values for all proteins identified in the experiment. For the calculation of NSAF, the length of a protein was replaced by the protein mass. Proteins displaying less than 50% increase or decrease when comparing abundance between CG and CB were excluded from the dataset. In order to highlight the most altered functional categories, a pie chart was built from results obtained using Mapman (Thimm *et al*. 2004). Proteins were classified in the different bins according to the mapping file resulting from the *Malus* x *domestica* genome draft V1.0 (Velasco *et al*. 2010).

G. Triterpene analysis

Powdered apple skin material (400 mg) was mixed with 10 mL ethyl acetate:hexane (50:50 *v*/*v*). This mixture was then homogenized using a vortex for 30 s and shaken for 1 h at room temperature. After centrifugation at 4,816 *g* for 20 min, the supernatant was collected and evaporated to dryness using a

centrifugal vacuum evaporator. The pellet was re-extracted using 10 mL ethanol:H_2O (80:20 *v/v*), homogenized and shaken for 2 h at room temperature and centrifuged as above. The supernatant was collected, combined with the lipophilic dried extract and evaporated to dryness. Triterpenes were re-suspended in 1.5 mL EtOH and filtered (0.2 μm) before Ultra Performance Liquid Chromatography analysis. Analyses were performed in triplicate (n =3).

Extracts were analyzed with a Waters Acquity UPLC system (Milford, MA, USA) hyphenated to a Diode Array Detector (UPLC-DAD). The separation of the 5 μL aliquot was performed on a reverse-phase Acquity UPLC BEH C18 column (2.1 × 100 mm, 1.7 µm particle size, Waters, Milford, MA, USA). The eluents were 0.05 % o-phosphoric acid in water (A) and 0.05 % o-phosphoric acid in acetonitrile (B). The gradient was as follows: 0 min, 75% B; 2 min, 75 % B; 16 min, 82% B; 25 min, 100% B; 26.5 min, 100% B; 27 min, 75% B; 30 min, 75% B. The flow rate was of 0.3 mL min^{-1} and the column temperature was 40 °C. Identification and quantification of triterpenes was performed as described in Andre *et al* (2013). Ursolic acid (UA), oleanolic acid (OA), betulinic acid (BA) as well as BA-transCaffeate (BA-transC) were identified by their retention time and spectral data compared with authentic standards and were quantified at 210 nm (UA, OA, and BA) and 320 nm (BA-transC) using five-point calibration curves. Excellent linearity ($R^2 > 0.99$) was obtained in the concentration range 100–6.25 μg mL^{-1} for all compounds.

III. Results and discussion

A. Phenotypic and genetic characterization

1. Fruit growth and phenotype

CG and CB already displayed a strong difference in the skin phenotype during the early stage of the fruit development (57 DAFB, Fig 4-1).

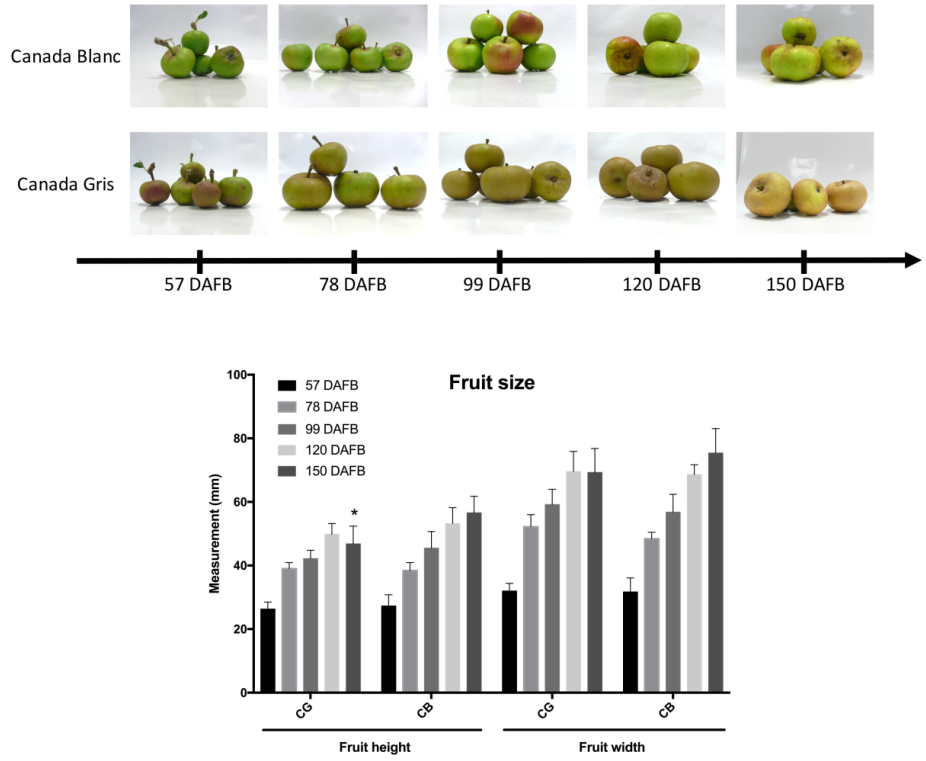

Figure 4-1: Above: skin phenotype of 'Canada Gris' (CG) and 'Canada Blanc' (CB) during fruit growth (from 57 Days After Full Bloom (DAFB) to 150 DAFB). Below: Fruit height and width measured in mm) during the fruit growth kinetics. The star displays the significant difference between CG and CB (p-value< 0,05).

Indeed, CG exhibited a medium russeting 57 DAFB, which gradually increased during the course of the experiment. In addition to this, the skin reddening occurring 57 DAFB was not observable anymore in the latest time points. The CB variety showed a waxy skin with a slight russeting on the stalk and calyx ends during the early sampling dates. whereas an increase in russeting spots and patches was more and more observed during the latest sampling dates (Fig 4-1). Fruit growth was measured during the whole time-course of the experiment and showed a strong increase in fruit width and height between 57 and 78 DAFB in both varieties, which is in accordance with previous observations and suggests that extreme tensions might occur on the surface of the fruit during these crucial stages (Fig 4-1, Walter 1967, Faust and Shear 1967, Skene 1982, Khanal *et al*. 2013, Legay *et al*. 2015). Both varieties did not show any significant difference in their fruit development except at 150 DAFB, when CG showed a slightly reduced fruit height compared to CB (Fig 4-1).

2. Genetic analysis using SSR markers

In order to better characterize the CG and CB varieties, a genetic diversity study was performed using 16 simple sequence repeats (SSR) markers on a reduced subset of old heritage and commercial *M*. x *domestica* varieties. Two individuals of *M*. *Sieboldii* and *M*. *Floribunda* were also tested. The 16 SSR markers spread over the genome correctly amplified in all the selected samples. Polymorphism was good with an allele number per marker ranging from 8 to 14 different alleles per marker and a major allele frequency between 0.20 and 0.43 (Table 4-1). Three variety groups have been determined from the genetic analysis results (Fig. 4-2). A first group was constituted by a large number of non-russeted commercial varieties such as ‘Jonagold’, ‘Gala’, ‘Fiesta’. Two waxy cultivars developed by the CRA-W (Belgium), which were used in our previous work were also clustered within this group (Legay *et al*. 2015).

Table 4-1: Overview of the Single Sequence Repeat (SSR) markers used for the phylogenetic analysis of Canada Gris and Canada Blanc.

SSR Name	Linkage group	Fw sequence	5' Labelling	Rev sequence	SSR repeat type	Osberved size range	Allele number	Major allele frequency
CH05g08	1	CCAAGACCAAGGCAACATTT	FAM	CCCTTCACCTCATTCTCACC	imperfect	156-203	11	0.43
CH03d01	2	CGCACCACAAATCCAACTC	FAM	AGAGTCAGAAGCACAGCCTC	imperfect	86-120	10	0.25
MS14h03	3	CGCTCACCTCGTAGACGT	HEX	ATGCAATGGCTAAGCATA	perfect	107-139	12	0.27
Ch01f02	7	ACCACATTAGAGCAGTTGAGG	HEX	CTGGTTTGTTTTCCTCCAGC	perfect	164-206	14	0.3
CH03a09	5	GCCAGGTGTGACTCCTTCTC	FAM	CTGCAGCTGCTGAAACTGG	perfect	116-139	10	0.4
CH03d07	6	CAAATCAATGCAAAACTGTCA	FAM	GGCTTCTGGCCATGATTTTA	perfect	161-225	11	0.2
CH02c09	15	TTATGTACCAACTTTGCTAACCTC	HEX	AGAAGCAGCAGAGGAGGATG	perfect	225-256	10	0.26
CH05g03	17	GCTTTGAATGGATACAGGAACC	HEX	CCTGTCTCATGGCATTGTTG	perfect	133-207	12	0.24
CH02g09	8	TCAGACAGAAGAGGAACTGTATTTG	FAM	CAAACAAACCAGTACCGCAA	perfect	94-136	10	0.23
CH02b03b	10	ATAAGGATACAAAAACCCTACACAG	HEX	GACATGTTTGGTTGAAAACTTG	perfect	70-104	11	0.26
CH04c07	14	GGCCTTCCATGTCTCAGAAG	FAM	CCTCATGCCCTCCACTAACA	perfect	93-133	9	0.21
CH01h02	9	AGAGCTTCGAGCTTCGTTTG	FAM	ATCTTTTGGTGCTCCCACAC	imperfect	224-261	10	0.34
CH01g05	14	CATCAGTCTCTTGCACTGGAAA	HEX	GACAGAGTAAGCTAGGGCTAGGG	perfect	136-171	10	0.25
CH03b10	15	CCCTCCAAAATATCTCCTCCTC	HEX	CGTTGTCCTGCTCATCATACTC	perfect	91-117	11	0.24
CH01f03b	9	GAGAAGCAAATGCAAAACCC	FAM	CTCCCCGGCTCCTATTCTAC	imperfect	137-177	8	0.28
CH01h01	17	GAAAGACTTGCAGTGGGAGC	HEX	GGAGTGGGTTTGAGAAGGTT	perfect	102-138	8	0.22

The second group gathered two older varieties, ‘Saint Edmund Pippin’ and ‘Discovery’, developed during the first half of the 20th century and originating from England. The last group included the ‘Canada Blanc’ and ‘Canada Gris’ varieties and also gathered other russeted varieties such as ‘Patte de Loup’, ‘Court Pendu gris’. Finally, ‘Lord Lambourne’ is clustered out of these three groups. As expected, CG and CB displayed a perfect identity in alleles, suggesting that the difference in the genotype might result from one or more localized gene mutations (Fig. 4-2). One of the explanation might be that apple seemed to be particularly sensitive to sport mutations triggered by multiple causes such as transposable element (Flaginella *et al*. 2015). As an example, ‘Golden Delicious’ has also a russeted isogenic homolog called ‘Golden Russet’ (Gardner *et al*. 1948). A recent study identified an ATP binding cassette family G (ABCG) linked with the cuticle deposition as a major QTL leading to russeting, but many other genes (metabolic, regulatory, etc…) might also result in the development of russeting (Flaginella *et al*. 2015). As an example we can imagine that mutation of the *MdSHN3* gene might also result in a russeting phenotype.

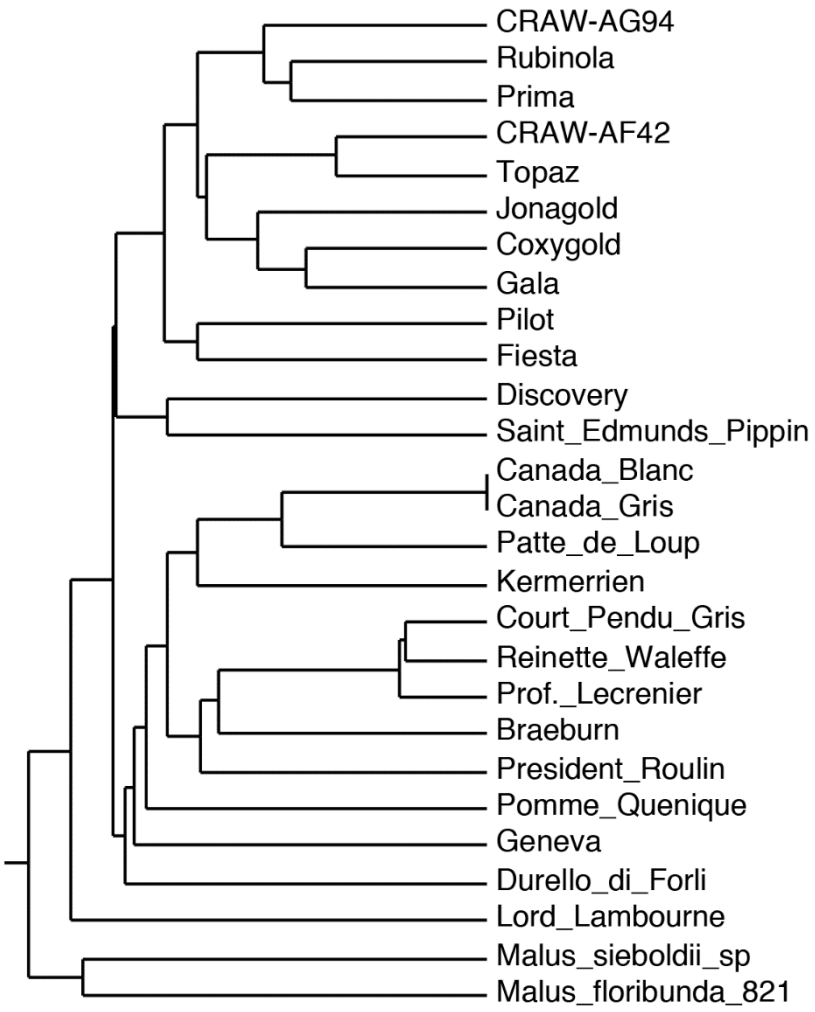

Figure 4-2: Phenogram gathering the 27 selected individuals performed with the allelic data obtained from 16 Simple Sequence Repeats (SSR) markers. Alleles were coded in a binary matrix, which was further used to build the Pearson correlation-based distance matrix. The tree was generated using the Unweighted Pair Group Method with Arithmetic Mean (UPGMA) method with 100 bootstraps.

B. Overview of the transcriptomic and proteomic data

1. Sequencing, mapping and selection of differentially expressed genes

Sequencing of the 30 cDNA libraries constituted by two varieties, five time-points and three biological replicates produced 3 056 442 350 paired-end reads with between 70 and 130 million reads per library. After uploading in CLC genomics workbench V8.5, sequenced reads were filtered and trimmed to remove nucleotide ambiguity, short reads and remaining adaptor residues. Between 7 and 15% of raw sequences were discarded from the analysis and it is noteworthy that a significant difference in the filtering results (*p*-value=0,0008) was observed between the CG and CB samples (Table 4-2). The filtered reads were then mapped to the *Malus* x *domestica* predicted transcriptome v1.0 (Velasco *et al*. 2010), which was previously used in our previous work. Taking into account that both varieties are quite distant genetically from the reference transcriptome ('Golden Delicious'), several mapping with different criteria (percentage of identity and/or coverage, and mismatch cost) were performed and evaluated. The best criteria were chosen to obtain an acceptable number of mapped reads and without lowering the specificity of the hits. The mapping results were good with around 74 and 71% of the reads mapped to the reference for CB and CG, respectively (Table 4-2). Interestingly, the mapping was also slightly lower in the CG libraries (-1,37%, *p*-value=0,0011). However, it is difficult to conclude whether these differences in filtering and mapping rates are due a technical artefact or biological variations. However, the CG and CB libraries were sequenced in distinct NextSeq500 runs, which could partly explain the difference in the sequence filtering. The difference in the mapping performance remains however unclear.

Table 4-2: Overview of the sequencing, filtering and mapping statistics. The read number is expressed in million.

Library name	Raw reads number (M)	Remaining reads after trimming and filtering (M)	% of remaining reads removed after trimming and filtering	Number of reads mapped to the reference (M)	% reads mapped to the reference	Reads specifically mapped (M)	Reads with multiple hits (M)	% of reads specifically mapped
CB_57DAFB_Rep1	91.65	83.01	**9.42**	61.52	**74.11**	47.46	14.06	**57.18**
CB_57DAFB_Rep2	93.95	84.41	**10.15**	62.35	**73.87**	48.08	14.27	**56.96**
CB_57DAFB_Rep3	91.62	82.54	**9.91**	61.00	**73.90**	46.96	14.04	**56.90**
CB_78DAFB_Rep1	147.33	130.29	**11.56**	96.33	**73.93**	74.78	21.55	**57.39**
CB_78DAFB_Rep2	115.38	105.58	**8.50**	78.93	**74.76**	61.58	17.35	**58.33**
CB_78DAFB_Rep3	110.93	100.94	**9.00**	74.31	**73.62**	57.67	16.64	**57.14**
CB_99DAFB_Rep1	90.38	80.94	**10.45**	59.96	**74.08**	46.89	13.07	**57.93**
CB_99DAFB_Rep2	93.78	83.89	**10.54**	62.27	**74.23**	48.49	13.78	**57.80**
CB_99DAFB_Rep3	100.81	91.00	**9.73**	67.27	**73.93**	52.43	14.84	**57.62**
CB_120DAFB_Rep1	108.61	97.51	**10.22**	72.06	**73.90**	55.51	16.55	**56.93**
CB_120DAFB_Rep2	95.68	88.59	**7.41**	64.76	**73.10**	49.91	14.86	**56.33**
CB_120DAFB_Rep3	91.25	83.91	**8.04**	60.69	**72.32**	46.67	14.01	**55.62**
CB_150DAFB_Rep1	88.80	81.98	**7.68**	59.92	**73.09**	46.65	13.26	**56.91**
CB_150DAFB_Rep2	96.35	84.98	**11.81**	60.56	**71.27**	47.02	13.54	**55.33**
CB_150DAFB_Rep3	117.01	105.88	**9.51**	76.25	**72.02**	59.18	17.07	**55.90**
CG_57DAFB_Rep1	81.89	73.36	**10.41**	54.20	**73.88**	41.63	12.57	**56.74**
CG_57DAFB_Rep2	87.66	77.06	**12.09**	56.41	**73.20**	43.59	12.82	**56.57**
CG_57DAFB_Rep3	91.53	82.08	**10.33**	60.24	**73.40**	46.43	13.82	**56.57**
CG_78DAFB_Rep1	88.49	77.87	**12.00**	56.46	**72.50**	43.75	12.70	**56.19**
CG_78DAFB_Rep2	112.57	100.39	**10.82**	72.05	**71.77**	55.60	16.45	**55.38**
CG_78DAFB_Rep3	109.33	97.80	**10.55**	71.69	**73.31**	55.56	16.13	**56.81**
CG_99DAFB_Rep1	82.98	70.25	**15.34**	51.01	**72.62**	39.41	11.60	**56.11**
CG_99DAFB_Rep2	69.89	61.50	**12.00**	44.40	**72.20**	34.37	10.03	**55.89**
CG_99DAFB_Rep3	99.53	86.52	**13.07**	62.78	**72.56**	48.83	13.95	**56.44**
CG_120DAFB_Rep1	99.21	88.62	**10.68**	62.89	**70.97**	48.93	13.97	**55.21**
CG_120DAFB_Rep2	107.31	96.31	**10.25**	69.09	**71.74**	53.69	15.40	**55.74**
CG_120DAFB_Rep3	109.84	98.23	**10.58**	70.38	**71.65**	54.64	15.74	**55.63**
CG_150DAFB_Rep1	144.76	128.14	**11.48**	90.19	**70.38**	69.87	20.32	**54.53**
CG_150DAFB_Rep2	115.35	104.07	**9.78**	74.16	**71.26**	57.91	16.25	**55.65**
CG_150DAFB_Rep3	122.59	107.20	**12.56**	75.24	**70.19**	58.56	16.67	**54.63**
Total	3 056.44	2 734.82						

The proportion of the specifically mapped reads represented around 77,5% of the mapped reads which is quite low but similar to previous studies (Table 4-2, Legay *et al*. 2015). This lower rate compared to what is currently observed in RNA-seq studies on other plant species using the Illumina technology, could be due the redundant structure of the *Malus* x *domestica* genome. Indeed, recent sequencing of the apple genome showed an important redundancy between large segments of chromosomes *i.e*. 3 and 11, 5 and 10, 9 and 17, and 13 and 16. As the haploid chromosome number of a large majority of Rosaceae species ranges from x=7 to

x=9, the uncommon genome structure of the *Malus* ancestor called *Pyrae* (x=17) was first attributed to a probable allopolyploidization between species related to *Spiraeoideae* (x=9) and *Amygdaleoideae* (x=8). However, investigation of genome sequence concluded in a genome duplication with rearrangement of the *Pyrae* ancestor (x=9) resulting in 17 haploid chromosomes (Velasco *et al*. 2010). Nevertheless, this quite high amount of non-specifically mapped reads was counted in the present data, the total amount of non-specifically mapped reads being proportionally spread among their different contigs according to the ratio observed for the specific reads.

2. Overview of the differentially expressed genes

In order to highlight interesting candidate genes differentially expressed between CG and CB during fruit growth development, stringent statistical test (FDR corrected *p*-value < 0,05) and fold change cut off ($-2<\log_2$ (ratio(RPKM CG/ RPKM CG))<2) were applied at each time point. A merged dataset was built gathering the differentially expressed genes from each time point (SI Table 4-1). A large majority of the differentially expressed genes were more expressed in the russeted (or suberized) tissues. Gene expression profiling studies, using either microarrays or RNA-Seq techniques, usually display a balanced number of up and down regulated genes (Legay *et al*. 2008, Legay *et al*. 2011). This assessment was commonly used for the normalization of the dataset displaying technical bias (Jaeger and Spang 2006). However, unbalanced repartition of the up- and down-regulated genes have been previously observed in our bulk transcriptomic RNA-Seq analysis and a gene expression profiling study of the cork differentiation, suggesting that this may not be attributed to a technical bias and, consequently, that this postulate may not be applicable to the gene expression profiling of the suberized tissues (Soler *et al*. 2007, Legay *et al*. 2015). To structure the dataset

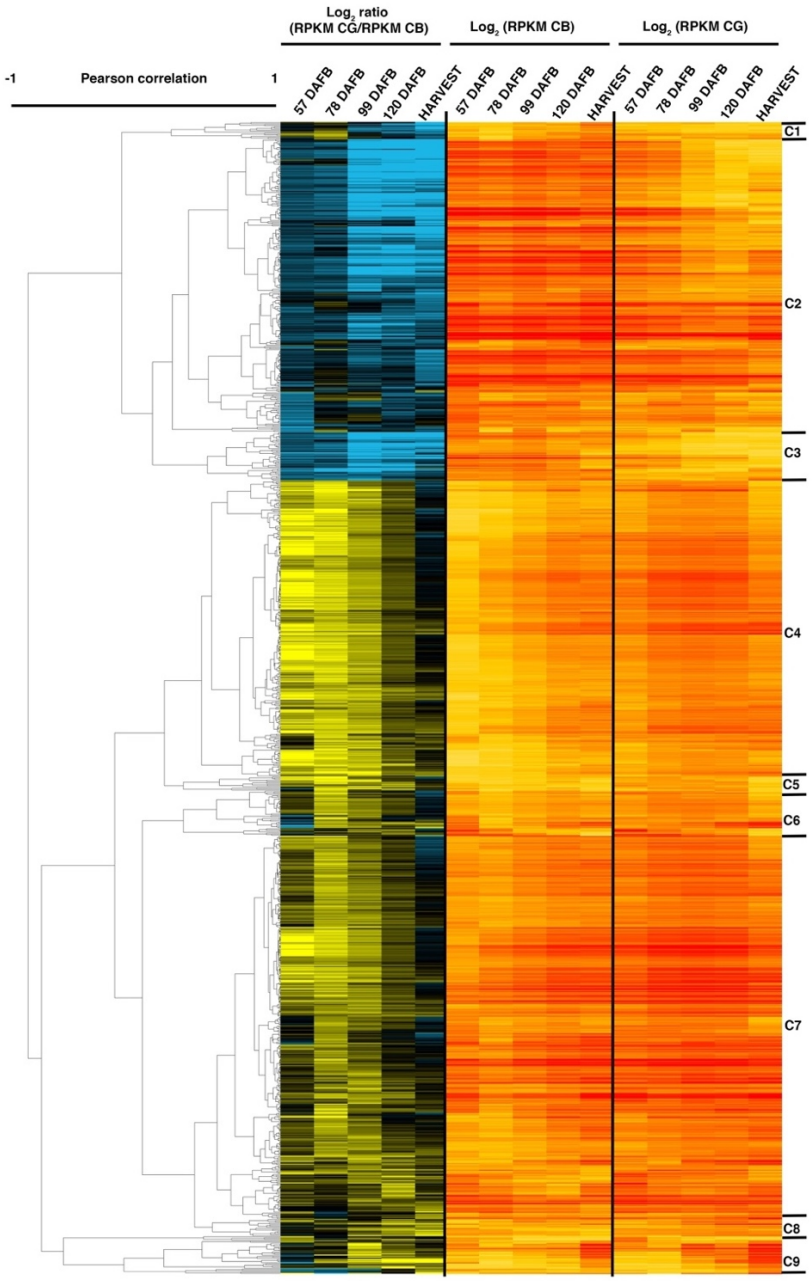

Figure 4-3: see legend on the next page

Figure 4-3: Hierarchical clustering of the 1070 differentially expressed genes across the kinetics. Computing was performed in Cluster3 using Pearson uncentered correlation and complete linkage clustering method. The tree was built using Treeview. On the left, the expression is displayed in Log_2 ratio (RKPM CG/RPKM CB), positive and negative fold changes are displayed in yellow and blue, respectively. On the right side the log_2 RPKM of CB and CG are displayed. Low, medium and high log_2 RPKM values are displayed in yellow, orange and red respectively.

and to group genes with similar expression profiles across time-points and varieties, a hierarchical clustering based on Pearson correlation and a complete linkage clustering methodology was performed (Fig. 4-3). Nine clusters with variable size were defined from the resulting heatmap with three clusters exhibiting genes which were more expressed in CB and six cluster displaying a higher expression in CG. In order to increase the readability of the analysis, clusters displaying similar expression pattern have been grouped. The clusters C1 (16 genes), C2 (272 genes) and C3 (45 genes) encompassed genes which were more expressed in CB and seemed to be associated with the cuticle metabolism (Fig. 4-3). C4 (275 genes), C5 (13 genes), C6 (42 genes) and C7 (356 genes) included genes with an enhanced expression pattern in CG at 78, 99 and 120 DAFB, that belong to the suberin biosynthesis pathway. Finally, the C8 (16 genes) and C9 (35 genes) clusters include only moderately correlated genes with higher expression in CG at later sampling dates and seemed to be associated with aging and senescence (Fig. 4-3).

3. Proteome analysis overview

The proteome analysis of the fruit growth development of CG and CB displayed 522 identified proteins in at least one of the five time points (SI Table 4-2, SI Table 4-3). A fold change cut off value was set in order to retain proteins

displaying at least 50% increase or decrease between NSAF values (-0,58<$\log_2$ ratio (NSAF CG/NSAF CB)>0,58). The MapMan tool was used to highlight proteins and pathways which are the most affected by the phenotype difference of CG and CB (Thimm *et al*. 2004). Among these, it is not surprising that the protein metabolism and the RNA processing were among the most affected functional categories. Similar patterns have been observed in our previous RNA-Seq data (Fig. 4-4, Legay *et al*. 2015). Interestingly, a large number of proteins involved in photosynthesis displayed differences between CB and CG. Among these we found a large number of photosystem and rubisCO subunits displaying chaotic profiles in CG over the kinetics, suggesting that they were not correlated with the studied trait. Such differences were not observed in the corresponding gene expression study, thereby suggesting that these differences might result from some post-transcriptional regulation or protein turnover. Only few proteins being involved in the major and minor carbohydrate metabolism were differentially regulated, corroborating previous works suggesting that russeting only slightly impacts the carbohydrate metabolism (Fig. 4-4, Soler *et al*. 2007, Legay *et al*. 2015). Conversely, we expected that the cell wall, lipid and secondary metabolism would be strongly altered by russeting. It should be noted that, although these pathways displayed a number of differentially expressed proteins, the proportion was not as obvious as it was in the gene expression profiling results (Fig. 4-4, Legay *et al*. 2015). We can speculate that these differences might be due to the relatively lower abundance of proteins participating in these pathways, particularly in the secondary metabolism. Moreover, as russeting involved a significant number of membrane and cell wall protein, the analysis of the soluble proteome might result in a partial picture of the differentially regulated protein being part of this process.

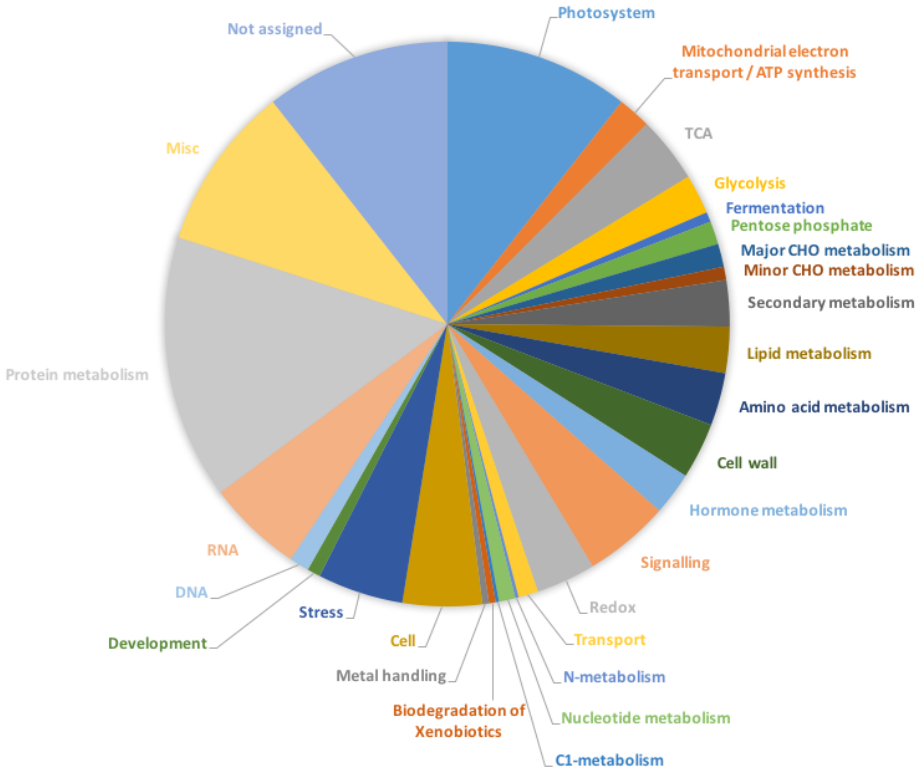

Figure 4-4: Distribution of the significantly and differentially expressed proteins ($-0{,}58 < \log_2$ ratio (NSAF CG/NSAF CB)$> 0{,}58$) according to the MapMan bins classification.

Table 4-3: Subset of the differentially expressed proteins (FC>0,5). Features found in both datasets are displayed in the first part of the table. Annotations were obtained from the *Malus* x *domestica* genome draft v1.0. Protein abundance obtained from the liquid chromatography (LC) is expressed as Normalized Spectral Abundance Factor (NSAF100), transcript abundance obtained from RNA sequencing (RNA-Seq) is expressed as RPKM.

				Canada Blanc					Canada Gris				
Dataset	Contig code	Gene symbol	Annotation description	57 DAFB	78 DAFB	99 DAFB	120 DAFB	150 DAFB	57 DAFB	78 DAFB	99 DAFB	120 DAFB	150 DAFB
Features found in the RNA-Seq and proteomic data													
LC	MDP0000120594		HXXXD-type acyl-transferase family protein					0.25					
RNAseq	MDP0000120594		HXXXD-type acyl-transferase family protein	270.7	252.8	332.3	207.8	455.1	138.7	98.7	75.3	64.6	115.3
LC	MDP0000166457		HXXXD-type acyl-transferase family protein										0.23
RNAseq	MDP0000166457		HXXXD-type acyl-transferase family protein	4.8	6.3	15.3	8.3	30.0	1.1	0.3	0.4	0.2	3.5
LC	MDP0000184619		Li-tolerant lipase 1	1.98	1.76	2.42	2.38			0.68			
RNAseq	MDP0000184619	ATLTL1,LTL1	Li-tolerant lipase 1	1967.7	1372.9	2047.1	560.5	59.0	450.2	302.3	47.2	6.0	0.3
LC	MDP0000197743		Bifunctional inhibitor/lipid-transfer protein							0.87			
RNAseq	MDP0000197743		Bifunctional inhibitor/lipid-transfer protein	0.6	1.5	4.4	8.5	13.0	11.3	18.6	23.9	16.5	10.2
LC	MDP0000208152		peroxidase 2		0.62	0.18	0.23	0.71		0.35	0.79	1.94	0.26
RNAseq	MDP0000208152	ATPA2,PA2	peroxidase 2	0.4	2.8	3.2	13.3	10.1	1.7	8.5	20.5	32.1	16.0
LC	MDP0000231084		acetoacetyl-CoA thiolase 2	0.47	0.18	0.23	0.25	0.96					0.28
RNAseq	MDP0000231084	ACAT2	acetoacetyl-CoA thiolase 2	1195.0	848.8	1219.7	834.9	1366.9	532.4	287.9	282.8	218.9	396.1
LC	MDP0000285074		lipid transfer protein 3	16.35	10.52	24.23	22.81	11.37	10.84	5.03	9.44	14.46	6.51
RNAseq	MDP0000285074	LTP3	lipid transfer protein 3	23540.0	29906.7	49936.6	32077.5	64941.5	6517.5	5625.1	2116.9	2379.1	19183.5
LC	MDP0000304369		lipid transfer protein 3	5.98	4.45	8.75	8.04	1.25	6.90				
RNAseq	MDP0000304369	LTP3	lipid transfer protein 3	543.4	284.9	245.1	150.0	778.1	194.2	62.9	25.3	26.6	539.6
LC	MDP0000306867		Peroxidase superfamily protein			0.55		0.47	1.15	0.74			0.67
RNAseq	MDP0000306867	PRX52	Peroxidase superfamily protein	22.6	29.3	77.2	183.4	210.9	127.6	204.2	138.5	128.5	107.5
LC	MDP0000312095		Peroxidase superfamily protein					0.21					
RNAseq	MDP0000312095	PRX72	Peroxidase superfamily protein	4.2	3.0	7.5	14.0	19.7	13.1	19.8	26.0	23.1	32.0
LC	MDP0000319048		Peroxidase superfamily protein	3.06	2.04	2.48	1.37	0.68	2.36	1.29	1.06		
RNAseq	MDP0000319048	PRX52	Peroxidase superfamily protein	297.8	133.7	149.7	44.0	29.1	80.9	28.3	4.4	1.5	3.6

continued...

Table 4-3: continued…

Dataset	Contig code	Gene symbol	Annotation description	Canada Blanc 57 DAFB	78 DAFB	99 DAFB	120 DAFB	150 DAFB	Canada Gris 57 DAFB	78 DAFB	99 DAFB	120 DAFB	150 DAFB
Features found in the proteomic data only													
LC	MDP0000231084		acetoacetyl-CoA thiolase 2	0.47	0.18	0.23	0.25	0.96					0.28
LC	MDP0000157284		acetyl Co-enzyme a carboxylase					0.73					
LC	MDP0000166116		acyl activating enzyme 5					0.81					
LC	MDP0000323883		acyl-CoA oxidase 1					0.60					
LC	MDP0000129664		peroxisomal 3-ketoacyl-CoA thiolase 3					0.48					
LC	MDP0000231304		peroxisomal 3-ketoacyl-CoA thiolase 3					0.62					
LC	MDP0000251803		alpha/beta-Hydrolases superfamily protein					0.35					
LC	MDP0000697378		alpha/beta-Hydrolases superfamily protein					0.49					
LC	MDP0000122785		alpha/beta-Hydrolases superfamily protein		0.83								
LC	MDP0000197743	LTPG20	Bifunctional inhibitor/lipid-transfer protein							0.87			
LC	MDP0000293049	LTPG20	Bifunctional inhibitor/lipid-transfer protein									1.48	
LC	MDP0000476415	LTL1,GDSL1	Li-tolerant lipase 1					1.17					
LC	MDP0000496434	LTL1,GDSL1	Li-tolerant lipase 1		2.62		2.00						
LC	MDP0000322755	CCR	cinnamoyl coa reductase 1					0.48					
LC	MDP0000227287		Terpenoid cyclases family protein					0.51					
LC	MDP0000478473	CYP716A1	cytochrome P450, family 716A1					0.21					
LC	MDP0000130449	CYP716A1	cytochrome P450, family 716A1					0.22					
LC	MDP0000432497	EXPA15	expansin A15					0.23					
LC	MDP0000431696	EXPA8	expansin A8					0.52					
LC	MDP0000525641	FLA1	FASCICLIN-like arabinogalactan 1	0.33	0.58	0.34		0.24		0.50	0.24	1.19	0.34
LC	MDP0000904458	FLA2	FASCICLIN-like arabinogalactan 2	1.29	0.67	1.37	1.38	0.65	0.92	1.01	2.05	4.01	0.83
LC	MDP0000658332	FLA11	FASCICLIN-like arabinogalactan-protein 10	1.26	0.48	0.74	0.38	0.44	1.27	0.63	1.09	1.72	0.15
LC	MDP0000220665	PA2,PRX53	peroxidase 2			0.32	0.25						
LC	MDP0000301828	PA2,PRX53	peroxidase 2	0.52		0.83	0.56	0.45	1.08	0.48	1.90	3.37	0.59
LC	MDP0000539299	PA2,PRX53	peroxidase 2					0.72					
LC	MDP0000208152	PA2,PRX53	peroxidase 2		0.62	0.18	0.23	0.71		0.35	0.79	1.94	0.26
LC	MDP0000209189		Peroxidase superfamily protein	1.65	1.32	2.12	1.74	2.05	3.08	1.73	5.45	8.17	2.61
LC	MDP0000207215		Peroxidase superfamily protein	1.50	1.25	1.88	1.00	0.98	2.07	1.38	2.69	4.74	1.31
LC	MDP0000283650		Peroxidase superfamily protein	0.62	0.66	1.27	0.43	0.49	0.73	0.65	1.26	2.26	0.66
LC	MDP0000319048		Peroxidase superfamily protein	3.06	2.04	2.48	1.37	0.68	2.36	1.29	1.06		
LC	MDP0000129664		peroxisomal 3-ketoacyl-CoA thiolase 3					0.48					
LC	MDP0000231304		peroxisomal 3-ketoacyl-CoA thiolase 3					0.62					
LC	MDP0000519318	WAK3	wall associated kinase 3						0.68	0.38			
LC	MDP0000323987	XTH5	xyloglucan endotransglucosylase/hydrolase 5					0.26					0.53
LC	MDP0000269483	XTH6	xyloglucan endotransglucosylase/hydrolase 6					0.35					0.63
LC	MDP0000127521	MYB17	myb domain protein 17		0.18								

The signaling and hormone metabolism pathways were also well represented in this dataset supporting their role in the regulation of these two different phenotypes. Finally, the miscellaneous bin grouping features with no clear or multiple association in these different pathways was one of the most represented group in these data (Fig. 4-4). However, in this category we found some particularly interesting proteins regarding our topic such as some lipase and peroxidase. As the transcriptomic data were much more complete, in the next sections, proteomic data will be discussed in more details as a complement or validation the transcriptomic work.

C. Integrative analysis

1. Cuticle deposition genes displayed inversed expression patterns in CG and CB during fruit growth

Clusters C1, C2 and C3 displayed genes which were globally more expressed in CB. C1 is a small cluster grouping genes with less correlated expression profiles and relatively lower expression compared to C2 and C3 (Fig. 4-3). These few genes displayed a slightly higher expression in CG as compared to CB in the early time-points whereas an inverse trend occurred in the later sampling dates with an increased expression in CB compared to CG. Expression profiles of C2 and C3 were similar, however genes from the C3 cluster were slightly less expressed (Fig. 4-3). In both clusters, genes showed a strong and increasing expression in CB during all the fruit growth development. In CG, at the early time points of the kinetics (57 and 78 DAFB), these genes were slightly less expressed compared to the CB variety and their expression further decreased in the latest time-points (99, 120, 150 DAFB). The GO analysis of clusters 2 and 3 displayed five groups which can be summarized as lipid metabolism (orange), lipid transport (pink), response to stress (light blue), plant epidermis morphogenesis (purple) and hormone

biosynthesis (dark blue), the fatty acid, cutin and waxes biosynthesis being the most significant biological processes (Fig. 4-5). As observed in our previous work, the primary fatty acid metabolism seemed to be repressed in CG as compared to CB (Legay *et al*. 2015). The proteomic analysis displayed some acyl activating enzyme and acyl-Coenzyme A (CoA) oxidase, which were up-regulated in CB at the harvest time-point (Table 4-3). These two proteins are involved in the CoA activation and the dehydration of carboxylic acids occurring during the synthesis and modification of the carboxylic acid precursors. Acetoacetyl-CoA thiolase, which belongs to the β-oxidation process, displayed an increased gene expression and protein abundance in CB during all the time course of the experiment (Table 4-3, Table 4-4). Several fatty acid desaturase (FAD), which are involved in the core fatty acid synthesis were up-regulated in CB as compared to CG (Table 4-4). The enhancement of the β-oxidation process was also supported by two peroxisomal 3-ketoacyl-CoA thiolase proteins displaying an increased expression in CB 150 DAFB.

A noticeable number of 3-ketoacyl-CoA synthase 6 (*KCS6*) genes, which encode fatty acid condensing enzymes, belonged to these clusters. KSCs play a crucial role in the synthesis of epicuticular waxes and suberin precursors (Millar *et al*. 1999, Serra *et al*. 2009a, Wang *et al*. 2014a, Wang *et al*. 2014b). Among these, the KCS6 (CER6, CUT1) gene belongs to the well-known CER gene family, which is implicated in wax synthesis (Table 4-4). Other members of this *A. thaliana* mutant family were also found in our dataset, such as CER8, long chain acyl-CoA synthetase 1(LACS1); CER1(WAX1) and CER3 (WAX2), some fatty acid hydroxylase; CER2, a BAHD acyl-transferase (Aarts *et al*. 1995, Xia *et al*. 1996, Rowland *et al*. 2007, Lü *et al*. 2009). The differential expression of the wax synthesis related genes between CG and CB was also confirmed by the increased

expression of a wax ester synthase-like gene (*WSD1*), which is responsible for the final synthesis of the wax esters (Table 4-4, Li *et al*. 2008).

The expression of cutin synthesis-related genes was strongly decreased in CG (Fig. 4-3, Fig 4-6). As an example, the well-known glycerol-3-phospahate acyltransferase 6, which is involved in the production of the cutin monomers, displayed a strongly decreased expression in CG (Table 4-4, Li and Beisson 2009). This decrease was observed in other genes involved in this biological process, *i.e*. the *DCR* (*PEL3*) BAHD acyl transferase, the cytochrome P450(CYP)77A4, which is responsible for the epoxidation of fatty acids (Sauveplane *et al*. 2008), the fatty acid hydroxylases *CYP86A2* (*ATT1*) and *CYP86A8* (*LCR*) and finally the *LACS2* gene (Table 4-4, Wellesen *et al*. 2001, Schnurr *et al*. 2004, Xiao *et al*. 2004, Panikashvili *et al*. 2009). In addition to the above-mentioned DCR gene, other BAHD acyl-transferases were found in both transcriptomic and proteomic data, and might be implicated in the preliminary oligomerization step of cutin synthesis (Table 4-4, Panikashvili *et al*. 2009). A significant number of GDSL-lipase and α/β-fold hydrolase displayed a strong decrease in expression in CG during the fruit growth compared to CB. These data were corroborated by the proteome analysis, where different α/β-fold hydrolase displayed an increase abundance at 78 and 150 DAFB (Table 4-3). Although GDSL-lipase and α/β-fold hydrolase were not associated with the cutin and wax synthesis GO terms, some members of these families are major actors of the cutin polymerization (Girard *et al*. 2012, Yeats *et al*. 2012, Jakobson *et al*. 2016). As an example, genes and proteins annotated as a Li-tolerant lipase-like, which were similar to the LTL1 GDSL-lipase, might be major actors of the cutin assembly in the apple fruit skin (Table 4-3, Table 4-4, Yeats *et al*. 2012, Girard *et al*. 2012).

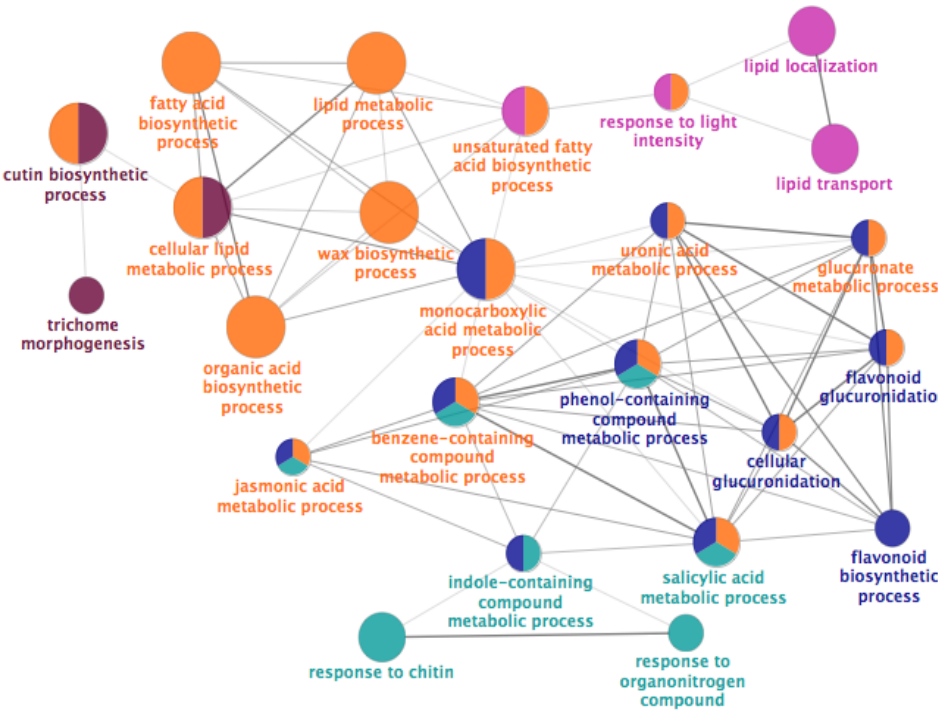

Figure 4-5: Gene ontology enrichment analysis of the significantly differentially expressed genes ordered in clusters C2 and C3. Only significant biological processes were represented and the circle size of each of them represents its *p*-value (the bigger the circle, the higher the *p*-value). The colors represent the grouping results of the ClueGO/CluePedia analysis: lipid metabolism (orange), lipid transport (pink), response to stress (light blue), plant epidermis morphogenesis (purple) and hormone biosynthesis (dark blue).

The lipid transport linked to the cutin and wax deposition seemed to be also strongly affected in the russeted CG apple. *WBC11* (*ABCG11*), which is involved in extracellular transport of the cutin monomers and wax esters, displayed a similar trend as the one observed for the metabolic enzymes: the expression in CG decreases over the time course, while this gene was strongly expressed during the fruit development of the CB variety (Table 4-4, McFarlane *et al*. 2010). The *ABCG32* (*PDR4*) and *ABCG15* transporters were also more expressed in the CB

variety during the whole time course of the fruit development. ABCG32 has been recently described in *A. thaliana* to be a major transporter of cuticle (Fabre *et al*. 2016), while ABCG15 is involved in anther cuticle synthesis in rice (Qin *et al*. 2012, Langraf *et al*. 2014). An acyl-CoA binding protein 6 (*ACBP6*), displayed an increasing expression during the CB fruit growth, while its expression decreased in CG over the time (Table 4-4). ACBP6 is localized both in the extracellular space and in the cytosol, its function being mainly associated with transport of C16, C18 and C18:1 fatty acids synthetized in plastids. In *A. thaliana*, the *acbp6* loss-of-function mutant displayed an impaired development of the cuticle layer, suggesting that ACBP6 might be associated with the strong decrease in expression of the cutin and wax synthesis genes observed in our data (Xia *et al*. 2012). Three genes coding lipid transfer protein 3 (*LTP3*) were also strongly repressed in CG compared to CB (Table 4-4). LTPs are thought to be involved in several biological processes including the cell lipid homeostasis and the cutin assembly (Arondel *et al*. 2000). In the present data, one of these three *LTP3* displayed extremely high expression values in CB ranging from 23540 RPKM at 57 DAFB to 64941 KPKM at the commercial harvest time point. In CG, this gene exhibited the same expression pattern as the one observed in cluster 2: a decreasing expression until 120 DAFB and a slight increase at the commercial harvest time point (150 DAFB) ranging from 2116 RPKM (99 DAFB) to 19183 RPKM (150 DAFB). Moreover, two proteins corresponding to two of the three LTP3 contigs were also found in the proteomic data (Table 4-3). These showed the highest abundance in the dataset and displayed a decreased abundance in the russeted CG. Interestingly, this transporter was not significantly regulated between waxy and russeted exocarps during our previous bulk gene expression profiling study (Legay *et al*. 2015). Differences in expression between the varieties were also observed, but these were not correlated with the russet/waxy

phenotype, suggesting that, in the present data, the strong differential expression of this *LTP3* gene might be specific to the CB/CG variety couple. As *LTP3* expression was correlated with the cutin and wax biosynthesis biological processes and massively expressed in CB, LTP3 gene might (i) play a crucial role in the transport of waxes or cutin monomers and (ii) be a valuable candidate gene which may explain part of the differential development and phenotype of these two varieties.

In addition to the differential expression of the lipid metabolism-related genes, some biological processes linked to the hormone metabolism were also represented in clusters C2 and C3. Among these, several UDP-glucosyl transferase (UGT) such as the *UGT72E1*, *UGT74F1*, *UGT74F2* were found. UGT74F1 and UGT74F2 have been previously described to participate in the synthesis of salicylic acid 2-O-D-glucose and salicylic acid-glucose esters (Dean and Delaney, 2008). Salicylic acid (SA) is involved in a number of physiological and developmental responses such as the response against pathogen and environmental stresses and has antagonistic effect to abscisic acid (ABA). In potato, the feruloyl-hydroxycinnamoyl transferase (FHT), which is responsible for the synthesis of suberin monomer precursors, was shown to be negatively regulated by salicylic (SA) acid after wounding (Boher *et al*. 2013). The lower expression of UGT74F1 and UGT74F2 might be linked with a lower synthesis of SA in CG, but additional experiment has to be performed to verify this hypothesis. The allene oxide cyclase 4 (AOC4), which is involved in the jasmonic acid biosynthesis was also differentially regulated in both proteomic and transcriptomic data. However, its expression was not following clearly discernible trends across the kinetics of CB. *AOC4* was significantly expressed at the early stage and latest stage of the development of CB, suggesting an increased synthesis

Table 4-4: Subset of the significantly differentially expressed genes observed in clusters C2-C3 (Fold change > 4, FDR corrected *p*-value <0.05 in at least one sampling date). Genes were sorted in pathways according to the literature cited in the manuscript).

					Log2 ratio (RPKM CG/RPKM CB)				
	Contig code	Gene symbol	TAIR code	Annotation description	57 DAFB	78 DAFB	99 DAFB	120 DAFB	150 DAFB
Cutin and wax synthesis									
	MDP0000250127	KAS1	AT5G46290.1	3-ketoacyl-acyl carrier protein synthase I	-1.17	-0.35	-1.18	-0.75	-2.00
	MDP0000411575	KCS1	AT1G01120.1	3-ketoacyl-CoA synthase 1	-1.92	-0.12	-0.73	-0.32	-2.41
	MDP0000134273	FDH,KCS10	AT2G26250.1	3-ketoacyl-CoA synthase 10	-1.94	-2.43	-4.98	-5.77	-3.74
	MDP0000341591	KCS11	AT2G26640.1	3-ketoacyl-CoA synthase 11	-0.90	0.22	-0.79	-0.55	-2.26
	MDP0000784053	KCS19	AT5G04530.1	3-ketoacyl-CoA synthase 19	1.58	0.51	-3.13	-3.51	-5.40
	MDP0000625646	KCS2	AT1G04220.1	3-ketoacyl-CoA synthase 2	-0.60	0.25	-0.55	-0.44	-2.20
	MDP0000218282	CER6,KCS6,	AT1G68530.2	3-ketoacyl-CoA synthase 6	-1.49	-2.22	-5.11	-6.52	-4.92
	MDP0000305778	ACBP6	AT1G31812.1	Acyl-CoA-binding protein 6	-0.50	0.40	-0.58	-1.11	-2.28
	MDP0000874252	CYP77A4	AT5G04660.1	Cytochrome P450, family 77, subfamily A, polypeptide 4	-1.88	-2.39	-5.69	-7.64	-7.17
	MDP0000941955	CYP86A8,LCR	AT2G45970.1	Cytochrome P450, family 86, subfamily A, polypeptide 8	-1.42	-1.99	-5.26	-6.04	-5.74
	MDP0000218683	CER1	AT1G02205.1	Fatty acid hydroxylase superfamily	-1.53	-2.44	-5.03	-6.63	-6.70
	MDP0000479163	GPAT6	AT2G38110.1	Glycerol-3-phosphate acyltransferase 6	-1.30	-0.88	-2.27	-1.86	-3.33
	MDP0000334757	FAD5	AT3G15850.1	Fatty acid desaturase 5	-2.21	-2.07	-4.40	-6.73	-2.16
	MDP0000268854	LTL1,GDSL1	AT3G04290.1	Li-tolerant lipase 1	-1.48	-2.48	-4.65	-3.10	-0.81
	MDP0000184929		AT1G72110.1	O-acyltransferase (WSD1-like) family protein	-1.60	-1.90	-5.02	-5.29	-4.07
Phenylpropanoid									
	MDP0000037251	ATCAD9,CAD9	AT4G39330.1	Cinnamyl alcohol dehydrogenase 9	-1.58	-2.05	-5.20	-5.87	-7.10
Transport									
	MDP0000729313	LTP1	AT2G38540.1	Lipid transfer protein 1	-1.47	-2.34	-5.08	-7.40	-7.60
	MDP0000285074	LTP3	AT5G59320.1	Lipid transfer protein 3	-1.87	-2.42	-4.53	-3.69	-1.68
	MDP0000200335	ABCG11,WBC11	AT1G17840.1	White-brown complex homolog protein 11	-1.71	-2.52	-5.38	-5.44	-3.40
	MDP0000094058	ABCG15	AT3G21090.1	ABC-2 type transporter family protein	-1.11	-1.81	-4.31	-4.65	-4.00
	MDP0000263761	ABCG32,PDR4	AT2G26910.1	pleiotropic drug resistance 4	-1.89	-2.21	-4.07	-3.34	-3.46
Trancription factors									
	MDP0000430870	SHN1,WIN1	AT1G15360.1	Integrase-type DNA-binding superfamily protein	-0.72	0.01	-2.66	-3.30	-3.86
	MDP0000228673	RD22	AT5G25610.1	BURP domain-containing protein RD22	-1.02	-1.55	-3.01	-1.85	-1.60
	MDP0000407613	MYB15	AT3G23250.1	myb domain protein 15	-2.70	0.72	-1.05	-1.19	-1.13
	MDP0000121476	MYB16	AT5G15310.1	myb domain protein 16	-2.23	-1.33	-2.72	-1.85	-1.27
	MDP0000308403	MYB17	AT3G61250.1	myb domain protein 17	-0.66	-0.93	-3.45	-3.72	-3.76
	MDP0000894463	MYB73	AT4G37260.1	myb domain protein 73	-3.10	0.90	0.04	-0.16	0.50
	MDP0000149535	MYB94	AT3G47600.1	myb domain protein 94	-1.23	-1.61	-3.96	-3.68	-2.71
	MDP0000742771	MYB106	AT3G01140.1	myb domain protein 106	-1.87	-0.98	-2.08	-1.12	-0.71
Misc.									
	MDP0000857446	SQE1,XF1	AT1G58440.1	FAD/NAD(P)-binding oxidoreductase family protein	-2.21	1.17	1.55	-1.59	-0.50
	MDP0000120594		AT1G24430.1	HXXXD-type acyl-transferase family protein	-0.98	-1.36	-2.12	-1.62	-1.90
	MDP0000183197		AT5G17540.1	HXXXD-type acyl-transferase family protein	-2.82	-4.57	-6.40	-5.82	-2.99
	MDP0000137138		AT4G13840.1	HXXXD-type acyl-transferase family protein	-0.89	-1.80	-5.02	-5.92	-3.12
	MDP0000126620		AT5G02890.1	HXXXD-type acyl-transferase family protein	-1.91	-1.80	-3.09	-2.53	-4.01
	MDP0000120595		AT1G24430.1	HXXXD-type acyl-transferase family protein	-0.95	-1.32	-2.36	-1.77	-2.01
	MDP0000928830		AT3G16370.1	GDSL-like Lipase/Acylhydrolase superfamily protein	-1.50	-1.85	-4.10	-3.73	-3.22

of jasmonic acid at these time-points. Finally some methyl esterase *MES13* and *MES17* displayed an increased expression in CB during the whole time course. MES17 has been shown to participate in the hydrolysis and activation of the indole-3-acetic acid methyl ester (Me-IAA) into IAA (Yang *et al*. 2008). Me-IAA may play a similar role as Me-jasmonate in plants, being a transport and storage form of IAA. Thus the increased expression of *MES17* might reflect a higher release of IAA in epidermal cells of CB, favoring the cell elongation and cell division during the fruit growth. Despite the limited knowledge available, it appears that plant hormones might participate in the regulation of the russeting process by altering the expression of genes involved in their cell homeostasis. Investigation of the hormonal pool might be very informative to elucidate the role of each of them in the deposition of suberin.

The decreased expression of the cutin synthesis genes was also accompanied by a lower expression of a number of regulatory factors *i.e*. the SHN1-like(*MdSHN3*) and *MYB94*, *MYB15*, *MYB16*, *MYB17*, *MYB73*, *MYB106* and *RD22* (Table 4-4). But, only one protein, similar to MYB17, displayed a slightly higher accumulation in CB (Table 4-3). In *A. thaliana*, overexpression of *MYB94* triggered the expression of waxes synthesis genes such as *WSD1*, *KCS1* or *CER1* with a concomitant increased accumulation of cuticular waxes (Lee and Suh 2013). The SHN1 transcription factor was described as a major regulator of the cutin synthesis in *A. thaliana*. When overexpressed, strong increases of C16 and 18:1 ῼ-hydroxyacids which are characteristic monomers of the cutin, were observed (Kannangara *et al*. 2007). Moreover, recent studies showed that *MdSHN3*, the *SHN1* orthologous gene in apple, regulates the cuticle deposition and inhibits russeting (Lashbrooke *et al*. 2015). Recent studies showed that MYB16 and MYB106 MIXTA-like transcription factor coordinately regulated the cuticle synthesis with SHN1 (Oshima *et al*. 2013). Silencing of the MYB16 resulted in a

decreased expression of the *LCR* (*CYP86A8*), and *CER1* (fatty acid hydroxylase) genes, with an associated increased cuticle permeability (Oshima and Mitsuda, 2013). MYB17 is similar to MYB106 and MYB16 and is implicated in the early inflorescence development and seed germination (Zhang *et al*. 2009, Oshima and Mitsuda, 2013). In *A. thaliana*, MYB15 has been previously associated with drought tolerance and abscisic acid (ABA) hypersensitivity in *A. thaliana*. Interestingly in the *A. thaliana* MYB15 overexpressing seedlings, an increased expression of the well-known *RESPONSE TO DEHYDRATION 22* (*RD22*) gene was observed (Ding *et al*. 2009). In the present experiment, a similar co-expression pattern was observed, *MYB15* and *RD22* being more expressed in CB. Altogether, the decrease in expression of transcriptional regulators observed in CG supports the hypothesis that, during the fruit growth of the CG variety, russeting is strongly associated with a lower cuticle and wax synthesis. Additionally, it seemed that the ABA-mediated signaling pathway might play a role in the regulation of cuticle in apple through the differential expression of *MYB15* and *RD22*. Cuticle development has been previously associated with abiotic stress responses, such as dehydration and is tightly regulated by ABA, and it is tempting to propose that these genes are also involved in the regulation of cuticle development (Hen-Avivi *et al*. 2014).

2. Differential increased expression of the suberin and cell wall metabolism between Canada Blanc and Canada Gris

Clusters C4, C5, C6, C7, C8 and C9 exhibited genes which were globally more expressed in CG (Fig. 4-3). In clusters C4 to C7, the expression in CG was higher than CB at the early time-point (57 DAFB). The gene expression profile in CG strongly increased until 120 DAFB and then part of the genes had their expression slightly decreased while others remained stable until the commercial harvest time-point (Fig. 4-3). In CB, the gene expression level was low 57 DAFB and gradually

increased until the commercial harvest (150 DAFB). Interestingly, at this sampling date, a large part of the genes displayed similar or higher expression levels as those observed in CG (Fig. 4-3). In order to unravel the biological processes which were represented in these clusters, a GO enrichment analysis was performed on the merged data of the C4 to C7 clusters (Fig-4-6). Four groups, gathering different biological processes, were defined by the ClueGO/CluePedia plugins in Cytoscape v3. These reflect the differential expression of genes involved the fatty acid and secondary metabolism (purple), in the cell wall biosynthesis and regulation (dark blue and light blue) and finally the organ morphogenesis (orange). Among these, the most significant and represented biological processes were closely related to the phenylpropanoid, lignin, flavonoid, suberin metabolisms and the secondary cell wall biogenesis (Fig. 4-6). Similar results were obtained from the STRING online tool (Table 4-5). The most preponderant biological processes belong to the secondary and phenylpropanoid metabolism and the lignin and suberin biosynthesis. Analysis against the KEGG pathway database provided additional details such as the probable involvement of the hormone signal transduction and the flavonoids, sesquiterpenes and triterpenes synthesis pathways in these clusters. The functional localization of these genes was associated with cell wall, apoplast and extracellular matrix, which is in agreement with the represented metabolic pathways and biological processes. Finally, the most redundant molecular functions characterized in these clusters were oxidoreductase, transferase and hydroxylase activities. It is noteworthy that the triterpene synthesis seemed to be also represented, as four genes with β-amyrin synthase activity were highlighted. An important number of genes involved in the fatty acid metabolism were tightly linked with the suberin biosynthesis. A large part of the genes described below (Table 4-6) displayed a tight and isolated

interaction network in the STRING tool, suggesting that all these are driven by a common regulatory network (Fig. 4-7).

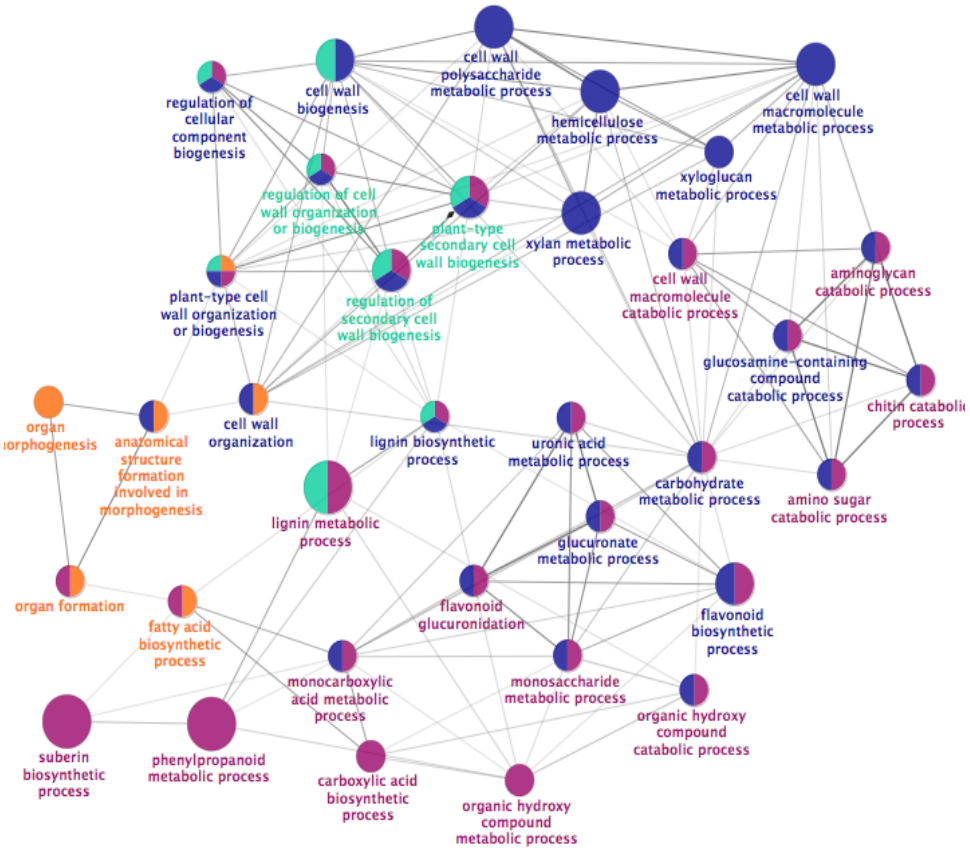

Figure 4-6: Gene ontology enrichment analysis of the significantly differentially expressed genes ordered in the cluster C4 to C7. Only significant biological processes were represented and the circle size of each of them represents its *p*-value (the bigger the circle, the higher the *p*-value). The colors represent the grouping results of the ClueGO/CluePedia analysis: the fatty acid and secondary metabolism (purple), in the cell wall biosynthesis and regulation (dark blue and light blue, respectively) and the organ morphogenesis (orange).

Table 4-5: Gene ontology and KEGG pathway analysis performed from clusters C4, C5, C6 and C7 performed using the STRING functional analysis tool.

Gene ontology (GO)

Pathway ID	Pathway description	Count in gene set	FDR corrected p-value
GO:0009698	phenylpropanoid metabolic process	28	1.05E-22
GO:0009699	phenylpropanoid biosynthetic process	24	1.54E-22
GO:0044550	secondary metabolite biosynthetic process	27	2.89E-15
GO:0019748	secondary metabolic process	32	6.60E-15
GO:0009808	lignin metabolic process	15	1.08E-11
GO:0009809	lignin biosynthetic process	11	1.56E-09
GO:0010345	suberin biosynthetic process	9	3.28E-09
GO:0044710	single-organism metabolic process	104	1.16E-07

KEGG pathway

Pathway ID	Pathway description	Count in gene set	FDR corrected p-value
940	Phenylpropanoid biosynthesis	20	1.34E-10
941	Flavonoid biosynthesis	9	1.77E-09
1110	Biosynthesis of secondary metabolites	46	1.57E-08
360	Phenylalanine metabolism	12	1.30E-05
909	Sesquiterpenoid and triterpenoid biosynthesis	6	4.82E-05
73	Cutin, suberin and wax biosynthesis	5	0.000788
4075	Plant hormone signal transduction	14	0.00432
40	Pentose and glucuronate interconversions	6	0.0422
4712	Circadian rhythm - plant	4	0.0456

Cellular component (GO)

Pathway ID	Pathway description	Count in gene set	FDR corrected p-value
GO:0005576	extracellular region	57	7.80E-08
GO:0005618	cell wall	26	0.000473
GO:0048046	apoplast	21	0.00109
GO:0071944	cell periphery	68	0.00286
GO:0005575	cellular_component	229	0.0292
GO:0031012	extracellular matrix	5	0.0326

Molecular function (GO)

Pathway ID	Pathway description	Count in gene set	FDR corrected p-value
GO:0003824	catalytic activity	159	2.70E-08
GO:0016491	oxidoreductase activity	44	6.96E-05
GO:0042300	beta-amyrin synthase activity	4	6.96E-05
GO:0003674	molecular_function	201	0.000818
GO:0016758	transferase activity, transferring hexosyl groups	18	0.00754
GO:0016757	transferase activity, transferring glycosyl groups	20	0.00777
GO:0020037	heme binding	15	0.0102
GO:0004553	hydrolase activity, hydrolyzing O-glycosyl compounds	13	0.0385
GO:0016209	antioxidant activity	10	0.0455

Alternative isoforms of the KCS genes (*KCS2* and *KCS4*) were also more expressed in the russeted CG and might be tightly linked to the suberin biosynthesis (Table 4-6). Interestingly, in our previous work, we did not observe any differentially expressed *KCS* genes specific to the russeted tissues. In *A. thaliana*, KCS2 was previously described to be a major actor of the synthesis of the very long chain fatty acids, which are one of the characteristic components of suberin (Lee *et al*. 2009). Little is known about the KCS4 function, but in *A. thaliana* a *KCS4* gene expressed in flowers and old siliques was not able to use the C16 and C18:1 fatty acid precursor as substrate (Blacklock and Jaworski 2006, Joubès *et al*. 2008). This might suggest that this enzyme may use fatty acids with a longer chain which are produced by other KCS enzymes such as KCS2. The fatty acyl-ACP thioesterases B (FATB) which are involved in the production of C16 fatty acid seemed to share some functions with GPAT5 in the STRING network built from data obtained in clusters C4-C7 (Fig. 4-7). This *FATB* gene has been also linked with russeting in our bulk transcriptomic analysis, supporting its putative involvement in the remobilization and/or synthesis of fatty acids dedicated to the suberin biosynthesis (Legay *et al*. 2015). An increased expression of fatty acid hydroxylase *CYP86A1* and very long chain fatty acid hydroxylase *CYP86B1* genes, which are involved in the biosynthesis of ω-hydroxyacids, was also observed (Table 4-6, Fig. 4-7, Hofer *et al*. 2008, Compagnon *et al*. 2009). A fatty acyl-coenzyme A reductase 5 (*FAR5*) gene was also differentially expressed in these clusters (Table 4-6, Fig. 4-7). FAR5 is involved in the reduction of acyl-CoA into primary alcohols which compose the suberin associated waxes (Domergue *et al*. 2010). Two suberin biosynthesis-related glycerol-3-phosphate acyltransferase 5 (*GPAT5*) genes, which displayed an enhanced expression in the russeted apple exocarps, were also more expressed in CG compared to CB (Table 4-6, Legay *et al*. 2015).

Table 4-6: Subset of the significant differentially expressed genes observed in clusters C4 to C7 (Fold change > 4, FDR corrected *p*-value <0.05 in at least one sampling date). Genes were sorted in pathways according to the literature cited in the manuscript).

					Log2 ratio (RPKM CG/RPKM CB)				
	Contig code	**Gene symbol**	**TAIR code**	**Annotation description**	**57 DAFB**	**78 DAFB**	**99 DAFB**	**120 DAFB**	**150 DAFB**
Suberin synthesis									
	MDP0000433567	KCS2	AT1G04220.1	3-ketoacyl-CoA synthase 2	0.49	2.04	1.59	0.90	-0.60
	MDP0000922301	KCS4	AT1G19440.1	3-ketoacyl-CoA synthase 4	3.28	2.84	2.62	1.18	1.48
	MDP0000150502	GPAT5	AT3G11430.1	glycerol-3-phosphate acyltransferase 5	4.00	3.24	2.49	1.23	-0.18
	MDP0000923760	CYP86A1	AT5G58860.1	cytochrome P450, family 86, subfamily A,	4.02	3.01	2.38	1.08	-0.21
	MDP0000306273	CYP86B1	AT5G23190.1	cytochrome P450, family 86, subfamily B,	3.81	3.34	2.66	1.43	-0.07
	MDP0000138841	FAR5	AT3G44550.1	fatty acid reductase 5	2.77	3.41	2.57	1.20	-0.39
	MDP0000312412	FATB	AT1G08510.1	fatty acyl-ACP thioesterases B	4.24	3.42	2.54	1.33	-0.17
	MDP0000258308	RWP1,FCT,FHT	AT5G41040.1	Feruloyl-hydroxycinnamoyl acytransfearase	4.18	3.22	2.53	1.24	-0.18
Phenylpropanoid									
	MDP0000219895	C4H	AT2G30490.1	cinnamate-4-hydroxylase	0.16	2.32	2.77	0.79	0.47
	MDP0000260512	4CL2	AT3G21240.1	4-coumarate:CoA ligase 2	1.67	2.06	1.56	0.94	-0.35
	MDP0000287919	CHS,TT4	AT5G13930.1	Chalcone and stilbene synthase family protein	-2.87	2.63	2.53	0.67	2.41
	MDP0000274127	CHI,TT5	AT3G55120.1	Chalcone-flavanone isomerase family protein	2.26	2.06	1.89	0.60	0.15
	MDP0000264424	HCT	AT5G48930.1	shikimate O-hydroxycinnamoyltransferase	0.66	2.80	2.33	0.55	0.11
	MDP0000479113	OMT1	AT5G54160.1	O-methyltransferase 1	3.80	3.44	2.79	1.26	-0.26
	MDP0000246535	CCoAOMT1	AT4G34050.1	Caffeoyl CoA methyltransferase	2.59	3.33	2.71	1.13	-0.24
	MDP0000164173	CYP84A1,FAH1	AT4G36220.1	ferulic acid 5-hydroxylase 1	3.34	3.15	2.63	1.68	0.40
Transport									
	MDP0000265619	ABCG2	AT2G37360.1	ABC-2 type transporter family protein	1.88	2.01	1.92	1.06	-0.05
	MDP0000299379	ABCG6	AT5G13580.1	ABC-2 type transporter family protein	3.17	3.08	2.67	0.90	0.00
	MDP0000731415	ABCG23	AT5G19410.1	ABC-2 type transporter family protein	4.06	3.20	2.40	1.26	-0.25
	MDP0000193438	ABCG11	AT1G17840.1	white-brown complex homolog protein 11	-1.84	2.43	2.01	0.74	-0.45
	MDP0000940078	LTP1	AT2G38540.1	lipid transfer protein 1	-2.01	2.79	1.72	1.90	0.76
	MDP0000197743	LTPG20	AT3G22620.1	Bifunctional inhibitor/lipid-transfer protein	4.23	3.60	2.46	1.02	-0.28
	MDP0000304463	LTPG16,EDA4	AT2G48140.1	Bifunctional inhibitor/lipid-transfer protein	4.14	3.40	2.67	1.29	-0.18
	MDP0000137283	LTPG5	AT3G22600.1	Bifunctional inhibitor/lipid-transfer protein	1.96	2.17	1.98	1.05	-0.11
Pentacyclic triterpene synthesis									
	MDP0000207731		AT1G78950.1	beta amyrin synthase	3.69	3.18	3.01	1.50	1.81
	MDP0000661381	CYP96A2	AT4G32170.1	cytochrome P450, family 96, subfamily A,	1.91	2.55	2.12	0.64	1.54
	MDP0000266125	CAMS1	AT1G78955.1	camelliol C synthase 1	3.74	3.17	3.04	1.59	1.64
	MDP0000212688	LUP1	AT1G78970.1	lupeol synthase 1	4.19	3.08	3.27	1.40	2.20
	MDP0000151814	LUP2	AT1G78960.1	lupeol synthase 2	2.84	3.15	2.69	1.42	1.44
	MDP0000634676	SQE1	AT1G58440.1	FAD/NAD(P)-binding oxidoreductase family protein	-2.70	1.15	1.99	-0.50	0.08

Table 4-6 continued…

				Log2 ratio (RPKM CG/RPKM CB)				
Contig code	Gene symbol	TAIR code	Annotation description	57 DAFB	78 DAFB	99 DAFB	120 DAFB	150 DAFB
Cell wall metabolism								
MDP0000139485	XTH30	AT1G32170.1	xyloglucan endotransglucosylase/hydrolase 30	1.34	2.68	1.59	0.86	-0.16
MDP0000311765	XTH32	AT2G36870.1	xyloglucan endotransglucosylase/hydrolase 32	1.99	3.01	2.51	1.23	-0.24
MDP0000398765	XTH5	AT5G13870.1	xyloglucan endotransglucosylase/hydrolase 5	2.23	3.14	2.32	0.80	0.01
MDP0000320017	XTH23	AT4G25810.1	xyloglucan endotransglycosylase 6	1.69	3.48	1.98	1.49	-0.48
MDP0000205889	AGP16	AT2G46330.1	arabinogalactan protein 16	-0.14	2.13	1.02	0.94	-0.89
MDP0000287357	AGP30	AT2G33790.1	arabinogalactan protein 30	1.81	2.10	2.39	1.54	0.17
MDP0000165381	AGP31	AT1G28290.1	arabinogalactan protein 31	0.63	1.83	2.35	1.11	-0.02
MDP0000133529	PEL	AT3G53190.1	Pectin lyase-like superfamily protein	2.78	3.31	1.83	0.94	-0.61
MDP0000297071	PMEI	AT5G09760.1	Pectin methylesterase inhibitor	0.85	2.69	1.71	0.74	-0.26
MDP0000560112	EXPA1	AT1G69530.1	expansin A1	0.35	2.05	2.50	4.62	2.58
MDP0000195798	EXPA4	AT2G39700.1	expansin A4	1.96	2.31	1.02	0.85	-1.22
MDP0000290170	EXPB2	AT1G65680.1	expansin B2	1.43	3.04	1.34	0.90	0.86
MDP0000208152	PA2,PRX53	AT5G06720.1	peroxidase 2	1.96	1.60	2.72	1.33	0.74
MDP0000312095	PRX72	AT5G66390.1	Peroxidase superfamily protein	1.63	2.71	1.83	0.78	0.77
MDP0000306867	PRX52	AT5G05340.1	Peroxidase superfamily protein	2.49	2.79	0.87	-0.44	-0.90
MDP0000126274	LAC7	AT3G09220.1	laccase 7	1.10	4.16	1.27	0.09	-1.68
MDP0000262848	LAC14	AT5G09360.1	laccase 14	1.24	2.26	2.29	0.09	0.51
MDP0000655646	LAC15	AT5G48100.1	laccase 15	0.72	2.16	1.60	0.18	0.28
Transcription factor								
MDP0000211677	MYB4	AT4G38620.1	myb domain protein 4	0.81	1.37	2.10	1.39	1.18
MDP0000210851	MYB7	AT2G16720.1	myb domain protein 7	2.13	3.11	1.82	0.90	0.58
MDP0000124049	MYB36	AT5G57620.1	myb domain protein 36	3.52	3.35	2.67	1.26	1.20
MDP0000787808	MYB42	AT4G12350.1	myb domain protein 42	0.32	2.01	1.28	-0.29	-0.20
MDP0000291518	MYB52	AT1G17950.1	myb domain protein 52	3.57	3.52	2.67	1.42	0.79
MDP0000133542	MYB58	AT1G16490.1	myb domain protein 58	3.70	3.40	1.86	0.74	-0.81
MDP0000157506	MYB67	AT3G12720.1	myb domain protein 67	4.11	3.24	2.90	1.63	1.18
MDP0000786507	MYB68	AT5G65790.1	myb domain protein 68	3.87	3.39	3.29	1.42	0.80
MDP0000682032	MYB85	AT4G22680.1	myb domain protein 85	3.28	2.91	2.46	1.12	0.11
MDP0000320772	MYB93	AT1G34670.1	myb domain protein 93	4.11	3.19	2.54	1.34	-0.15
MDP0000197283	MYB102	AT4G21440.1	myb domain protein 102	2.12	2.26	0.82	0.11	-1.20
MDP0000262032	ANAC072,RD26	AT4G27410.2	NAC domain containing protein 72	1.17	1.12	2.01	1.07	0.68
MDP0000129335	NAC100	AT5G61430.1	NAC domain containing protein 100	1.45	2.19	1.06	0.31	-0.36
MDP0000480581	NAC036	AT2G17040.1	NAC domain containing protein 36	-2.03	1.66	0.28	-0.10	1.27
MDP0000690168	NAC038	AT2G24430.1	NAC domain containing protein 38	3.23	3.08	2.64	1.22	0.84
MDP0000235213	NAC058	AT3G18400.1	NAC domain containing protein 58	3.59	3.44	2.49	1.19	0.00
MDP0000124509	NAC075	AT4G29230.1	NAC domain containing protein 75	3.29	3.20	2.11	1.27	0.39
MDP0000126517	NAC083,VNI2	AT5G13180.1	NAC domain containing protein 83	2.73	3.11	2.52	1.18	0.71
MDP0000481448	ATNAP,NAP	AT1G69490.1	NAC-like, activated by AP3/PI	0.41	1.37	2.76	0.71	0.36

Table 4-6 continued…

	Contig code	Gene symbol	TAIR code	Annotation description	Log2 ratio (RPKM CG/RPKM CB) 57 DAFB	78 DAFB	99 DAFB	120 DAFB	150 DAFB
Misc.									
	MDP0000660239		AT1G74460.1	GDSL-like Lipase/Acylhydrolase superfamily protein	4.45	3.52	2.54	1.32	-0.41
	MDP0000174332		AT1G75900.1	GDSL-like Lipase/Acylhydrolase superfamily protein	3.01	2.91	2.64	1.21	0.23
	MDP0000698860		AT4G13840.1	HXXXD-type acyl-transferase family protein	3.87	3.28	2.52	1.35	0.01
	MDP0000593263		AT1G32910.1	HXXXD-type acyl-transferase family protein	3.05	2.92	2.50	1.22	-0.10
	MDP0000172849		AT3G03990.1	alpha/beta-Hydrolases superfamily protein	1.06	2.05	1.94	1.24	1.29
	MDP0000594621		AT1G47480.1	alpha/beta-Hydrolases superfamily protein	3.47	3.04	2.54	1.06	0.01
	MDP0000930224		AT2G18360.1	alpha/beta-Hydrolases superfamily protein	3.37	3.07	2.79	1.09	0.68
	MDP0000188790		AT5G06570.1	alpha/beta-Hydrolases superfamily protein	1.66	1.20	2.59	0.51	0.47
	MDP0000927926		AT4G18550.1	alpha/beta-Hydrolases superfamily protein	3.48	2.81	3.04	1.13	0.85

GPAT5 produces sn-2 monoacyl-glyceryls which are among the most abundant monomers in suberin (Beisson *et al*. 2007). Three HXXXD-motif BAHD acyl transferase similar to the *A. thaliana* feruloyl hydroxycinnamoyl transferase (Table 4-6, Fig. 4-7 FHT/RWP1) were also co-expressed with these suberin biosynthesis genes. In *A. thaliana*, FHT(RWP1) is involved in the synthesis of the feruloyl-ω-hydroxyacids and alkyl-hydroxycinamates, which are found in the suberin matrix and suberin-associated waxes, respectively (Molina *et al*. 2009, Molina and Kosma 2015). As observed in clusters C2 and C4, a significant number of GDSL-motif lipases and α/β-fold hydrolases were also found and seemed to share similar metabolic processes with the suberin synthesis core metabolic pathway, namely CYP86A1, CYP86B1, GPAT5 and FHT (Table 4-6, Fig 4-7). As described in the previous part related to cuticle synthesis, recent studies identified, in *Solanum lycopersicum*, a GDSL-motif esterase/lipase (GDSL1) which is able to perform the transesterification of monoacylglycerol monomers enabling the linear polymerization of the cutin (Yeats *et al*. 2012, Girard *et al*. 2012). Additionally, the cell wall-associated α/β-fold hydrolase protein, BODYGUARD (BDG), is also a major actor of the cutin synthesis in *A. thaliana* (Kurdyukov *et al*. 2006). Loss-of-function *bdg* mutant strongly impaired the suberin deposition in roots, suggesting that this hydrolase might act in both suberin and cutin synthesis in the light of the high similarity between these two polymers (Jakobson *et al*. 2016). Additionally, a number of α/β-fold hydrolases and GDSL-motif lipases were also highlighted in previous works supporting their putative involvement in the apple russeting and more speculatively in the suberin final polymerization steps (Soler *et al*. 2007, Legay *et al*. 2015).

In addition to the suberin monomer synthesis metabolic enzymes, a significant number of genes coding for non-enzymatic proteins seemed to participate in the russeting process. Several hydroxyproline-rich glycoproteins were strongly

expressed in CG during the early time-point of the growth development. Among them, some Pro-Glu-Leu, Ile, Val-Pro-Lys-motif PELPK1 and PELPK2 were tightly associated with the suberin core (Fig. 4-7). PELPK-motif proteins function has not been fully elucidated yet, but PELPK1 was previously annotated as a cell wall related hydroxyproline rich glycoprotein and seemed to favor seed germination and growth rate in *A. thaliana* (Rashid *et al*. 2012). As PELPK1 is localized in the cell wall and responsive to pathogen attack, it has been proposed that PELPK1 might play a role in the cell wall integrity signaling cascade (Rashid 2011). Its involvement in the suberin deposition might be linked to the cuticle microcracking, which might also affect the cell wall integrity, but further work should be performed to validate this point.

As observed for cutin, a specific lipid transport process seemed to be associated with the russeting phenotype and the suberin deposition and gathered two large families. First, the ABC family G half size transporters were well represented with *ABCG2*, *ABCG6 ABCG11* and *ABCG23*, and shared biological functions with suberin genes (Table 4-6, Fig. 4-7). In *A. thaliana*, ABCG2 and ABCG6 are crucial partners of the suberin deposition in seed coat and ABCG23 was co-expressed with some suberin synthesis genes such as the GPAT5 (Yadav *et al*. 2014). ABCG11 transporter has been previously associated with the cutin and wax deposition (Bird *et al*. 2004). However, a more recent study described that ABCG11 affected the normal development of both cuticle, in reproductive organs, and suberin, in roots (Panikashvili *et al*. 2010). In apple, we previously observed two ABCG11 genes which displayed inverse expression patterns depending on apple skin phenotype (russet/waxy), suggesting that there might be a cuticle- and a suberin-specific ABCG11 transporters (Legay *et al*. 2015).

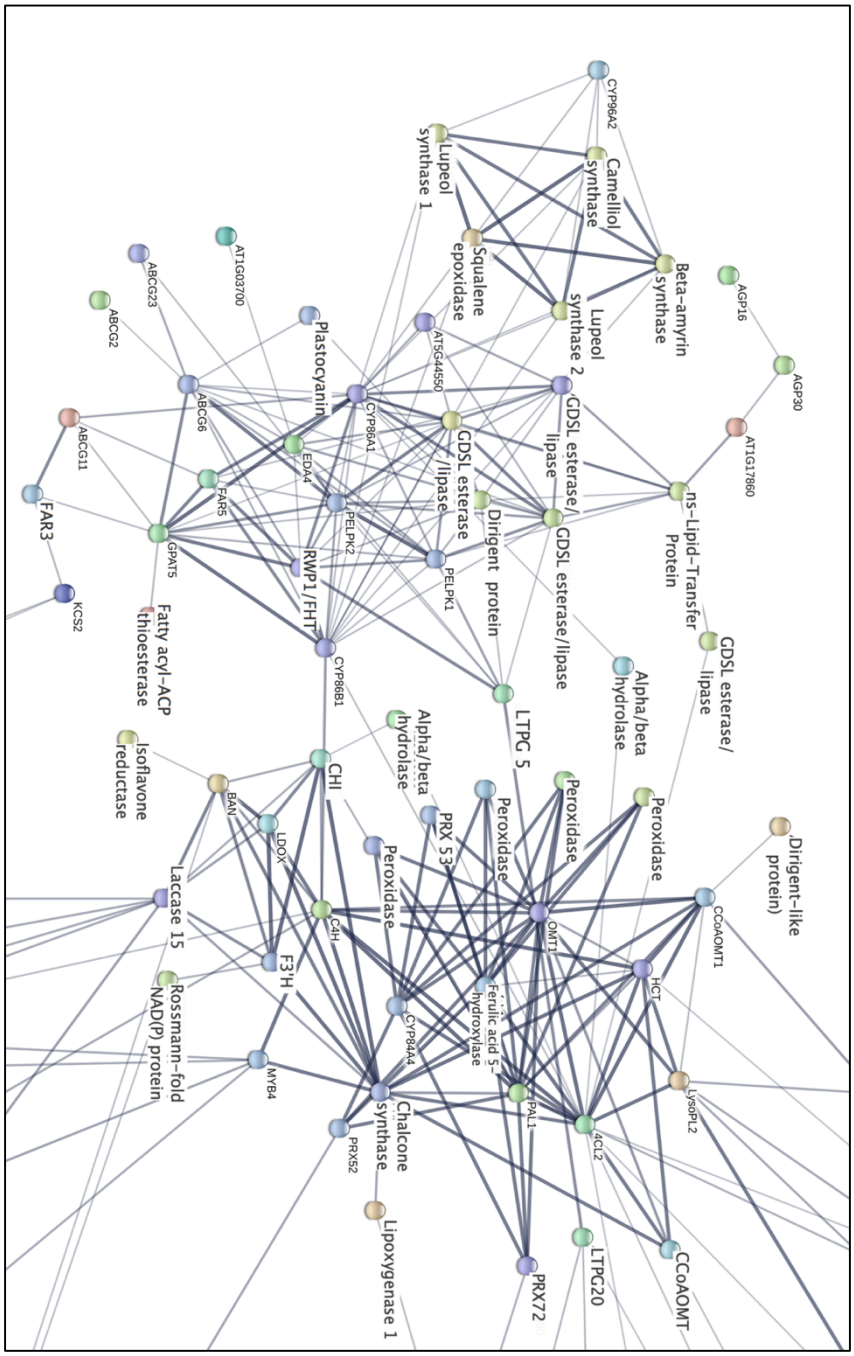

Figure 4-7: see legend on the next page

Figure 4-7 (previous page): Subset of the co-expression matrix performed using STRING from clusters C4 to C7. The full matrix was restricted to the neighbours of the suberin, phenylpropanoid and triterpene synthesis biosynthesis pathway. Grey lines display the confidence of associations between two genes, which share a role in biological processes. The thickness of the lines corresponds to the significance of the interaction with a minimum cut-off value of 0.4. Interactions with genes which were not included in this network are represented by the lines going to the borders of the figure. Genes that displayed lower than this cut-off value are not represented. Genes with unknown function were coded with their corresponding TAIR code, others were coded as follows : 4CL : 4-coumarate-CoA ligase, ABCG : ATP-binding cassette family G transporter, AGP : arabinogalactan protein, BAN : BANYULS, C4H : Cinnamate-4-hydroxylase, CCoAMT : Caffeoyl-CoA methyltransferase, CHI : Chalcone isomerase, CYP : cytochrome P450, EDA4 : embryo sac development arrest 4, F3'H : Flavonoid-3'-hydrolase, FAR : fatty acid reductase, GPAT5 : Glycerol-3-phosphate acyl transferase 5, HCT : hydroxycinnamoyl transferase, KCS : 3-ketoacyl-CoA synthase, LDOX : lipoxygenase, LTPG: Lipid transfer protein family G, LysoPL2 : lysophospholipase 2, PELPK : hydroxyproline-rich glycoprotein.

The non-specific lipid transfer proteins constitute the second group of transporters being co-expressed with the suberin synthesis gene in CG (Table 4-6). LTP subfamily G transporters were among the most represented with LTPG5, LTPG16 (EDA4) and several LTPG20. One LTPG20 protein also accumulated 78 DAFB (Table 4-3). LTPG transporters are non-specific lipid transfer protein presenting a GPI-anchor at the C-terminal region, which linked the protein to the external side of the plasma membrane. *In silico* analysis of the expression pattern of the *A. thaliana* LTPGs showed that LTPG5, LTPG16 and LTPG20 participate in the phenylpropanoid and suberin metabolism, however their exact function remained undefined (Edstam *et al*. 2013). In addition to the GPI-anchored LTPG transporter genes, an LTP1-like gene was also upregulated in the CG variety. LTPs are involved in the transport of cutin and waxes but, to date, their implication if the suberin deposition is only hypothesized (Li-Beisson *et al*. 2010).

Suberin is a complex biopolymer constituted by a polyaliphatic and a polyphenolic domain (Bernards 2002). As observed for genes involved in the synthesis of the aliphatic domain of suberin, a differential gene expression was observed in the phenylpropanoid pathway and might be linked to the suberin polyphenolic domain synthesis (Fig. 4-6, Fig. 4-7, Table 4-6). Among these, several genes involved in the synthesis of hydroxycinnamic acids were highlighted: the phenylalanine ammonia lyase 1 (*PAL1*), the 4-coumarate-CoA Ligase (*4CL*), the ferulic acid-5 hydroxylase 1 (*FAH1*), some hydroxycinnamoyl-CoA shikimate/quinate hydroxycinnamoyl transferase (*HCT*), a large number of *O*-methyltransferase 1 (*OMT1*) and caffeoyl-CoA *O*-methyltransferase 1 (*CCoAMT1*) (Table 4-6). Taken together, and according to the recent understanding of the phenylpropanoid synthesis pathway, the enhanced expression of these genes strongly suggest that an increased synthesis of hydroxycinnamic acids and particularly of ferulic acid occurred in the russeted CG (Fraser and Chapple 2011, Graca 2015, Wishwanath *et al*. 2015). Inversely, and, as observed in previous works, the hydroxycinnamoyl alcohols synthesis seemed to be repressed (Wang *et al*. 2014a, Wang *et al*. 2014b, Legay *et al*. 2015). Indeed, a gene coding for a cinnamyl alcohol dehydrogenase 9-like (*CAD*), which catalyzes a crucial step of the hydroxycinnamyl alcohols, displayed a decreased expression and was grouped into clusters C2 and C3 (Table 4-4). In addition to this, a cinnamoyl-CoA reductase (*CCR*) showed a decreased abundance 150 DAFB (Table 4-3). A similar decreased expression of *CCR* and *CAD* was previously observed in transcriptomic works focusing on russeting (Wang *et al*. 2014a, Wang *et al*. 2014b, Legay *et al*. 2015). The analysis of the polyphenolic domain of suberin (SPPD), which is anchored in the primary cell wall, displays a similar structure as lignin, with a higher amount of polymerized ferulic acid (Bernard *et al*. 2002). The decreased expression of *CCR* and *CAD* might be linked

to the higher synthesis of hydroxycinnamate content found in the lignin-like SPPD. Furthermore, the content in free hydroxycinnamic acids have been shown to be significantly higher in russeted apple skin (Andre *et al*. 2012). Altogether, the present data corroborate the previous works and suggest that the synthesis of hydroxycinnamic acids is strongly enhanced in russeted apples (Bernards 2002, Molina *et al*. 2009).

As the SPPD is covalently linked to the primary cell wall, it is not surprising that a noticeable number of genes involved in cell wall biosynthesis and modification, particularly the expression of those involved in the modification of hemicelluloses, were found in clusters C4 to C7 (Fig. 4-6, Table 4-3, Table 4-6). Genes involved in the xylan and xyloglucan synthesis suggested that a strong modification of the hemicellulose occurred in the cell wall (Fig. 4-6). The xyloglucan synthesis biological process was mainly represented by different isoforms of the xyloglucan endotransglucosylase/hydrolase (XET, Table 4-6). This was corroborated by the increased abundance of two XET proteins, 150 DAFB (Table 4-3). Previous studies showed that XETs play a crucial role in cell wall loosening enabling an increased cell wall extension (Van Sandt *et al*. 2007). Additionally, XETs also participate in some remodeling activities aiming at increasing cohesion between primary and secondary cell wall (Bourquin *et al*. 2002). In the present case, XET might be involved in a remodeling process aiming at favoring SPPD anchoring in the cell wall but this has to be further investigated. This cell wall loosening process has also affected pectin-related genes (Table 4-6). In the present dataset, we observed a number of pectin lyase and pectin methylesterase inhibitors. A recent study showed that the cell wall elasticity is dependent on the degree of methylation of pectins. In *A. thaliana*, these genes are associated with cell wall loosening and their overexpression results in a higher root extension (Xu *et al*. 2014). Multiple expansins genes, similar to *AtEXPA1*,

AtEXPA4 and *AtEXPB2*, were also grouped in clusters C4 to C7, but other expansin-like proteins genes (EXPA15 and EXPA8) were also downregulated in CG (Table 4-3, Table 4-6). Expansins are also involved in cell wall loosening, by unlocking the network of polysaccharides and enabling cell expansion (Cosgrove 1998, Cosgrove 2000, Cosgrove 2005). Arabinogalactan protein genes AGP16, AGP30 and AGP31 were more expressed in CG and seemed to be linked to the suberin synthesis (Table 4-6, Fig. 4-7). Some fasciclin-like arabinogalactan (FLA) protein genes displaying a higher accumulation in CG were also found (Table 4-3). AGP are complex proteins belonging to a large family and display multiple functions associated, among other things, with the assembly cell wall polysaccharides (Ellis *et al*. 2010). FLAs are suspected to be involved in processes related to cell adhesion. Some members play a crucial role in the continuum apoplast-plasma membrane. Therefore, their involvement in the suberin deposition is plausible (Johnson *et al*. 2003). However, their exact function in cell wall modification during the suberin deposition process remains unclear.

In addition to this cell wall modification process, GO analysis performed on the C4-C7 clusters revealed biological processes linked with lignin synthesis (Fig. 4-6). These were mostly represented by some peroxidase genes which displayed strong interactions with the phenylpropanoid synthesis genes cited above (Fig. 4-7). Indeed, according to the gene interaction network, some of these have been already associated with the phenylpropanoid metabolism and the suberin deposition. PRX2, *PRX52* and *PRX72* genes and corresponding proteins were found in both data and displayed a similar expression pattern (Table 4-3, Table 4-6). PRX72 is a crucial actor of the lignification process and the secondary cell wall thickening, PRX52 is involved in the synthesis of lignin syringyl units and PRX2 (also coded as PA2 or PRX53) displays multiple functions implicated in wounding responses or flower development (Jin *et al*. 2011, Fernandez-Perez *et*

al. 2015a, Fernandez-Perez *et al*. 2015b). In addition to peroxidases, laccases (LACs) might also be involved in the suberin deposition process. As observed in our previous work, *LAC7*, *LAC14* and *LAC15* were more expressed in the russeted variety and were tightly correlated with the expression of suberin synthesis genes (Table 4-6, Legay *et al*. 2015). The LAC15/TT10 gene plays a role in the lignin synthesis but its role in the suberization remains unclear (Liang *et al*. 2006, Pourcel *et al*. 2005). The involvement of peroxidase and laccase genes in the suberin deposition process has not been clearly demonstrated yet. However, as the SPPD is suspected to have a lignin like structure, we can speculate that similar assembling processes, involving PRXs and the above-mentioned cell wall modification, might occur during the formation of this complex domain (Bernards *et al*. 1995, Bernards 2002). The regulation of the cell wall modification is still under discussion and involves a complex network including signaling cascades and transcription factors (Zhong *et al*. 2008, Cassan-Wang *et al*. 2014). Interestingly, the proteomic analysis revealed a wall associated kinase 3 (WAK3) displaying an increased abundance in CG at 57 and 78 DAFB (Table 4-3). In *A. thaliana*, WAK seems to participate in the pathogen response and the cell wall expansion during plant development (Kohorn and Kohorn 2012). In the present case, we can speculate that WAK might be implicated in a sensing process that involved the above-described cell wall modification process.

Moreover, C4, C5, C6 and C7, displayed a large number of genes for transcription factors, which were correlated with the suberin deposition and cell wall modification process. Among these, a number of MYB and NAC family transcription factors were represented (Table 4-6). It is noteworthy that part of these regulators were grouped into a biological process implicated in the regulation of the secondary cell wall biogenesis. Among these, *MYB42*, *MYB52*, *MYB58* and *MYB85*, are regulated by the SND1 master regulator and associated

with the secondary cell wall thickening. As an example, in *A. thaliana,* MYB52 repression resulted in a strong reduction of the secondary cell wall thickening (Zhong *et al.* 2008). However, recent studies displayed opposite conclusions, suggesting that it might be a negative regulator of the lignification process (Cassan-Wang *et al.* 2013). NAC075 seems to be also implicated in the secondary cell wall formation (Sakamoto and Mitsuda 2015). The role of the other MYB (MYB4, MYB67), NAC (NAC58, NAC38) and WRKY (WRKY45, WRKY56) transcription factors remains unclear. Finally, our previous work highlighted the strong correlation of *MYB93* and the suberin synthesis genes. Noteworthy, the differentially regulated transcription factors set is highly conserved with respect to our previous work, supporting their potential implication in russeting. Future functional analyses will assess their specific role in this complex process.

3. Expression of genes for triterpene metabolism in CG and CB strongly differed during fruit growth

Pentacyclic triterpenes are among the most abundant metabolites in the apple skin reaching up to 60% of the total wax content (André *et al.* 2012). Three main triterpene series have been identified in the apple skin so far. These differentially accumulated in non-russeted and russeted apple skin. The oleane and ursane series are predominantly found in the non-russeted fruit skin, whereas lupane triterpene series are found in russeted apples (André *et al.* 2012, Brendolise *et al.* 2011). The first step of the triterpene biosynthetic pathway is catalyzed by the squalene epoxidase (SQE), which converts squalene into 2,3 oxidosqualene. Interestingly, we found two genes coding for a squalene epoxidase, which were differentially regulated between the CB and CG varieties. Despite these were clustered into both clusters 2 and 6, they displayed a quite irregular expression pattern during the growth kinetics of these varieties. The next step of this metabolic pathway is determinant, shunting 2,3 oxidosqualene towards the synthesis of phytosterols or

of the different series mentioned above and is catalyzed by the oxidosqualene cyclase (OSC). Surprisingly, the gene expression data did not show any OSC specifically expressed in the non-russeted variety CB. In previous works, several OSC genes and particularly *MdOSC1*, were predominantly expressed in the non-russeted apple skin and the encoded enzymes produced α-amyrin and β-amyrin (Brendolise *et al*. 2011, Legay *et al*. 2015). However, a protein similar to MdOSC1, displaying an enhanced expression in the russeted CB at the harvest time point, was found in the proteomic data (Table 4-3). To clarify this unexpected result, we carefully investigated the full dataset and found two OSC-like genes similar to *MdOSC1* (MDP0000227287 and MDP0000474746), which were statistically more expressed in CB during the whole kinetics (FDR *p*-value <0.05), but did not raise the fold change cut-off value (Fold change>4). A CYP716A1-like gene and protein corresponding to MDP0000478473, displayed a higher expression and abundance in CB (Table 4-6). MDP0000478473 is highly similar to the monoxygenase CYP716A175 which is responsible for the final conversion step of α-amyrin, β-amyrin and lupeol into ursolic, oleanolic and betulinic acid, respectively (André *et al*. 2016). Interestingly, *CYP716A175* did not exhibit any tissue-specific expression when tested against a panel of russeted and non-russeted varieties (André *et al*. 2016). The differential expression observed in the present work might be considered as specific for the CG/CB couple.

A number of other *OSCs* displayed a similar expression pattern compared to the core suberin synthesis genes with slight differences (Table 4-6). However, in CG at 150 DAFB, a decreased expression of the suberin biosynthesis genes was observed, whereas the triterpene synthesis gene expression remained stable.

These *OSC* genes were annotated as lupeol synthase, terpenoid cyclase/beta amyrin synthase and cameliol synthase, the latter being not fully appropriate considering the different triterpene metabolic profiles recently found in apple

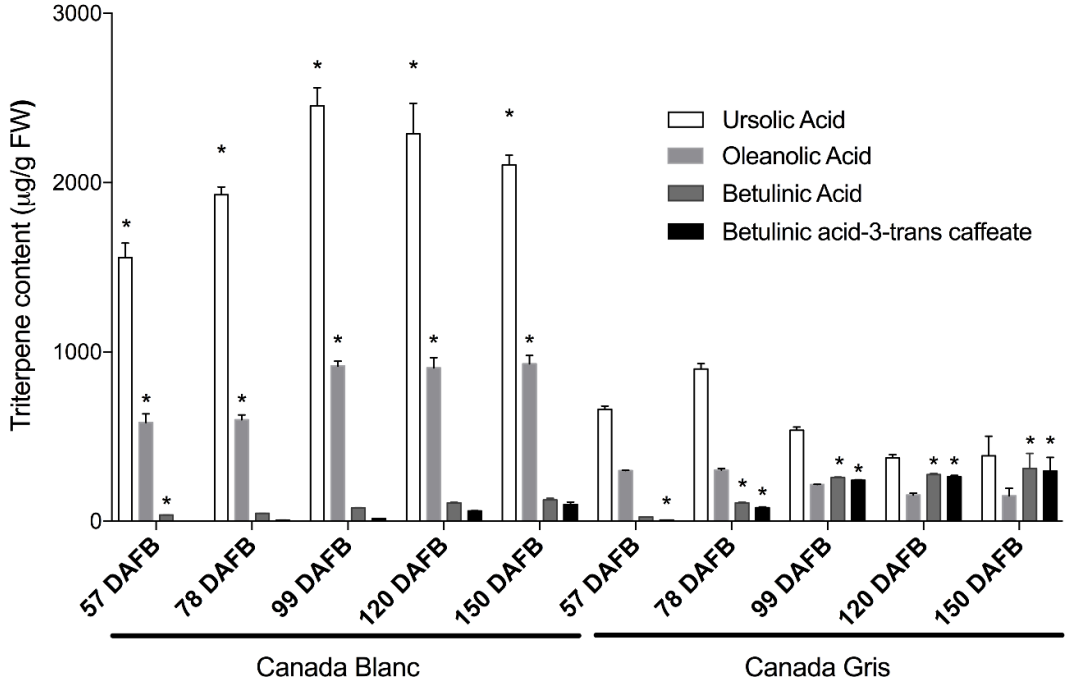

Figure 4-8: Oleanolic acid, ursolic acid, betulinic acid and betulinic acid-3-trans caffeate content in the "Canada Blanc" (non-russeted) and "Canada Gris" (russeted) skins. Measurement were performed at each time-point of the kinetics: 57, 78, 99, 120 and 150 days after full bloom. Stars display a statistically significant increase (p-value<0,05) content resulting from a Student t-test between Canada Gris and Canada Blanc.

(Table 4-6, Andre *et al*. 2012). For example, an *OSC* gene identified as a camelliol synthase was in fact the recently described MdOSC5 (MDP0000266125), which produced lupeol and β-amyrin in a 95:5 ratio (André *et al*. 2016). The strong interaction between the *OSC* genes and the suberin biosynthetic pathway was also supported by the STRING association network, with *CYP86A1* and *CYP86B1* sharing some biological processes with triterpene synthesis genes (Fig 4-7). In addition to this, a *CYP96A2* fatty acid hydroxylase-like gene also displayed interactions with the triterpene synthesis genes, however its function and involvement in the triterpene biosynthetic pathway remain unknown (Fig. 4-7).

In order to assess the tight correlation which seemed to occur between the suberin and triterpene biosynthesis, a targeted analysis of the apple triterpenes already described in previous works was performed (Fig. 4-8). The triterpene contents in both varieties showed strong differences which are comparable with the previous data (André *et al*. 2012, André *et al*. 2016). The non-russeted variety CB, exhibited a significantly higher accumulation of oleanolic and ursolic acid which increased during the first stages of the fruit growth (57 to 99 DAFB) and remained stable or slightly decreased at 120 and 150 DAFB. In CG, these two metabolites displayed a much lower accumulation, increasing until 78 DAFB and then decreasing until the commercial harvest (150 DAFB). Conversely, the betulinic and betulinic acid-3-*trans* caffeate contents increased in the russeted variety CG during in fruit growth but to a lower extent as compared to oleanolic and ursolic acids in CB.

Interestingly, triterpene-caffeates present potent biological activities and are therefore of major pharmaceutical interest (Rao *et al*. 2008, André *et al*. 2013). However, as they have only been recently discovered in apple skin, their biosynthesis remains unclear. Their synthesis might be assumed by enzymes showing acyltransferase and/or condensation activities. In model plants such as *A*.

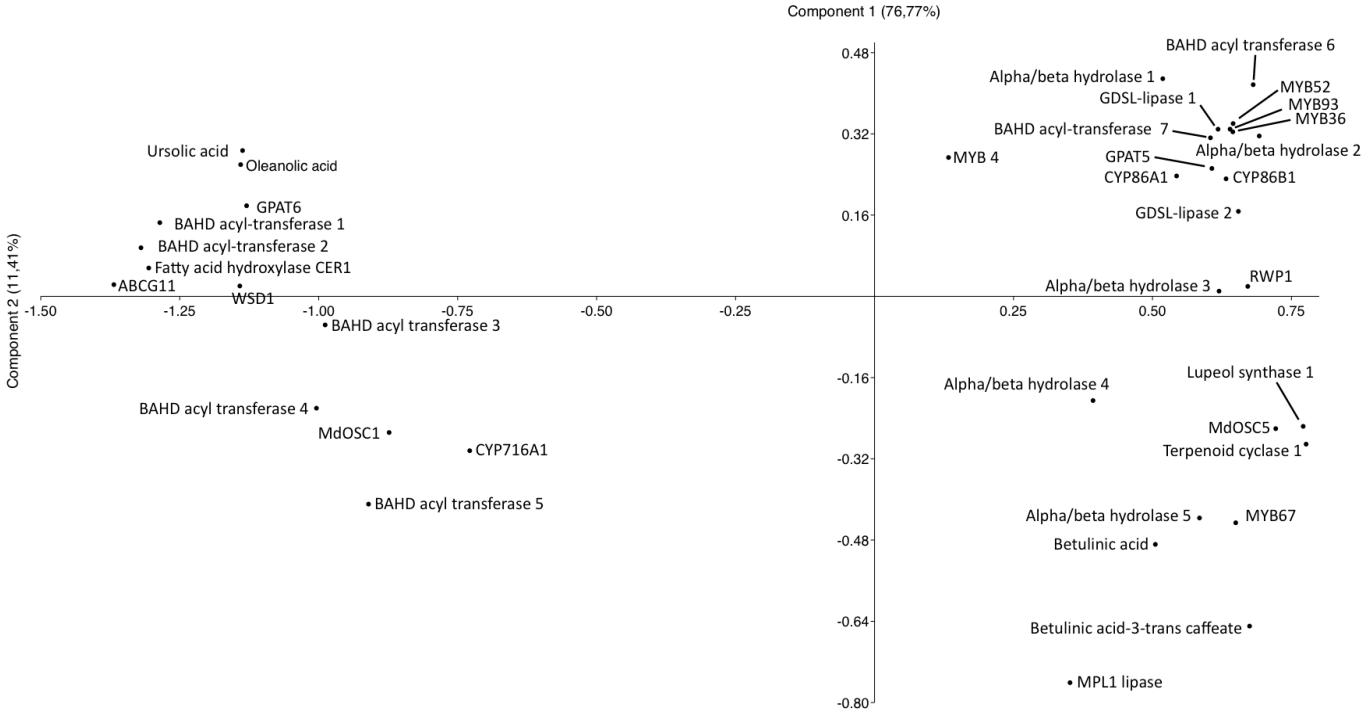

Figure 4-9 : See plegend on the next page

Figure 4-9: Principal component analysis performed using differentially expressed genes coding for α/β-fold hydrolases (1 to 5, respectively MDP0000172849, MDP0000594621, MDP0000930224, MDP0000188790, MDP0000927926), GDSL-lipases (1 and 2, respectively, MDP0000660239, MDP0000174332) and BAHD acyl-transferases (1 to 7,MDP0000120594, MDP0000183197, MDP0000137138, MDP0000126620, MDP0000120595,MDP0000698860, MDP0000593263) and transcription factors (MYB4, MYB52, MYB67, MYB93) genes implicated in cutin (GPAT6, CER1, ABCG11, WSD1) suberin (GPAT5, CYP86A1, CYP86B1, RWP1) and triterpene synthesis (MdOSC1, Lupeol synthase 1, MdOSC5, a terpenoid cyclase-like) and the triterpene contents (37 variables and 10 individuals).

thaliana, suberin-associated waxes comprise a large amount of alkyl-hydroxycinnamate conjugates which are produced by BAHD hydroxycinnamoyl transferases (Molina and Kosma 2015). Thus, it can be postulated that other members of this family might participate in the biosynthesis of triterpene-hydroxycinnamate conjugates. However, there is a broad range of enzymes able to perform condensation or acylation activities.

As an example, in tomato, a GDSL-lipase holding acyltransferase activity, uses chlorogenic acid as caffeate donor to form caffeoyl glutarate conjugate (Teutschbein *et al*. 2010). In the same way, protein of the α/β-fold hydrolase family display a large panel of functions including esterase activities, which might also undertake this task (Jakobson *et al*. 2016). As multiple members of these protein families were co-expressed with the triterpene and suberin synthesis pathways in our work, we performed a principal component analysis using expression data of cutin, suberin and triterpene biosynthesis markers (genes), together with some representative candidates of the protein family previously cited and the triterpene contents (Fig. 4-9). In addition to this, transcription factors co-expressed within the suberin deposition and triterpene biosynthesis clusters were also added (C4-C7). As expected, the first component was tightly linked to the russet trait and explained 76% of the variance of the data. Ursolic and oleanolic

acid contents were grouped with *MdOSC1*, *CYP716A1* and the cutin synthesis genes (Fig. 4-9). Cuticle-associated triterpene synthesis genes and contents were spread across the component 2 (11% of the total variance). This might be explained by the massive accumulation of ursolic and oleanolic acid, which correlated more with strong expression of cuticle biosynthesis genes. On the other side of the Y-axis, the suberin synthesis genes were grouped with the GDSL-lipase, part of the α/β-fold hydrolase, the BAHD-acyltransferase genes belonging to cluster C4-C7 such as *RPW1*, *MYB93*, *MYB4* and *MYB52* (Fig 4-9). Interestingly, the OSC genes, which clustered within C4-C7 (including MdOSC5), the betulinic acid and the betulinic acid-3-*trans* caffeate contents were grouped on the opposite side of the X-axis (component 2) compared to the suberin genes. Moreover, *MYB67* and three α/β-fold hydrolase genes also grouped with these triterpene genes and compounds, suggesting that they might participate in the synthesis and regulation of russeting-related triterpene biosynthesis pathway (Fig. 4-9).

D. Global outlines and key features

The present work constitutes the first expression profiling study comparing the fruit growth kinetics of russeted and non-russeted closely related apple varieties. Part of the identified biological processes implicated in this trait have been already described in our previous bulk transcriptomic study (Legay *et al*. 2015). However, although this preliminary work allowed us to draw a consistent snapshot of the russet trait-associated gene expression profiles, it did not provide a clear understanding of the interplay occurring between the different biological processes which are crucial actors in the establishment of russeting in apple. As an example, we previously concluded that the cutin and waxes synthesis biological processes were downregulated in fully russeted skin compared to non-

russeted skin. In the present data, these pathways also displayed a lower expression level in the russeted variety. However, it is interesting to notice that these were expressed in the early time-points (57 DAFB) and drastically decreased from 78 days to 150 DAFB, suggesting that the cuticle deposition process was repressed during the early fruit development in CG. Furthermore, in the russeted CG variety, it is obvious that the decreased expression of the cuticle deposition related genes is inversely correlated with the expression of suberin biosynthesis genes which increased from 57 DAFB, reaching a maximum of expression 78 DAFB and slightly decreasing 150 DAFB. These data were also corroborated by a recent study describing that the MdSHN3 transcription factor is able to trigger the cuticle deposition in the apple skin and to inhibit russeting (Lashbrooke *et al*. 2015).

We previously proposed that, in fully russeted apples, the decreased expression of cutin and wax synthesis gene might result in a thinner cuticle layer which favors the development of microcracking on the fruit skin surface leading to the development of russeting (Legay *et al*. 2015). However, the present work allowed us to refine our hypothesis. In CB, despite the fact that the cuticle synthesis-related genes were strongly and stably expressed over the time course of the fruit growth, expression of genes linked with russeting continuously increased and reached a similar expression level compared to CG at 150 DAFB (Fig. 4-10). This suggests that there might be multiple factors which lead to the development of russeting. Previous studies described multiple causes leading to russeting, such as the extended periods of humidity, drought, pesticides application, extreme tangential tensions on the surface of the fruit occurring during the fruit growth, etc (Walter 1967, Faust and Shear 1969, Skene 1982). All these factors seemed to have a common consequence, *i.e*. the development of cuticle microcracking (Faust and Shear 1969, Skene 1982, Curry 2009, Khanal *et al*. 2013). As in CB, the

expression of the cuticle biosynthesis genes is comparable to those previously observed in non-russeted waxy commercial apples, we can speculate that, in CB, the cuticle deposition may sustain the production of a consistent cuticle layer. The lower but significant increase of the suberin deposition process observed in this variety might be also caused by cuticle microcracking, but these might be less abundant than in CG due to a higher cuticle thickness. If so, the decreased expression of cuticle biosynthesis genes might be considered as an aggravating factor more than the main cause of the cuticle microcracking formation, increasing the effect of developmental and environmental factors in fruit skin. However, further integrative studies combining chemistry, biomechanics, transcriptomics have to be performed to support this critical point.

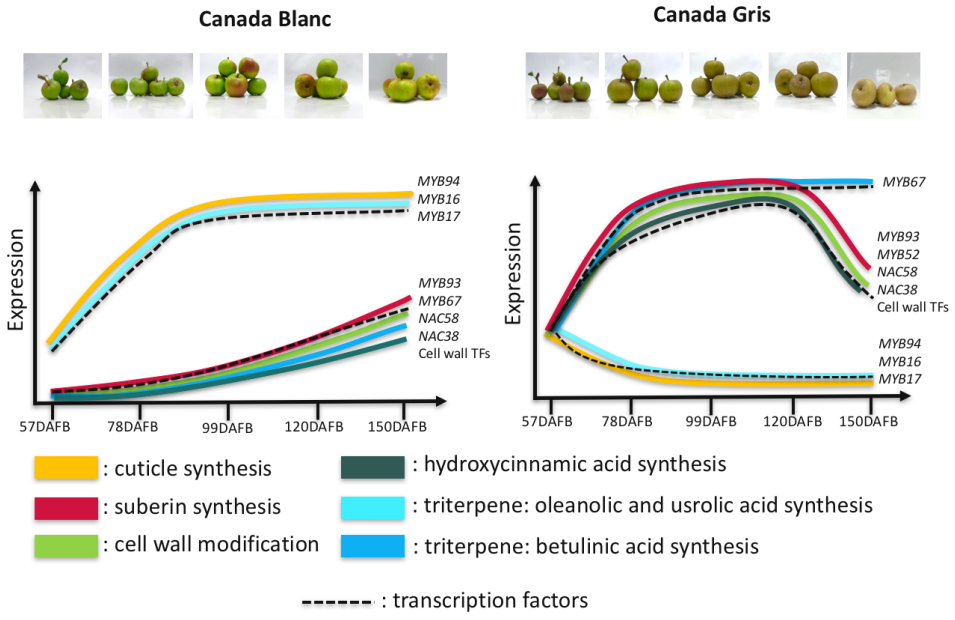

Figure 4-10: Trend in expression of genes being involved in the cuticle, suberin, hydroxycinnamic acid, triterpene biosynthesis and cell wall modification, during the fruit growth kinetic of Canada Gris and Canada Blanc. Cell wall modification-related transcription factor (cell wall TF) genes include: *NAC75*, *NAC73*, *MYB42*, *MYB52*, *MYB58* and *MYB85*. DAFB: days after full bloom.

The suberin biosynthesis pathway has not been fully elucidated yet, neither in model plants nor in apple. A large majority of the metabolic genes already described in model plants were found in our dataset. But interestingly, an important number of new candidates were also found. Among these, a particular interest has been given to the suberin deposition regulators. Transcription factors from the NAC and MYB families displayed correlations with genes suspected to be involved in the russet trait and nearly all of them were also described in our previous work (Fig. 4-10). Among these, some have been already linked with the cell wall metabolism (see below) but others, which were not described, might be involved in the regulation of the suberin deposition (Zhong *et al*. 2008, Cassan-Wang *et al*. 2013). MYB93 is probably one of the most promising candidates, considering its recently-reported expression patterns, which were tightly correlated with the suberin biosynthesis pathway in apple (Legay *et al*. 2015). As expected, we also found similar results, *MYB93* being clustered with suberin synthesis genes. The other remaining black boxes rely to the final assembly of the polyaliphatic domain of suberin. Genes belonging to the GDSL-lipase and/or α/β-fold hydrolase families have been suggested and recent works in the field of cutin synthesis, which shares similar structure and precursors, also support this hypothesis (Yeats *et al*. 2012, Vishwanath *et al*. 2015, Jakobson *et al*. 2016). In the present data, multiple candidates were found and corroborated our previous work. However, these two families also gathered a broad diversity in functions which make the selection of candidate genes difficult.

The alteration of the cell wall metabolism, which was similar to our previous observation, was highly correlated with the suberin biosynthesis pathway in term of expression level and time coordination (Fig. 4-10, Legay *et al*. 2015). These genes were associated with the modification of the hemicelluloses, more particularly with xylan and xyloglucan modifications, and with the lignification

process. The increased activities of these hemicellulose modification enzymes might be explained by a cell wall loosening process which results from the needs of the cell wall to expand during the fruit growth. But, as the SPPD has a structure similar to lignin, the mechanisms enabling the anchoring of the SPPD to cell wall might be similar and hemicellulose modifications (xylan, more specifically) might be part of this process (Bernards *et al*. 1995, Bernards 2002). The increased expression of lignin-related peroxidases (*PRX52*, *PRX72*) and laccase (*LAC7*, *LAC14*, *LAC15*) completes the picture and allows us to speculate that the cell wall modification and lignin synthesis genes might be considered as part of the SPPD polymerization process (Fernandez-Perez *et al*. 2015a, Fernandez-Perez *et al*. 2015b). This point was also supported by the increased expression of transcription factors such as *NAC75*, *NAC73*, *MYB42*, *MYB52*, *MYB58* and *MYB85* which were regulated by the secondary cell wall biogenesis master regulator, SND1, and associated with cell wall lignification (Fig. 4-10, Zong *et al*. 2008, Zhao *et al*. 2010).

Finally, a particular interest has been also given to the triterpene biosynthesis pathway. Compared to model plants such *A. thaliana* and *S. tuberosum*, the composition of both cuticle and suberin-associated waxes in the apple skin is dissimilar due to the massive content in triterpenic acids (André *et al*. 2016). In previous studies, a differential accumulation of triterpenes, highly dependent on the russeting degree, was observed (André *et al*. 2012, André *et al*. 2016). The transcriptomic and targeted triterpene analyses strongly support this observation and provide new insights about the regulation of the triterpene synthesis pathway. Indeed, during the fruit growth kinetics, a similar expression pattern was observed between the cutin and wax synthesis, and genes involved in the ursane and oleane triterpene series (Fig. 4-10). In the russeted variety, genes responsible for the lupane series synthesis, such as the *MdOSC5*, displayed a differential expression

which was highly correlated with the suberin-related genes excepted at the harvest sampling date. Interestingly, all genes belonging to the triterpene synthesis that are more expressed in the CG variety displayed this difference. Moreover, other genes such as α/β-fold hydrolases and *MYB67* also displayed this difference in expression pattern, suggesting that they might be linked to the regulation of the lupane synthesis (Fig. 4-10). Considering the relatively high proportion of triterpenes in the apple waxes and since their differential accumulation is highly correlated with the russet/non-russeted trait, we might speculate that the lupanes and their caffeate conjugates biosynthesis pathway might share common regulatory network with the cutin and suberin deposition pathway. Further investigation of transcriptional regulators putatively implicated in the triterpene and suberin synthesis, such as MYB67 or MYB93, might provide new insights about the regulatory and metabolic interplay potentially occurring between triterpene accumulation and the suberin biosynthesis pathway.

References

Aarts MG, Keijzer CJ, Stiekema WJ, Pereira A. 1995. Molecular characterization of the CER1 gene of *Arabidopsis* involved in epicuticular wax biosynthesis and pollen fertility. *The Plant Cell* **7**: 2115-27.

Andre CM, Greenwood JM, Walker EG, Rassam M, Sullivan M, Evers D, Perry NB, Laing WA. 2012. Anti-inflammatory procyanidins and triterpenes in 109 apple varieties. *Journal of Agricultural Food Chemistry* **60**: 10546-10554.

Andre CM, Larsen L, Burgess EJ, Jensen DJ, Cooney JM, Evers D, Zhang J, Perry NB, Laing WA. 2013. Unusual immuno-modulatory triterpene-caffeates in the skins of russeted varieties of apples and pears. *Journal of Agricultural Food Chemistry* **61**: 2773-2779.

Andre CM, Legay S, Deleruelle A, Nieuwenhuizen N, Punter M, Brendolise C, Cooney JM, Lateur M, Hausman JF, Larondelle Y, Laing WA. 2016. Multifunctional oxidosqualene cyclases and cytochrome P450 involved in the biosynthesis of apple fruit triterpenic acids. *New Phytologist* **211**: 1279-1294.

Arondel VV, Vergnolle C, Cantrel C, Kader J. 2000. Lipid transfer proteins are encoded by a small multigene family in *Arabidopsis thaliana*. *Plant Science* **157**: 1-12.

Baggerly KA, Deng L, Morris JS, Aldaz CM. 2003. Differential expression in SAGE: accounting for normal between-library variation. *Bioinformatics* **19**: 1477-1483.

Bernards MA. 2002. Demystifying suberin. *Canadian Journal of Botany* **80**: 227-240.

Bernards MA, Lopez ML, Zajicek J, Lewis NG. 1995. Hydroxycinnamic acid-derived polymers constitute the polyaromatic domain of suberin. *Journal of Biological Chemistry* **270**: 7382-7386.

Beisson F, Li Y, Bonaventure G, Pollard M, Ohlrogge JB. 2007. The acyltransferase GPAT5 is required for the synthesis of suberin in seed coat and root of *Arabidopsis*. *The Plant Cell* **19**:351-368.

Bindea G, Galon J, Mlecnik B 2013. CluePedia Cytoscape plugin: pathway insights using integrated experimental and *in silico* data. *Bioinformatics* **29**: 661-663.

Bindea G, Mlecnik B, Hackl H, Charoentong P, Tosolini M, Kirilovsky A, Fridman WH, Pages F, Trajanoski Z, Galon J. 2009. ClueGO: a Cytoscape plug-in to decipher functionally grouped gene ontology and pathway annotation networks. *Bioinformatics* **25**:1091-1093.

Bird D, Beisson F, Brigham A, Shin J, Greer S, Jetter R, Kunst L, Wu X, Yephremov A, Samuels L. 2007. Characterization of *Arabidopsis* ABCG11/WBC11, an ATP binding cassette (ABC) transporter that is required for cuticular lipid secretion. *The Plant Journal* **52**: 485-498.

Blacklock BJ, Jaworski JG. 2006. Substrate specificity of *Arabidopsis* 3-ketoacyl-CoA synthases. *Biochemical and Biophysical Research Communications* **346**: 583-590.

Boher P, Serra O, Soler M, Molinas M, Figueras M. 2013. The potato suberin feruloyl transferase FHT which accumulates in the phellogen is induced by wounding and regulated by abscisic and salicylic acids. *Journal of Experimental Botany* **64**: 3225-3236.

Bourquin V, Nishikubo N, Abe H, Brumer H, Denman S, Eklund M, Christiernin M, Teeri TT, Sundberg B, Mellerowicz EJ. 2002. Xyloglucan endotransglycosylases have a function during the formation of secondary cell walls of vascular tissues. *The Plant Cell* **14**: 3073-3088.

Brendolise C, Yauk YK, Eberhard ED, Wang M, Chagne D, Andre C, Greenwood DR, Beuning LL. 2011. An unusual plant triterpene synthase with predominant alpha-amyrin-producing activity identified by characterizing oxidosqualene cyclases from *Malus* x *domestica*. *FEBS Journal* **278**: 2485-2499.

Buschhaus C, Jetter R. 2012. Composition and physiological function of the wax layers coating *Arabidopsis* leaves: β-amyrin negatively affects the intracuticular water barrier. *Plant Physiology* **160**: 1120-1128.

Cassan-Wang H, Goue N, Saidi MN, Legay S, Sivadon P, Goffner D, Grima-Pettenati J. 2013. Identification of novel transcription factors regulating secondary cell wall formation in *Arabidopsis*. *Frontiers in Plant Science* **4:** 189.

Compagnon V, Diehl P, Benveniste I, Meyer D, Schaller H, Schreiber L, Franke R, Pinot F. 2009.CYP86B1 is required for very long chain omega-hydroxyacid and alpha, omega-dicarboxylic acid synthesis in root and seed suberin polyester. *Plant Physiology* **150**:1831-1843.

Cosgrove DJ. 1998. Cell Wall Loosening by Expansins. *Plant Physiology* **118**: 333-339.

Cosgrove DJ. 2000. Loosening of plant cell walls by expansins. *Nature* **407**: 321-326.

Cosgrove DJ. 2005. Growth of the plant cell wall. Nature Reviews. *Molecular Cell Biology*. **6**: 850-861.

Curry EA. 2009. Growth-induced microcracking and repair mechanisms of fruit cuticles. *Proceedings of the SEM annual conference*.

Curry EA. 2012. Increase in epidermal planar cell density accompanies decreased russeting of 'Golden Delicious' apples treated with Gibberellin A_{4+7}. *Hortscience* **47**: 232-237

Dean JV, Delaney SP. 2008. Metabolism of salicylic acid in wild-type, ugt74f1 and ugt74f2 glucosyltransferase mutants of *Arabidopsis thaliana*. *Physiologia Plantarum* **132**: 417-425.

Ding Y, Liu N, Virlouvet L, Riethoven JJ, Fromm M, Avramova Z1. 2013. Four distinct types of dehydration stress memory genes in *Arabidopsis thaliana*. *BMC Plant Biology* **13**: 229.

Domergue F, Vishwanath SJ, Joubes J, Ono J, Lee J *et al.* 2010. Three *Arabidopsis* fatty acyl-CoA reductases, FAR1, FAR4, and FAR5, generate primary fatty alcohols associated with suberin deposition. *Plant Physiology* **153**:1539-1554.

Edstam MM, Blomqvist K, Eklöf A, Wennergren U, Edqvist J. 2013. Coexpression patterns indicate that GPI-anchored non-specific lipid transfer proteins are involved in accumulation of cuticular wax, suberin and sporopollenin. *Plant Molecular Biology* **83**: 625-649.

Ellis M, Egelund J, Schultz CJ, Bacic A. 2010. Arabinogalactan-proteins: key regulators at the cell surface? *Plant Physiology* **153**: 403-419.

FAOSTAT: www.faostat.foa.org

Faust M, Shear C. 1972. Russeting of apples, an interpretative review. *HortScience* **7**: 233-235.

Khanal BP, Grimm E, Knoche M. 2013. Russeting in apple and pear: a plastic periderm replaces a stiff cuticle. *Annals of Botany – Plants* **5**: ls048.

Fabre G, Garroum I, Mazurek S, Daraspe J, Mucciolo A, Sankar M, Humbel BM, Nawrath C. 2016. The ABCG transporter PEC1/ABCG32 is required for the formation of the developing leaf cuticle in *Arabidopsis*. *New Phytologist* **209**: 192-201.

Falginella L, Cipriani G, Monte C, Gregori R, Testolin R, Velasco R, Troggio M, Tartarini S. 2015. A major QTL controlling apple skin russeting maps on the linkage group 12 of 'Renetta Grigia di Torriana'. *BMC Plant Biology* **15**: 150.

Fernández-Pérez F, Pomar F, Pedreño MA, Novo-Uzal E. 2015a. Suppression of *Arabidopsis* peroxidase 72 alters cell wall and phenylpropanoid metabolism. *Plant Science* **239**: 192-199.

Fernández-Pérez F, Pomar F, Pedreño MA, Novo-Uzal E. 2015b. The suppression of AtPrx52 affects fibers but not xylem lignification in *Arabidopsis* by altering the proportion of syringyl units. *Physiologia Plantarum* **154**: 395-406.

Fraser CM, Chapple C. 2011. The phenylpropanoid pathway in *Arabidopsis*. *Arabidopsis Book* **9**: e0152.

Gardner VR, Toenjes W, Giefel M, Kremer JC. 1948. Variability and segregation in the Golden Russet apple. *Journal of Agricultural Research* **76**: 231–240.

Gasic K, Hernandez A, Korban S. 2004. RNA extraction from different apple tissues rich in polyphenols and polysaccharides for cDNA library construction. *Plant Molecular Biological Report* **22**: 437a-437g.

Gianfranceschi L, Seglias N, Tarchini R, Komjanc M, Gessler C. 1998. Simple sequence repeats for the genetic analysis of apple. *Theoretical and Applied Genetics* **96**: 1069-1076.

Gibbs DJ, Coates JC. 2014. AtMYB93 is an endodermis-specific transcriptional regulator of lateral root development in *Arabidopsis*. *Plant Signaling and Behavior* **9**: e970406.

Gibbs DJ, Voß U, Harding SA, Fannon J, Moody LA, Yamada E, Swarup K, Nibau C, Bassel GW, Choudhary A *et al.* 2014. AtMYB93 is a novel negative regulator of lateral root development in *Arabidopsis*. *New Phytologist* **203**: 1194-1207.

Girard AL, Mounet F, Lemaire-Chamley M, Gaillard C, Elmorjani K *et al.* 2012. Tomato GDSL1 is required for cutin deposition in the fruit cuticle. *The Plant Cell* **24**: 3119-3134.

Guilford P, Prakash S, Zhu JM, Rikkerink E, Gardiner S, Bassett H, Forster R. 1997. Microsatellites in Malus X domestica (apple): abundance, polymorphism and cultivar identification. *Theoretical and Applied Genetics* **94**: 249-254.

Hen-Avivi S, Lashbrooke J, Costa F, Aharoni A. 2014. Scratching the surface: genetic regulation of cuticle assembly in fleshy fruit. *Journal Experiment Botany* **65**: 4653-4664.

Hofer R, Briesen I, Beck M, Pinot F, Schreiber L, Franke R. 2008. The *Arabidopsis* cytochrome P450 CYP86A1 encodes a fatty acid omega-hydroxylase involved in suberin monomer biosynthesis. *Journal of Experimental Botany* **59**: 2347-2360.

Jaeger J, Spang R. 2006. Selecting normalization genes for small diagnostic microarrays. *BMC Bioinformatics* **22**: 388.

Jakobson L, Lindgren LO, Verdier G, Laanemets K, Brosché M, Beisson F, Kollist H. 2016. BODYGUARD is required for the biosynthesis of cutin in *Arabidopsis*. *New Phytologist* **211**: 614-626.

Jiang ZH, Tanaka T, Kouno I. 1995. A lupane triterpene and two triterpene caffeates from *Rhoiptelea chiliantha*. *Plant chemistry* **40**: 1223-1226.

Jin J, Hewezi T, Baum TJ. 2011. *Arabidopsis* peroxidase AtPRX53 influences cell elongation and susceptibility to *Heterodera schachtii*. *Plant Signaling and Behaviour* **6**: 1778-1786.

Johnson KL, Jones BJ, Bacic A, Schultz CJ. 2003. The fasciclin-like arabinogalactan proteins of *Arabidopsis*. A multigene family of putative cell adhesion molecules. *Plant Physiology* **133**: 1911-1925.

Joubès J, Raffaele S, Bourdenx B, Garcia C, Laroche-Traineau J, Moreau P, Domergue F, Lessire R. 2008. The VLCFA elongase gene family in *Arabidopsis thaliana:* phylogenetic analysis, 3D modelling and expression profiling. *Plant Molecular Biology* **67**: 547-566.

Kannangara R, Branigan C, Liu Y, Penfield T, Rao V, Mouille G, Höfte H, Pauly M, Riechmann JL, Broun P. 2007. The transcription factor WIN1/SHN1 regulates Cutin biosynthesis in *Arabidopsis thaliana*. *The Plant Cell* **19**: 1278-1994.

Knoche M, Grimm E. 2008. Surface moisture induces microcracks in the cuticle of 'Golden Delicious' apple. *Hortscience* **43**: 1929–1931

Knoche M, Khanal BP, Stopar M. 2011. Russeting and microcracking of 'Golden Delicious' apple fruit concomitantly decline due to Gibberellin A4+7 application. *Journal of the American Society for Horticultural Science* **136**: 159-164.

Kohorn BD, Kohorn SL. 2012. The cell wall-associated kinases, WAKs, as pectin receptors. *Frontiers in Plant Science*. **8**: 88.

Kosma DK, Molina I, Ohlrogge JB, Pollard M. 2012. Identification of an *Arabidopsis* fatty alcohol:caffeoyl-Coenzyme A acyltransferase required for the synthesis of alkyl hydroxycinnamates in root waxes. *Plant Physiology* **160**: 237–248.

Kosma DK, Murmu J, Razeq FM, Santos P, Bourgault R, Molina I, Rowland O. 2014. AtMYB41 activates ectopic suberin synthesis and assembly in multiple plant species and cell types. *Plant Journal* **80**: 216-229.

Kurdyukov S, Faust A, Nawrath C, Bär S, Voisin D, Efremova N, Franke R, Schreiber L, Saedler H, Métraux J-P *et al.* 2006. The epidermis-specific extracellular BODYGUARD controls cuticle development and morphogenesis in *Arabidopsis*. *The Plant Cell* **18**: 321-339.

Liang M, Davis E, Gardner D, Cai X, Wu Y. 2006. Involvement of AtLAC15 in lignin synthesis in seeds and in root elongation of *Arabidopsis*. *Planta* **224**: 1185-1196.

Landgraf R, Smolka U, Altmann S, Eschen-Lippold L, Senning M *et al.* 2014. The ABC transporter ABCG1 is required for suberin formation in potato tuber periderm. *The Plant Cell* **26**: 3403-3415.

Lashbrooke J, Aharoni A, Costa F. 2015. Genome investigation suggests MdSHN3, an APETALA2-domain transcription factor gene, to be a positive regulator of apple fruit cuticle formation and an inhibitor of russet development. *Journal of Agricultural Food Chemistry* **63**: 185-91.

Lee SB, Jung SJ, Go YS, Kim HU, Kim JK, Cho HJ, Park OK, Suh MC. 2009. Two *Arabidopsis* 3-ketoacyl CoA synthase genes, KCS20 and

KCS2/DAISY, are functionally redundant in cuticular wax and root suberin biosynthesis, but differentially controlled by osmotic stress. *Plant Journal* **60**: 462-475.

Lee SB, Suh MC. 2013. Recent advances in cuticular wax biosynthesis and its regulation in *Arabidopsis*. *Molecular Plant* **6**: 246-249.

Legay S, Guerriero G, Deleruelle A, Lateur M, Evers D, André CM, Hausman, J-F. 2015. Apple russeting as seen through the RNA-seq lens: strong alterations in the exocarp cell wall. *Plant Molecular Biology* **88**: 21-40.

Legay S, Lefèvre I, Lamoureux D, Barreda C, Tincopa LR, Gutierrez R, Quiroz R, Hoffmann L, Hausman JF, Bonierbale M, Evers D, Schafleitner R. 2011. Carbohydrate metabolism and cell protection mechanisms differentiate drought tolerance and sensitivity in advanced potato clones (*Solanum tuberosum* L.). *Functional & integrative genomics* **11**: 275-291.

Li F, Wu X, Lam P, Bird D, Zheng H, Samuels L, Jetter R, Kunst L. 2008. Identification of the wax ester synthase/acyl-coenzyme A: diacylglycerol acyltransferase WSD1 required for stem wax ester biosynthesis in *Arabidopsis*. *Plant Physiology* **148**: 97-107.

Li Y, Beisson F. 2009. The biosynthesis of cutin and suberin as an alternative source of enzymes for the production of bio-based chemicals and materials. *Biochimie* **91**: 685-691.

Li-Beisson Y, Shorrosh B, Beisson F, Andersson MX, Arondel V *et al.* 2010. Acyl-lipid metabolism. *The Arabidopsis Book* **8**: e0133.

Liebhard R, Gianfranceschi L, Koller B, Ryder CD, Tarchini R, Van de Weg WE, Gessler C. 2002. Development and characterisation of 140 new microsatellites in apple (*Malus* x *domestica* Borkh.). *Molecular Breeding* **10**: 217-241.

Lü S, Song T, Kosma DK, Parsons EP, Rowland O, Jenks MA. 2009. *Arabidopsis* CER8 encodes LONG-CHAIN ACYL-COA SYNTHETASE 1

(LACS1) that has overlapping functions with LACS2 in plant wax and cutin synthesis. *Plant Journal* **59**: 553-564.

McFarlane HE, Watanabe Y, Yang W, Huang Y, Ohlrogge J, Samuels AL. 2014. Golgi- and trans-Golgi network-mediated vesicle trafficking is required for wax secretion from epidermal cells. *Plant Physiology* **164**: 1250-1260.

Millar AA, Clemens S, Zachgo S, Giblin EM, Taylor DC, Kunst L. 1999. CUT1, an *Arabidopsis* gene required for cuticular wax biosynthesis and pollen fertility, encodes a very-long-chain fatty acid condensing enzyme. *The Plant Cell* **11**: 825-838.

Molina I, Kosma D. 2015. Role of HXXXD-motif/BAHD acyltransferases in the biosynthesis of extracellular lipids. *Plant Cell Reports* **34**: 587-601.

Molina I, Li-Beisson Y, Beisson F, Ohlrogge JB, Pollard M. 2009. Identification of an *Arabidopsis* feruloyl-coenzyme A transferase required for suberin synthesis. *Plant Physiology* **151**: 1317-1328.

Mortazavi A, Williams BA, McCue K, Schaeffer L, Wold B. 2008. Mapping and quantifying mammalian transcriptomes by RNA-Seq. *Nature Methods* **5**: 621-628.

Oufir M, Legay S, Nicot N, Van Moer K, Hoffmann L, Renaut J, Hausman JF, Evers D. 2008. Gene expression in potato during cold exposure: changes in carbohydrate and polyamine metabolisms. *Plant science* **175**: 839-852.

Oshima Y, Mitsuda N. 2013. The MIXTA-like transcription factor MYB16 is a major regulator of cuticle formation in vegetative organs. *Plant Signaling and Behaviour* **8**: e26826.

Oshima Y, Shikata M, Koyama T, Ohtsubo N, Mitsuda N, Ohme-Takagi M. 2013. MIXTA-like transcription factors and WAX INDUCER1/SHINE1 coordinately regulate cuticle development in *Arabidopsis* and *Torenia fournieri*. *The Plant Cell* **25**: 1609-1224.

Pan H, Lundgren LN, Andersson R. 1994. Triterpene caffeates from bark of *Betula pubescens*. *Phytochemistry* **37**: 795-799.

Panikashvili D, Shi JX, Bocobza S, Franke RB, Schreiber L, Aharoni A. 2010. The *Arabidopsis* DSO/ABCG11 transporter affects cutin metabolism in reproductive organs and suberin in roots. *Molecular Plant* **3**: 563-575.

Panikashvili D, Shi JX, Schreiber L, Aharoni A. 2009. The *Arabidopsis* DCR Encoding a Soluble BAHD Acyltransferase Is Required for Cutin Polyester Formation and Seed Hydration. *Plant Physiology* **151**: 1773-1789.

Pourcel L, Routaboul JM, Kerhoas L, Caboche M, Lepiniec L, Debeaujon I. 2005.
TRANSPARENT TESTA10 encodes a laccase-like enzyme involved in oxidative polymerization of flavonoids in *Arabidopsis* seed coat. *The Plant Cell* **17**: 2966-2980.

Qin P, Tu B, Wang Y, Deng L, Quilichini TD, Li T, Wang H, Ma B, Li S. 2013. ABCG15 encodes an ABC transporter protein, and is essential for post-meiotic anther and pollen exine development in rice. *Plant Cell Physiology* **54**: 138-154.

Rao YK, Fang SH, Tzeng YM. 2008. Antiinflammatory activities of flavonoids and a triterpene caffeate isolated from Bauhinia variegata. *Phytotherapy Research*. **22**: 957-962.

Rashid A. 2011. Functional characterization of a novel cell-wall annotated PELPK1 gene in *Arabidopsis thaliana*. *Thesis Manuscript* University of Alberta.

Rashid A, Hobson N, Deyholos MK. 2012. A genomic region upstream of *Arabidopsis thaliana* PELPK1 promotes transcription in aleurone tissues and in response to *Pseudomonas syringae* or *Pythium irregulare*. *Plant Molecular Biology Reporter* **31**: 1025-1030.

Renaut J, Lutts S, Hoffmann L, Hausman JF. 2004. Responses of poplar to chilling temperatures: proteomic and physiological aspects. *Plant Biology (Stuttg)* **6**: 81-90.

Rowland O, Lee R, Franke R, Schreiber L, Kunst L. 2007. The CER3 wax biosynthetic gene from *Arabidopsis thaliana* is allelic to WAX2/YRE/FLP1. *FEBS Letters* **581**: 3538-3544.

Sakamoto S, Mitsuda N. 2015. Reconstitution of a secondary cell wall in a secondary cell wall-deficient *Arabidopsis* mutant. *Plant Cell Physiology* **2**: 299-310.

Sauveplane V, Kandel S, Kastner PE, Ehlting J, Compagnon V, Werck-Reichhart D, Pinot F. 2009. *Arabidopsis thaliana* CYP77A4 is the first cytochrome P450 able to catalyze the epoxidation of free fatty acids in plants. *FEBS Journal* **276**: 719-735.

Schnurr J, Shockey J, Browse J. 2004. The acyl-CoA synthetase encoded by LACS2 is essential for normal cuticle development in *Arabidopsis*. *The Plant Cell* **16**: 629-642.

Skene DS. 1982. The development of russet, rough russet and craks on the fruit of the apple Cox's Orange Pippin during the course of the season. *Journal of Horticultural Science* **57**: 165-174.

Serra O, Soler M, Hohn C, Franke R, Schreiber L, Prat S, Molinas M, Figueras M, 2009a. Silencing of StKCS6 in potato periderm leads to reduced chain lengths of suberin and wax compounds and increased peridermal transpiration. *Journal of Experimental Botany* **60**: 697-707.

Soler M, Serra O, Molinas M, Huguet G, Fluch S, Figueras M. 2007. A genomic approach to suberin biosynthesis and cork differentiation. *Plant Physiology* **144**: 419-431.

Teutschbein J, Gross W, Nimtz M, Milkowski C, Hause B, Strack D. 2010. Identification and Localization of a Lipase-like Acyltransferase in Phenylpropanoid Metabolism of Tomato (*Solanum lycopersicum*). *The Journal of Biological Chemistry* **285**: 38374-38381.

Thimm O, Blaesing O, Gibon Y, Nagel A, Meyer S, Krüger P, Selbig J, Müller

LA, Rhee SY, M Stitt. 2004. MAPMAN: a user-driven tool to display genomics data sets onto diagrams of metabolic pathways and other biological processes. *Plant Journal* **37**: 914-39.

Velasco R, Zharkikh A, Affourtit J, Dhingra A, Cestaro A, Kalyanaraman A, Fontana P *et al.* 2010. The genome of the domesticated apple (*Malus* x *domestica* Borkh.). *Nature Genetics* **42**: 833-839.

Van Sandt VS, Suslov D, Verbelen JP, Vissenberg K. 2007. Xyloglucan endotransglucosylase activity loosens a plant cell wall. *Annals of Botany* **100**: 1467-1473.

Vishwanath SJ, Kosma DK, Pulsifer IP, Scandola S, Pascal S, Joubes J, Dittrich-Domergue F, Lessire R, Rowland O, Domergue F. 2013. Suberin-associated fatty alcohols in *Arabidopsis thaliana*: distributions in roots and contributions to seed coat barrier properties. *Plant Physiology* **163**: 1118-1132.

Walter TE.1967. Russeting and cracking in apples. A review of world literature. *Report of East Mailing Research Station* **1966**: 83-95.

Wang YZ, Dai MS, Zhang SJ, Shi ZB. 2014a. Exploring candidate genes for pericarp russet pigmentation of sand pear (*Pyrus pyrifolia*) via RNA-Seq data in two genotypes contrasting for pericarp color. *PLoS One* **9**: e83675.

Wang, YZ, Zhang S, Dai MS, Shi ZB. 2014b. Pigmentation in sand pear (*Pyrus pyrifolia*) fruit: biochemical characterization, gene discovery and expression analysis with exocarp pigmentation mutant. *Plant Molecular Biology* **85**: 123-134.

Wellesen K, Durst F, Pinot F, Benveniste I, Nettesheim K, Wisman E, Steiner-Lange S, Saedler H, Yephremov A. 2001. Functional analysis of the LACERATA gene of *Arabidopsis* provides evidence for different roles of fatty acid ω-hydroxylation in development. *Proceedings of the national Academy of of Sciences of USA* **98**: 9694-9699.

Xia Y, Nikolau BJ, Schnable PS. 1996. Cloning and characterization of CER2, an *Arabidopsis* gene that affects cuticular wax accumulation. *The Plant Cell* **8**: 1291-304.

Xia Y, Yu K, Gao QM, Wilson EV, Navarre D, Kachroo P, Kachroo A. 2012. Acyl CoA Binding Proteins are Required for Cuticle Formation and Plant Responses to Microbes. *Frontiers in Plant Science* **8**: 224.

Xiao F, Goodwin M, Xiao Y, Sun Z, Baker D,Tang X, Matthew A, Jenks MA, Zhou JM. 2004. *Arabidopsis* CYP86A2 represses *Pseudomonas syringae* type III genes and is required for cuticle development. *EMBO Journal* **23**: 2903-2913.

Xu P, Cai XT, Wang Y, Xing L, Chen Q, Xiang CB. 2014. HDG11 upregulates cell-wall-loosening protein genes to promote root elongation in *Arabidopsis*. *Journal Experimental Botany* **65**: 4285-4295.

Yang Y, Xu R, Ma CJ, Vlot AC, Klessig DF, Pichersky E. 2008. Inactive methyl indole-3-acetic acid ester can be hydrolyzed and activated by several esterases belonging to the AtMES esterase family of *Arabidopsis*. *Plant Physiology* **147**: 1034-1045.

Yeats TH, Huang W, Chatterjee S, Viart HM, Clausen MH, Stark RE, Rose JK. 2014. Tomato Cutin Deficient 1 (CD1) and putative orthologs comprise an ancient family of cutin synthase-like (CUS) proteins that are conserved among land plants. *Plant Journal* **77**: 667-675.

Yeats TH, Laetitia BB, Martin Viart HMF, Isaacson T, He Y, Zhao L *et al.* 2012. The identification of cutin synthase: formation of the plant polyester cutin. *Nature Chemical Biology* **8**: 609-611.

Yadav V, Molina I, Ranathunge K, Castillo IQ, Rothstein SJ, Reed JW. 2014. ABCG transporters are required for suberin and pollen wall extracellular barriers in *Arabidopsis*. *The Plant Cell* **26**: 3569-3588.

Zhao Q, Wang H, Yin Y, Xu Y, Chen F, Dixona RA. 2010. Syringyl lignin biosynthesis is directly regulated by a secondary cell wall master switch. *Proceedings of the national Academy of of Sciences of USA* **107**: 14496-14501.

Zhang Y, Cao G, Qu LJ, Gu H. 2009. Characterization of *Arabidopsis* MYB transcription factor gene AtMYB17 and its possible regulation by LEAFY and AGL15. *Journal of Genetics and Genomics* **36**: 99-107.

Zhong R, Lee C, Zhou J, McCarthy RL, Ye ZH. 2008. A battery of transcription factors involved in the regulation of secondary cell wall biosynthesis in *Arabidopsis*. *The Plant Cell* **20**: 2763-2782.

Chapter III

Integrative analysis of two russeted and non-russeted closely related apple varieties during fruit development provides new insights about the cuticle/suberin interplay

Summary and Perspectives

In apple, the development of suberized fruit skin has been linked with a decreased expression of the cutin and wax biosynthetic genes. This observation is supported by previous studies and our Chapter II on the analysis of the semi-russeted apple 'Cox Orange Pippin', which displayed a drastic decrease in cutin monomers and wax components. Moreover, our bulk transcriptomic analysis (Chapter I) showed an expected increased expression of the suberin biosynthetic pathway and allowed to identify key genes already identified in model plants such as *Arabidopsis thaliana*. This was also confirmed by the analysis of the russeted skin of 'Cox Orange Pippin', which showed an increased content in suberin-distinctive monomers and precursors, such as very long chain ω-hydroxyacids and α,ω-diacids, or ferulic acid. In the present chapter, the growth kinetics of the 'Canada Gris' and 'Canada Blanc' cultivars provide new insights about the regulation of cuticle synthesis and suberin development. Indeed, during the early stages of the fruit growth of the 'Canada Gris' variety, it was unexpected to observe that genes involved in the cutin and the wax biosynthesis displayed a basal expression, which further decreased during the latest stages of the fruit growth. This decrease was

concomitant with the massive expansion of the fruit and the increased expression of suberin biosynthesis-related genes, suggesting that there might be a direct or indirect antagonist effect of the suberization process on the cuticle biosynthesis. The reason leading to this cuticle biosynthesis repression remains unclear, but we can speculate that there might be some regulatory elements, triggered by microcracking generated by the fruit growth, which have antagonistic effects on the cuticle development and the suberization process. However, we still do not have any proof of such mechanisms and further work should be performed to validate or reject these hypotheses.

Conversely, the 'Canada Blanc' variety showed a constant increased expression of the suberin biosynthetic genes during fruit growth reaching similar levels as those observed in 'Canada Gris' variety, whereas cutin and wax synthesis-related genes remained stably expressed at a relatively high level. This observation does not perfectly fit with conclusions drawn from 'Canada Gris'. However, this implies that russeting can also occur in varieties displaying a normal expression of cutin and wax biosynthesis genes and suggests that the impairment of cuticle biosynthesis observed in the russeted and semi-russeted cultivars might be a worsening factor whose effects go beyond that of the main cause of russeting. In both varieties, the initiation of russeting might be caused by environmental and/or developmental factors through the development of cuticle microcracking, which are more or less predominant depending on the cuticle development.

In our first transcriptomic study, the apple suberized cell wall seemed to undergo a strong modification of its structure as several genes implicated in the hemicellulose modification, which have been associated with cell wall loosening, were strongly upregulated in the russeted tissues. As the skin surface has to face extreme tensions due to fruit growth, we postulated that this enhancement of the cell wall-modifying genes might help to relax this tension. However, the present

work showed that the expression of genes involved in this cell wall modification is tightly correlated with the suberization process, suggesting that it might have a role in the suberin deposition. Additionally, genes involved in this cell wall modification have been previously associated with the lignification process. As the suberin polyphenolic domain of suberin shares a similar structure with lignin, we proposed that this process might also involve primary cell wall modification, *i.e.* the anchoring process of the suberin polyphenolic domain in the cell wall.

Finally, we focused in this chapter on the suberin-associated triterpenic acid, betulinic acid, and its conjugated form, the betulinic acid-3-trans-caffeate. We observed again that the suberin-associated triterpene contents were closely correlated with the russeting degree in both varieties, reinforcing the putative co-regulation of these pathways. However, the expression pattern of genes implicated in the suberin-associated pentacyclic triterpenes displayed a slight, distinctive difference at the latest time-point of the kinetics in 'Canada Gris', which allowed us to cluster suberin and their triterpene biosynthesis genes in two different groups. Interestingly, genes for some α/β-fold hydrolase, lipase and a MYB67 transcription factor present some correlations with the betulinic acid and the betulinic acid-3-trans-caffeate contents, suggesting that they may be implicated in their biosynthesis. In addition to this, *MYB93*, *MYB52* and *MYB36* seemed to be associated with the suberin synthesis.

As MYB93 presented a correlated expression with suberin biosynthetic genes and contents in all parts of our study, a functional validation of this transcription factor is described in the next chapter, to evaluate its putative role as regulator of the suberin deposition. For this, a transient expression of *MdMYB93* (MDP0000320772) was performed in *Nicotiana benthamiana* leaves, followed by a GC/MS analysis of the free and depolymerized fraction of the leaf extracts.

These data was matched to a gene expression profiling of the genes induced and repressed by this transcription factor.

Chapter III highlights:

Outcome:

- The decreased cuticle deposition can be considered as an worsening factor of suberin deposition.
- In 'Canada Gris', the enhanced expression of suberin biosynthetic genes seemed to inhibit the cutin and wax synthesis.
- The cell wall-modifying genes might be associated with the anchoring of suberin to the primary cell wall
- MYB67, some α/β-fold hydrolases, lipases have been identified as new candidate genes implicated in the biosynthesis of suberin-associated triterpenes.
- *MYB93* is a major candidate gene for the regulation of suberin biosynthesis.

Questions raised:

- Is there an antagonistic regulatory pathway between cuticle and suberin biosynthesis?
- Does MYB67 play a role in the suberin-associated triterpene synthesis?

Chapter IV: MdMyb93 is a regulator of suberin deposition in russeted apple fruit skins

---

Adapted from the published article:

Legay S, Guerriero G, André CM, Guignard C, Cocco E, Charton S, Boutry M, Rowland O, Hausman JF. 2016. MdMyb93 is a regulator of suberin deposition in russeted apple fruit skins. *New phytologist* Epub head of print.

Contributions:

S. Legay designed the experimental setup, performed the sampling and the laboratory work (cloning, transient expression in *N. benthamiana*, sample preparation, RNA extraction, library preparation, sequencing, U.V. microscopy and the bioinformatic work). He also performed the GC-MS metabolite identification. Finaly, he performed the statistical analysis and wrote the article.

Gea Guerriero participated in the transient expression work.

S. Charton and C. André performed the UPLC-triple TOF analysis.

E. Cocco performed the GC-MS data extraction. She also participated in the manuscript refinement.

C. Guignard supervised the analytical chemistry work.

M. Boutry, O. Rowland and J.-F. Hausman were involved in the manuscript refinement.

Abstract

A comparison of the transcriptomes of russeted vs. non-russeted apple skins previously highlighted a tight relationship between a gene encoding a MYB-type transcription factor, MdMYB93, and some key suberin biosynthetic genes. The present work assesses the role of this transcription factor in the suberization process. A phylogenetic analysis of MdMYB93 and *Arabidopsis thaliana* MYBs was performed and the function of MdMYB93 was further investigated using *Agrobacterium*-mediated transient expression in *Nicotiana benthamiana* leaves. An RNA-Seq analysis was performed to highlight the MdMYB93-regulated genes. UPLC-TripleTOF and GC-MS were used to investigate alterations in phenylpropanoid, soluble free lipid, and lipid polyester contents. A massive accumulation of suberin and its biosynthetic precursors in MdMYB93 agro-infiltrated leaves was accompanied by a remobilization of phenylpropanoids and an increased amount of lignin precursors. Gene expression profiling displayed a concomitant alteration of lipid and phenylpropanoid metabolism, cell wall development, and extracellular transport, with a large number of induced transcripts predicted to be involved in suberin deposition. The present work supports a major role of MdMYB93 in the regulation of suberin deposition in russeted apple skins, from the synthesis of monomeric precursors, their transport, polymerization, and final deposition as suberin in primary cell wall.

Keywords: Russeting, Suberin, *Malus* x *domestica*, *Nicotiana benthamiana*, MYB-family transcription factor, MYB93, Transcriptomics, Lipid metabolism

I. Introduction

Suberin deposition in apple fruit skins, also called russeting, is one of the most important trait defects leading to decreases in the commercial value of some apple varieties. Suberin is an insoluble biopolyester composed of poly-aliphatic (SPAD) and poly-phenolic (SPPD) domains (Bernards 2002). SPPD is a lignin-like polymer with higher amount of hydroxycinnamic acids, whereas SPAD is a bio-polyester based on glycerol and ferulic acid esterified with saturated and unsaturated ω-hydroxy fatty acids, α,ω-dicarboxylic acids, fatty alcohols, and alkanoic acids. Suberin deposition occurs on the inner part of the primary cell wall in a broad spectrum of tissues such as the subepidermal cells of apple fruit and tuber, the bark of trees, and the endodermis and periderm of roots, to name of few (Meyer 1944, Boher *et al*. 2013, Graca 2015). The suberin biosynthetic pathways have been studied in various plant models, such as *Arabidopsis thaliana* (Beisson *et al*. 2007, Franke and Schreiber 2007, Li and Beisson 2009, Beisson *et al*. 2012, Kosma *et al*. 2014) and *Solanum tuberosum* (Lulai and Corsini 1998, Graca and Pereira 2000, Serra *et al*. 2009, 2010, Boher *et al*. 2013). A large number of genes involved in the synthesis of suberin have been identified, ranging from those involved in the upstream lipid and phenylpropanoid metabolic pathways to the more suberin-specific genes, such as those encoding fatty acyl reductases, fatty acid hydroxylases, glycerol-3-phosphate acyltransferases, and feruloyl-CoA transferases (Vishwanath *et al*. 2015). However, despite these important advancements, many aspects of suberin biosynthesis remain undetermined. This is particularly the case for the process leading to the final polymerization of suberin, as well as for the regulatory mechanisms governing suberin deposition developmentally (*e.g*. in fruit epidermis) or in response to stress.

The regulation of suberin deposition on the surface of tree fruit is complex as it appears to be triggered by multiple causes. Previous studies have highlighted that

environmental stresses, such as extended rainfalls periods extreme temperatures, or the application of agrochemicals can promote the appearance of the russeted phenotype, especially at early stages of fruit development (Faust and Shear 1972, Skene 1982, Khanal *et al*. 2013). Among these, the duration of skin surface wetness seemed to be a critical factor leading to skin spot and russeting in apple (Winkler *et al*. 2014, Tukey 1969). These developmental factors have been linked to the deposition and integrity of the fruit cuticle and the occurrence of suberization. Indeed, during the early state of fruit development, the extreme tension occurring at the surface of the periderm may lead to microcracking in the cuticle layer and promote suberization. For example, in *Malus* x *domestica* cv. Golden Delicious, a decrease in epidermal cell surface tension occurring after gibberellic acid ($GA_{4+7)}$ application leads to less microcracking of the cuticle and a significant decrease of the russeting phenotype (Knoche and Khanal 2011, Curry 2012). Furthermore, in fully russeted apple varieties, which consistently present a suberized phenotype at an early stage of fruit growth, the expression levels of cuticle biosynthetic genes (cutin and wax) are significantly lower compared to non-russeted commercial apples such as 'Gala' (Legay *et al*. 2015). This decreased expression is accompanied by an enhanced expression of genes implicated in suberin biosynthesis, stress signaling, and cell wall modification (Legay *et al*. 2015). In *M*. x *domestica*, a recent study showed that enhanced expression of the MdSHN3 transcription factor increased cuticle deposition and prevented apples from russeting. However, the downstream gene regulatory network governing suberin deposition is still under investigation (Lashbrooke *et al*. 2015). Recently, a MYB family transcription factor, AtMYB41, was found to be a major regulator of suberin deposition in *A. thaliana* roots under stress conditions (Kosma *et al*. 2014). Whereas this transcriptional regulator was shown to be specifically expressed under abiotic stress conditions in *A. thaliana*, no

significant differential expression of its predicted *Malus* x *domestica* ortholog was observed between russeted and non-russeted apple varieties (Legay *et al*. 2015), suggesting that additional transcription regulators more related to a developmental process participate in suberin deposition in russeted apple fruit. Indeed, in our gene expression profiling studies we observed a contig presenting sequence similarities with *Arabidopsis* MYB93 (*AtMYB93*) that was significantly enhanced in the suberized (russeted) skin. The expression of this contig was closely correlated with some key suberin biosynthetic genes (cytochrome P450 (CYP) 86A1, Glycerol-3-phosphate acyltransferase 5 (GPAT5) and CYP86B1). In *A. thaliana* roots, *AtMYB93* is specifically expressed in endodermal cells and negatively regulates lateral root development (Gibbs and Coates 2014, Gibbs *et al*. 2014). However, no indication of a putative involvement of AtMYB93 in suberization process has yet been shown.

In the present paper, we demonstrate using transient expression in *Nicotiana benthamiana* leaves combined with transcriptomics and analytical chemical profiling, that the predicted apple ortholog of AtMYB93, MDP0000320772 (MdMYB93), is able to orchestrate the synthesis and organization of suberin.

II. Material and methods

A. RNA extraction and reverse transcription

A total RNA extract was obtained from semi-russeted *Malus* x *domestica* cv. 'Cox Orange Pippin' as described previously (Legay *et al*. 2015). For the *Nicotiana benthamiana* leaves total RNA extracts from four biological replicates were used for each group (35S::MdMYB93/p19 (overexpression) and p19 alone (control)). Each biological replicate was comprised of a pool of six plants with four agoinfiltrated leaves per plant. Total RNA extracts were obtained using the

RNeasy plant mini kit (QIAGEN, Leusden, The Netherlands) coupled with the on-column DNase I treatment, following the manufacturer's guidelines. Total RNA integrity (RIN>8) was assessed using a 2100 Bioanalyzer (Agilent Technologies, Santa Clara, CA, USA). RNA purity was assessed using a Nanodrop ND1000 spectrophotometer (Thermo scientific, Villebon-sur-Yvette, France). Total RNA was quantified using a Qubit RNA assay kit (Life technologies, Carlsbad, CA, USA).

B. Gene isolation and cloning

The MDP0000320772 contig was isolated from a cDNA library made from RNA extracted from *M*. x *domestica* cv. 'Cox Orange Pippin'. The following primers were used: Forward(F) 5'-CACCATGGGAAGATCTCCTT-3' and Reverse(R) 5'-AGCAATCTCATTGGAAAAAGG-3'. Amplification was carried out using the Q5 High Fidelity 2X Master Mix (New England Biolabs, Ipswich, MA, USA) following the manufacturer's instructions (Tm=60°C). The PCR product was purified using the QIAquick PCR purification Kit (QIAGEN) and cloned into pENTR/D-TOPO. *E. coli* TOP10 competent cells were transformed and grown on LB/kanamycin plate according to manufacturer guidelines (Thermo scientific). The plasmid was extracted using the QIAprep Spin Miniprep Kit (QIAGEN, Leusden, The Netherlands) and insert was sequenced. The LR clonase cloning protocol (Thermo scientific) was used with the pENTR/D-TOPO and pEarleyGate103(p103) vectors to obtain a MDP0000320772-GFP fusion driven by the CaMV35S promoter (Earley *et al*. 2006).

C. Infiltration by *Agrobacterium tumefaciens*

The two *Agrobacterium tumefaciens* GV3101-pMP90 strains (p103::MDP0000320772 and pBIN61-p19) were grown in 50 mL of LB liquid medium supplemented with gentamycin (30 mg/L), rifampicin (10 mg/L),

kanamycin (50 mg/L), and acetosyringone (30 mg/L). The cultures in 100 mL Erlenmeyer flasks were agitated at 130 rpm/28°C for 48 h. After centrifugation (1000 *g*/10 min), cultures were re-suspended in 20 mM MES, 20 mM $MgSO_4$ infiltration buffer supplemented with 150 mg/L acetosyringone. After 2 hours, p103::MDP0000320772 and pBIN61-p19 *A. tumefaciens* cultures were adjusted to OD_{600}=0.8 and 1, respectively. Three weeks-old *N. benthamiana* plants were used for the transient expression study. Plants were divided into two groups, p103::MDP0000320772/pBIN61-p19 and pBIN61-P19(control), each with four biological replicates constituted by a pool of six plants. For each plant, the four first leaves were infiltrated with 0.5 mL infiltration buffer using a 1 mL needleless syringe. After six days, the leaves were collected and flash frozen in liquid nitrogen.

D. Library preparation and sequencing

cDNA libraries were prepared from 10 ng mRNA using the SMARTer Stranded RNA-Seq kit according to the manufacturer's guidelines (ClonTech laboratories, Mountain View, CA, USA). Libraries were analyzed and quantified as described in Legay *et al*. 2015. The pooled libraries were sequenced on an Illumina MiSeq using five consecutive runs (Illumina MiSeq reagent V3-150 cycles) to generate 76 base-pairs paired-end reads. Raw sequences have been deposited at the NCBI Gene Expression Omnibus website (GEO, http://www.ncbi.nlm.nih.gov/geo, accession number: GSE83618).

FASTQ files were imported in CLC genomics workbench v8.0.1 discarding poor quality reads (<Q30). For each library, reads were trimmed and filtered using the following criteria: sequence quality <0.01, no ambiguous nucleotides, minimum read length >35 nucleotides, trimming against the Illumina adaptor sequence, and finally a hard trim of 10 nucleotides at the 5' end and 2 nucleotides at the 3' end. The filtered reads were mapped to the *N. benthamiana*

transcriptome v5-primary transcript (Nakasugi *et al*. 2014) obtained from the *N. benthamiana* genome and transcriptome website (http://benthgenome.qut.edu.au/) with the following criteria: a mismatch, gap and insertion cost on the maximum settings (stringent mapping), mapped reads having more than five hits were removed, reads should have 80% identity and 50% coverage to the reference transcriptome. The remaining unmapped reads were then re-mapped against the transcriptome v5-alternate transcripts following the same criteria. An additional annotation of the transcriptome was performed against the *A. thaliana* database using BLAST2GO Pro v3.0. Expression values were calculated using the RPKM (Reads per kilobase transcript per million reads) method (Mortazavi *et al*. 2008). Differentially expressed genes between the tobacco leaves infiltrated with *A. tumefaciens* GV3101 (pMP90, P103::MDP0000320772) and control were statistically determined using a Baggerley's 'on proportions' weighted test (Baggerly *et al*. 2003), a false discovery rate corrected *p*-value (Benjamini-Hotchberg correction) was set at 0.01, a fold-change cut-off value set at 10-fold increase or decrease in expression, and a minimum mean RPKM difference between both groups set at 10. The gene ontology enrichment analysis was performed from the significantly regulated genes in Cytoscape (v3.1.0) with the ClueGO v2.1.1 and CluePedia v1.1.1 plugins (Bindea *et al*. 2009, Bindea *et al*. 2013) to highlight regulated biological processes following these criteria: gene ontology from level 3 to level 8, kappa score set at 0.2. A functional association network was performed using STRING with default settings (http://string-db.org) from the TAIR code obtained from the significantly up-regulated genes. RT-qPCR validation details and protocols are described in the supporting Information Table 5-1.

E. Targeted gene expression analysis using RT-qPCR

Four biological replicates of leaves expressing MdMYB93 and control leaves (p19) were analyzed on a subset of height representative genes and two primer couples targeting the transiently expressed MdMY93 using RT-qPCR. Reverse transcription was carried out using the M-MuLV Reverse Transcriptase (RNase H-), the Murine RNase Inhibitor (New England Biolabs, Ipswich, MA, USA) and random primers (Invitrogen, Carlsbad, NM, USA) following the manufacturers' instructions. qPCR primers were designed using the Primer3 software (http://frodo.wi.mit.edu/) with the following criteria: primer size between 18 and 25 base pairs, GC content between 30 and 70%, amplicon size from 80 to 200 base pairs, primer annealing temperatures in the 57-61°C range. Matching primer sets were checked using NetPrimer (http://www.premierbiosoft.com/netprimer/index.html) for unexpected secondary structures. In order to test the specificity of the primers, a BLAST search against the *N. benthamiana* transcriptome v5 and the NCBI *Viridiplantae* Non redundant database was carried out. qPCR runs were carried out, using three technical triplicates on a Viia7 384-well real-time PCR instrument (Thermo Fisher, Waltham, MA, USA) with Takyon SYBR Green low ROX (Eurogentec, Liège, Belgium) following the manufacturer's guidelines. Experiments were carried out following the MIQE guidelines (Bustin *et al*. 2009) and a melting curve was performed at the end of all the runs to assess the specificity of the primers. The normalized relative expression of genes was calculated using Biogazelle qbase+ V3.0, taking into account multiple reference gene normalization and specific PCR efficiencies (Table 5-1). The geNorm^{PLUS} tool described the Uridylate kinase (UK) and the Sand family protein (SAND) genes as the most suitable for optimal normalization of the data. A Mann-Whitney statistical analysis of the normalized

Table 5-1: Primer data: for each investigated gene, primer sequences, accession, amplicon size, melting temperature (Tm in °C) and references are displayed

Name	Gene Name	Accession	Sens	Sequence	Amplicon size	Tm	Reference
NB_GPAT5	Glycerol-3-phosphate acyltransferase 5	Nbv5tr6232718	F	TCATGCAACAACAGCTAGGG	113	80.5	
			R	ACGTGGCTTCTACTGGCAAC			
NB_CYP86A1	Fatty acid omega-hydroxylase	Nbv5tr6408715	F	GGAGCGTCATGAACAATCG	188	81	
			R	AGGGACCGAAGGGTACAGAC			
NB_FCoAT	Feruloyl-CoA Acyl transferase	Nbv5tr6212895	F	TTCATGGCAAATGAGAGCTG	159	81	
			R	TGTGGCTTTGCCAGAGAAG			
NB_FAR3_1	Fatty acid reductase	Nbv5tr6203423	F	CTGACGATCCGACCTGGTAT	122	81	
			R	CGACCCTAAAGCCGTTATTG			
NB_FAR3_2	Fatty acid reductase	Nbv5tr6203422	F	TACCTTCAACCCAACCAGGA	149	79.5	
			R	TTATGGATGGCCAAACACCT			
NB_KCS2	3-ketoacyl-CoA synthase 2	Nbv5tr6245119	F	CCAATTTCATCCATCCAAGG	101	78.5	
			R	ATTGCATTTGGCTCAGGATT			
NB_GDSL esterase/lipase	GDSL esterase/lipase	Nbv5tr6216569	F	TTTGCACATGTTCCTGGAGA	119	81.5	
			R	TTGTCACTCACCCAGCTGAT			
NB_GDSL esterase/lipase	GDSL esterase/lipase	Nbv5tr6222730	F	CAACGGATGATGTTGGACAG	145	78	
			R	AGTCGCCCATGTTCTGAATC			
MdMYB93	Myb family transcription factor 93	MDP0000320772	F	TATCCAACACCACCAAGCAA	145	80.5	Legay et al. 2015
			R	CCACCGAAGTAGGAGATGGA			
GFP	Green fluorescent protein		F	CAACTTCAAGACCCGCCACA	102	83	Leckie and Stewart 2011
			R	TCTGGTAAAAGGACAGGGCCA			
UK	Uridylate kinase	EH363935	F	CTAGGAGTATATTGGAAGAGCG	107	79	Liu et al. 2012
			R	AAAGATACATCGCCTTGCTGAA			
TUB	b-Tubulin	EH371301	F	CAAGATGCTACTGCAGACGAG	126	79	Liu et al. 2012
			R	CTGGAAGTTGTGGTTTTGGC			
SAND	Sand family protein	Niben.v0.3.Ctg25188435	F	ACCACCAACACCTATGAATGCT	83	80	Liu et al. 2012
			R	CAGTCTCGCCTCATCTGGGTCA			

relative quantities was performed using Qbase^{PLUS} v3.0 (Vandesompele *et al*. 2002).

F. Suberin depolymerization and free fatty acid analysis

Extraction and transesterification

Frozen leaves samples (500 mg) of were freeze-dried for 24 h in a 2 mL Eppendorf tube. Dried samples were then ground in a bead shaker for 5 min at 25 Hz with two 4.5 mm steel beads. To extract the merged cytosolic and suberin-associated soluble lipid fraction, three consecutive extractions were performed with 1 mL dichloromethane by shaking at 25 Hz for 10 min. The extracts were then evaporated in a SpeedVac and recovered in 1 mL dichloromethane. The remaining material was then oven-dried for 48 hours at 35°C. Suberin depolymerization was performed according to the protocol described by Franke *et al*. (2005). Six mL of boron trifluoride methanolic solution (10% BF_3/MeOH, Sigma Aldrich) was added to 20 mg of powder in a glass tube sealed with a Teflon cap. After 16 h at 70°C, the transesterification reaction was stopped using 10 mL aqueous $NaHCO_3$ saturated solution. An internal standard *i.e*. nonadecanoic acid (1 μg) was added to the solution. The methylesters were then extracted three times (3 mL dichloromethane, 25 Hz for 10 min), evaporated, and recovered in 1mL dichloromethane. A 200 μL aliquot of the soluble lipid and suberin depolymerization extracts in dichloromethane were placed in GC-MS vials and dried under gentle nitrogen flow, then 50 μL of a Bis-Trimethylsilyl-trifluoroacetamide: Trimethylchlorosilane mixture (BSTFA:TMCS 99:1) was added. The reaction was carried out for 60 min at 60 °C, then the derivatized extract was directly analyzed by GC-MS.

GC-MS Analysis

The identification and quantification of derivatized compounds in both extracts were achieved on an Agilent 7890B/5977A GC-MS coupled to a Gerstel

Multipurpose Sampler. The injection was performed at 280°C in splitless mode (1 μL). The carrier gas was He at a constant flow of 1.2 mL/min. The column was an Agilent HP5-MS (30 m x 0.25 mm i.d. x 0.25 μm film thickness) and the oven temperature was programmed as follows: 80°C (2 min) to 210°C (8°C/min), then 280°C (3°C/min) and 320°C (15°C/min, 15 min isotherm). The MS transfer line was kept at 280°C. MS spectra were recorded in Full-Scan mode between 50 and 900 amu. The identification of compounds in the soluble lipid and suberin polyester fractions and the determination of their relative peak areas were performed using the Agilent MassHunter Software suite.

G. Phenylpropanoid analysis

Extraction

Leaf tissue sample (100 mg) from pooled material (three leaves) was homogenized in liquid nitrogen and extracted with 1 mL of methanol:water (4:1, v/v). This mixture was then vortexed for 30 s, sonicated for 10 min, and shaken for 4 h at room temperature. After centrifugation at 10,000 *g* for 15 min, the supernatant was collected and evaporated to dryness using a centrifugal vacuum evaporator. Dried *N. benthamiana* extracts were made up in 600 μL of ethanol:water (1:1, v/v) and filtered through a syringe filter (0.2 μm, PTFE Millex-LG (Merck KGaA, Darmstadt, Germany).

UPLC-TripleTOF Analysis

Extracts were analyzed with a Waters Acquity UPLC system (Milford, MA) hyphenated to a high-resolution time-of-flight mass spectrometer (TripleTOF 5600+, AB Sciex, Concord, Ontario, Canada). The separation of the 5 μL aliquot was performed on a reverse-phase Acquity UPLC BEH C18 column (2.1 × 100 mm, 1.7 µm particle size, Waters). In positive mode, the eluents were 0.1% formic acid in water (A) and 0.1% formic acid in acetonitrile (B). In negative mode, the

solvents were (A) H_2O with 2.5 mM (v/w) ammonium acetate and (B) acetonitrile. The gradient was as follows: 0 min, 1% B; 4 min, 1% B; 16 min, 5% B; 35 min, 40% B; 45 min, 100% B; 50 min, 100% B; 53 min, 1% B; 60 min, 1% B. The flow rate was of 0.5 mL min^{-1} and the column temperature was 50 °C. Analyses were positively ionized with electrospray ionization (ESI) source using the following parameter values for the positive and negative mode: source temperature of 650°C, ion spray voltage of 4.5 and – 4.5 kV, respectively, curtain gas (nitrogen) of 30, nebulizer gas (air) of 55, and turbine gas (air) of 50. Precursor charge state selection was set at 1. For information-dependent acquisition (IDA in high sensitivity mode), survey scans were acquired in 175 ms and the 10 most abundant product ion scans were collected if exceeding a threshold of 100 count per second. The total cycle time was fixed at 2.25 s. Four time bins were summed for each scan at a pulser frequency value of 16.4 kHz. A sweeping collision energy setting of 15 eV in positive and – 15 eV in negative mode, and was applied to all precursor ions for collision-induced dissociation. The declustering potential was set at 60 eV and – 60 eV in positive and negative mode, respectively. Dynamic exclusion was set for 8 s after two occurrences, and then the precursor was refreshed of the exclusion list. For MS1, full HR-MS spectra between 100 and 1300 mass-to-charge ratio (m/z) were recorded. MS2 scans were recorded between 25 and 1300 m/z.

Data Processing

Data were first processed with MS Data Converter (Beta v1.3, AB SCIEX, Concord, Ontario, Canada). The software converts the raw data (*.wiff) into peak lists (*.mzML). The Proteowizard software (v3.0, Chambers *et al*. 2012) was then used to transform the files into *.mzXML. The *.mzXML files (containing MS1 data only) were processed using XCMS online (https://xcmsonline.scripps.edu/)

for feature detection, alignment, and statistical analysis to highlight metabolites of interest. The software PeakView (v 1.2 0.3, AB SCIEX, Concord, Ontario, Canada) combined with the Metlin (https://metlin.scripps.edu/index.php) and PubChem database (https://pubchem.ncbi.nlm.nih.gov) as well as literature data were used for structure elucidation.

III. Results

A. The MDP0000320772 contig is orthologous to the *Arabidopsis thaliana* AtMYB93 transcription factor

MDP0000320772 was aligned with 126 *A. thaliana* MYB transcription factors (http://planttfdb.cbi.pku.edu.cn/, http://www.ncbi.nlm.nih.gov/). Additional differentially expressed russeting-related MYB-domain transcription factors, identified in our previous work, were also included (Legay *et al*. 2015, Fig. 1). Sequence alignments were performed using MUSCLE, which computes distances based on the full length protein sequence (Fig. 5-1). MDP0000320772 clustered close to MDP0000228252 and AtMYB93 into a larger clade, which includes the stress inducible suberin transcriptional regulator AtMYB41 (Fig. 5-1). The close similarity between MDP0000320772 and MDP0000228252, located on linkage groups 15 and 2, respectively, might be explained by an ancestral genome duplication, which occurred in the *Pyreae* ancestor genome, leading to high redundancy in gene functions (Velasco *et al*. 2010, Legay *et al*. 2015). Interestingly, MDP0000197283, which was annotated as a MYB102-like transcription factor, is grouped with the stress responsive suberin regulator AtMYB41 (Kosma *et al*. 2014). A deeper investigation revealed than the N-terminal region of MDP0000320772 (1-150 amino acids) is conserved compared to AtMYB93 with 86% identity, whereas the C-terminal region (150-

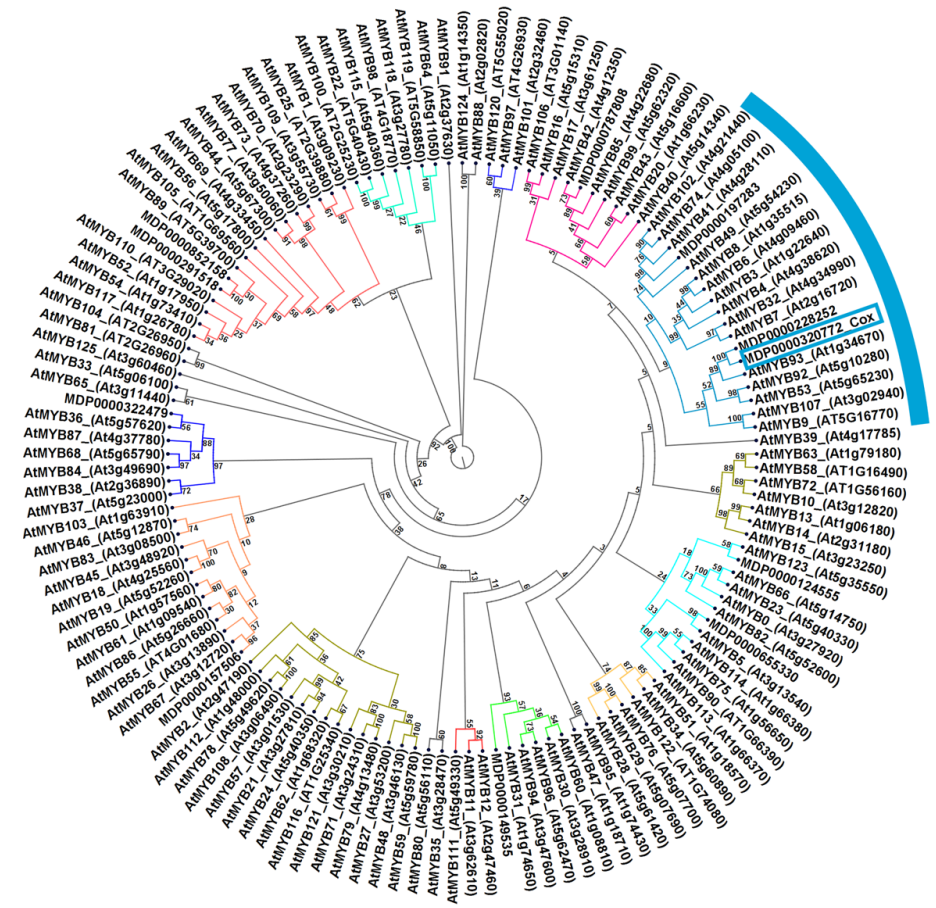

Figure 5-1: Phylogenetic analysis of the apple MYB transcription factors, namely MDP0000320772, MDP0000228252, MDP0000787808, MDP0000655330, MDP0000291518, MDP0000852158, MDP0000291518, MDP0000124555, MDP0000157506, MDP0000322479, MDP0000149535 and MDP0000197283, that were differentially regulated between russeted and non-russeted apple skins. The predicted amino acid sequences of these genes were compared to the 126 MYB transcription sequences identified in *A. thaliana* using the MUSCLE tool. The cladogram was generated using UGMA algorithm from Jukes-Cantor based distances bootstrapped with 1000 replicates in CLC genomics main workbench v7.0.2. Branch supported values are represented on each dichotomy. The clade containing the MdMYB93, AtMYB93 and AtMYB41 is highlighted in blue.

280 amino acids) displayed a low identity (30%).

The protein sequence analysis and modeling, performed using the Phyre2 web portal for protein modelling, revealed that the C-terminal region is predicted to be an intrinsically disordered region in both *A. thaliana* MYB93 and MDP0000320772, although they share low similarity (Fig. 5-2).

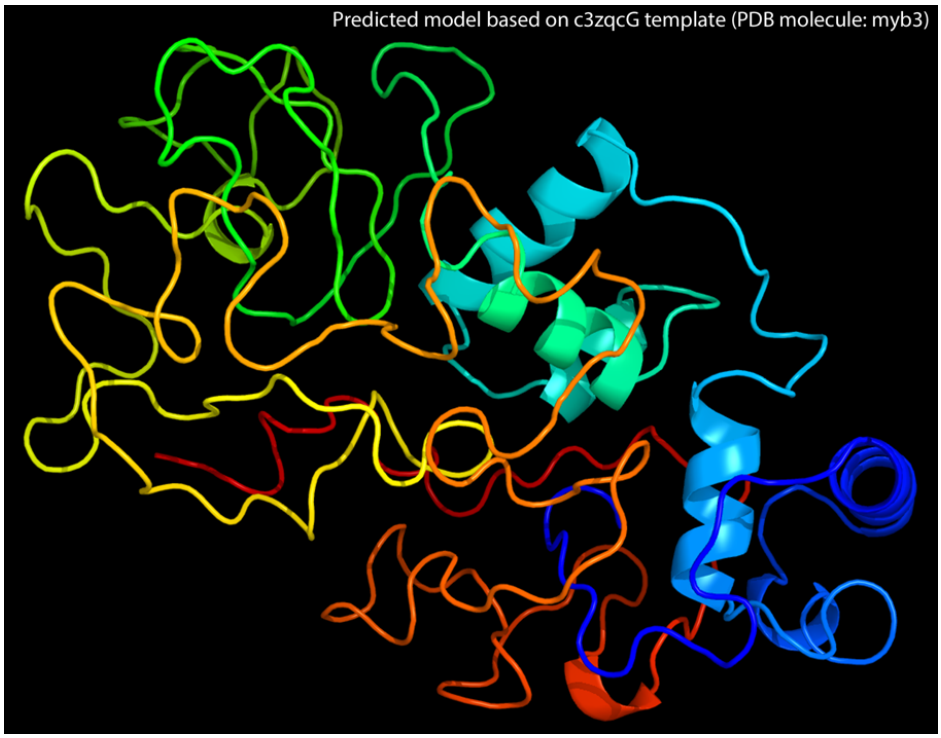

Figure 5-2: Phyre2 protein modeling of MdMYB93. The Model (myb3: c3ZqcG, Confidence index: 100, protein identity: 42%) obtained from the MdMYB93 (MDP0000320772) using Phyre2 displayed an intrinsically disordered region on the C-terminal region (on the left side) and the two SANT domains on the N-terminal region (on the right side).

B. Whole gene expression profiling of the MDP0000320772-regulated genes in *Nicotiana benthamiana*

In order to validate the role of MDP0000320772 (MdMYB93) in the apple russeting and, by extension, in the suberin deposition, we expressed MdMYB93 in *N. benthamiana* and performed a whole gene expression profiling using RNA-Seq. A total of 204 359 302 paired-end reads were generated with about 21 to 30 million reads per library. After trimming and filtering, each library was mapped against the primary transcripts of the *N. benthamiana* transcriptome assembly v5 with about 75% of successfully mapped reads. Three hundred and seventy-four differentially expressed genes, with about 80% being up-regulated, were found in leaves overexpressing MdMYB93 versus that of control (P19) with high redundancy in the functions (Supporting information (SI) Table 5-1). RT-qPCR validation was performed on a subset of genes previously described (*FAR*, *KCS2*, *CYP86A1*, *CYP86B1*, *ASFT*, *GPAT5*, Vishwanath *et al*. 2015) or suspected (GDSL-motif esterase/lipase, Legay *et al*. 2015) to be involved in the suberin biosynthesis. These displayed similar results with a strong increased expression of MdMYB93 and genes which are known or suspected to be involved in the suberin biosynthesis (Fig. 5-3, SI Table 5-2).

The gene ontology enrichment analysis using ClueGO/CluePedia, based on the orthologous genes found in *A. thaliana*, showed that *MdMYB93* overexpression altered the expression of several metabolic processes including lipid and phenylpropanoid biosynthetic pathways, xylan metabolism, and suberin biosynthesis (Fig. 5-4). In addition to this, the expression of some downstream transcription factors was also enhanced (Table 5-2).

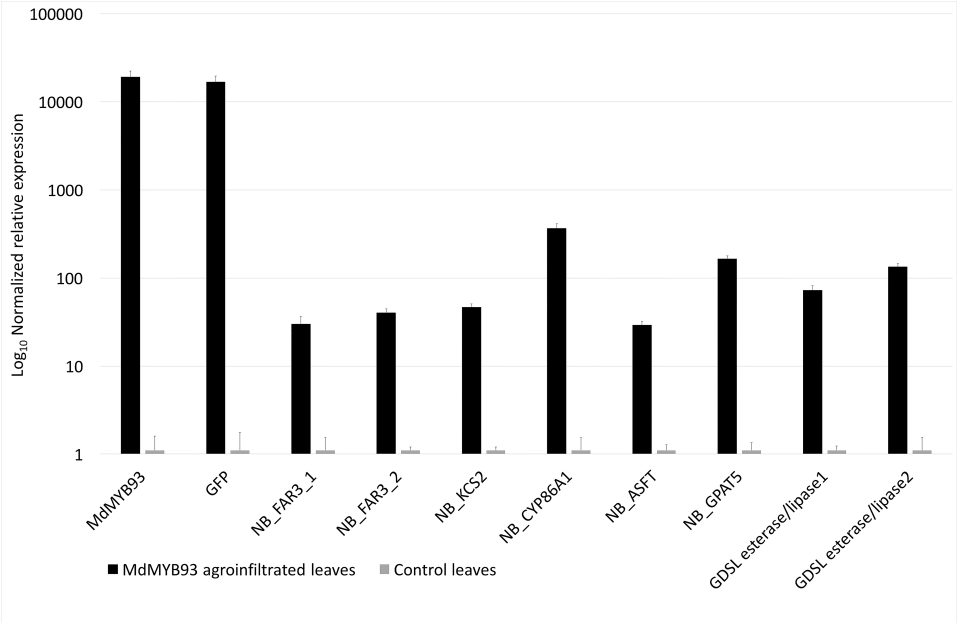

Figure 5-3: RTqPCR validation of transient expression of MdMYB93 in *N. benthamiana*. Normalized relative expression of MdMYB93/GFP, glycerol phosphate acyl transferase 5 (NB_GPAT5, Nbv5tr6232718), fatty acid hydroxylase (NB_CYP86A1, Nbv5tr6408715), feruloyl-CoA-Acyl transferase (NB_ASFT, Nbv5tr6212895), two fatty acyl reductases (FAR3_1 (Nbv5tr6203423) and FAR3_2 (Nbv5tr6203422)), 3-ketoacyl-CoA synthase 2 (KCS2, Nbv5tr6245119), and GDSL-esterase/lipase1 and two *N. benthamiana* orthologs of MDP0000174332 and MDP0000660239 respectively (Nbv5tr6216569, Nbv5tr6222730). Each gene was normalized using a SAND family and a uridylate kinase genes as reference genes. In the control condition (leaves agroinfiltrated with p19 only), the relative quantities of MdMYB93 and the GFP transcripts were calculated from the detection limits (35 cycles). The error bars display the standard deviation calculated from four biological replicates in each group. Normalized expression results for each gene were tested using a Mann-Whitney test in qbase^{PLUS} v.3.0 and all displayed significant differences (p-value < 0,05).

A large part of the MdMYB93 responsive genes are implicated in lipid metabolism. Among them, 3-ketoacyl-CoA synthase (KCS) genes, *KCS1*, *KCS2* and *KCS4*, were highly expressed (Fig. 5-3, Table 5-2). The KCS proteins are part of the fatty acid elongation complex (FAE) producing very-long-chain fatty acids, which are further used for suberin monomer synthesis (Vishwanath *et al*. 2015). Genes encoding a long-chain fatty acid ω-hydroxylase (*CYP86A1*) and a very long-chain fatty acid ω-hydroxylase (*CYP86B1*) were also strongly upregulated (Fig. 5-3, Table 5-2). *CYP86A1* displayed, as observed in the RT-qPCR validation, the highest expression rate and fold change in the present data. Additional genes encoding cytochrome P450 enzymes, *CYP86A8* and *CYP94C1*, which have a fatty acid hydroxylase function in the cutin biosynthesis pathway (Wellesen *et al*., 2001), were also induced (Table 5-2). These two genes displayed tight associations with some suberin biosynthetic genes, suggesting they are involved together in common biological processes (Fig. 5-5), and may also participate in the fatty acid hydroxylation process concomitantly with CYP86A1. Interestingly, a *LACS4-like* (long chain acyl-CoA-synthetase) gene was strongly up-regulated in response to MdMYB93 expression. LACSs are responsible for the CoA-activation of α,ω-dicarboxylic and ω-hydroxy fatty acids and have been linked with the cutin synthesis, but not yet with suberin synthesis (Vishwanath *et al*. 2015). Genes encoding GPAT5 and ASFT (RWP1), also showed an increased gene expression (Table 5-2). GPAT5 has been tightly linked with suberin deposition in *A. thaliana* roots and seeds (Beisson *et al*. 2007) and its predicted ortholog is also strongly expressed in the russeted apple skins (Legay *et al*. 2015). Interestingly, a *GPAT6*-like gene, which has been linked to cutin synthesis, was also induced in MdMYB93 agroinfiltrated leaves, whereas only weak expression was detected in the control leaves. The expression of other *GPAT* genes annotated in the transcriptome remained stable at a low level. Four α/β-fold protein

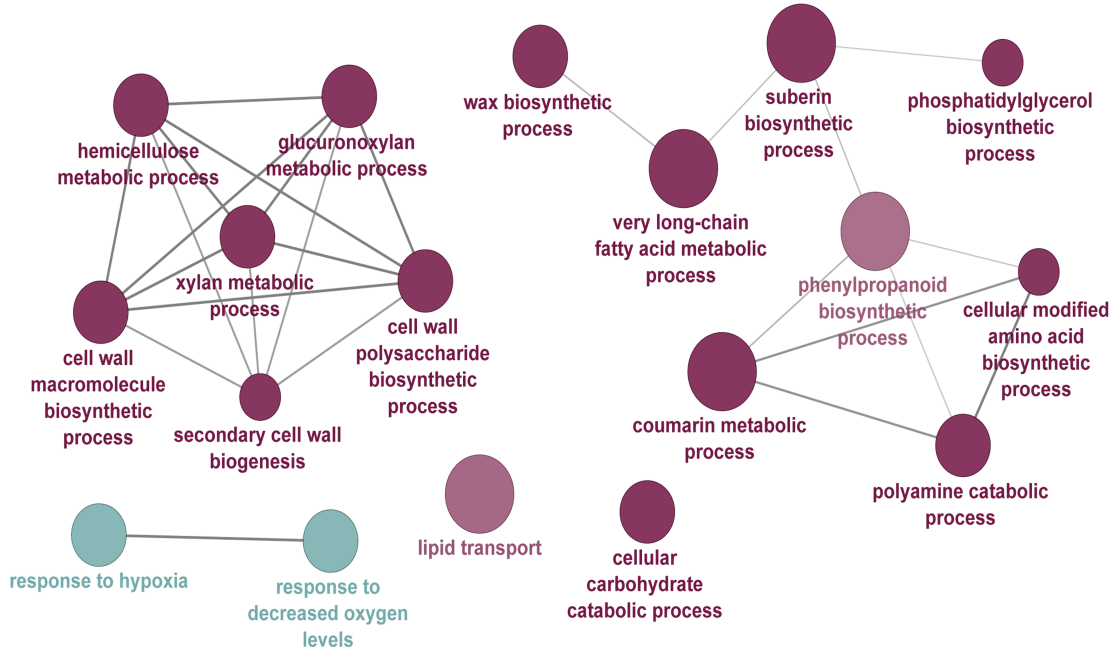

Figure 5-4: Gene ontology enrichment analysis of the MdMYB93 responsive biological processes. The network was generated using cytoscape and the ClueGO/CluePedia plugins performed from the differential expressed genes in *N. benthamiana* leaves. GO term tree interval was set between 3 and 8, Kappa score at 0.2. The gene ontology was based on the *A. thaliana* orthologous genes of the differentially expressed genes (-10 > fold change > 10, FDR corrected p-Value < 0.01, mean group RPKM difference > 10). In red, the up-regulated biological processes; in blue, the down-regulated biological processes.

hydrolase genes, which displayed significantly increased expression in leaves overexpressing *MdMYB93*, are associated with the suberin synthesis cluster (*GPAT5*, *CYP86A1* or *CYP86B1*, Fig. 5-5). The expression of alcohol-forming fatty acyl-CoA reductase-like genes, which are responsible for the synthesis of primary fatty alcohols, another important component of suberin (Domergue *et al*. 2010, Vishwanath *et al*., 2013), were also enhanced in our dataset. In addition to the suberin gene cluster, a number of genes encoding GDSL-esterase/lipases were also induced, including those targeted in the RT-qPCR experiment (Fig. 5-3). Finally, the expression of genes involved in the phenylpropanoid pathway was also altered in response to *MdMYB93* expression, such as phenylalanine ammonia lyase (*PAL*), 4-coumarate-CoA ligase (*4CL*), cinnamyl-alcohol dehydrogenase (*CAD*), and some *O*-methyltransferases (Table 5-2).

Sterol metabolism was also altered by *MdMYB93* expression (Table 5-2). Expression of geranylgeranyl pyrophosphate synthase and *SMT1* (cycloartenol-C24-methyltransferase) were enhanced, whereas some sesquiterpene-synthase-like genes were down-regulated. The geranylgeranyl pyrophosphate synthase is a major actor of terpenoid synthesis, which leads to the synthesis of squalene, whereas SMT1 modulates the conversion of cycloartenol into C24 methyl sterol in *N. tabacum* (Schaeffer *et al*. 2000). The *SMT1* gene was already associated with *CYP86A1*, *CYP86B1* and *CYP86A8* (Fig. 5-5), suggesting a potential linked with the suberin biosynthetic pathway. Together with the enhancement of the suberin biosynthetic pathway, the expression of a large number of transmembrane transporters was also enhanced. A large part of these transporters belong to the ATP binding Cassette subfamily G (ABCG) half-transporter family (Table 5-2, Fig. 5-5). Among them are homologs of ABCG1, which has been found to be involved in the export of suberin components in potato

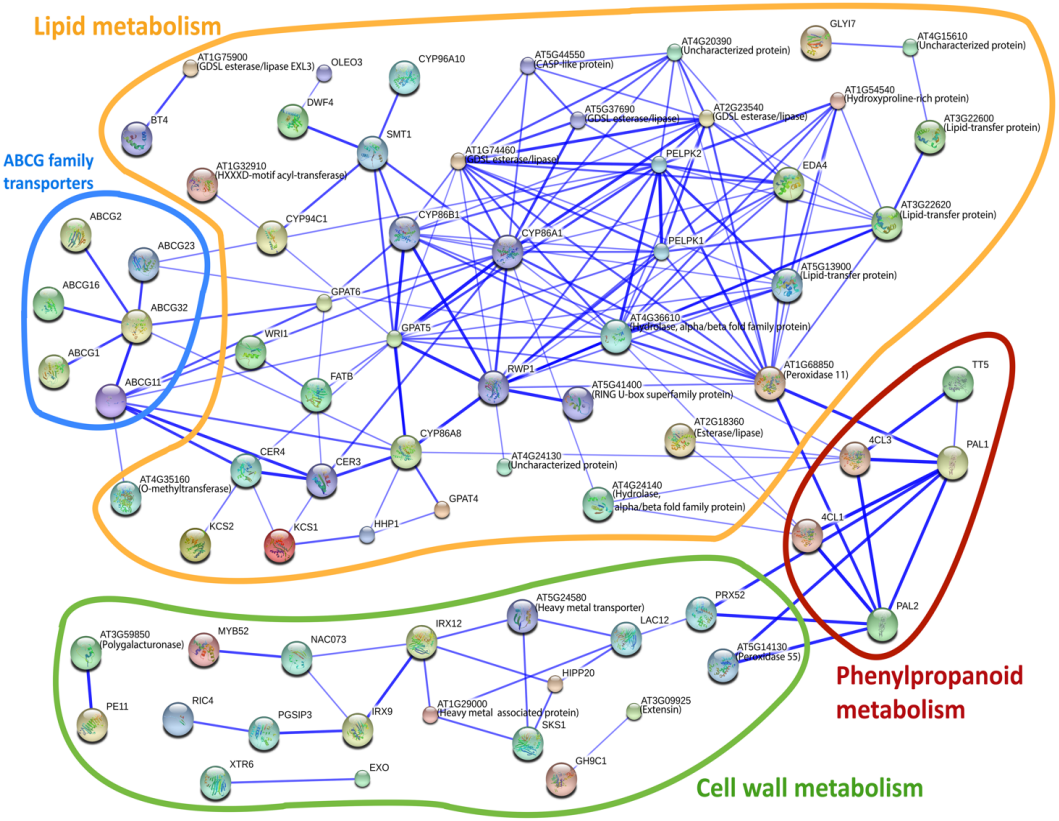

Figure 5-5 : see legend on the next page

Figure 5-5: Co-expression matrix performed using STRING from the significantly MdMYB93 up-regulated genes in *N. benthamiana*. Blue lines display the confidence of associations between two genes, which shared a role in some biological processes. The thickness of the line corresponds to the significance of the interaction with a minimum cut-off value of 0.4. Genes that displayed lower than this cut-off value are not represented. Colored nodes do not display any biological meanings.

(Landgraf *et al*. 2014), and ABCG2, which participates in suberin deposition in roots and seed coats of *A. thaliana* (Yadav *et al*. 2014). Interestingly, two *ABCG11*-like genes were also differentially expressed in response to *MdMYB93* expression, with one up-regulated and one down-regulated (Table 5-2). A significant number of lipid transfer proteins (LTP), such as a *LTP4*-like, lipid transfer protein *VAS*-like, and some seed storage lipid transfer proteins notably displayed high fold changes (Table 5-2).

MdMYB93 also triggered the expression of a significant number of genes involved in cell wall development. Specifically, pectin metabolism was altered with an enhanced expression of some pectin lyase and pectinesterase encoding genes (Table 5-2). Laccases and class III peroxidases were described or suggested to be major actors of the oxidative polymerization of lignin and suberin (Zhao *et al*. 2013, Bernards 2002). Notably, in the present data, genes encoding a peroxidase 11-like (PRX11) and a laccase 12-like (LAC12) proteins presented high expression with increased fold changes above 200. PRX11 showed some interactions with the phenylpropanoid and suberin biosynthetic pathways, whereas LAC12 seems to be more cell wall-related (Fig. 5-5). Expression of hemicellulose modification genes was also enhanced (Fig. 3). These include genes encoding xyloglucan endotransglucosylase hydrolase 6 (XETs), IRX9/beta-1,4-xylosyltransferase, and UDP-glucuronate:xylan alpha-glucuronosyltransferase (Table 5-2).

Table 5-2: Sub-selection of the differentially expressed genes obtained from comparison of *N. benthamiana* leaves expressing MdMYB93 against control infiltrated leaves. RPKM fold changes indicate the expression ratio (MdMYB93/control), with a negative value indicating higher expression in the control conditions. RPKM difference is the difference between the mean RKPM of both groups. Functional annotations against *Arabidopsis thaliana* were obtained from the Blast2Go Pro v3.1. Genes targeted in the qPCR experiment are displayed in bold.

Nicothiana benthamiana **contig assesion number**	**Gene symbol** ***(Arabidopsis thaliana)***	**Annotation (*Arabidopsis thaliana*)**	**Fold change (MdMYB93/p19)**	**RPKM Difference (MdMYB93-p19)**
Lipid metabolism				
Nbv5tr6328789	KCS1	3-ketoacyl- synthase 1	17.8	34.91
Nbv5tr6357319	**KCS2**	**3-ketoacyl- synthase 2**	**25.35**	**13.46**
Nbv5tr6222668	KCS4	3-ketoacyl- synthase 4	34.03	65.55
Nbv5tr6314011	AT4G36610	alpha beta fold family protein	194.47	23.53
Nbv5tr6389537	AT4G24140	alpha beta fold family protein	46.59	55.49
Nbv5tr6246568	LACS4	long chain acyl- synthetase 4	75.84	216.96
Nbv5tr6232718	**GPAT5**	**glycerol-3-phosphate acyltransferase 5**	**110.6**	**44.18**
Nbv5tr6218783	GPAT6	bifunctional sn-glycerol-3-phosphate 2-o-acyltransferase phosphatase	57.97	59.34
Nbv5tr6395628	GPAT4	bifunctional sn-glycerol-3-phosphate 2-o-acyltransferase phosphatase	34.81	64.25
Nbv5tr6408715	**CYP86A1**	**cytochrome p450 86a1**	**1 170.47**	**1 350.44**
Nbv5tr6237440	CYP86B1	cytochrome p450 86b1	70.01	236.18
Nbv5tr6220824	CYP94C1	cytochrome family subfamily polypeptide 1	15.44	18.07
Nbv5tr6346089	CYP86A8	cytochrome family subfamily polypeptide 8	11.82	35.17
Nbv5tr6203661	AT1G32910	hxxxd-type acyl-transferase-like protein	12.01	12.69
Nbv5tr6212895	**ASFT/RWP1**	**Omega-hydroxypalmitate O-feruloyl transferase**	**18.5**	**220.15**
Nbv5tr6203422	**CER4**	**fatty acyl- reductase cer4**	**29.74**	**76.3**
Nbv5tr6203423	**CER4**	**fatty acyl- reductase cer4**	**22.33**	**122.93**
Nbv5tr6369381	AT5G37690	gdsl esterase lipase	350.45	329.3
Nbv5tr6202105	AT5G03610	gdsl esterase lipase	176.24	125.39
Nbv5tr6222730	**AT1G74460**	**gdsl esterase lipase**	**60.87**	**68.63**
Nbv5tr6216569	**AT5G22810**	**gdsl esterase lipase**	**54.92**	**72**
Nbv5tr6228038	SMT1	24-sterol c-methyltransferase	96.27	81.7
Nbv5tr6202244		myrcene ocimene synthase	45.7	23.94
Nbv5tr6219443	AT4G38460	geranylgeranyl pyrophosphate synthase-related protein	27.53	22.8
Nbv5tr6237804	TPS21	alpha-humulene (-)- -beta-caryophyllene synthase	-18.74	-90.13

to be continued next page

Table 5-2: continued

Nicothiana benthamiana contig assesion number	Gene symbol (*Arabidopsis thaliana*)	Annotation (*Arabidopsis thaliana*)	Fold change (MdMYB93/p19)	RPKM Difference (MdMYB93-p19)
Phenolic metabolism				
Nbv5tr6211194	PAL1	phenylalanine ammonia lyase 1		
Nbv5tr6230676	PAL2	phenylalanine ammonia-lyase 2	15.91	105.75
Nbv5tr6215803	4CL1	4-coumarate-- ligase 1	29.33	39.75
Nbv5tr6233560	AT3G55120	chalcone flavanone isomerase	22.8	222.64
Nbv5tr6237359	AT4G35160	o-methyltransferase-like protein	149.39	373.96
Nbv5tr6231206	CAD9	cinnamyl-alcohol dehydrogenase cad1	-16.45	-24.4
Nbv5tr6204890	TT7	flavonoid 3 -monooxygenase	-10.19	-128.01
Nbv5tr6204044	TAA1	l-tryptophan--pyruvate aminotransferase 1	35.84	25.17
Nbv5tr6227276		monooxygenase	88.76	238.48
Transport				
Nbv5tr6236478	AT2G39350	abc transporter g family member 1	72.89	236.83
Nbv5tr6220564	AT2G37360	abc transporter g family member 2	41.64	27.29
Nbv5tr6217020	WBC11	abc transporter g family member 11	22.55	30.06
Nbv5tr6391581	AT5G19410	abc transporter g family member 23	317.7	217.57
Nbv5tr6241891	WBC11	abc transporter g family member 11	-12.69	-111.71
Nbv5tr6200284	LP1	non-specific lipid-transfer protein 1	12.27	10.45
Nbv5tr6201754	LTP4	non-specific lipid-transfer protein 4	172.13	974.95
Nbv5tr6222894	AT5G13900	lipid transfer-like protein vas	59.88	27.34
Nbv5tr6217812	AT3G22600	protease inhibitor seed storage lipid transfer protein family protein	74.66	112.37
Cell wall metabolism				
Nbv5tr6225572	AT5G55180	beta-glucanase-like, O-Glycosyl hydrolases family 17 protein	14.74	144.64
Nbv5tr6391909	GH9C1	glycosyl hydrolase 9c1	155.85	19.07
Nbv5tr6230638	XTR6	probable xyloglucan endotransglucosylase hydrolase protein 23	33.82	163.15
Nbv5tr6223206	PGSIP3	udp-glucuronate:xylan alpha-glucuronosyltransferase 2	40.55	64.36
Nbv5tr6394602	IRX9	probable beta- -xylosyltransferase irx9	41.74	52.4
Nbv5tr6228735	LAC12	laccase 12	216.97	320.95
Nbv5tr6392208	AT1G68850	peroxidase 11	876.79	60.68
Nbv5tr6235366	AT5G14130	peroxidase 55	30.34	32.97
Nbv5tr6369799	AT3G59850	pectin lyase-like superfamily protein	13.19	16.6
Nbv5tr6216642	PE11	pectinesterase 11	39.94	15.05
Nbv5tr6237815	MIOX2	myo-inositol oxygenase 2	81.97	131.38

to be continued next page

Table 5-2: continued

Nicothiana benthamiana contig assesion number	Gene symbol (*Arabidopsis thaliana*)	Annotation (*Arabidopsis thaliana*)	Fold change (MdMYB93/p19)	RPKM Difference (MdMYB93-p19)
Cell structure and misc.				
Nbv5tr6232726	AT4G15610	csplm_arath ame: full=casp-like protein 1d1 short= 1d1	101.5	227.79
Nbv5tr6223406	AT5G44550	csplw_arath ame: full=casp-like protein 1b1 short= 1b1	220.33	412.02
Nbv5tr6206592	AT5G09520	hydroxyproline-rich glycoprotein family protein	249.8	1 120.28
Nbv5tr6221489	AT5G09530	protein pro-glu-leu	46.01	88.72
Nbv5tr6207869	EDA4	protein embryo sac development arrest 4	96.06	161.15
Nbv5tr6221993	AT5G23750	remorin family protein	79.26	29.63
Nbv5tr6316960	AT3G52790	peptidoglycan-binding domain-containing protein	114.25	26.88
Nbv5tr6243328	AT3G09925	pollen ole e 1 allergen and extensin family protein	30.6	19.65
Gene regulation				
Nbv5tr6217099	MYB67	myb domain protein 67	208.86	41.27
Nbv5tr6316376	MYB52	myb domain protein 52 (partial)	436.84	25.44
Nbv5tr6228633	AT2G36890	transcription factor RAX2	37.1	49.18
Nbv5tr6226272	NAC038	nac domain containing protein 38	37.42	56.77
Nbv5tr6292509	NAC058	nac domain containing protein 58	283.71	406
Nbv5tr6205412	NAC073	nac domain containing protein 73	19.72	82.39
Nbv5tr6338894	NAC075	nac domain containing protein 75	228.36	32.2

Interestingly, *MdMYB93* expression also altered gene expression of cell wall structural proteins. Among these, we found some genes coding for CASP-like proteins and extensins, which were significantly more expressed in leaves expressing *MdMYB93* (Table 5-2). The STRING association network (Fig. 5-5) also highlighted additional up-regulated hydroxyproline-rich glycoprotein genes similar to *PELPK1* and *PELPK2*, which display strong co-expression with the suberin-related genes discussed in the previous section. In addition to its effect on metabolic and structural genes, *MdMYB93* induced the expression of several transcription factors. The MYB and the NAC family transcription factors were the most represented. NAC073 and NAC075 have been previously linked to the regulation of the secondary cell wall biogenesis (Zhong *et al*. 2008). MYB67, MYB52, NAC038 and NAC058 have no clear function established yet, but NAC058 presented a weak interaction with CYP86A1 in the STRING database (Legay *et al*. 2015).

C. *MdMYB93* triggered the accumulation of suberin monomers and suberin deposition.

In order to assess whether enhanced expression of suberin biosynthetic genes caused suberin deposition in *MdMYB93*-agroinfiltrated leaves, the free soluble lipid fraction (DCM fraction), as well as the BF3/Methanol depolymerized suberin fraction, were analyzed using GC-MS analysis (Fig. 5-6, Fig. 5-7). In the DCM fraction, a significant increase of ferulic acid was observed wheras coumaric acid did not displayed any differential accumulation. This is in occordance with results obtained when AtMYB41 was overexpressed in *N. benthamiana* leaves (Kosma *et al*. 2014). Accumulation of eicosanoic (20:0), docosanoic (22:0) and tetracosanoic (24:0) acids were observed, but no ω-hydroxy acids nor α,ω-dicarboxylic acids were differentially accumulated in the

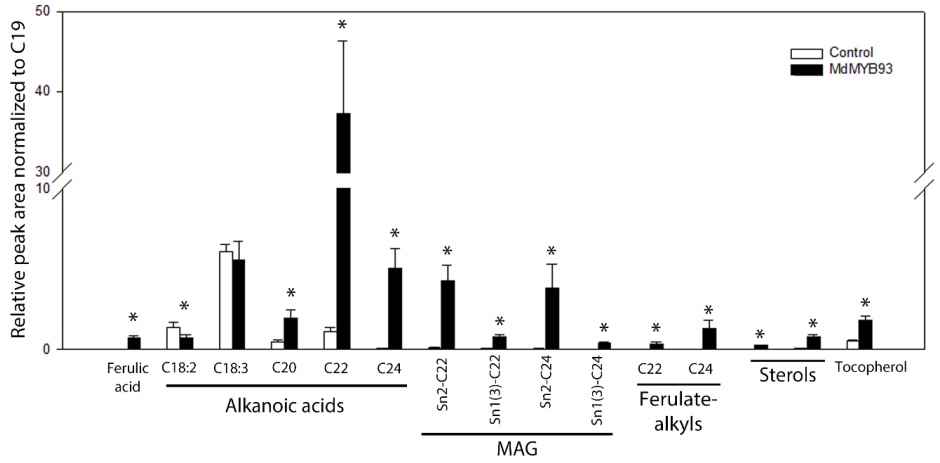

Figure 5-6: Composition of the free lipid fraction of *N. benthamiana* leaves agro-infiltrated with either MdMYB93/p19 or p19 alone (control). Data are represented by the mean value and standard deviation of four biological replicates of the peak areas normalized to the nonadecanoic acid internal standard. Statistical significance was evaluated using a t-test and displayed with asterisk.

DCM fraction (Fig. 5-6). Notably, *sn*-1(3), *sn*-2 docosanoyl and tetracosanoyl-glycerols, which are the main building blocks of the suberin in plants (Vishwanath *et al*. 2015), accumulated in leaves overexpressing MdMYB93. Two alkyl-ferulates, which are the main component of the suberin waxes (Molina and Kosma 2015), also displayed significant increase. Finally, two sterol derivatives also displayed a slight increased amount in response to MdMYB93 induction and may be linked with increased expression of the three cycloartenol-c-24-methyltransferase 1 (*SMT1)* genes observed in the RNA-Seq data, but further analyses need to be performed to confirm the implication of *MdMYB93* in the terpenoid synthesis pathway (Fig. 5-6).

The suberin depolymerized fraction supported the results obtained with the DCM fraction. A large amount of suberin polymer accumulated in *MdMYB93* agroinfiltrated tobacco leaves, whereas an extremely low amount was detected in

the control leaves (Graca and Pereira 2000, Graca *et al*. 2002, Bento *et al*. 1998, Franke *et al*. 2005). As observed in the DCM fraction, ferulic acid strongly accumulated (Fig. 5-7). An important part of the depolymerized fraction was composed of alkanoic acids, ranging from C20 to C28; ω-hydroxyacids, ranging from C16 to C22, and α,ω-dicarboxylic acids, ranging from C16 to C24, which is in accordance with the results obtained for the DCM fraction and the gene expression profiling results (Fig. 5-7). Finally, an increased amount of primary fatty alcohols, ranging from C20 to C24, was observed.

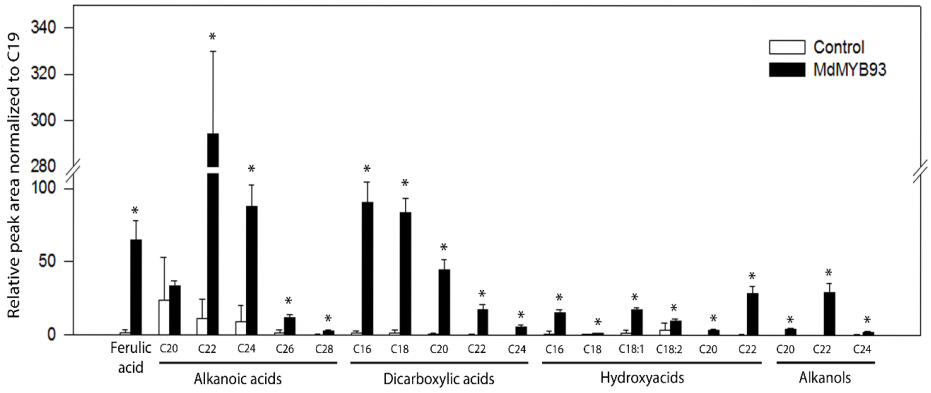

Figure 5-7: Polyester monomer composition of *N. benthamiana* leaves agro-infiltrated with either MdMYB93/p19 or p19 alone (control). Data are represented as the mean value and standard deviation of four biological replicates of the peaks area normalized to the nonadecanoic acid internal standard. Statistical significance was evaluated using a t-test and displayed with asterisk.

These data were also confirmed by UV microscopy and berberine/aniline blue staining, A clear increase of light blue color, which corresponds to the suberin staining, appeared in the cell walls of tissues expressing *MdMYB93*, whereas control tissues remained in grey/dark blue color, which corresponds to the cell wall (Cellulose) staining (Fig. 5-8, Brundrett *et al*. 1988, Fig. 5-8).

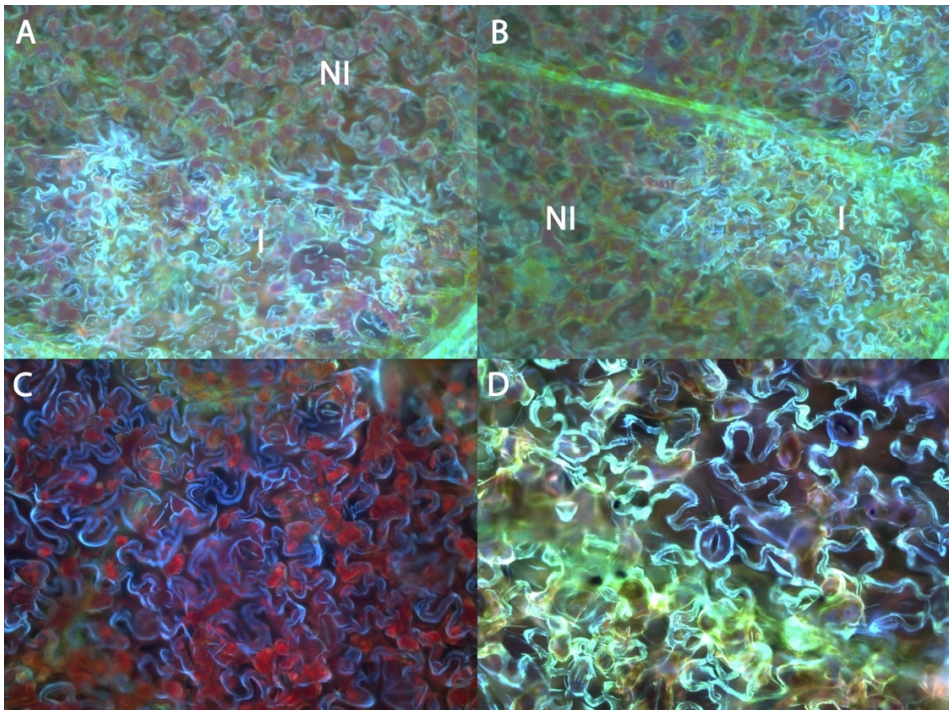

Figure 5-8: Ultraviolet microscopy performed on *N. benthamiana* leaves expressing *MdMYB93* and control leaves after staining with berberine/aniline blue. A, B: 10X zoom of tobacco leaves. In light blue, suberin appears in MdMYB93-infiltrated area (I) and not in non-infiltrated area (NI). C: control leaves (zoom 20X). D: Leaves overexpressing MdMYB93 (20X), suberin appears in light blue.

D. *MdMYB93* expression remobilizes phenylpropanoids and influences the lignin precursor accumulation.

To better understand the metabolic changes associated with transient expression of apple *MYB93* in tobacco leaves, metabolic profiling was performed using UPLC-TripleTOF in both positive and negative mode. In negative mode, we identified 90 metabolite features that significantly changed after agro-infiltration with *MdMYB93* (with p-value < 0.01 and fold change > 1.5). After removal of isotopes, fragment ions, and unclear mass spectra, 13 metabolites matched the

PubChem and METLIN database (Table 5-3). In positive mode, 89 metabolite features significantly changed in response to *MdMYB93* over-expression (with *p*-value < 0.01 and fold change > 1.5). After removal of isotopes, fragment ions, unclear mass spectra, and compounds previously described in negative mode, three metabolites were putatively identified.

Strong and significant decreases of different caffeoyl-quinic acid and *p*-coumaroyl-quinic acid isomers were observed (Table 5-3). The levels of tryptophan were significantly higher (about 4 fold) after *MdMYB93* expression, although no significant difference was observed for the other aromatic amino acids (phenylalanine, tyrosine, Table 5-3). Interestingly, several feruloyl-derivatives accumulated in transiently expressing *MdMYB93*-leaves (feruloyl-putrescine, N-feruloyl-tyramine, Table 5-3). Another feruloyl derivative was also detected, but we could not infer its identity. The exact mass of the parent ion corresponded to a feruloyl-hexoside, but the retention time (16.5 min) indicated a more lipophilic compound. In addition, this compound was not detected in control tobacco leaves, indicating a *MdMYB93*-specific metabolite. The synthesis of three flavonoids (including one flavone that is likely an apigenin derivative, Schmidt 2016) and two flavonols (kaempferol derivatives) were also reduced in transformed tobacco plants (Table 5-3). Two oligolignols, previously described in the stem of flax (Huis *et al*. 2012) accumulated in transiently transformed tobacco leaves (lariciresinol hexoside and a dimer of guaiacyl (8-5) hexoside, Table 5-3). A third compound with a molecular formula of $C_{30}H_{34}O_7$, eluting at 26.5 min in negative mode, could not be identified but presented fragment ions that are typical of a *p*-coumaryl alcohol hexoside derivative. It was only detected in the *MdMYB93* transformed plants. Finally, two hydroxy-fatty acids were also specifically produced in *MdMYB93* transformed plants (Table 5-3).

Table 5-3: List of compounds differentially accumulated in *N. benthamiana* leaf samples after transient expression of *MdMYB93*. MS/MS data were obtained by UPLC–TTOF in in positive and negative ESI mode. The relative abundance of each peak in transiently overexpressing *MdMYB93* and control (p19) tissues is based on the selected ion current and is presented as the average value of four biological replicates (n = 4). Abbreviations: t_r, retention time; nd, not detected.

$t_{r\ (min)}$	Relative abundance		Fold	[M-H]	Error (ppm)	Molecular Formula	MSMS [M-H]	Putative identity
	p19 + MYB93	p19						
Positive mode								
1.7	2.59×10^7	4.35×10^7	0.6	353.087	-1.4	C16H18O9	191.0558	5-*O*-caffeoyl-quinic acid (neochlorogenic acid) *
3	2.13×10^5	1.61×10^6	0.13	337.092	-2.3	C16H18O8	191.0552	p-coumaroyl-quinic acid isomer 1 (Torras-Claveria et al, 2012)
4.2	2.18×10^7	4.27×10^7	0.51	353.087	-4	C16H1809	191.0553	3-0-Caffeoyl-quinic acid*
7.3	4.07×10^5	1.90×10^6	0.21	337.092	1.8	C16H18O8	191.056	p-coumaroyl-quinic acid isomer 2 (Torras-Claveria et al, 2012)
11.1	3.60×10^4	1.82×10^5	0.2	711.213	-1.7	C32H40O18	269.0598	Apigenin-derivative [b]
19.3	7.17×10^5	1.15×10^6	0.62	755.203	0.6	C33H40O20	447.0954; 285.0396	Kaempferol-3-O-hexosyl-rhamnosyl-hexoside*
22.03	8.64×10^5	8.99×10^4	9.61	579.207	0.1	C28H36O13	339.1227; 327.1223; 324.0991	Guaiacyl (8-5) guaiacyl hexoside (Huis et al., 2012)
22.1	2.42×10^5	5.03×10^5	0.48	593.15	-1.3	C27H30O15	285.0383	Kaempferol-3-0-rutinoside*
22.1	4.38×10^5	5.13×10^4	7.9	521.201	-2.4	C26H34O11	359.1491; 329.1390	Lariciresinol hexoside (Huis et al, 2012)
24.6	1.17×10^5	nd	MYB Only	327.218	-0.6	C18H32O5		Tri-hydroxy-octadecadienoic acid (Fahy et al., 2007)
24.8	5.58×10^5	4.95×10^4	11.6	312.124	-0.7	C18H19NO4		Feruloyl-tyramine (Scalabrin et al, 2015)
26.5	1×10^4	nd	MYB Only	505.224	-0.7	C30H34O7	311.0981; 149.0439; 131.0345	Unknown [b]
33.3	2.93×10^5	nd	MYB Only	293.212	3.3	C18H30O3		Hydroxy–octodeca-trienoic acid (Fahy et al., 2007)
Negative mode								
5.2	2.98×10^6	7.76×10^5	3.8	205.097	-1.7	C11H12N2O2	177.0541	Tryptophan (PubChem)
8.5	6.57×10^6	1.63×10^6	4	265.155	0.1	C14H20N2O3	195.0635	Feruloyl-putrescine (Torras-Claveria et al, 2012)
16.9	9.60×10^5	nd	MYB only	357.117	3.3	C16H20O9	163.0604	Feruloyl-derivative (Huis et al., 2012)

[a]Identity of the compound was confirmed with an authentic standard. [b] No bibliographic references for the MS data were available. Reference number after a compound name refers to a bibliographic reference for MS data.

IV. Discussion

Russeting is one of the most important agronomical defects that occurs at the surface of fruit, drastically downgrading the profitability of fruit tree production. This rough and brown phenotype is mainly due to the accumulation of suberin in the primary cell wall of plants and is linked to defects on the cuticular surface (Knoche and Khanal 2011, Khanal *et al*. 2013, Lashbrooke *et al*. 2015). Suberin deposition has been widely studied in *A. thaliana*, *S. tuberosum* and *Quercus suber* (Vishwanath *et al*. 2015, Graca 2015). However, despite the important progress that has been made in the last decade regarding the functional description of suberin synthesis, some key points, such as the final polymerization steps and the regulation of suberin synthesis, remain unclear. In *A. thaliana*, a recent study described AtMYB41, a transcription factor that can trigger suberin deposition via the upregulation of suberin biosynthetic genes, including those encoding GPAT5, fatty acid hydroxylases (CYP86A1 and CYP86B1), KCS2, AFST and fatty acyl reductases (FAR1, FAR4, and FAR5), with a concomitant synthesis of suberin monomers and suberin lamellae deposition in the primary cell wall (Kosma *et al*. 2014). This transcription factor is expressed in root endodermis under stress conditions, for example high salt, but not under non-stress conditions. In russeted apple fruit, although a significant number of stress signaling genes has been observed, no expression of an AtMYB41 ortholog was observed in our previous RNA-Seq experiment, suggesting that other transcription factors are involved in the regulation of suberin deposition in the apple fruit skin. Indeed, another MYB-like transcription factor was co-expressed with some key suberin biosynthetic genes, such as the apple orthologs of *CYP86A1*, *CYP86B1*, and *GPAT5*. The amino acid sequence of this MYB transcription factor displayed high similarity with AtMYB93, which has been already described in *A. thaliana* to be specifically expressed in endodermal cells and acts as a negative regulator of lateral root

development. However, no evidence has yet been established between AtMYB93 and suberin deposition (Gibbs and Coates 2014, Gibbs *et al*. 2014). The structure of MdMYB93 was investigated and showed high similarity with AtMYB93 on the N-terminal region sharing two SANT DNA binding domains, whereas the C-terminal sequence codes for an intrinsically disordered region that has a low identity level with AtMYB93. The role of intrinsically disordered regions in proteins remains unclear. The disordered and flexible structure of these regions may have a role in post translational regulation or in conferring binding affinities with different protein partners (promiscuity/moonlighting; Uversky 2013). We can thus speculate that MdMYB93 may also be influenced by other partners, which may alter its affinity for its DNA binding site and/or its communication with the basal transcriptional machinery (Pazos *et al*. 2013).

Transient overexpression of *MdMYB93* in *N. benthamiana* triggered the expression of a large number of genes involved in lipid and phenylpropanoid metabolism, which covered the synthesis of central metabolites as well as advanced suberin building blocks (Fig. 5-4, Fig. 5-9, Fig. 5-5, Table 5-2). This finding suggests that MdMYB93 acts on the whole synthesis pathway as an upstream regulator. The major influence of MdMYB93 on suberin monomer synthesis via upregulation of the *KCS*, *CYP86*A1, *CYP86B1*, *GPAT* or *LACS* genes is strongly supported by the accumulation of their products in the DCM fraction. For example, enhanced expression of *GPAT* and *ASFT* genes by the synthesis of advanced monomers composing the SPAD such as the *sn*-1(3) and *sn*-2 acylglycerols and the feruloyl acyl chains (Table 5-2, Vishwanath *et al*. 2015, Graca 2015).

Suberin deposition was observed by fluorescence microscopy imaging coupled with berberine/aniline blue staining and ultraviolet light illumination (Fig. 5-8) and was confirmed by the analysis of depolymerized aliphatic suberin,

specifically ferulic acid, alkanoic acids, ω-hydroxacids, α,ω-diacids and primary fatty alcohols with a remarkable fraction of long chain C22 and C24-derived methyl-esters that are characteristic of suberin (Fig. 5-6, Fig. 5-6). Similar results were described with AtMYB41 overexpression in *N. benthamiana*, suggesting that these two transcription factors, which seem to be expressed in different organs and conditions, regulate in a similar manner the synthesis of the SPAD and their dedicated metabolic processes (Kosma *et al*. 2014).

Besides, MdMYB93 also influences genes belonging to sterol metabolism. In apple, skin suberization has been linked with the expression of dedicated oxidosqualene cyclase and the occurrence of some specific triterpene compounds (Andre *et al*. 2013, Andre *et al*. 2016). Thus, even though data are lacking to support this hypothesis, we can postulate that MdMYB93 might influence the regulation of the terpenoid pathways.

Still, in order to feed the massive enhancement of suberin metabolism previously described, MdMYB93 transient expression seems to trigger a remobilization of secondary metabolites, *i.e.,* hydroxycinnamic esters and flavonoids (Table 5-3). In potato, it has been suggested that chlorogenic acids, as well as coumaroyl-quinic acids, accumulate in the tuber as phenolic compound storage pools, which can be re-mobilized according to the plant's needs (e.g. detoxification of reactive oxygen species in the case of oxidative stress, or lignin / suberin production) (Valinas *et al*. 2015). It is therefore likely that the hydroxycinnamic esters and flavonoids molecules observed in the present experiment serve as precursors of feruloyl-CoA through the action of hydroxycinnamoyl transferase (HCT), caffeoyl-CoA O-methyltransferase (CCoAOMT), and caffeic/5-hydroxyferulic acid O-methyltransferase (COMT1), directing the flux towards suberin production (Fig. 5-9). Inversely, the increase in feruloyl putrescine may reflect transitory storage of ferulic acid, which strongly accumulated in response to

MdMYB93 overexpression (Table 5-3). In potato tubers, silencing the fatty ω-hydroxyacid/fatty alcohol hydroxycinnamoyl transferase (FHT), which uses mainly caffeoyl and feruloyl-CoA as substrates, leads to the accumulation of caffeoyl and feruloyl-putrescine (Serra *et al*. 2010). However, it is difficult to assess whether this remobilization occurs because of altered physiological conditions, which may be due to a disequilibrium triggered by the MdMYB93 transient overexpression.

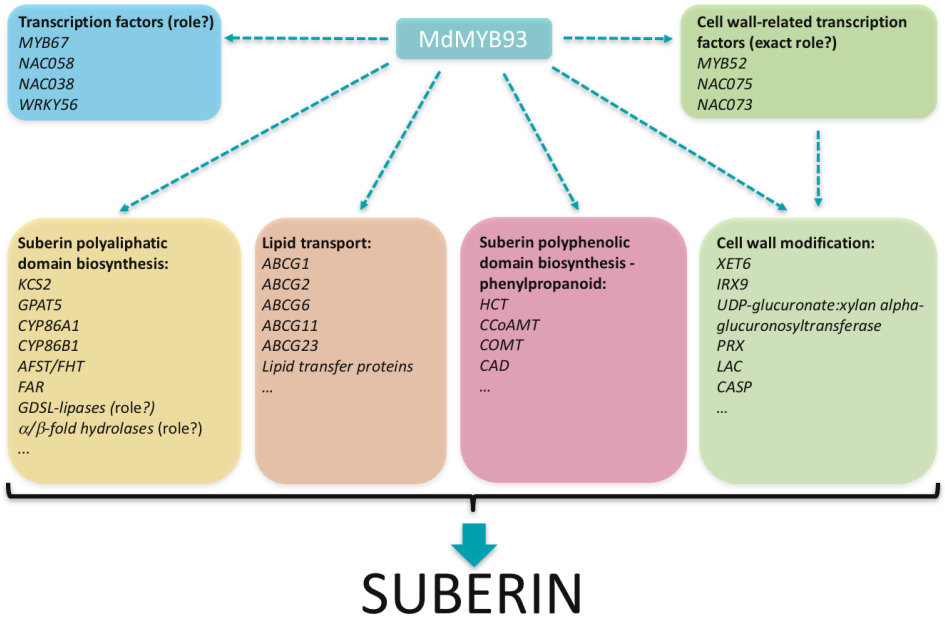

Figure 5-9: Summary of the biological processes and genes altered by the expression of *MdMYB93* in *N. benthamiana* leaves. *GPAT*: glycerol phosphate acyl transferase, *CYP86A1*: fatty acid hydroxylase, *CYP86B1*: very long chain fatty acid hydroxylase, *ASFT/FHT*: feruloyl-CoA-Acyl transferase, *FAR*: fatty acyl reductase, *KCS2*: 3-ketoacyl-CoA synthase 2, *ABCG*: ATP-binding cassette family G, *HCT*: hydroxycinnamoyl transferase, *CCoAMT*: caffeoyl-CoA O-methyltransferase, *COMT*: caffeic/5-hydroxyferulic acid O-methyltransferase, *CAD*: cinnamyl alcohol dehydrogenase, *XET*: xyloglucan endotransglucosylase transferase, *IRX9*: glycosyl transferase, *LAC*: laccase, *PRX*: peroxidase, *CASP*: CASP protein gene.

The exportation of suberin monomers and/or oligomers is not fully understood, however number of transporters have been already linked with the suberin deposition. In the present work, expression patterns of ABC transporters and lipid transfer proteins suggest that MdMYB93 also orchestrates the transport of these monomers (Fig. 5-9). In addition to the ABCG1, ABCG2 and ABCG6 transporters, which are involved in the transport of suberin monomers (Yadav *et al*. 2014, Landgraf *et al*. 2014, Vishwanath *et al*. 2015), an ABCG23 transporter showed some interactions with suberin biosynthetic genes (Fig. 5-5) and was previously shown to be co-expressed with some suberin biosynthetic genes in *A. thaliana* (Yadav *et al*. 2014), suggesting it may also have a role in the export of suberin monomers under the tight control of MdMYB93. ABCG11, a major transporter of cutin monomers (Bird *et al*. 2007), may participate in lipid/sterol homeostasis (le Hir *et al*. 2013) and alters the expression of some cutin genes in reproductive organs and suberin biosynthetic genes in roots (Panikashvili *et al*. 2010). Thus, ABCG11 might also participate in the exportation of suberin monomers. In addition to the ABCG transporters, non-specific lipid transfer proteins (LTPs) were also induced by MdMYB93. LTPs have been suggested to be involved in cuticular wax, cutin and suberin deposition but no *LTP* gene has been clearly linked to suberin deposition in *A. thaliana* or in other species (Edstam *et al*. 2013, Edstam and Edqvist 2014). However, because the present *LTP* genes were significantly regulated by *MdMYB93* and seemed to contribute to the suberin biosynthetic gene cluster (Fig. 5-5), we hypothesize that they play a crucial role, in conjunction with the ABCG transporters, in the exportation of suberin monomers to the primary cell wall for further assembly.

To date, the final suberin polymerization process remains unknown (Vishwanath *et al*. 2015). However, in the present study, the protein-protein co expression analysis showed strong interactions between some GDSL-esterase/lipases, some

α,β-fold protein hydrolases, and the suberin biosynthetic gene cluster. Indeed, recent advances in the field of cutin polyester synthesis described a GDSL-esterase/lipase as being able to perform this critical step in tomato (Girard *et al*. 2012). Through our experiments on suberized apple skin (Legay *et al*. 2015) and on the heterologous expression of *MdMYB93* in *N. benthamiana* leaves, we highlighted a link between GDSL-esterase/lipases and suberin (Fig. 5-9). Genes identified in the current experiment appear therefore excellent candidates for further functional validation. The α/β-fold protein hydrolases, regulated by MdMYB93, might also participate in this process. Indeed, in *A. thaliana*, an α,β-fold protein hydrolase called BODYGUARD is a crucial actor of the polymerization of carboxylic esters of cutin and might be implicated in the attachment of suberin to the cell wall (Kurdyukov *et al*. 2006, Jakobson *et al*. 2016). However, the functions of these proteins are broad and caution should be taken regarding their function in suberization, as they might also participate generally in the hydroxylation of fatty acids (Blee and Schuber 1993).

MdMYB93 also influenced the expression of genes linked to lignin and/or to the SPPD. Indeed, the decreased expression of CAD genes, which was observed in our previous work on apple russeting (Legay *et al*. 2015) or similar work in pear (Wang *et al*. 2014), also occurred in MdMYB93 overexpressing leaves. Decreased CAD expression in suberized tissues was associated with a concomitant decrease of lignin precursors in the SPPD leading to a contrasted ratio of monolignols/hydroxycinnamic acids compared to lignin (Bernards *et al*. 1995, Bernards 2002). Moreover, the accumulation of oligolignols (lariciresinol hexoside and a dimer of guaiacyl (8-5) hexoside) raises the question whether these are lignin-specific or if they are also involved in SPPD composition; the accumulation of feruloyl derivatives (N-feruloyl-tyramine and a feruloyl-hexoside) strengthens the hypothesis that MdMYB93 may be able to orchestrate

the polymerization of suberin SPPD (Graca 2015, Bernards *et al*. 2004). Due to its lignin-like structure, it has been proposed that the SPPD assembly may engage some oxidative pathways using peroxidase, but no gene has been clearly identified yet. MdMYB93 altered the expression of members of the peroxidase and laccase families, which is in accordance with our observations in apple russeted skins, without being able to distinguish whether these were dedicated to SPPD assembly or to the cell wall lignification. Overall, MdMYB93 seemed to alter the phenolic composition of *N. benthamiana* leaves. We speculate that this might be linked to synthesis of the polyphenolic domain of suberin but further experiments need to be performed to test this.

In russeted apple skin, deposition of suberin was associated with altered expression of cell wall modification genes (Legay *et al*. 2015). The present data suggest that MdMYB93 may drive this cell wall reconstruction and more precisely xylans, pectins and cell wall structural genes (Fig. 5-9). As an example, CASP proteins are involved in the ordering of the primary cell wall Casparian strip and may have a role in the localization and the regulation of cell wall biosynthetic enzymes (Roppolo *et al*. 2011). Hydroxyproline-rich glycoproteins, such as the extensins, participate in cell wall organization by altering its plasticity through the formation of covalent bonds (Hijazi *et al*. 2014). The PELPK1 protein, which is localized in the cell wall, is involved in seed germination, growth and flowering in *A. thaliana* (Rashid *et al*. 2012). PELPK1 is thought to participate in a stress signaling cascade linked to the cell wall integrity during pathogen attack. As an increased expression of *PELPK1* has been also observed in the russeted variety 'Reinette Grise du Canada', we can speculate that PELPK1 might be involved in a cell wall signaling cascade enabling the coordination between cell wall modification and suberin deposition (Rashid 2011). Xylan is a major hemicellulose of secondary cell walls, which acts as an anchor for lignin

deposition. However, only a slight accumulation of xylan has been observed in the primary cell wall, where suberin deposition occurs (Mortimer *et al*. 2015). As the suberin poly-aromatic domain has been described as a lignin-like biopolymer (Bernards 2002), this modification in xylan metabolism might reflect a remodeling process of the primary cell wall that favors the anchoring of the suberin poly-aromatic domain. The expression changes of cell wall-related genes might be mediated by the NAC073 and NAC075 transcriptional regulators, which regulate secondary cell wall biogenesis (Zhong *et al*. 2008).

Altogether, this study demonstrates the important role of MdMYB93 in the suberization process, regulating the biogenesis of suberin fatty acid precursors and the organization of their deposition and polymerization in the cell wall. Importantly, MdMYB93 is expressed in apple during fruit growth, specifically in russeted tissues as previously shown in 'Cox orange Pippin' variety. The discovery of this transcriptional regulator inspires new strategies enabling the control of russeting in fruit, thereby enhancing the market value of fruit tree production.

Acknowledgements: The authors acknowledge Aude Corvisy and Laurent Solinhac for their precious technical help. Sylvain Legay and Jean-Francois Hausman are grateful to the National Research Funds (FNR, Luxembourg) for partial funding (AFR ID: 9208308).

References

Andre CM, Larsen L, Burgess EJ, Jensen DJ, Cooney JM, Evers D, Zhang J, Perry NB, Laing WA. 2013. Unusual immuno-modulatory triterpene-caffeates in the skins of russeted varieties of apples and pears. *Journal of Agricultural Food Chemistry* **61**: 2773-2779.

Andre CM, Legay S, Deleruelle A, Nieuwenhuizen N, Punter M, Brendolise C, Cooney JM, Lateur M, Hausman JF, Larondelle Y, Laing WA. 2016. Multifunctional oxidosqualene cyclases and cytochrome P450 involved in the biosynthesis of apple fruit triterpenic acids. *New Phytologist*. **211**: 1279-1294.

Baggerly KA, Deng L, Morris JS, Aldaz CM. 2003. Differential expression in SAGE: accounting for normal between-library variation. *Bioinformatics* **19**: 1477-1483.

Beisson F, Li Y, Bonaventure G, Pollard M, Ohlrogge JB. 2007. The acyltransferase GPAT5 is required for the synthesis of suberin in seed coat and root of Arabidopsis. *The Plant Cell* **19**: 351-368.

Beisson F, Li-Beisson Y, Pollard M. 2012. Solving the puzzles of cutin and suberin polymer biosynthesis. *Current Opinion in Plant Biology* **15**: 329-337.

Bento MF, Pereira H, Cunha MA, Moutinho AMC, van den Berg KJ, Boon JJ. 1998. Thermally assisted transmethylation gas chromatography-mass spectrometry of suberin components in cork from *Quercus suber* L. *Phytochemical Analysis* **9**: 75-87.

Bernards MA, Lopez ML, Zajicek J, Lewis NG. 1995. Hydroxycinnamic acid-derived polymers constitute the polyaromatic domain of suberin. *Journal of Biological Chemistry* **270**: 7382-7386.

Bernards MA. 2002. Demystifying suberin. *Canadian Journal of Botany* **80**: 227-240.

Bernards, MA, Summerhurst, DK, Razem, FA. 2004. Oxidases, peroxidases and hydrogen peroxide: The suberin connection. *Phytochemistry Reviews* **3**: 113-126.

Bindea G, Mlecnik B, Hackl H, Charoentong P, Tosolini M, Kirilovsky A, Fridman WH, Pages F, Trajanoski Z, Galon J. 2009. ClueGO: a Cytoscape plug-in to decipher functionally grouped gene ontology and pathway annotation networks. *Bioinformatics* **25**: 1091-1093.

Bindea G, Galon J, Mlecnik B. 2013. CluePedia Cytoscape plugin: pathway insights using integrated experimental and *in silico* data. *Bioinformatics* **29**: 661-663.

Bird D, Beisson F, Brigham A, Shin J, Greer S, Jetter R, Kunst L, Wu X, Yephremov A, Samuels L. 2007. Characterization of Arabidopsis ABCG11/WBC11, an ATP binding cassette (ABC) transporter that is required for cuticular lipid secretion. *The Plant Journal* **52**: 485-498.

Blee E, Schuber F. 1993. Biosynthesis of cutin monomers: involvement of a lipoxygenase/peroxygenase pathway. *The Plant Journal* **41**:113-123.

Boher P, Serra O, Soler M, Molinas M, Figueras M. 2013. The potato suberin feruloyl transferase FHT which accumulates in the phellogen is induced by wounding and regulated by abscisic and salicylic acids. *Journal of Experimental Botany* **64**: 3225-3236.

Brundrett MC, Enstone DE, Peterson CA. 1988. A berberine-aniline blue fluorescent staining procedure for suberin, lignin, and callose in plant tissue. *Protoplasma* **146**: 133-142.

Bustin SA, Benes V, Garson JA, Hellemans J, Huggett J *et al.* 2009. The MIQE guidelines: minimum information for publication of quantitative real-time PCR experiments. *Clinical Chemistry* **55**: 611-22.

Chambers MC, MacLean B, Burke R, Amode D, Ruderman DL, *et al.* 2012. A cross-platform toolkit for mass spectrometry and proteomics. *Nature Biotechnology* **30**: 918-920.

Curry E. 2012. Increase in epidermal planar cell density accompanies decreased russeting of "Golden Delicious" apples treated with gibberellin A_{4+7}. *HortScience* **47**: 232-237.

Domergue F, Vishwanath SJ, Joubès J, Ono J, Lee JA, Bourdon M, Alhattab R, Lowe C, Pascal S, Lessire R, *et al.* 2010. Three Arabidopsis fatty acyl-

coenzyme A reductases, FAR1, FAR4, and FAR5, generate primary fatty alcohols associated with suberin deposition. *Plant Physiology* **153**: 1539-1554.

Earley KW, Haag JR, Pontes O, Opper K, Juehne T, Song K, Pikaard CS. 2006. Gateway-compatible vectors for plant functional genomics and proteomics. *The Plant Journal* **45**: 616-629.

Edstam MM, Blomqvist K, Eklöf A, Wennergren U, Edqvist J. 2013. Coexpression patterns indicate that GPI-anchored non-specific lipid transfer proteins are involved in accumulation of cuticular wax, suberin and sporopollenin. *Plant Molecular Biology* **83**: 625-649.

Edstam MM, Edqvist J. 2014. Involvement of GPI-anchored lipid transfer proteins in the development of seed coats and pollen in *Arabidopsis thaliana*. *Physiologia Plantarum* 152: 32-42.

Fahy E, Sud M, Cotter D, Subramaniam S. 2007. LIPID MAPS online tools for lipid research. *Nucleic Acids Research* **35**: p.W606-12.

Faust M, Shear C. 1972. Russeting of apples, an interpretative review. *HortScience* **7**: 233-235.

Franke R, Briesen I, Wojciechowski T, Faust A, Yephremov A, Nawrath C, Schreiber L. 2005. Apoplastic polyesters in Arabidopsis surface tissues - a typical suberin and a particular cutin. *Phytochemistry* **66**: 2643-2658.

Franke R, Schreiber L. 2007. Suberin - a biopolyester forming apoplastic plant interfaces. *Current Opinion in Plant Biology* **10**: 252-259.

Gibbs DJ, Coates JC. 2014. AtMYB93 is an endodermis-specific transcriptional regulator of lateral root development in Arabidopsis. *Plant Signaling and Behavior* **9**: e970406.

Gibbs DJ, Voß U, Harding SA, Fannon J, Moody LA, Yamada E, Swarup K, Nibau C, Bassel GW, Choudhary A *et al.* 2014. AtMYB93 is a novel negative regulator of lateral root development in Arabidopsis. *New Phytologist* **203**: 1194-1207.

Girard A-L, Mounet F, Lemaire-Chamley M, Gaillard C, Elmorjani K, Vivancos J, Runavot J-L, Quemener B, Petit J, Germain V *et al.* 2012. Tomato

GDSL1 is required for cutin deposition in the fruit cuticle. *The Plant Cell* **24**: 3119-3134.

Graça J, Pereira H. 2000. Suberin structure in potato periderm: glycerol, long-chain monomers, and glyceryl and feruloyl dimers. *Journal of Agricultural and Food Chemistry* **48**: 5476-5483.

Graça J, Schreiber L, Rodrigues J, Pereira H. 2002. Glycerol and glyceryl esters of omega-hydroxyacids in cutins. *Phytochemistry* **61**: 205-15.

Graça J. 2015. Suberin: the biopolyester at the frontier of plants. *Frontiers in Chemistry* **3**: 62.

Hijazi M, Velasquez SM, Jamet E, Estevez JM, Albenne C. 2014. An update on post-translational modifications of hydroxyproline-rich glycoproteins: toward a model highlighting their contribution to plant cell wall architecture. *Frontiers in Plant Science* **5**: 395.

Huis R, Morreel K, Fliniaux O, Lucau-Danila A, Fénart S, Grec S, Neutelings G, Chabbert B, Mesnard F, Boerjan W, Hawkins S. 2012. Natural hypolignification is associated with extensive oligolignol accumulation in flax stems. *Plant physiology* **158:** 1893-1915.

Jakobson L, Lindgren LO, Verdier G, Laanemets K, Brosché M, Beisson F, Kollist H. 2016. BODYGUARD is required for the biosynthesis of cutin in Arabidopsis. *New Phytologist* **211**: 614-626.

Khanal BP, Grimm E, Knoche M. 2013. Russeting in apple and pear: a plastic periderm replaces a stiff cuticle. *AoB Plants* **5**: ls048.

Knoche M, Khanal BP. 2011. Russeting and microcracking of 'Golden Delicious' apple fruit concomitantly decline due to gibberellin A_{4+7} application. *Journal of the American Society for Horticultural Science* **136**: 159-164.

Kosma DK, Murmu J, Razeq FM, Santos P, Bourgault R, Molina I. Rowland O. 2014. AtMYB41 activates ectopic suberin synthesis and assembly in multiple plant species and cell types. *The Plant Journal* **80**: 216-229.

Kurdyukov S, Faust A, Nawrath C, Bär S, Voisin D, Efremova N, Franke R, Schreiber L, Saedler H, Métraux J-P *et al.* 2006. The epidermis-specific

extracellular BODYGUARD controls cuticle development and morphogenesis in Arabidopsis. *The Plant Cell* **18**: 321-339.

Landgraf R, Smolka U, Altmann S, Eschen-Lippold L, Senning M, Sonnewald S, Weigel B, Frolova N, Strehmel N, Hause G *et al.* 2014. The ABC transporter ABCG1 is required for suberin formation in potato tuber periderm. *The Plant Cell* **26**: 3403-3415.

Lashbrooke J, Aharoni A, Costa F. 2015. Genome investigation suggests MdSHN3, an APETALA2-domain transcription factor gene, to be a positive regulator of apple fruit cuticle formation and an inhibitor of russet development. *Journal of Experimental Botany* Epub head of print.

Legay S, Guerriero G, Deleruelle A, Lateur M, Evers D, André CM, Hausman, J-F. 2015. Apple russeting as seen through the RNA-seq lens: strong alterations in the exocarp cell wall. *Plant Molecular Biology* **88**: 21-40.

Le Hir R, Sorin C, Chakraborti D, Moritz T, Schaller H, Tellier F, Robert S, Morin H, Bako L, Bellini C. 2013. ABCG9, ABCG11 and ABCG14 ABC transporters are required for vascular development in Arabidopsis. *The Plant Journal* **76**: 811-824.

Leckie BM, Neal Stewart CJ. 2011. Agroinfiltration as a technique for rapid assays for evaluating candidate insect resistance transgenes in plants. *Plant Cell Reports* **30**: 325-34.

Li Y, Beisson F. 2009. The biosynthesis of cutin and suberin as an alternative source of enzymes for the production of bio-based chemicals and materials. *Biochimie* **91**: 685-691.

Liu D, Shi L, Han C, Yu J, Li D, Zhang Y. 2012. Validation of reference genes for gene expression studies in virus-infected *Nicotiana benthamiana* using quantitative real-time PCR. *PLoS One* **7**: e46451.

Lulai EC, Corsini DL. 1998. Differential deposition of suberin phenolic and aliphatic domains and their roles in resistance to infection during potato tuber (*Solanum tuberosum* L.) wound-healing. *Physiological Molecular Plant Pathology* **53**: 209-222.

Meyer A. 1944. A study of the skin structure of Golden Delicious apples. *Proceedings of the American Society for Horticultural Science* **45**: 105-110.

Molina I, Kosma D. 2015. Role of HXXXD-motif/BAHD acyltransferases in the biosynthesis of extracellular lipids. *Plant Cell Reports* **34**: 587-601.

Mortazavi A, Williams BA, McCue K, Schaeffer L, Wold B. 2008. Mapping and quantifying mammalian transcriptomes by RNA-Seq. *Nature Methods* **5**: 621-628.

Mortimer JC, Faria-Blanc N, Yu X, Tryfona T, Sorieul M, Ng YZ, Zhang Z, Stott K, Anders N, Dupree P. 2015. An unusual xylan in Arabidopsis primary cell walls is synthesised by GUX3, IRX9L, IRX10L and IRX14. *The Plant Journal* **83**: 413-426.

Nakasugi K, Crowhurst R, Bally J, Waterhouse P. 2014. Combining transcriptome assemblies from multiple *de novo* assemblers in the allo-tetraploid plant *Nicotiana benthamiana*. *PLoS ONE* **9**: e91776.

Panikashvili D, Shi JX, Bocobza S, Franke RB, Schreiber L, Aharoni A. 2010. The Arabidopsis DSO/ABCG11 transporter affects cutin metabolism in reproductive organs and suberin in roots. *Molecular Plant* **3**: 563-575.

Pazos F, Pietrosemoli N, García-Martín JA, Solano R. 2013. Protein intrinsic disorder in plants. *Frontiers in Plant Science* **4**: 363.

Rashid A. 2011. Functional characterization of a novel cell-wall annotated PELPK1 gene in *Arabidopsis thaliana*. *Thesis Manuscript* University of Alberta.

Rashid A, Hobson N, Deyholos MK. 2012. A genomic region upstream of *Arabidopsis thaliana* PELPK1 promotes transcription in aleurone tissues and in response to *Pseudomonas syringae* or *Pythium irregulare*. *Plant Molecular Biology Reporter* **31**: 1025-1030.

Roppolo D, De Rybel B, Dénervaud Tendon V, Pfister A, Alassimone J, Vermeer JEM, Yamazaki M, Stierhof, Y-D, Beeckman T, Geldner. N 2011. A novel protein family mediates Casparian strip formation in the endodermis. *Nature* **473**: 380-383.

Scalabrin E, Radaelli M, Rizzato G, Bogani P, Buiatti M, Gambaro A, Capodaglio G. 2015. Metabolomic analysis of wild and transgenic *Nicotiana langsdorffii* plants exposed to abiotic stresses: unraveling metabolic responses. *Analytical and bioanalytical chemistry* **407**: 6357-6368.

Schaeffer A, Bouvier-Navé P, Benveniste P, Schaller H. 2000. Plant sterol-C24-methyl transferases: different profiles of tobacco transformed with SMT1 or SMT2. *Lipids* **35:** 263-269.

Schmidt J. 2016. Negative ion electrospray high-resolution tandem mass spectrometry of polyphenols. *Journal of Mass Spectrometry* **51**: 33-43.

Serra O, Soler M, Hohn C, Sauveplane V, Pinot F, Franke R, Schreiber L, Prat S, Molinas M, Figueras M. 2009. CYP86A33-targeted gene silencing in potato tuber alters suberin composition, distorts suberin lamellae, and impairs the periderm's water barrier function. *Plant Physiology* **149**: 1050-1060.

Serra O, Hohn C, Franke R, Prat S, Molinas M, Figueras M. 2010. A feruloyl transferase involved in the biosynthesis of suberin and suberin-associated wax is required for maturation and sealing properties of potato periderm. *The Plant Journal* **62**: 277-290.

Skene DS. 1982. The development of russet, rough russet and craks on the fruit of the apple Cox's Orange Pippin during the course of the season. *Journal of Horticultural Science* **57**: 165-174.

Torras-Claveria L, Jáuregui O, Codina C, Tiburcio AF, Bastida J, Viladomat F. 2012. Analysis of phenolic compounds by high-performance liquid chromatography coupled to electrospray ionization tandem mass spectrometry in senescent and water-stressed tobacco. *Plant Science* **182:** 71-78.

Tukey LD. 1969. Observations on the russeting of apples growing in plastic bags. *Journal of American Society for Horticultural science* **74**: 30-39.

Uversky VN. 2013. A decade and a half of protein intrinsic disorder: Biology still waits for physics. *Protein Science: a publication of the protein society* **22**: 693-724.

Valinas MA, Lanteri ML, Ten Have A, Andreu AB. 2015. Chlorogenic acid biosynthesis appears linked with suberin production in potato tuber (*Solanum tuberosum*). *Journal of Agricultural and Food Chemistry* **63:** 4902-4913.

Vandesompele J, De Preter K, Pattyn F, Poppe B, Van Roy N, De Paepe A, Speleman F. 2002. Accurate normalization of real-time quantitative RT-PCR data by geometric averaging of multiple internal control genes. *Genome Biology* **3**: RESEARCH0034.

Velasco R, Zharkikh A, Affourtit J, Dhingra A, Cestaro A, Kalyanaraman A, Fontana P *et al.* 2010. The genome of the domesticated apple (*Malus* x *domestica* Borkh.). *Nature Genetics* **42**:833-839.

Vishwanath SJ, Delude C, Domergue F, Rowland O. 2015. Suberin: biosynthesis, regulation, and polymer assembly of a protective extracellular barrier. *Plant Cell Reports* **34**: 573–586.

Vishwanath SJ, Kosma DK, Pulsifer IP, Scandola S, Pascal S, Joubès J, Dittrich-Domergue F, Lessire R, Rowland O, Domergue F. Suberin-associated fatty alcohols in Arabidopsis: distributions in roots and contributions to seed coat barrier properties. *Plant Physiology* **163**: 1118-1132.

Wang YZ, Dai MS, Zhang SJ, Shi ZB. 2014. Exploring candidate genes for pericarp russet pigmentation of sand pear (*Pyrus pyrifolia*) via RNA-Seq data in two genotypes contrasting for pericarp color. *PLoS One* **9**: e83675.

Wellesen K, Durst F, Pinot F, Benveniste I, Nettesheim K, Wisman E, Steiner-Lange S, Saedler H, Yephremov A. 2001. Functional analysis of the LACERATA gene of Arabidopsis provides evidence for different roles of fatty acid ω-hydroxylation in development. *Proceeding of the National Academy of Sciences* USA **98**: 9694-9699.

Winkler A, Grimm E, Knoche M, Lindstaedt J, Köpcke D. 2014. Late-season surface water induces skin spot in apple. *HortScience* **49**: 1324-1327.

Yadav V, Molina I, Ranathunge K, Castillo IQ, Rothstein SJ, Reed JW. 2014. ABCG transporters are required for suberin and pollen wall extracellular barriers in Arabidopsis. *The Plant Cell* **26**: 3569-3588.

Zhao Q, Nakashima J, Chen F, Yin Y, Fu C, Yun J, Shao H, Wang X, Wang Z-Y, Dixon RA. 2013. Laccase is necessary and nonredundant with peroxidase for lignin polymerization during vascular development in Arabidopsis. *The Plant Cell* **25**: 3976-3987.

Zhong R, Lee C, Zhou J, McCarthy RL, Ye ZH. 2008. A battery of transcription factors involved in the regulation of secondary cell wall biosynthesis in Arabidopsis. *The Plant Cell* **20**: 2763-278.

Chapter IV

MdMyb93 is a regulator of suberin deposition in russeted apple fruit skins

Summary and Perspectives

During the last decade, reverse genetics studies in model plants such as *A. thaliana* strongly improved our understanding of the suberin biosynthesis pathways. Numerous genes involved in the biosynthesis of the precursors and more advanced suberin monomers are now identified. The remaining unknown steps relate to the final assembly of these suberin monomers into suberin and to the regulation of the suberin deposition.

In apple, a recent study showed that the MdSHN3 transcription factor regulates cuticle deposition and inhibits russeting. However, it is still unclear whether the antagonistic effect of this transcription factor on russeting is direct or indirect. In *A. thaliana*, AtMYB41 induces the expression of key suberin biosynthetic genes, such as the *A. thaliana* suberin feruloyl-acyl transferase (*ASFT*), the ketoacyl-CoA synthase 2 (*KCS2*), the *CYP86A1* and *CYP86B1* fatty acid hydroxylase, the glycerol-3-phosphate acyltransferase 5 (*GPAT5*) or the fatty acid reductases (*FAR1*, *FAR4*, *FAR5*), which was supported by the increased suberin deposition. It is noteworthy that AtMYB41 is expressed in the root endodermis under stress condition, such as high salinity.

In russeted apples, our previous study (Chapter I and III) showed that the AtMYB41orthologous gene did not display any differential expression between russeted and waxy skins and was expressed at a low level, suggesting that other transcription factors might be specific to the development of the fruit. Conversely,

our transcriptomic works (Chapter I and III) highlighted other members of the MYB family transcription factors which were more expressed in the russeted apple skin. These include transcription factors similar to the *Arabidopsis* MYB36, MYB52, MYB67, MYB93 and MYB102. The function of MYB36 and MYB67 are unknown, whereas MYB102 has been presented as a new stress-inducible suberin regulator, at the International Symposium on Plant Lipids (July 2016, Kosma team), MYB52 has been previously linked with the cell wall lignification. Finally, MYB93 was previously described as a negative regulator of the lateral root formation in *A. thaliana*. However, in our work, the expression of MdMYB93 and some of the above-cited key suberin biosynthetic genes showed strong correlations.

In order to assess its role in the suberin biosynthesis, transient expression of MdMYB93 in *N. benthamiana* using the Gateway® cloning methodology has been performed. *N. benthamiana* is a powerful model to study the effect of MdMYB93, as its leaves do not accumulate suberin in normal growth conditions. A gene expression profiling, using RNA-Seq, showed a strong induction of genes involved in the core suberin biosynthesis, which was comparable to those observed with AtMYB41. The enhanced expression of these genes was supported by the strong accumulation of suberin monomers such as the C22 and C24 monoacylglycerols. Moreover, alkyl-ferulates, which are crucial components of the suberin-associated waxes, also accumulated. This enhanced suberin monomer synthesis was accompanied by the increased expression of a number of ATP-binding cassette subfamily G half transporters (ABCG) and lipid transfer proteins, which might be involved in the export of the suberin building blocks outside of the cell. As observed in the biochemical analysis of 'Cox orange Pippin', the depolymerisation of the *N. benthamiana* leaves transformed with MdMYB93 showed a drastic increase in alkanoic acids, ω-hydroxacids, α,ω diacids and

primary fatty alcohols, with a remarkable fraction of long chain C22 and C24-derived methyl-esters supporting the *de novo* synthesis of suberin. The observation of the epidermal cell walls using berberine/aniline blue staining and ultra-violet microscopy also confirmed the enhanced accumulation of suberin in leaves transformed with MdMYB93.

Apart from the core suberin biosynthesis pathway, MdMYB93 seems to trigger directly or indirectly the remobilization of conjugated-hydroxycinnamic acids, which might be further used for the synthesis of ferulic acid. We found increased contents of the feruloyl putrescine and feruloyl-tyramine. The feruloyl-putrescine can be considered as a storage form of ferulic acid which might accumulate in abnormal proportion due to the MdMYB93 overexpression, while the feruloyl-tyramine has been considered as a component of the lignin-like suberin polyphenolic domain (SPPD). It is noteworthy that MdMYB93 regulates numerous genes implicated in the cell wall modification as those observed in our previous RNA-Seq studies, suggesting that this transcription factor also orchestrates cell wall remodelling to facilitate the anchoring of the SPPD (Chapter III). However, a deeper investigation of this part of the suberin polymer had to be performed to better understand the interaction between the SPPD and the primary cell wall (Chapter III, this chapter).

Finally, the gene expression profiling of the MdMYB93-induced genes showed a number of interesting new candidates. Among them, GDSL-motif lipases and α,β-fold protein hydrolases might be implicated in the final assembly of suberin. Moreover, the *MYB52*, and *MYB67* genes were also induced by MdMYB93 and constitute highly valuable candidate genes for further functional validation studies. Indeed, in Chapter III, *MYB67* has been linked to the suberin-associated pentacyclic triterpenes, whereas *MYB52* seemed to be linked with the core suberin synthesis.

Altogether, the discovery of MdMYB93 constitutes a major improvement in the understanding of the suberin biosynthesis regulation in apple. However, the upstream-regulatory elements which drive MdMYB93 and, by extension, the russeting development, remain unknown. Additionally, MdMYB93 also provides new insights for further industrial applications aiming at producing raw or modified suberin for eventual use as source of long chain fatty acid or coatings. In this context, a patent has been filed in 2016, which describes a suberin production process using MdMYB93.

Chapter IV highlights:

Outcome:

- MdMYB93 is a master regulator of suberin synthesis in russeted apple.
- The cell wall modification process observed in chapter I and III is also regulated by MdMYB93.
- Gene expression profiling of the MdMYB93 transcription factor provides candidate genes putatively implicated in the suberin assembly.
- From this chapter, a patent has been filed in Luxembourg n°93026.

Questions raised:

- What are the upstream regulatory elements, which drive the expression of MdMYB93?
- What are the functions of MYB67 and MYB52?

General discussion

During the last decades, apple russeting has been increasingly considered as a default by consumers, causing part of the fruit production to be devaluated due the appearance of this unexpected phenotype on the fruit skin surface. This is particularly true for the old heritage fully russeted apple cultivars such as the 'Patte de Loup' or 'Canada Gris', which are difficult to find in the market stalls and supermarkets for this particular reason. However, the particularly problematic aspect is that russeting is also observed in commercial apples, where suberized patches randomly spread on the fruit surface. An example of such a phenotype is observed in the well-studied variety 'Cox Orange Pippin'. Since the 60s, russeting has been widely studied at the horticultural, histological and rheological level, providing crucial progresses in the knowledge of factors favoring the development of this undesired phenotype (Walter 1967, Tukey 1969, Watanabe 1969, Skene 1982, Knoche and Grimm 2008, Lashbrooke *et al*. 2015). Environmental and developmental factors seem to have an impact on the fruit skin surface and, more particularly, on the cuticle layer (Walter 1967, Tukey 1969, Knoche and Grimm 2008). Indeed, several histological studies have associated the apple russeting with the development of a thinner cuticle layer (Skene 1982, Knoche and Grimm 2008). A recent work showed that the MdSHN3 transcription factor regulates the cuticle synthesis in apple (Lashbrooke *et al*. 2015). In addition to be correlated with a thinner cuticle layer, a low *MdSHN3* expression has been also linked to russeting. Inversely, fruits showing a thicker cuticle layer, display a higher expression of this regulator, which seems to inhibit russeting (Lashbrooke *et al*.

2015). However, it is still difficult to assess whether MdSHN3 has a direct effect on the suberin biosynthesis or if it is due to indirect effects. In this perspective, this thinner cuticle seems to be more fragile and stiffer favoring the development of multiple defects called microcracking (Knoche *et al*. 2011, Curry 2012, Khanal *et al*. 2013). Cuticle microcracking is already observed in young fruits and seems to be due to the extreme tangential tensions occurring on the fruit surface during this period of exponential growth (Knoche *et al*. 2011, Curry 2012, Khanal *et al*. 2013). These damages in the cuticle layer are suspected to induce a mechanical or wounding response, which might further trigger the suberization process, the latter being considered as a healing mechanism (Sironval and Clijters 1962, Walter 1967, Faust and Shear 1972, Skene 1982). The cuticle and suberin biosynthesis pathways have been extensively studied in model plants, such as *Arabidopsis thaliana*, *Solanum tuberosum* L., *Solanum lycopersicum* and *Quercus suber* L. (Yeats and Rose 2013, Wishwanath *et al*. 2015, Graca 2015, Ayvaz *et al*. 2016, and citations). In apple, as the first genome draft has been released in 2010, only few studies describing gene expression data and functional validation are currently available (Velasco *et al*. 2010, Lashbrooke *et al*. 2015). Key genes involved in the russeting process are only hypothesized from annotations obtained against model plants and their selection is a hard task due to the high redundancy of the apple genome structure. Moreover, the apple russeting process is not restricted to a differential accumulation of the cuticle and suberin, since other metabolic processes are implicated in this particular phenotype. As an example, the pentacyclic triterpenes have been previously shown to be differentially represented in the russeted and waxy apple skins (André *et al*. 2012). In order to get a global overview of the genes involved in the apple russeting, we performed two large transcriptomic analyses with distinct approaches (Legay *et al*. 2015, Legay *et al*. Chapter III). The bulk transcriptomic analysis allowed us to extract

the most relevant biological processes implicated in the establishment of russeted and waxy apple skin and to discard traits which are more specific to each variety. However, this methodology is highly stringent because it requires individuals within groups which are closely related to each other in terms of expression levels. We can expect that a small part of genes implicated in these traits might have been lost during the statistical analysis due to higher variability between cultivars. Additionally, these apple varieties were collected at commercial maturity stage (roughly 150 days after full bloom) and did not provide any information about the early stages of the fruit development. For these reasons, a second gene expression study was set up from two closely related varieties differing in the skin surface, which were collected at 5 time-points during the fruit development. Although 5-times more sequence reads were generated in this second experiment, the differentially regulated genes selected from both work were quite similar. Indeed, for gene expression profiling studies, a deep sequencing provides a better detection limit for genes which are expressed at a low level. However, these usually do not pass the statistical filtering. In addition, we can speculate that genes displaying a strong expression might have more influence on the final trait of interest than copies expressed at a lower level. Inversely, deep sequencing is crucial for alternative splicing detection and new genes discovery, but this was not the aim of the present thesis. Finally, it is also crucial to keep in mind that gene expression is only one of the numerous steps which leads to the synthesis of proteins and/or metabolites. As a number of post-transcriptional modifications can occur after mRNA synthesis, caution should be taken with the interpretation of gene expression data. In order to strengthen our data, we compared, in the chapter III, results obtained from transcriptomic and proteomic approaches. Despite the fact that the proteomic dataset was less rich, both -omics displayed strong similarities in terms of trends in gene expression and gene identification. It is

noteworthy that the use of a common reference (*M*. x *domestica* predicted transcriptome v1) for each approach made easier the comparision between these two powerful tools.

A. Synthesis of cutin and suberin and their associated waxes was inversely regulated between russeted and waxy apple skin

Globally, russeted apples displayed a lower expression of genes involved in the cuticle and wax synthesis. Part of these genes are orthologous to those already identified in *A. thaliana*, but the function of other genes remain undetermined. The primary synthesis of very long chain acyl-CoA, which is further used for the wax synthesis, was impaired in russeted apples. As an example, several 3-ketoacyl-CoA synthase (*KCS1*, *KCS2*, *KCS6*, *KCS10*, *KCS11* and *KCS19*) and other *ECERIFERUM* (*CER*) genes such as *CER1*, *CER2*, *CER3*, *CER8* to name a few, displayed a decreased expression in the russeted apples (Aarts *et al*. 1995, Xia *et al*. 1996, Millar *et al*. 1999, Rowland *et al*. 2007, Joubes *et al*. 2008, Lü *et al*. 2009). Moreover, cutin biosynthesis genes showed an analogous expression pattern in our experiments (RNA-Seq and RT-qPCR), suggesting that both pathways might be regulated by common actors. As an example, apple orthologues of the cytochrome P450 family 86 sub-family A2 (*CYP86A2*) and *CYP86A8* fatty acid hydroxylases, the *CPY77A4* monooxygenase, displayed a decreased expression in russeted apples (Sauveplane *et al*. 2009, Wellesen *et al*. 2001, Xiao *et al*. 2004). These genes are involved in the synthesis of ω-hydroxyacids and α,ω-diacids constituting the basic precursors of the cutin monomers, the latter being putatively synthesized by the apple orthologous gene of the *A. thaliana* glycerol-3-phosphate acyl transferase 6 (*GPAT6*, Li and Beisson 2009). Conversely, a specific increased expression of suberin biosynthesis genes occurred in the russeted tissues including the well-known *CYP86A1* and *CYP86B1*

fatty acid hydroxylase and very long chain fatty acid hydroxylase, respectively, a feruloyl hydroxycinnamoyl transferase similar to the *A. thaliana* suberin feruloyl transferase gene (*ASFT*), and a suberin specific *GPAT5*, which is responsible for the core suberin monomer synthesis in thale cress (Benveniste *et al*. 1998, Beisson *et al*. 2007, Höfer *et al*. 2008, Compagnon *et al*. 2009). Interestingly, two *KCS* genes (*KSC2, KCS4*) were also specifically induced in the suberized tissues (Fig. 6-1). In *A. thaliana*, KCS2 is a major actor of the very long chain fatty acid synthesis and displays a redundant function in both the cuticular wax and suberin biosynthesis, producing predominantly C22 and C24 very long chain fatty acids (VLCFA, Lee *et al*. 2009). In apple, we speculate that these two differentially and inversely regulated *KCS2* copies found in the transcriptomic data might also have a similar function, *i.e*. the synthesis of 22 and 24 carbon chain suberin precursors (Lee *et al*. 2009). The role of KCS4 remains unclear. In *A. thaliana*, KCS4 is not able to use the 16 and 18 carbon chain fatty acids as precursors suggesting that it might participate in the elongation of longer carbon chains (Blacklock and Jaworski 2006, Joubès *et al*. 2008). In suberized tissues, the synthesis of C16 fatty acid precursors, which are further elongated by these KCS, seemed to involve a fatty acyl-ACP thioesterase B (Bonaventure *et al*. 2003). Similarly, some upregulated triacylglycerol lipase 3 and lipase 1 might also be implicated in the remobilization of fatty acids and glycerol and provide an alternative source of precursors for the suberin biosynthesis process. Interestingly, these anti-correlated expression patterns of the cuticle and suberin biosynthesis genes were observed in fully russeted apples, as well as in the suberized patches of the semi russeted varieties, suggesting that the russeting process might be similar in all apple varieties and might differ in terms of intensity. The comparison of the lipid composition of the waxy and russeted skin surface strongly supported these observations. The russeted patches of the 'Cox Orange Pippin' showed a drastic

decrease in the cuticle components. As an example, the wax composition showed a strong decrease in very long chain (C26 to C30) fatty acids, alkanes, primary alcohols and aldehydes, which is in accordance with the decreased expression of wax synthesis-related *CER* and *KCS* genes discussed above (Aarts *et al*. 1995, Millar *et al*. 1999, Rowland *et al*. 2007, Lee *et al*. 2009, Lü *et al*. 2009, Von Wettstein-Knowles 2012, Lee and Suh 2013). Additionally, the global decrease of C16, C18, and C18:2 ω-hydroxyacids, which compose the cutin biopolymer (Franke *et al*. 2005), also supports the transcriptomic results and corroborates previous works which showed a deficient/thinner cuticle layer in russeted skin (Knoche and Grimm 2008, Khanal *et al*. 2013, Lashbrooke *et al*. 2015). Conversely, russeted tissues specifically accumulated C20, C22 and C24 chain suberin monomer, higher levels of α,ω-dicarboxylic acids and ferulic acid, a finding which is similar to previous observations in other plant species such as *A. thaliana* roots, *S. tuberosum* tubers or *Q. suber* bark (Graca and Pereira 2000a, Graca and Pereira 2000b, Franke *et al*. 2005, Molina *et al*. 2006). It is noteworthy that the suberin monomers and their associated waxes seemed to be restricted to C chain size ranging from 20 to 24, suggesting that KCS2 and KCS4 might not be able to produce fatty acid precursors with longer chain size. Interestingly, fatty acids, which accumulated in *N. benthamiana* leaves expressing *MdMYB93*, showed similar results, as well as alkyl-hydroxycinnamates which usually specifically accumulate in the russeted/suberized apple skin. Indeed, primary alcohols constituting the aliphatic moieties of these suberin-associated waxes were also predominantly composed by C22 and C24 C chains. As observed in model plants, the fatty acid precursors produced by the above-mentioned KCSs might be converted into primary alcohols by the fatty acid reductases (FAR), which were more expressed in the russeted tissues (Schreiber *et al*. 2005, Serra *et*

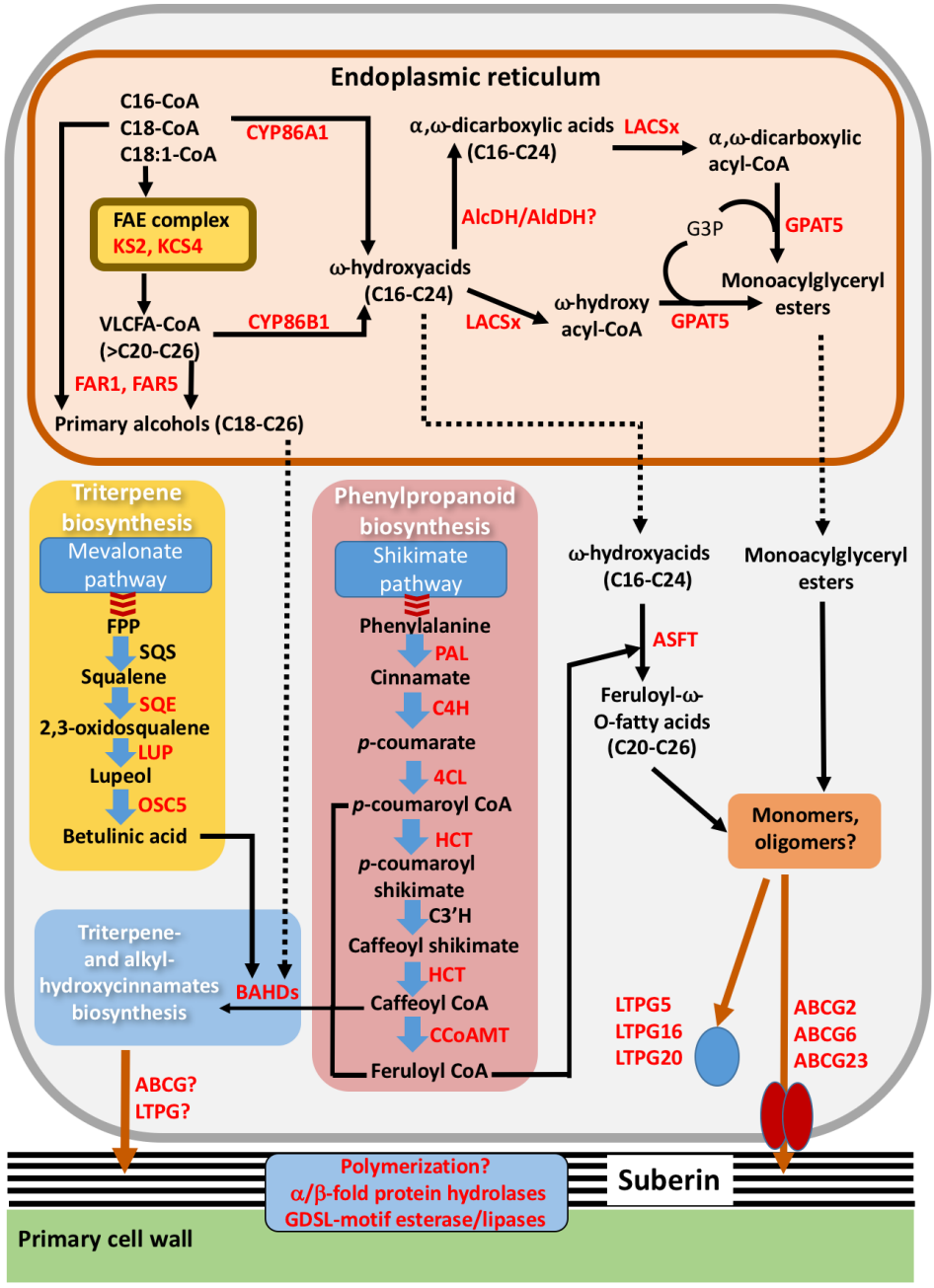

Figure 6-1: see legend on next page.

Previous page: figure 6-1: Schematic representation of the suberin polyaliphatic domain biosynthesis pathway in russeted apple. Enzymes highlighted in red displayed an increased expression of their respective genes in russeted apple skin. KCS: 3-ketoacyl-CoA synthase, FAR: fatty acid reductase, CYP86A1: fatty acid hydroxylase, CYP86B1: very long chain fatty acid hydroxylase, AlcDH: alcohol dehydrogenase, AldDH: aldehyde dehydrogenase, LACS: long chain acyl-CoA synthetase, GPAT: glycerol-3-phosphate acyltransferase, ASFT: aliphatic suberin feruloyl transferase, ABCG: ATP-binding cassette family G, LTPG: lipid transfer protein family G. VLCFA: very long chain fatty acid, PAL: phenylalanine ammonia-lyase, C4H: cinnamic acid 4-hydroxylase, 4CL: 4-coumarate-CoA ligase, HCT: hydroxycinnamoyl-coenzyme A shikimate:quinate hydroxycinnamoyl-transferase, C3'H: *p*-coumaroyl shikimate 3'-hydroxylase, CCoAOMT: caffeoyl-CoA 3-*O*-methyltransferase, SQS: squalene synthase, SQE: squalene epoxidase, LUP: lupeol synthase, OSC: oxidosqualene cyclase, BAHD: BAHD acyl transferase.

al. 2010, Kosma *et al*. 2012, Kosma *et al*. 2015, Molina and Kosma 2015, Delude *et al*. 2016). Interestingly, only genes encoding FAR5 and a putative FAR1 were differentially regulated in our data, whereas, in *A. thaliana* roots, an additional FAR4 has been described to participate in the synthesis of these suberin-associated fatty alcohols (Fig. 6-1, Domergue *et al*. 2010).

Apart from the lipid metabolism, the phenylpropanoid biosynthesis pathway was also strongly impacted in russeted tissues. Several genes involved in the synthesis of hydroxycinnamic acids were highlighted, such as phenylalanine ammonia lyase (*PAL1*), cinnamate-4-hydroxylase (*C4H*), 4-coumarate-CoA Ligase (*4CL*), ferulic acid-5 hydroxylase (*FAH*), hydroxycinnamoyl-CoA shikimate/quinate hydroxycinnamoyl transferase (*HCT*), a large number of *O*-methyltransferase (*OMT*) and caffeoyl-CoA *O*-methyltransferase (*CCoAMT*), suggesting an enhanced biosynthesis of hydroxycinnamic acids and, particularly, ferulic acid (Fig. 6-1, Fraser and Chapple 2011, Graca 2015, Wishwanath *et al*. 2015). A previous work showed that free hydroxycinnamic acid contents are significantly higher in russetted apple skin (Andre et al 2012). This was also supported by the

increased content in ferulic acid observed in the depolymerized extract of the 'Cox Orange Pippin' russeted patches and in the *N. benthamiana* leaves overexpressing *MdMYB93*. Furthermore, in the same tissues, a concomitant decreased expression of some cinnamoyl-CoA reductase (*CCR*) and cinnamyl alcohol dehydrogenase (*CAD*) genes was observed, suggesting that a decreased biosynthesis in monolignols, which are crucial precursors of lignin, occurred. Moreover, this decreased monolignol synthesis might also favor the increased accumulation of hydroxycinnamic acids observed in our data. One of the proposed suberin structure models suggests that the suberin polyphenolic domain, which is anchored in the primary cell wall, shares a similar structure with lignin, with, notably, increased contents in hydroxycinnamic acids, mainly ferulic acid (Bernards *et al*. 1995, Bernards 2002). The present data support this hypothesis and further analyses of the suberin polyphenolic domain composition produced by the MdMYB93 overexpression might validate this crucial point.

Our data also highlighted numerous genes involved in the pentacyclic triterpenes biosynthesis, which constitute a major part of the apple skin wax compared to other plant models, such as *A. thaliana* (Jägger *et al*. 2009, André *et al*. 2012). As suggested by previous studies performed on apple, a differential accumulation of the ursane, oleane and lupane series triterpenes was observed between russeted and waxy skin, the triterpenic acids ursolic acid and oleanolic acid being strongly accumulated in the waxy skin whereas lower contents were observed in the russeted apple. Conversely, betulinic acid and betulinic acid-3-*trans*-caffeate specifically accumulated in the russeted tissues, suggesting their synthesis might be co-regulated with the suberin synthesis pathway (André *et al*. 2012, André *et al*. 2013). Interestingly, in 'Cox Orange Pippin', betulinic acid was found only in the depolymerized extract, suggesting that this compound might be embedded in the suberin matrix, strengthening the tight relationship observed between the

suberin and the lupane triterpene series biosynthesis. In addition to the already identified genes involved in the biosynthesis of the different triterpene series, numerous new candidates, which were also differentially regulated in both tissues, have been found (Brendolise *et al*. 2011, André *et al*. 2016). This provides an extensive list of valuable candidates putatively involved in the biosynthesis of already identified triterpenes, as well as minor undetermined ones, which were found in 'Cox Orange Pippin'. Finally, the synthesis process leading to betulinic acid-3-*trans*-caffeate remains unclear due the difficulty to extract, among the large number of genes, a reduced number of relevant candidates putatively responsible for the synthesis of this compound.

From a more global point of view, the transcriptomic profiling of the growth kinetics of the 'Canada Gris' and 'Canada Blanc' varieties provided important insights in the regulation of the cutin, suberin and their associated waxes (including triterpenes) biosynthesis. As an example, it is noteworthy that during the early stage of the russeted apple fruit growth, the expression of the cuticle biosynthesis genes further decreased with the fruit enlargement and the increased expression of the suberin biosynthesis gene. However, it is difficult to assess whether this was caused by the exponential growth of the fruit and concomitant appearance of cuticle microcracking, or if the enhanced suberin biosynthesis directly impacted the cuticle biosynthesis (Knoche and Grimm 2008). Conversely, 'Canada Blanc' showed a persistent higher expression of the cuticle synthesis genes from the early stage to the latest stages of the fruit growth. However, this variety also showed a constant increasing expression of the suberin biosynthesis genes during the time course of the experiment with a concomitant development of russeting of the fruit surface. It is tempting to speculate that this increasing suberin deposition in 'Canada Blanc' might also result from cuticle microcracking, which might be caused by developmental and environmental

factors. However, this phenomenon seemed to be less pronounced compared to the russeted variety, suggesting that the decreased expression of cuticle biosynthesis genes might be considered as an aggravating factor more than the main cause of the cuticle microcracking formation.

B. The role of α/β-fold hydrolases, GDSL esterase/lipases and BAHD acyltransferases

Our three different gene expression profiling highlighted, among the differentially expressed genes, a relatively high proportion of members of the α/β-fold hydrolase, GDSL esterase/lipase and BAHD acyltransferase families, which might participate in crucial steps of (i) the suberin and cutin assembly, as well as the synthesis of conjugates found in the suberin-associated waxes, such as the triterpene- and alkyl-hydroxycinnamates (Fig. 6-2). As an example, a Li-tolerant lipase, which was similar to the LTL1 GDSL-lipase, might be a major actor of the cutin assembly in the apple fruit skin (Yeats *et al*. 2012, Girard *et al*. 2012). Moreover, since suberin and cutin share a similar structure, we can speculate that the suberin assembly might use enzymes displaying similar functions to these cutin-specific GDSL-lipase and α/β-fold hydrolase (Kurdyukov *et al*. 2006, Girard *et al*. 2012, Yeats *et al*. 2012, Yeats *et al*. 2014, Vishwanath *et al*. 2015). This was also supported by our different co-expression networks which clearly associate part of these genes with the core suberin biosynthesis network. Among the BAHD acyltransferases found in our data, genes highly similar to the *A. thaliana* gene for defective in cuticular ridges (*DCR*) or the *Arabidopsis* gene for suberin feruloyl transferase (ASFT), which is involved the suberin monomer synthesis, have been identified (Panikashvili *et al*. 2009, Molina *et al*. 2009). However, the role of a large number of these family members remained undetermined. Since expression patterns correlated with the suberin and triterpenes biosynthesis genes were observed, it is plausible that some candidates

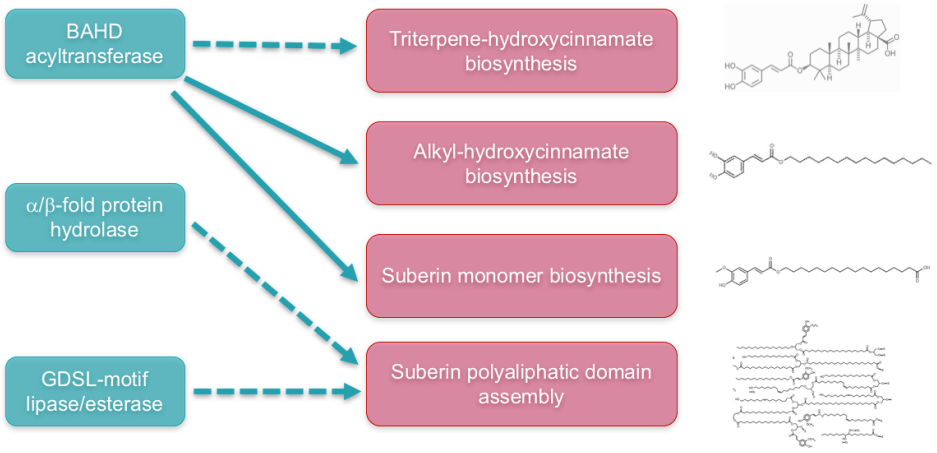

Figure 6-2: Involvement of BAHD acyltransferase, GDSL-motif esterase/lipase and α/β-fold protein hydrolase in the suberization process. Full arrows show functions, which were already described, whereas dashed arrows display functions, which are suspected or under investigation.

might play a critical role in these metabolic pathways. As an example, in other plant models, BAHD acyltransferases have been described as key players in the biosynthesis of alkyl-hydroxycinnamates, suggesting that some apple members might be involved in this process, too (Molina and Kosma 2015). Furthermore, it is also tempting to speculate that similar enzymes might be responsible for the synthesis of the triterpene-3-*trans*-caffeates found in the russeted tissues (André *et al*. 2013). In order to answer this question, we are currently working on some members of this family, trying to assess their role in the suberization process in apple.

C. Transport of cutin and suberin precursors was likely supported by dedicated ATP-binding cassette subfamily G and lipid transfer protein transporters

The ATP-binding cassette subfamily G (ABCG) members were the most represented transporters in both transcriptomic datasets. A number of these half

transporters seem to be involved in the extracellular export of cutin and suberin monomers and their associated waxes. In the waxy skin, an increased expression of *ABCG11* (also called White-Brown Complex 11, WBC11), *ABCG15*, *ABCG32* was observed. ABCG11 is a major transporter of cutin monomers and waxes in *A. thaliana*, while ABCG32 seems to be less specific as it also participates in the transport of suberin monomers (Bird *et al*. 2004, McFarlane *et al*. 2010, Langraf *et al*. 2014). In *Oryza sativa* ABCG15 is involved in the anther cuticle synthesis. (Qin *et al*. 2012). Conversely, some suberin-specific ABCG transporters were also found. Interestingly, in both gene expression profiling experiments, a second *ABCG11* was found, suggesting that there might be cutin- and suberin-specific ABCG11 transporters. In addition, *ABCG2*, *ABCG6* and *ABCG23* were co-expressed with suberin biosynthesis genes. ABCG2 and ABCG6 are major players of the suberin deposition in *A. thaliana* seed coat, whereas the function of ABCG23 is less clear. As observed in our data, only co-expression with some suberin synthesis genes such as *GPAT5* was established (Yadav *et al*. 2014).

Suberin and cutin monomers transport also involved a large number of lipid transfer proteins (LTP). Remarkably, our time course experiment revealed an *LTP3* gene, which showed a drastic expression decrease in the russeted apple, whereas a massive expression rate was observed in the waxy variety. Additionally, it was the most abundant protein observed in our proteomic analysis, suggesting that it might play a crucial role in the transport of waxes and/or cutin monomers (Li-Beisson *et al*. 2010). Conversely, some genes for lipid transfer proteins subfamily G (LTPG), including *LTPG5*, *LTPG16* and *LTPG20*, displayed a correlated expression with suberin biosynthesis genes. LTPG transporters are non-specific lipid transfer protein presenting a GPI-anchor at the C-terminal region, which links the protein to the external side of the plasma membrane (Edstam *et al*. 2013). Their exact function is still under investigation,

but they are thought to be involved in the transport of suberin monomers and phenylpropanoids (Edstam *et al*. 2013). Other genes coding for transporters were also differentially expressed in our datasets. However, their annotations and functions remain unclear, and further work focusing on these should be performed to elucidate their implication in the russet and waxy traits. Finally, the export of pentacyclic triterpenes out of the cell remains undetermined. However, we can speculate that some of the above-cited transporters might also be involved in this process (Yazaki 2006).

D. Russeting triggered a cell wall-modification process linked to the suberization process

Remarkably, our transcriptomic experiments showed a relevant number of genes which belong to the cell wall modification and organization processes. As an example, a number of genes coding for arabinogalactan proteins (AGPs), fasciclin-like arabinogalactan proteins (FLAs) and COBRA proteins, were up-regulated in the suberized skin. AGPs belong to a large family displaying multiple functions associated with cell wall polysaccharide assembly (Ellis *et al*. 2010). FLAs and COBRA proteins are thought to have a role in cell adhesion, cell wall expansion and the cellulose microfibril orientation, which is known to impact the cell wall stiffness and mechanical properties (Roudier *et al*. 2005; Liepman *et al*. 2010; MacMillan *et al*. 2010). This putative cell wall expansion process was also reinforced by the increased expression of xyloglucan endotransglycosylases (XETs), which are involved in the modification of xyloglucan, one of the most abundant hemicelluloses in primary plant walls, which is cross-linked with cellulose microfribrils. XETs are considered as the major regulator of cell wall expansion. These are able to cleave and elongate xyloglucan, leading to some remodeling activities aiming at increasing cohesion between primary and secondary cell wall (Bourquin *et al*. 2002). Expansins, which rapidly disrupt

hydrogen bonds between cellulose and hemicellulose and thus participate in cell wall expansion (Cosgrove 2005, Sampedro and Cosgrove 2005), showed a similar expression pattern compared to *XETs* and *FLAs*.

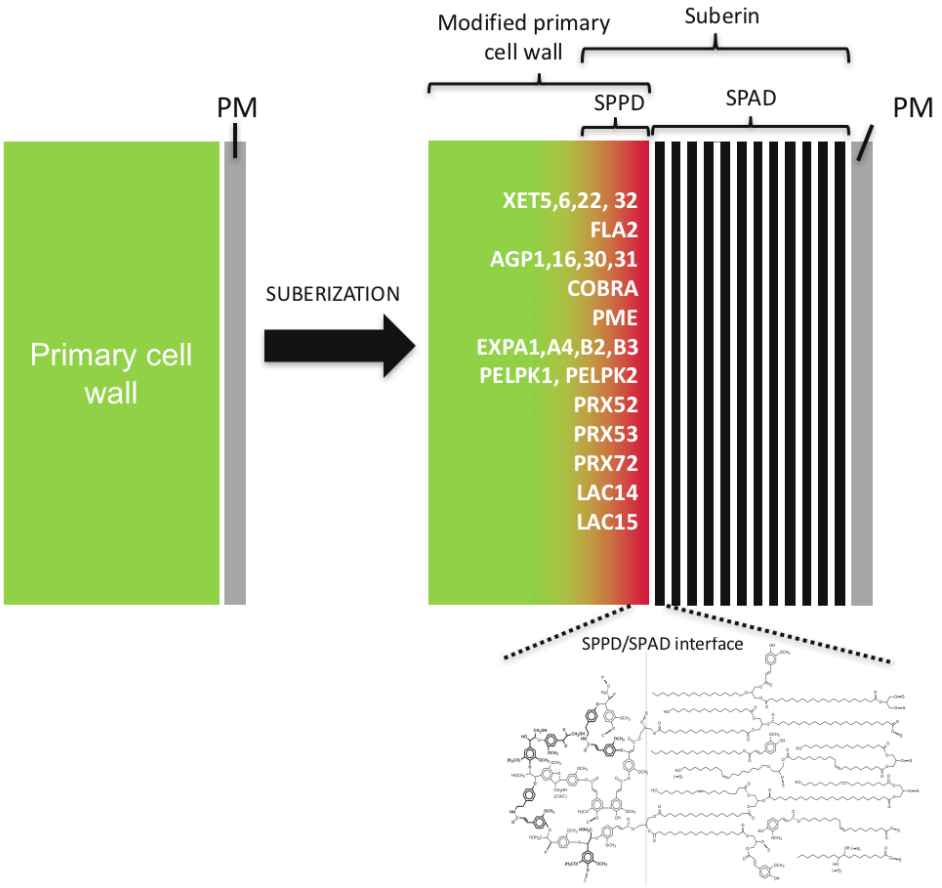

Figure: 6-3: Hypothetical model of the cell wall modification process built from gene expression data observed in russeted apple skin and based on the model described by Bernards (2002). PM: plasma membrane, SPPD: suberin polyphenolic domain, SPAD: suberin polyaliphatic domain, XET: xyloglucan endotransglycosylase, FLA: fasciclin-like arabinogalactan protein, AGP: arabinogalactan protein, COBRA: COBRA protein, PME: pectin methyl esterase, EXP: expansin, PELPK: Pro-Glu-LeuIIelVal-Pro-Lys protein, PRX: peroxidase, LAC: laccase.

Finally, the pectin structure might also be affected in the russeted tissues as a number of genes encoding modifying enzymes, such as pectin methylesterase inhbitors, showed an increased expression in suberized skin. The sigmoidal increase of fruit size triggers extreme biaxial tangential tensions and mechanical stresses leading to microcracking in the primary fruit skin *i.e*. cuticle, epidermis and hypodermis and, in certain cases, to tissue disruption (as observed in the 'Patte de Loup') (Watanabe 1969, Skene 1982, Curry 2009, Khanal *et al*. 2013). Thus, this strong alteration of the epidermal cell walls might be interpreted as a mechanism aiming to relax these tensions. Moreover, as observed for the suberin-related genes, the increased expression of these cell wall modification genes started in the early stage of the fruit development when the growth rate is maximal, suggesting that there is a robust link between fruit enlargement, cell wall modification and suberization process.

In addition to cell wall modification, the expression of peroxidases and laccases was also associated with russeting in our data. Among them, PRX72 is involved in the lignification process and the secondary cell wall thickening, while PRX52 participates in the polymerization of lignin S-units and PRX53 displays multiple functions, namely wound responses or flower development (Jin *et al*. 2011, Fernandez-Perez *et al*. 2015a, Fernandez-Perez *et al*. 2015b). The *Laccase 15* gene participates in the lignin synthesis in *A. thaliana* seeds and roots (Liang *et al*. 2006). However, the exact function of these laccases and peroxidases in the suberization process has been proposed, but never proven (Soler *et al*. 2007, Pollard *et al*. 2008). Indeed, as the suberin polyphenolic domain seems to share a similar structure with lignin (Bernards 2002), it is tempting to speculate that its assembly might engage similar processes. Phenolic monomers such as the G-units and the ferulic acid, which were found in the *N. benthamiana* leaves overexpressing *MdMYB93* might be polymerized by oxidizing enzymes such as

peroxidase and laccase described above. Moreover, XETs involved in xyloglucan modification, seem to play a role in the restructuration of the primary cell wall, favoring the interconnections with the secondary cell wall of vascular tissues (Bourquin *et al*. 2002). As some XETs and other cell wall modification enzymes were induced by *MdMYB93* in *N. benthamiana* leaves, it is plausible that these might also participate in the structural modification of the primary cell wall, favoring the anchoring of the suberin polyphenolic domain in the primary cell wall. Further investigation of the role of these cell wall modification proteins and oxidative enzymes in the suberization process might provide new insights into how the suberin polyphenolic domain is synthetized and linked within the cell wall; a question, which has been given less consideration compared to the suberin polyaliphatic domain synthesis pathway.

E. The russeting transcriptional regulatory network

The establishment of russeting in apple altered the expression of a large number of transcription factors, which were mostly represented by members of the MYB, NAC and WRKY family. Interestingly, a majority of these were repeatedly found in our data, suggesting that they could be considered as consistent candidates for further functional validation. MYBs, NACs and WRKYs are involved in a broad spectrum of biological processes such as senescence, the responses against biotic and abiotic stresses, seed dormancy and germination (Olsen *et al*. 2005, Dubos *et al*. 2010, Rushton *et al*. 2010). In our work, the majority of the differentially regulated transcription factors was spread across two groups and showed a correlated expression with (i) genes involved in the cuticle deposition process and (ii) genes related to the suberin biosynthesis and cell wall modification. Among the cuticle biosynthesis-related group, *MYB94*, *MYB15*, *MYB16*, *MYB17*, *MYB73*, *MYB106* and a *NAC90* displayed a decreased expression in the russeted apple skin. In *A. thaliana*, overexpression of MYB94 triggered the expression of waxes

synthesis genes, such as *WSD1*, *KCS1* or *CER1*, with a concomitant increased accumulation of cuticular waxes (Lee and Suh 2015). The MYB16 and MYB106 MIXTA-like transcription factors coordinately regulate the cuticle synthesis with SHN1 (Oshima *et al*. 2013). Silencing of the MYB16 resulted in a decreased expression of the *LCR* (*CYP86A8*), and *CER1* (fatty acid hydroxylase) genes, with an associated increased cuticle permeability (Oshima and Mitsuda 2013). The SHN1 transcription factor was described as a major regulator of the cutin synthesis in *A. thaliana*.

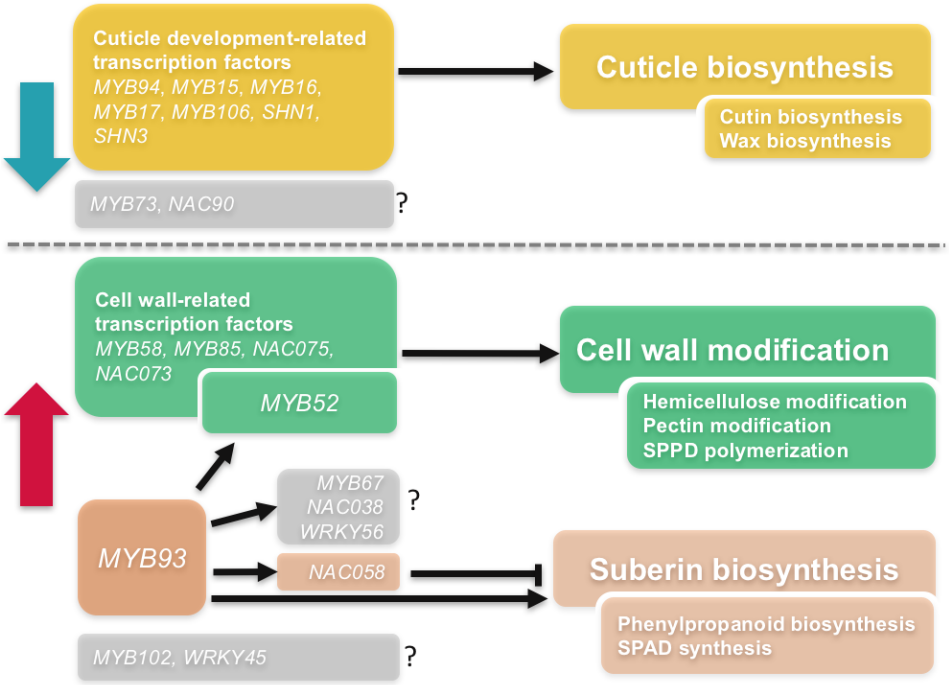

Figure 6-4: Tentative regulatory network occurring during apple russeting. The blue and red arrows show the gene expression trend found in RNA-Seq data. Transcription factor genes, which were previously associated with the cuticle development (yellow), cell modification (green) and suberin deposition (brown) are highlighted with the corresponding colour. Transcription factor genes with unknown functions are highlighted in grey.

When overexpressed, strong increases in C16 and 18:1 ω-hydroxyacids which are characteristic monomers of the cutin, were observed (Kannangara *et al*. 2007). In our work, the apple *MdSHN3*, which is similar to *SHN1*, was also down-regulated in the russeted apple. Moreover, a recent work showed that a higher expression of this cuticle biosynthesis master regulator leads to an increased deposition of cuticle, which seemed to inhibit russeting (Lashbrooke *et al*. 2015). However, as explained above, it is not clear whether MdSHN3 directly or indirectly impacts the suberization process. MYB17 is similar to MYB106 and MYB16 and seems to participate in the early inflorescence development and seed germination, but its role in the cuticle deposition process is still unclear (Zhang *et al*. 2009, Oshima and Mitsuda 2013). In *A. thaliana*, overexpression of the *MYB15* leads to an increased expression of the ABA-mediated *RESPONSE TO DEHYDRATION* (*RD22*) regulator gene and an improved drought tolerance. The cuticle development has been previously associated with abiotic stress responses, such as dehydration, which is partly regulated by ABA (Hen-Avivi *et al*. 2014). In our data, an *RD22* gene was also co-expressed with these transcription factors, suggesting that an ABA-mediated signaling cascade might play a role or is impacted by the regulation of cuticle synthesis in apple through the differential expression of MYB15. However, further work has to be performed to validate this hypothesis.

Transcription factors displaying a higher expression in the russeted tissues included MYB52, MYB58 and MYB85 which are regulated by the SND1 master regulator and associated with the secondary cell wall thickening. However, the role of these regulators is still under debate. As an example, in *A. thaliana,* previous studies showed antagonistic roles for MYB52 in secondary cell wall thickening (Zhong *et al*. 2008, Cassan-Wang *et al*. 2013). In a perspective work, we performed a gene expression profiling in *N. benthamiana* leaves

overexpressing *MdMYB52*, which showed a probable implication in the lignification and the senescence process, but further analysis of the cell wall composition has to be performed in order to assess these results (Legay *et al*. ongoing work).

Additionally, russeted tissues showed an increased expression of *NAC075* and *NAC073*/*SND2*, which are also implicated in secondary cell wall formation (Hussey *et al*. 2011, Sakamoto and Mitsuda 2015). SND2 regulates cellulose, xylan and mannan synthesis as well as lignin polymerization (by the action of laccases), but is not involved in the regulation of monolignol synthesis (Hussey *et al*. 2011). Altogether, these data support our hypothesis suggesting that the suberization process might engage cellular processes similar to the lignification of the secondary cell wall leading to the suberin polyphenolic domain assembly and anchoring. Moreover, MYB102, which was found in our dataset, has a dual role in cell wall modification and suberin deposition. Indeed, this transcription factor enhances the expression of expansins, XETs or pectin esterases in response to wounding in *A. thaliana* (De Vos *et al*. 2006). However, Kosma and coworkers very recently demonstrated that it also regulates suberin synthesis in similar conditions (personal communication: International Symposium on Plant Lipids). Finally, we focused our efforts on MYB93, which displayed high correlation with some suberin synthesis genes such as the *GPAT5*, *CYP86A1* and *CYP86B1*. In *A. thaliana*, AtMYB93 has been previously shown to negatively regulate the lateral formation (Gibbs *et al*. 2014). However, the transient expression of *MdMYB93* in *N. benthamiana* leaves clearly demonstrates its major role in suberin biosynthesis in apple. The increased expression of suberin synthesis genes was supported by the accumulation of characteristic suberin precursors with 22 and 24 C chains and their corresponding suberin monomers in the depolymerized extract. It is noteworthy that in addition to the already known suberin biosynthesis genes, the

gene expression data highlighted genes for other transcription factors, which might be also implicated in the suberin synthesis. These include *MYB67*, which has been linked with the suberization process in our time course experiment, *NAC058*, *NAC038*, *WRKY56* and *WRKY45*, which were associated with russeting in both gene expression studies in apple. NAC058 was previously described as a negative regulator of the suberin biosynthesis, suggesting that it might have a role in the feed-back regulation of the suberization process in russeted apples (Verdaguer *et al*. 2016). In a recent article, MYB67, NAC038 and WRKY56 were associated with the suberization process, but their exact respective functions remain unclear (Lashbrooke *et al*. 2016). Finally, the discovery of this crucial suberin regulator provides new opportunities for the development of industrial applications such as modified suberin production. In this perspective, a patent describing a process of suberin production using MYB93 has been filed recently (Patent n°93026, Luxembourg).

The present work provides a massive amount of data, which open multiple windows for further exploratory and functional validation studies in apple and more generally *in planta*. Indeed, a large amount of valuable candidates, which have been here highlighted, might provide an answer to the remaining questions about the suberin synthesis pathway and its regulation. More specifically to the apple model, it provides a strong basis in the knowledge of the multiple actors involved in the russet trait. Further studies have to be performed to establish the impact of these putative crucial actors, which favor the development of russeting in apple. Additionally, the very early sensing, which commits the apple epidermis to the russeting program, remains unclear. We are currently setting up a new project devoted to deciphering this crucial part of the russeting regulation, using russeting inducers, such as wounding or humidity exposure.

References

Aarts MG, Keijzer CJ, Stiekema WJ, Pereira A. 1995. Molecular characterization of the CER1 gene of arabidopsis involved in epicuticular wax biosynthesis and pollen fertility. *The Plant Cell* **7**: 2115-2127.

Andre CM, Greenwood JM, Walker EG, Rassam M, Sullivan M, Evers D, Perry NB, Laing WA. 2012. Anti-inflammatory procyanidins and triterpenes in 109 apple varieties. *Journal of Agricultural Food Chemistry* **60**: 10546-10554.

Andre CM, Larsen L, Burgess EJ, Jensen DJ, Cooney JM, Evers D, Zhang J, Perry NB, Laing WA. 2013. Unusual immuno-modulatory triterpene-caffeates in the skins of russeted varieties of apples and pears. *Journal of Agricultural Food Chemistry* **61**: 2773-2779.

Andre CM, Legay S, Deleruelle A, Nieuwenhuizen N, Punter M *et al.* 2016. Multifunctional oxidosqualene cyclases and cytochrome P450 involved in the biosynthesis of apple fruit triterpenic acids *New Phytologist* **211**: 1279-1294.

Ayvaz H, Santos AM, Rodriguez-Saona LE. 2016. Understanding Tomato Peelability
Comprehensive Reviews in Food Science and Food Safety **15**: 619-632.

Benveniste I, Tijet N, Adas F, Philipps G, Salaun JP, Durst F. 1998. CYP86A1 from *Arabidopsis thaliana* encodes a cytochrome P450-dependent fatty acid omega-hydroxylase. *Biochemical and Biophysical Research Communications* **243**: 688-693.

Beisson F, Li Y, Bonaventure G, Pollard M, Ohlrogge JB. 2007. The acyltransferase GPAT5 is required for the synthesis of suberin in seed coat and root of *Arabidopsis*. The *Plant Cell* **19**: 351-368.

Bernards MA. 2002. Demystifying suberin. *Canadian Journal of Botany* **80**: 227-240.

Bernards MA, Lopez ML, Zajicek J, Lewis NG. 1995. Hydroxycinnamic acid-derived polymers constitute the polyaromatic domain of suberin. *Journal of Biological Chemistry* **270**: 7382-7386.

Bird D, Beisson F, Brigham A, Shin J, Greer S, Jetter R, Kunst L, Wu X, Yephremov A, Samuels L. 2007. Characterization of *Arabidopsis* ABCG11/WBC11, an ATP binding cassette (ABC) transporter that is required for cuticular lipid secretion. *The Plant Journal* **52**: 485-498.

Bourquin V, Nishikubo N, Abe H, Brumer H, Denman S, Eklund M, Christiernin M, Teeri TT, Sundberg B, Mellerowicz EJ. 2002. Xyloglucan endotransglycosylases have a function during the formation of secondary cell walls of vascular tissues. *The Plant Cell* **14**:3073-3088.

Cosgrove DJ 2005. Growth of the plant cell wall. *Nature Reviews. Molecular Cell Biology* **6**: 850-861.

Blacklock BJ, Jaworski JG. 2006. Substrate specificity of *Arabidopsis* 3-ketoacyl-CoA synthases. *Biochemical and Biophysical Research Communications* **346**: 583-590.

Bonaventure G, Salas JJ, Pollard MR, Ohlrogge JB. 2003. Disruption of the FATB gene in *Arabidopsis* demonstrates an essential role of saturated fatty acids in plant growth. *The Plant Cell* **15**: 1020-1033.

Brendolise C, Yauk YK, Eberhard ED, Wang M, Chagne D, Andre C, Greenwood DR, Beuning LL. 2011. An unusual plant triterpene synthase with predominant alpha-amyrin-producing activity identified by characterizing oxidosqualene cyclases from *Malus* x *domestica*. *The FEBS Journal* **278**: 2485-2499.

Cassan-Wang H, Goue N, Saidi MN, Legay S, Sivadon P, Goffner D, Grima-Pettenati J. 2013. Identification of novel transcription factors regulating secondary cell wall formation in *Arabidopsis*. *Frontiers in Plant Science* **4:** 189.

Compagnon V, Diehl P, Benveniste I, Meyer D, Schaller H, Schreiber L, Franke R, Pinot F. 2009. CYP86B1 is required for very long chain omega-hydroxyacid and alpha, omega -dicarboxylic acid synthesis in root and seed suberin polyester. *Plant Physiology* **150**:1831-1843.

Curry EA 2009. Growth-induced microcracking and repair mechanisms of fruit cuticles. Proceedings of the SEM annual conference.

Curry EA. 2012. Increase in epidermal planar cell density accompanies decreased russeting of 'Golden Delicious' apples treated with Gibberellin A_{4+7}. *Hortscience* **47**: 232-237

De Vos M, Denekamp M, Dicke M, Vuylsteke M, Van Loon LC, Smeekens SC, Pieterse CM. 2006. The *Arabidopsis thaliana* transcription factor AtMYB102 functions in defense against the insect herbivore *Pieris rapae*. *Plant Signal and Behaviour* **1**: 305-311.

Delude C, Fouillen L, Bhar P, Cardinal MJ, Pascal S, Santos P, Kosma DK, Joubès J, Rowland O, Domergue F. 2016. Primary fatty alcohols are major components of suberized root tissues of *Arabidopsis* in the form of alkyl-hydroxycinnamates. *Plant Physiology* **171**: 1934-1950.

Domergue F, Vishwanath SJ, Joubes J, Ono J, Lee J *et al.* 2010. Three *Arabidopsis* fatty acyl-CoA reductases, FAR1, FAR4, and FAR5, generate primary fatty alcohols associated with suberin deposition. *Plant Physiology* **153**:1539-1554.

Dubos C, Stracke R, Grotewold E, Weisshaar B, Martin C, Lepiniec L. 2010. MYB transcription factors in Arabidopsis. *Trends in plant science* **15**: 573-581.

Edstam MM, Blomqvist K, Eklöf A, Wennergren U, Edqvist J. 2013. Coexpression patterns indicate that GPI-anchored non-specific lipid transfer proteins are involved in accumulation of cuticular wax, suberin and sporopollenin. *Plant Molecular Biology* **83**: 625-649.

Ellis M, Egelund J, Schultz CJ, Bacic A. 2010. Arabinogalactan-proteins: key regulators at the cell surface? *Plant Physiology* **153**: 403-419.

Faust M, Shear C. 1972. Russeting of apples, an interpretative review. *HortScience* **7**: 233-235.

Fernández-Pérez F, Pomar F, Pedreño MA, Novo-Uzal E. 2015a. Suppression of *Arabidopsis* peroxidase 72 alters cell wall and phenylpropanoid metabolism. *Plant Science* **239**: 192-199.

Fernández-Pérez F, Pomar F, Pedreño MA, Novo-Uzal E. 2015b. The suppression of AtPrx52 affects fibers but not xylem lignification in *Arabidopsis* by altering the proportion of syringyl units. *Physiologia Plantarum* **154**: 395-406.

Franke R, Briesen I, Wojciechowski T, Faust A, Yephremov A, Nawrath C, Schreiber L. 2005. Apoplastic polyesters in *Arabidopsis* surface tissues - a typical suberin and a particular cutin. *Phytochemistry* **66**: 2643-2658.

Fraser CM, Chapple C. 2011. The phenylpropanoid pathway in Arabidopsis. *Arabidopsis Book* **9**: e0152.

Gibbs DJ, Voß U, Harding SA, Fannon J, Moody LA, Yamada E, Swarup K, Nibau C, Bassel GW, Choudhary A *et al.* 2014. AtMYB93 is a novel negative regulator of lateral root development in Arabidopsis. *New Phytologist* **203**: 1194-1207.

Girard AL, Mounet F, Lemaire-Chamley M, Gaillard C, Elmorjani K *et al.* 2012. Tomato GDSL1 is required for cutin deposition in the fruit cuticle. *The Plant Cell* **24**: 3119-3134.

Graça J. 2015. Suberin: the biopolyester at the frontier of plants. *Frontiers in Chemistry* **3**: 62.

Graca J, Pereira H. 2000a. Methanolysis of bark suberins: analysis of glycerol and acid monomers. *Phytochemical Analysis* **11**: 45-51.

Graca J, Pereira H. 2000b. Suberin structure in potato periderm: glycerol, long-chain monomers, and glyceryl and feruloyl dimers. *Journal Agricultural Food Chemical* **48**: 5476-5483.

Hen-Avivi S, Lashbrooke J, Costa F, Aharoni A. 2014. Scratching the surface: genetic regulation of cuticle assembly in fleshy fruit. *Journal Experiment Botany* **65**: 4653-4664.

Hofer R, Briesen I, Beck M, Pinot F, Schreiber L, Franke R. 2008. The Arabidopsis cytochrome P450 CYP86A1 encodes a fatty acid omega-hydroxylase involved in suberin monomer biosynthesis. *Journal of Experimental Botany* **59**: 2347-2360.

Hussey SG, Mizrachi E, Spokevicius AV, Bossinger G, Berger DK, Myburg AA. 2011. SND2, a NAC transcription factor gene, regulates genes involved in secondary cell wall development in Arabidopsis fibres and increases fibre cell area in Eucalyptus. *BMC Plant Biology* **11**: 173.

Jäger S, Trojan H, Kopp T, Laszczyk MN, Scheffler A. 2009. Pentacyclic triterpene distribution in various plants - rich sources for a new group of multi-potent plant extracts. *Molecules* **14**: 2016-2031.

Jin J, Hewezi T, Baum TJ. 2011. *Arabidopsis* peroxidase AtPRX53 influences cell elongation and susceptibility to *Heterodera schachtii*. *Plant Signaling and Behaviour* **6**: 1778-1786.

Joubès J, Raffaele S, Bourdenx B, Garcia C, Laroche-Traineau J, Moreau P, Domergue F, Lessire R. 2008. The VLCFA elongase gene family in *Arabidopsis thaliana:* phylogenetic analysis, 3D modelling and expression profiling. *Plant Molecular Biology* **67**: 547-566.

Kannangara R, Branigan C, Liu Y, Penfield T, Rao V, Mouille G, Höfte H, Pauly M, Riechmann JL, Broun P. 2007. The transcription factor WIN1/SHN1 regulates Cutin biosynthesis in *Arabidopsis thaliana*. *The Plant Cell* **19**: 1278-1994.

Khanal BP, Grimm E, Knoche M. 2013. Russeting in apple and pear: a plastic periderm replaces a stiff cuticle. *Annals of Botany – Plants* **5**: ls048.

Knoche M, Grimm E. 2008. Surface moisture induces microcracks in the cuticle of 'Golden Delicious' apple. *Hortscience* **43**: 1929–1931.

Knoche M, Khanal BP, Stopar M. 2011. Russeting and microcracking of 'Golden Delicious' apple fruit concomitantly decline due to Gibberellin A4+7 application. *Journal of the American Society for Horticultural Science* **136**: 159-164.

Kosma DK, Molina I, Ohlrogge JB, Pollard M. 2012. Identification of an Arabidopsis fatty alcohol:caffeoyl-Coenzyme A acyltransferase required for the synthesis of alkyl hydroxycinnamates in root waxes. *Plant Physiology* **160**: 237–248.

Kosma DK, Rice A, Pollard M. 2015. Analysis of aliphatic waxes associated with root periderm or exodermis from eleven plant species. *Phytochemistry* **117**: 351-62.

Kurdyukov S, Faust A, Nawrath C, Bär S, Voisin D, Efremova N, Franke R, Schreiber L, Saedler H, Métraux J-P *et al.* 2006. The epidermis-specific extracellular BODYGUARD controls cuticle development and morphogenesis in *Arabidopsis*. *The Plant Cell* **18**: 321-339.

Landgraf R, Smolka U, Altmann S, Eschen-Lippold L, Senning M *et al.* 2014. The ABC transporter ABCG1 is required for suberin formation in potato tuber periderm. *The Plant Cell* **26**: 3403-3415.

Lashbrooke J, Aharoni A, Costa F. 2015. Genome investigation suggests MdSHN3, an APETALA2-domain transcription factor gene, to be a positive regulator of apple fruit cuticle formation and an inhibitor of russet development. *Journal of Agricultural Food Chemistry*. **63**: 185-91.

Lashbrooke J, Cohen H, Levy-Samocha D, Tzfadia O, Panizel I *et al.* 2016. MYB107 and MYB9 Homologs Regulate Suberin Deposition in Angiosperms. *Plant Cell* (Epub ahead of print).

Lee SB, Jung SJ, Go YS, Kim HU, Kim JK, Cho HJ, Park OK, Suh MC. 2009. Two *Arabidopsis* 3-ketoacyl CoA synthase genes, KCS20 and KCS2/DAISY, are functionally redundant in cuticular wax and root suberin biosynthesis, but differentially controlled by osmotic stress. *Plant Journal* **60**: 462-475.

Lee SB, Suh MC. 2013. Recent Advances in Cuticular Wax Biosynthesis and Its Regulation in Arabidopsis. *Molecular Plant* **6**: 246-249.

Lee SB, Suh MC. 2015. Cuticular wax biosynthesis is up-regulated by the MYB94 transcription factor in Arabidopsis. *Plant Cell Physiology* **56**: 48-60.

Legay S, Guerriero G, Deleruelle A, Lateur M, Evers D, André CM, Hausman, J-F. 2015. Apple russeting as seen through the RNA-seq lens: strong alterations in the exocarp cell wall. *Plant Molecular Biology* **88**: 21-40.

Li Y, Beisson F. 2009. The biosynthesis of cutin and suberin as an alternative source of enzymes for the production of bio-based chemicals and materials. *Biochimie* 91: 685-691.

Li-Beisson Y, Shorrosh B, Beisson F, Andersson MX, Arondel V *et al.* 2010. Acyl-lipid metabolism. *The Arabidopsis Book*. **8**: e0133.

Liang M, Davis E, Gardner D, Cai X, Wu Y. 2006. Involvement of AtLAC15 in lignin synthesis in seeds and in root elongation of Arabidopsis. *Planta* **224**: 1185-1196.

Liepman AH, Wightman R, Geshi N, Turner SR, Scheller HV. 2010. Arabidopsis - a powerful model system for plant cell wall research. *Plant Journal* **61**: 1107-1121.

Lü S, Song T, Kosma DK, Parsons EP, Rowland O, Jenks MA. 2009. *Arabidopsis* CER8 encodes LONG-CHAIN ACYL-COA SYNTHETASE 1 (LACS1) that has overlapping functions with LACS2 in plant wax and cutin synthesis. *Plant Journal* **59**: 553-564.

MacMillan CP, Mansfield SD, Stachurski ZH, Evans R, Southerton SG. 2010. Fasciclin-like arabinogalactan proteins: specialization for stem biomechanics and cell wall architecture in *Arabidopsis* and Eucalyptus. *Plant Journal* **62**: 689-703.

McFarlane HE, Watanabe Y, Yang W, Huang Y, Ohlrogge J, Samuels AL. 2014. Golgi- and trans-Golgi network-mediated vesicle trafficking is required for wax secretion from epidermal cells. *Plant Physiology* **164**: 1250-1260.

Millar AA, Clemens S, Zachgo S, Giblin EM, Taylor DC, Kunst L. 1999. CUT1, an *Arabidopsis* gene required for cuticular wax biosynthesis and pollen fertility, encodes a very-long-chain fatty acid condensing enzyme. *The Plant Cell* **11**: 825-838.

Molina I, Bonaventure G, Ohlrogge J, Pollard M. 2006. The lipid polyester composition of *Arabidopsis thaliana* and *Brassica napus* seeds. *Phytochemistry* **67**: 2597-2610.

Molina I, Kosma D. 2015. Role of HXXXD-motif/BAHD acyltransferases in the biosynthesis of extracellular lipids. *Plant Cell Reports* **34**: 587-601.

Molina I, Li-Beisson Y, Beisson F, Ohlrogge JB, Pollard M. 2009. Identification of an *Arabidopsis* feruloyl-coenzyme A transferase required for suberin synthesis. *Plant Physiology* **151**: 1317-1328.

Olsen AN, Ernst HA, Leggio LL, Skriver K. 2005. NAC transcription factors: structurally distinct, functionally diverse. *Trends in plant science* **10**: 79-87.

Oshima Y, Mitsuda N. 2013. The MIXTA-like transcription factor MYB16 is a major regulator of cuticle formation in vegetative organs. *Plant Signaling and Behaviour* **8**: e26826.

Oshima Y, Shikata M, Koyama T, Ohtsubo N, Mitsuda N, Ohme-Takagi M. 2013. MIXTA-like transcription factors and WAX INDUCER1/SHINE1 coordinately regulate cuticle development in *Arabidopsis* and *Torenia fournieri*. *The Plant Cell* **25**: 1609-1224.

Panikashvili D, Shi JX, Schreiber L, Aharoni A. 2009. The *Arabidopsis* DCR Encoding a Soluble BAHD Acyltransferase Is Required for Cutin Polyester Formation and Seed Hydration. *Plant Physiology* **151**: 1773-1789.

Pollard M, Beisson F, Li Y, Ohlrogge JB. 2008. Building lipid barriers: biosynthesis of cutin and suberin. *Trends in Plant Science* **13**: 236-246.

Roudier F, Fernandez AG, Fujita M, Himmelspach R, Borner GH, Schindelman G, Song S, Baskin TI, Dupree P, Wasteneys GO, Benfey PN. 2005. COBRA, an *Arabidopsis* extracellular glycosyl-phosphatidyl inositol-anchored protein, specifically controls highly anisotropic expansion through its involvement in cellulose microfibril orientation. *The Plant Cell* **17**:1749-1763.

Rowland O, Lee R, Franke R, Schreiber L, Kunst L. 2007. The CER3 wax biosynthetic gene from *Arabidopsis thaliana* is allelic to WAX2/YRE/FLP1. *FEBS Letters* **581**: 3538-3544.

Rushton PJ, Somssich IE, Ringler P, Shen QJ. 2010. WRKY transcription factors. *Trends in plant science* **15**: 247-258.

Sakamoto S, Mitsuda N. 2015. Reconstitution of a secondary cell wall in a secondary cell wall-deficient *Arabidopsis* mutant. *Plant Cell Physiology* **2**: 299-310.

Sampedro J, Cosgrove DJ. 2005. The expansin superfamily. *Genome Biology* **6**: 242

Sauveplane V, Kandel S, Kastner PE, Ehlting J, Compagnon V, Werck-Reichhart D, Pinot F. 2009. *Arabidopsis thaliana* CYP77A4 is the first cytochrome P450 able to catalyze the epoxidation of free fatty acids in plants. *FEBS Journal* **276**: 719-735.

Schreiber L, Franke R, Hartmann K. 2005. Wax and suberin development of native and wound periderm of potato (*Solanum tuberosum L.*) and its relation to peridermal transpiration. *Planta* **220**: 520–530.

Serra O, Hohn C, Franke R, Prat S, Molinas M, Figueras M. 2010. A feruloyl transferase involved in the biosynthesis of suberin and suberin-associated wax is required for maturation and sealing properties of potato periderm. *The Plant Journal* **62**: 277-290.

Sironval C, Clijsters H. 1962. Sur la nature de la rugosité chez la pomme Cox's Orange. *Bulletin de la société royale de botanique de Belgique* **94**: 35-44.

Skene DS. 1982. The development of russet, rough russet and craks on the fruit of the apple Cox's Orange Pippin during the course of the season. *Journal of Horticultural Science* **57**: 165-174.

Soler M, Serra O, Molinas M, Huguet G, Fluch S, Figueras M. 2007. A genomic approach to suberin biosynthesis and cork differentiation. *Plant Physiology* **144**: 419-431.

Tukey LD. 1969. Observations on the russeting of apples growing in plastic bags. *Proceedings of the American Society for Horticultural Science* **74**: 30-39.

von Wettstein PM 2012. Plant waxes. *eLS: citable reviews in the life sciences*. Wiley
press.

Velasco R, Zharkikh A, Affourtit J, Dhingra A, Cestaro A, Kalyanaraman A, Fontana P *et al.* 2010. The genome of the domesticated apple (*Malus* x *domestica* Borkh.). *Nature Genetics* **42**:833-839.

Verdaguer R, Soler M, Serra O, Garrote A, Fernández S, Company-Arumí D, Anticó E, Molinas M, Figueras M. 2016. Silencing of the potato StNAC103 gene enhances the accumulation of suberin polyester and associated wax in tuber skin. *Journal of Experimental Botany* **67**: 5415-5427.

Vishwanath SJ, Delude C, Domergue F, Rowland O. 2015. Suberin: biosynthesis, regulation, and polymer assembly of a protective extracellular barrier. *Plant Cell Reports* **34**: 573-86.

Walter TE. 1967. Russeting and cracking in apples. A review of world literature. *Report of East Mailing Research Station* **1966**: 83-95.

Watanabe S. 1969. Historical studies on the cause of apple russeting. *Bulletin of the Yamagata University* **5**: 205-267.

Wellesen K, Durst F, Pinot F, Benveniste I, Nettesheim K, Wisman E, Steiner-Lange S, Saedler H, Yephremov A. 2001. Functional analysis of the LACERATA gene of *Arabidopsis* provides evidence for different roles of fatty acid ω-hydroxylation in development. *Proceedings of the national Academy of of Sciences of USA* **98**: 9694-9699.

Xia Y, Nikolau BJ, Schnable PS. 1996. Cloning and characterization of CER2, an *Arabidopsis* gene that affects cuticular wax accumulation. *The Plant Cell* **8**: 1291-304.

Xiao F, Goodwin M, Xiao Y, Sun Z, Baker D,Tang X, Matthew A, Jenks MA, Zhou JM. 2004. *Arabidopsis* CYP86A2 represses *Pseudomonas syringae* type III genes and is required for cuticle development. *EMBO Journal* **23**: 2903-2913.

Yeats TH, Huang W, Chatterjee S, Viart HM, Clausen MH, Stark RE, Rose JK. 2014. Tomato Cutin Deficient 1 (CD1) and putative orthologs comprise an ancient family of cutin synthase-like (CUS) proteins that are conserved among land plants. *Plant Journal* **77**: 667-675.

Yeats TH, Laetitia BB, Martin Viart HMF, Isaacson T, He Y, Zhao L *et al.* 2012. The identification of cutin synthase: formation of the plant polyester cutin. *Nature Chemical Biology* **8**: 609-611.

Yeats TH, Rose JKC. 2013. The formation and function of plant cuticles. *Plant Physiology* **163**: 5–20.

Yadav V, Molina I, Ranathunge K, Castillo IQ, Rothstein SJ, Reed JW. 2014. ABCG transporters are required for suberin and pollen wall extracellular barriers in *Arabidopsis*. *The Plant Cell* **26**: 3569-3588.

Yazaki K. 2006. ABC transporters involved in the transport of plant secondary metabolites. *FEBS Letters* **580**: 1183-1191.

Zhang Y, Cao G, Qu LJ, Gu H. 2009. Characterization of *Arabidopsis* MYB transcription factor gene AtMYB17 and its possible regulation by LEAFY and AGL15. *Journal of Genetics and Genomics* **36**: 99-107.

Zhong R, Lee C, Zhou J, McCarthy RL, Ye ZH. 2008. A battery of transcription factors involved in the regulation of secondary cell wall biosynthesis in *Arabidopsis*. *The Plant Cell* **20**: 2763-2782.